US DOI, BUREAU OF SAFETY AND ENVIRONMENTAL
ENFORCEMENT(FORMERLY MINERALS MANAGEMENT SERVICE)[1]
TA&R PROJECT NUMBER 653
TEES A9390 PE
EVALUATION OF THE USE OF EPOXY-BASED MATERIALS IN WELL
ABANDONMENT
FINAL REPORT
OCTOBER 12, 2012

1. Executive Summary

Over the past several years, hurricanes have damaged or destroyed approximately 180 offshore oil and gas producing platforms (See Figure ES1). Because of this damage and destruction, many wells can no longer safely produce oil or gas, and/or have become an environmental and safety hazard. Most of the wells from damaged platforms can be plugged and abandoned by conventional means. However, when the platforms have been toppled or completely destroyed, conventional intervention methods may not be possible. Instead a subsea intersection well may have to be drilled to provide access to the wellbore. Depending on where the intersection takes place and the condition of the target well, it may not be possible to circulate or pump cement into the wellbore. In these cases, a plugging material may need to be spotted at the intersection of the target well, and allowed to fall through the annulus, and settle on top of a packer, where it is hoped that it will set properly.

Hurricane	No. Destroyed	No. Extremely Damaged
Rita & Katrina	113	144
Ike & Gustav	60	31
Ivan, Andrew & Lily	18	

Figure ES1 Damaged and Destroyed GOM Platforms by Recent Hurricanes

Although cement is currently the plugging material of choice, it is not always practical. One of the concerns of spotting cement and allowing it to fall to the packer, is that since cement is a water-based slurry, it will be diluted with seawater or brines that are present as packer fluids in many of these damaged wells. This dilution/contamination results in poor cement quality, if it hardens at all after falling up to several thousand feet through annular fluid.

The BSEE is considering the use of epoxy-based materials for abandonment of wells damaged by hurricanes. These wells do not have vertical access and may be buckled below the mud line, therefore preventing wire line operations via tubing to set plugs near the packer or punch the tubing to circulate cement into the casing. The major concern with using epoxy based plugging materials is that these materials have never been used as plugging materials nor has the

---

applicability of using such material been adequately studied. We have conducted an evaluation of epoxy based materials for use in plugging of oil and gas wells.

In this study we have evaluated materials and procedures for epoxy-based well abandonments by:

• Comparing epoxy-based materials against cement abandonments and other potential plugging materials

• Determining whether epoxy material can effectively drop 7000 feet through a casing annuli and accumulate on top of the packer

• Determining how long material takes to travel to the bottom of a casing annulus and cure

• Determining how material performs over time

• Determining how weighting of this material with BaSO4 affects the compressive and bond strength of the material

• Determining whether there are other weighting materials which may perform better than BaSO4

• Ranking various resin and hardener chemical systems for best performance in the field

• Evaluating the effects of various liquids such as calcium chloride, sea water, and formation hydrocarbons on the resin chemical systems.

2. Project Description
We have completed our study on the applicability of using epoxies and other gel, resin or grout materials as plugging agents in severely damaged wells where access is limited and may be only through subsurface intervention via intersection wells. This study was divided into six tasks as explained below.

Task 1 – A complete literature review was conducted to determine which epoxy (or other) materials may be applicable as plugging materials. Based on the literature review we made a first comparison of these unconventional plugging materials to oil well cement, including strength, potential for placement and good bonding under adverse conditions and expected lifetime. We tested these materials to determine how they will hold up over time at bottomhole conditions and compared these results to those of oilfield cements.

Task 2 - Rheology of plugging materials – these fluids are non-Newtonian fluids in most cases. Initially we thought the rheology was needed to determine pressure losses, and determine setting time. However, the rheological properties of these properties were such that the viscosity exceeded the measurement range of our Fann 35 type viscometers. But we did discover qualitatively that the rheological properties of the epoxy had no bearing on the fall rate (as long

as the formulation prevented separation of the weighting agent from the epoxy) or setting time and was not required for our evaluation.

Task 3 – We have data showing the likelihood that epoxy can effectively drop 7000 feet through a casing annulus, accumulate on top of the packer and set with effective strength and bonding. We have developed a methodology to determine the time for this material to travel to the bottom of the casing annulus compared to the curing time. This was done through both a theoretical analysis and experimental studies. An experimental apparatus was constructed where we measured the settling velocity of each material and determined the effect of the materials' densities on settling velocity. It was determined that density was the major contributor to the fall velocity and viscosity of the epoxy had little or no effect of the fall velocity. We utilized different size pipes (PVC and clear plastic) to visualize and measure the effect of cross section on the settling velocity. The apparatus was constructed so that the pipe can be placed at angles from vertical to horizontal so that we could determine the effect of hole angle on the settling velocity. We also built a second apparatus to measure the terminal velocity of an individual globule of epoxy. We intended to validate these small-scale tests by conducting larger scale tests in a 3000' test well owned and operated by Boots & Coots. However, an open time to use the Boots and Coots facility never became available.

Task 4 – Based on the results of Tasks 2 and 3, we developed a model where the optimized settling/setting times can be predicted for field applications. The model includes the ability to predict the volume of plugging material that is likely to adhere to the casing and tubing while falling to bottom. This will enable planners to make allowances for plugging material that will not make it to bottom, so that sufficient quantities can be mixed for a successful plug.

Task 5 – We performed lab studies to determine the curing time of these plugging materials at reservoir conditions. We utilized aging ovens to determine the effect of temperature on the curing time, as well as the effect of temperature on the compressive and bonding strength of these materials. We left several samples in the oven to determine (to a limited extent) if these materials will degrade over time, and compositional variations were studied to maximize time stability at temperature. We determined the compatibility of these fluids with potential wellbore fluids. The potential plugging materials may be contaminated by wellbore fluids which could have an effect on the rheology, curing time, compressive strength, and bonding strength of the plugging materials.

Task 6 – We determined how weighting these materials with $BaSO_4$ will affect settling velocity and the compressive and bond strength. We added different amounts of $BaSO_4$ to samples and measured the compressive and bond strength so that a comparison could be made to cement. We also conducted experiments to determine the degree to which $BaSO_4$ will separate during placement, whether it will settle prior to curing and any impacts of such effects on required behavior during placement, curing and lifetime of the material.

3. Results and Conclusions
This work was conducted by three professors, five graduate students, and two undergraduate students at Texas A&M University and was funded by the BSEE. Professors and the students working under their supervision, and the title of each student's thesis are:

Dr. Robert Lane

Suining Gao, "Curing Properties of Epoxy Resin for Use to Abandon Wells Destroyed by Hurricanes in the Gulf of Mexico", Texas A&M University, Dec. 2011.

Zhuo Gao, "Potential of Barite-Weighted Epoxy Systems to Plug Wells in the Gulf of Mexico", Texas A&M University, Dec. 2011

Dr. Hisham Nasr-el-Din

Ahmed Rami Abuelaish, "The Evaluation of the Mechanical Strength of Epoxy-Based Resin as a Plugging Material, and the Development of an Novel Plug and Abandon Technique Using Vitrified Solid Epoxy-Based Resin Beads", Texas A&M University, May, 2012

Dr. Jerome Schubert

Ibrahim El-Mallawany, "An Experimental Setup to Study the Fall Rate of Epoxy Based Fluids", Texas A&M University, December, 2010

Hasan Turkmenoglu, "Determining the Terminal Velocity and the Particle Size of Epoxy Based Fluids in the Wellbore", Texas A&M University, August 2012

Zaid Abdulsatter, and James Davis, Texas A&M University are undergraduate students who performed many of the fall rate experiments and their help was extremely valuable to the success of this project. The data obtained in their experiments were analyzed and reported in Turkmenoglu's thesis.

Dr. Lane and Nasr-el-Din and their students were charged with screening the literature to find epoxy compositions which would appear to have the curing, bonding, and strength properties which would be applicable as plugging material at wellbore conditions expected 7000' below the mud line. The students tested numerous blends commercially available to determine curing times at temperatures up to 200 degrees F, as well as bond strength and compressive strength. Once a suitable candidate was identified, these students tested the effect of various contaminants, and a barite densifier on these properties.

Dr. Schubert and his students designed and built two mechanism to measure the fall rate of the epoxy materials in an annulus with varying hole angle and density. These measurements were used to develop a model in which the time for the epoxy to reach a certain distance in both vertical and deviated wells, as well as a methodology to approximate the volume of the plugging material would adhere to the walls of the pipe on its trip to bottom. These estimates can be used to determine the pot time necessary, and the volume to mix so that a sufficient length plug can be obtained at the desired plug location.

Abstracts and conclusions of all five Master of Science theses are shown here.

Suining Gao, "Curing Properties of Epoxy Resin for Use to Abandon Wells Destroyed by Hurricanes in the Gulf of Mexico", Texas A&M University, Dec. 2011.

Abstract

Some Gulf of Mexico (GOM) wells destroyed by hurricanes have become environmental and safety hazards and cannot be abandoned by conventional methods since pumping and circulating cement into the casing is impossible when the platforms have been completely destroyed and toppled. This project tested the curing properties of several epoxy resin systems in different environments. A bisphenol-F/epichlorohydrin (BPF) resin cured by curing agent MBOEA system was successfully tested in the laboratory as a potential plugging material to abandon wells destroyed in the GOM. The BPF/MBOEA resin system had the most suitable curing time in a synthetic seawater environment. The system could be successfully weighted by barite up to 16.8 ppg and cured properly. Weighting allows the resin system fall more efficiently through the casing annulus. This laboratory verification of properties will lead to field test in the test wells.

Conclusions

The curing properties of the four epoxy resin systems were tested. From all the results and discussions, we draw conclusions as follow:

1. Curing properties of epoxy resin systems are consistent with needs for abandoning wells destroyed by hurricanes.

2. The BPF system which contains the RAR 9281 BPF resin, the RAC 9907 curing agent, and RAD 100 reactive diluent is the optimal system we tested in this project. This system has suitable pot life and curing time and large barite capacity which could weigh the system as much as 16.8 ppg.

3. BPF resin system has superior properties compared with BPA resin system. The BPA system which contains the RAR 901 and the RAC 9907 curing agent has suitable pot life, but the small filler capacity means this system could only be weighed to 10.5 ppg. Considering the lower price compared with BPF system, this BPA system may be used in the cases that require low density.

4. Laboratory verification of shear bond strength properties should lead to field test in test wells.

Zhuo Gao, "Potential of Barite-Weighted Epoxy Systems to Plug Wells in the Gulf of Mexico", Texas A&M University, Dec. 2011

Abstract

In the past ten years, there have been 194 hurricane-damaged platforms in the Gulf of Mexico (GOM), each with many wells that have not been permanently abandonment. This could lead to disastrous environmental consequences. Many wells where their platforms were destroyed by hurricanes cannot be abandoned by conventional methods. Our research showed that barite-weighted epoxy material could be potentially used for well abandonment for those wells in GOM. Shear bond strength tests showed that between two candidates epoxy systems—the bisphenol A system and the bisphenol F

system, the latter was less sensitive to barite weighting material. The shear bond strength of bisphenol A system was deteriorated as barite increased, while bisphenol F system showed slightly increasing trend when barite was added. The minimum bond strength given by bisphenol A system appears around 68 wt% of barite, which is around 1290 psi. The maximum value of 2200 psi comes at 0 wt% of barite. And the bisphenol F system can stand a minimum of 1010 psi bond strength at 0 wt% of barite, and a maximum of 1160 psi of bond strength with 70 wt% of barite. Moreover, mixing with seawater did influence the shear bond strength between epoxy system and low-carbon steel. The influence that seawater has on the F system is less than that of the A system. The time that the epoxy system needs to fully develop the bond is far longer than curing time determined in our parallel research. Bond strength is lower in both seawater environment and at high temperature.

Conclusions
Previous research in our lab has shown resin hardening time increased with the amount of barite added, which is good to give sufficient time to complete the abandonment work. Tests in this project were carried out in ideal conditions. Real world applications are likely to be affected by corrosion etc. Shear bond strength tests in this study showed further properties of epoxy systems:

1. A large number of mechanical tests verified that the shear bond strength of bisphenol F type epoxy bonded to low carbon steel remained stable when barite filler was added to the formulation.

2. Simulated environmental tests demonstrated that when epoxy contacts steel in the presence of synthetic seawater, shear bond strength decreases. We suspect that the strength decrease is due to the epoxy-steel contact area being decreased and the bond thus weakened due to some capture of some seawater between epoxy, steel, and epoxy, barite.

3. Even though strength reduction must be accounted for in determining pressure differential that the epoxy-steel bond can withstand, bisphenol F system with barite bonded to low carbon steel retains sufficient shear bond strength to exceed all established regulations.

4. Epoxy-Steel shear bond strength continues developing for six days, much longer than hardening time and reaches 725 psi more rapidly than cement formulations.

5. Increasing temperature weakens the bond strength of the barite-weighted epoxy with the low carbon steel. At least a portion of the observed weakening is due to unavoidable temperature cycling caused by the necessity of curing the samples in a separate oven from the testing device oven.

6. Even with weakening at high temperature, the shear bond strength of BPF/barite system bonded to low carbon steel is strong enough so that even a short length of plug in a wellbore will meet the most stringent regulatory criteria.

7. The BPF/barite system should be evaluated in a test wellbore where the epoxy system must drop through several thousand feet of synthetic seawater and bond to a section of steel casing in order to demonstrate strength of the bond under more realistic conditions.

Ahmed Rami Abuelaish, "The Evaluation of the Mechanical Strength of Epoxy-Based Resin as a Plugging Material, and the Development of an Novel Plug and Abandon Technique Using Vitrified Solid Epoxy-Based Resin Beads", Texas A&M University, May, 2012

Abstract
Over the past several years, some of the platforms in the Gulf of Mexico have been damaged completely, such that conventional P&A operations may not be possible. In these cases, plugging fluid needs to be pumped through an intervention well and dropped several thousand feet in water to settle above a packer and seal the well.

The current P&A material of choice is cement, but cement is miscible in water, which dilutes and contaminates the cement. Therefore, alternate plugging materials need to be used for these operations. This paper discusses the development of a cost-effective Epoxy P&A method and the challenges of using Epoxy. First, the impact of seawater, oil, and pipe dope on the curing process remains unknown. Secondly, the yield strength of Epoxy with and without the contaminating chemicals must be equal to or better than cement. Finally, previous tests have shown significant losses of Epoxy to the walls of the wellbore during the 7,000-ft drop.

Conclusions
1. Mixing the resin with seawater, oil, or pipe dope will reduce the ultimate strength and fracture strengths of the mixtures compared to the strengths of pure resin. The ultimate strength of contaminated resin will most likely drop to the value of the yield strength, and should be designed with that in mind. The fracture strengths of contaminated resin will experience a drop greater than a 25% compared to pure resin, while the yield strength, on the other hand, can remain relatively unaltered.

2. During a 6-hour cure, the cure process of resin mixed in with seawater can be accelerated by more than 2 hours compared to pure resin, while oil has no apparent effect on the cure process.

3. Quenching droplets of epoxy resin in 39°F diluted water before the initiation of gelation during the cure process was found to form solid beads through the reversible physical process of vitrification; using this effect as a plugging application can be successful.

4. The average fracture strength of reconsolidated epoxy resin beads was found to be 7,717 psi, indicating that an application utilizing solid resin beads, as discussed in this thesis, can be up to 89% stronger than the ASTM compressive strength values for Portland cements I & II.

5. From an operational cost standpoint, using vitrified epoxy resin beads has the potential to create up to USD 0.7 million in savings compared to conventional cement costs for cases similar to the one discussed herein. In Addition, using vitrified epoxy resin beads in place of pumping liquid epoxy resin could eliminate the 32% of material lost during settling, thus creating savings of approximately USD 60 thousand for a 7,000-ft application with a 550-ft plug height.

Ibrahim El-Mallawany, "An Experimental Setup to Study the Fall Rate of Epoxy Based Fluids", Texas A&M University, December, 2010

Abstract
This thesis is part of a project funded by BSEE to study the use of epoxy (or any cement alternative) to plug hurricane damaged wells. Some of the wells destroyed by hurricanes are damaged to an extent that vertical intervention from the original wellhead is not possible. The means to plug such wells, as sought by this project, is to drill an offset well and intersect the original at the very top and spot some epoxy (or any suitable non-cement plugging material) in the original well. The epoxy will then fall by gravity all the way until it reaches the packer and then set on top of the packer to plug the annulus of the well permanently.

One of the most important factors in this process is to be able to predict the settling velocity of the epoxy to be able to determine the required setting time of the epoxy so that the epoxy does not set prematurely. This thesis aims to design, build and run an experimental setup that would help develop a model to estimate settling velocities of different epoxies. The model itself will be part of a different dissertation. Part of this thesis is to also investigate how much epoxy will adhere to the pipe walls to be able to account for epoxy lost on the journey towards the packer. The thesis will also investigate whether weighting materials such as barite would separate from the epoxy when freefalling through water.

Conclusions
1. Denser formulations have a faster terminal velocity.

2. The fall rate during experiments at an angle other than vertical are much faster than experiments done at vertical position, almost double the terminal velocity.

3. The annulus size has no significant effect on terminal velocity for vertical pipes.

4. The pressure transducer is a good way to measure the time from the experiment's start until the lead of the epoxy passes it.

5. The greater the viscosity of the epoxy formulation the greater the adhesion to the pipe walls.

6. The larger the angle of inclination the greater the adhesion to the pipe walls.

7. The smaller the annulus size the greater the adhesion to the pipe walls.

8. Adhesion decreases with depth.

9. Recycled epoxy is not suitable to represent freshly mixed epoxy.

10. Although pure epoxy is less dense than water, it does not separate from the barite it is mixed with and therefore maintains a higher density and stays at the bottom.

Hasan Turkmenoglu, "Determining the Terminal Velocity and the Particle Size of Epoxy Based Fluids in the Wellbore", Texas A&M University, August 2012

Abstract
This thesis was inspired by the project funded by Bureau of Safety and Environment Enforcement (BSEE) to study the use of epoxy (or any cement alternative) to plug offshore wells damaged by hurricanes. The project focuses on non-cement materials to plug wells that are either destroyed or damaged to an extent where vertical intervention from the original wellhead is no longer possible. The proposed solution to this problem was to drill an offset well and intersect the original borehole at the very top and spot epoxy (or any suitable non-cement plugging material) in the original well. The spotted epoxy then would fall by gravitational force all the way down to the packer and then settle on top of the packer to plug the annulus of the damaged well permanently.

This thesis mainly concentrates on the factors affecting the fall rates and how to correlate them in order to derive an applicable test that can be conducted in the field or lab to calculate the terminal velocity of the known epoxy composition. Determining the settling velocity of the epoxy is crucial due to the fact that epoxy should not set prematurely for a better seal and isolation. The terminal velocity and the recovery for epoxy based plugging fluids were tested by using an experimental setup that was developed for this purpose. The results were also validated by using an alternative experiment setup designed for this purpose. Factors affecting the terminal velocity and recovery of epoxy were studied in this research since the settling velocity of the epoxy is crucial because epoxy should not set prematurely in order to achieve a better seal and isolation. The study was conducted by using an experimental setup that was specially developed for terminal velocity and recovery calculations for plugging fluids. Results obtained from the experiment setup were successfully correlated to epoxy's composition for estimating the terminal velocity of the mixture.

Conclusions
1. Denser epoxy formulations tend to have higher terminal velocity with some exceptions. The exceptions are thought to have a connection with the amount of diluent used. Further study needed to be done to increase the accuracy of terminal velocity estimations and "The Static Experiment Setup" was developed for this purpose.

2. The terminal velocity for any epoxy formulation can be calculated by using the equation provided.

3. For well inclinations from 30 degrees to 45 degrees, the fall rate of epoxy will increase by 100% to 130% compared to the vertical cases. It is recommended that the

velocity calculated from the equation should be used as the average velocity to be on the safe side.

4. Maximum amount of epoxy loss for a vertical well is estimated to be between 3.161 g/ft2 and 12.379 g/ft2.

5. For an inclined well which has a 30 degree inclination is expected to have 6.757 g/ft2 to 17.368 g/ft2 epoxy loss.

6. For 45 degree inclination this number varies between 9.142 g/ft2 and 19.055 g/ft2.

7. For a 60 degree inclination however, most of the tests failed to give any recovery of epoxy plugging material at the bottom of the apparatus. Therefore, at inclinations of 60 degree or greater, the material we tested would probably not provide an adequate plug.

8. As far as the tests conducted in the static experiment setup suggest, the density of the mixture should be kept around 14 ppg or less to increase the recovery of the epoxy. After 14 ppg, barite tends to break free from the mixture as it falls through water.

9. Higher inclinations will cause higher adhesion thus decrease the amount of epoxy delivered to the target. The volume of epoxy prepared for the inclined sections should always be kept more than the vertical case in order to assure the success of the work.

10. Smaller annular size will usually lead to less epoxy loss due to smaller inner surface area.

11. As the epoxy flow stabilizes towards the bottom of the well, interaction with the walls will decrease and the adhesion concentration will also decrease.

12. Barite is a good candidate for weighting epoxy mixtures up to 14 ppg density. It will however, break free from the mixture significantly if the density exceeds this number.

Full documentation of the work completed can be found in the individual theses, provided separate from this summary.

CURING PROPERTIES OF EPOXY RESIN FOR USE TO ABANDON WELLS

DESTROYED BY HURRICANES IN THE GULF OF MEXICO

A Thesis

by

SUINING GAO

Submitted to the Office of Graduate Studies of
Texas A&M University
in partial fulfillment of the requirements for the degree of

MASTER OF SCIENCE

December 2011

Major Subject: Petroleum Engineering

Curing Properties of Epoxy Resins for Use to Abandon Wells Destroyed by Hurricanes

in the Gulf of Mexico

CURING PROPERTIES OF EPOXY RESINS FOR USE TO ABANDON WELLS

DESTROYED BY HURRICANES IN THE GULF OF MEXICO

A Thesis

by

SUINING GAO

Submitted to the Office of Graduate Studies of
Texas A&M University
in partial fulfillment of the requirements for the degree of

MASTER OF SCIENCE

Approved by:

Chair of Committee,   Robert H. Lane
Committee Members,   David Schechter
                     Yuefeng Sun

Head of Department,   Akhil Datta-Gupta

December 2011

Major Subject: Petroleum Engineering

ABSTRACT

Curing Properties of Epoxy Resins for Use to Abandon Wells Destroyed by Hurricanes

in the Gulf of Mexico

(December 2011)

Suining Gao, M. S., Tsinghua University

Chair of Advisory Committee: Dr. Robert H. Lane

Some Gulf of Mexico (GOM) wells destroyed by hurricanes have become environment and safety hazard and cannot be abandoned by conventional methods since pumping and circulating cement into the casing is impossible when the platforms have been completely destroyed and toppled. This project tested the curing properties of several epoxy resin systems in different environments. A bisphenol-F/epichlorohydrin (BPF) resin cured by curing agent MBOEA system was successfully tested in the laboratory as a potential plugging material to abandon wells destroyed in the GOM. The BPF/MBOEA resin system had the most suitable curing time in a synthetic seawater environment. The system could be successfully weighted by barite up to 16.8 ppg and cured properly. Weighting allows the resin system fall more efficiently through the casing annulus. This laboratory verification of properties will lead to field test in the test wells.

DEDICATION

This thesis is dedicated to my wonderful husband, my lovely daughter, and my parents, for their support.

ACKNOWLEDGEMENTS

TABLE OF CONTENTS

LIST OF FIGURES

viii

LIST OF TABLES

1   INTRODUCTION

1.1 Statement of problem

About 400 offshore oil and gas producing platforms were destroyed or damaged by hurricanes in the past several years in the Gulf of Mexico (GOM) (BOEMRE, 2006, 2007, 2008). **Table 1.1** shows the detailed numbers of the wells destroyed or damaged.

TABLE 1.1– NUMBERS OF THE WELLS DESTROYED OR DAMAGED BY HURRICANES IN THE GOM			
Hurricanes	Ivan	Katrina and Rita	Gustav and Ike
Destroyed	7	116	60
Severe Damaged	18	163	31
Destroyed and Damaged	25	279	91
Total		395	

Since those wells have become an environment and safety hazard, they need to be plugged and abandoned. However, conventional abandonment methods may not be possible for some of the wells when the platforms have been completely destroyed and toppled (**Fig. 1.1**). Instead a subsea intervention well may have to be drilled to provide access to the wellbore (**Fig. 1.2**). The completion type and the well condition may limit or prevent the ability to pull tubing to circulate plugging material into the tubing or the annulus above or between packers. In these cases, the plugging material may have to be spotted at the intersection of the target well and dropped down the well's tubing and

_____

This thesis follows the style of *SPE style*

Fig. 1.1—Platform was destroyed by hurricane Ike in the East Cameron Area. (BOEMRE, 2010)
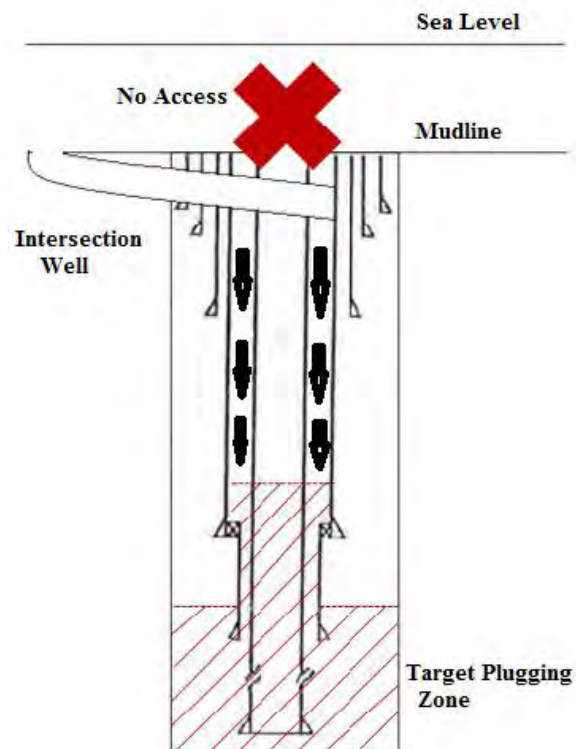
Fig. 1.2—Schematics of the situation of the wells destroyed by hurricanes.

annulus through existing packer fluids by gravity. The conventional plugging material, cement, may not be the optimum choice because cement is miscible with seawater. It is probable that many of the offshore wells would be filled with seawater due to its use as a packer fluid and/or entry of additional seawater if the wellbore is breached at or above the mudline during the destructive storm event. The seawater in the casing annulus and tubing would diluent cement as it fall to the bottom, then preventing it from obtaining sufficient compressive strength and bonding strength.

This thesis is part of the project funded by BOEMRE which aims to evaluate the use of epoxy resin as well abandonment material to permanently plug the wells destroyed by hurricanes. The current issue with using resins is that it is not yet known how effective they may be as a plugging material. Research must be conducted to determine if resin systems will provide sufficient properties, including suitable curing time and curing behavior, appropriate falling time and effective bonding and compressive strengths, as an alternative well abandonment material.

1.2 Literature Review

1.2.1   Offshore well abandonment technology

When production from a well drops below an economic level, the well will be abandoned temporarily or permanently. American Petroleum Institute (API) Bulletin E3 (API, 1993) provides guidance on environmentally-sound well abandonment practices in the petroleum industry. The main objective in well abandonment is controlling fluid

movement to minimize the risk of pollution of the environment. Typical offshore well abandonment steps are described as following (Jordan and Head, 1995):

"Step 1-Blow off tailpipe and deploy tubing non-return-valve (NRV);

Step 2-Bullhead the contents of tubing below the NRV into formation using burst disc plug assembly;

Step 3-Perforate tubing above packer;

Step 4-Run 2nd NRV and set 200ft above packer;

Step 5-Launch 2nd burst disc plug and pump X-linked gel into tubing annulus (barrier/seal for bullheading contents);

Step 6-Bullhead the contents simultaneously of both the tubing and tubing annulus below the back pressure valve;

Step 7-Pump cement into both the tubing and tubing annulus;

Step 8-Squeeze of cement (Monitor Nitrogen pressure);

Step 9-Perforate all upper casing annuli and drain into nitrogen sump;

Step 10-Pump cement into all upper annuli."

Traditional offshore abandonment operations are time and money consuming. Recently some innovative equipment and technology were developed to enhance safety and lower the cost. Vaucher and Brooks (2010) introduced the inflatable packer bridge plug technology which has been successfully used for temporary or permanent well abandonment in the GOM. Compared with the conventional mechanical packers, the inflatable packers have much more expansion ability and versatility. Olstad and McCormick (2011) developed the new pulling and jacking units which have been used in offshore operations that include intervention and well abandonment to address

hurricane damaged platforms in the GOM. These operating systems are the lightweight, modular units with minimal footprint and sufficient hoisting and jacking capabilities. Both of the two operating units have demonstrated an excellent safety record and significant cost savings.

1.2.2 Plugging materials used in petroleum industry

The most conventional plugging material, cement, cannot be the solution to the problem, as described in the statement of problem above. A wide range of unconventional plugging materials is actually used or has been proposed in petroleum industry for well abandonment or zone isolation, including epoxy resins (Gunningham et al., 1992), poly-acrylates (Cowan, 1996), phenol or melamine formaldehyde (De Landro and Attong, 1996) , compressed sodium bentonite (Engleharet et al., 2001), phenolic resins (Abdul-Rahman and Chong, 1997), and room temperature vulcanizing (RTV) silicone rubbers (Bosma et al., 1998). Although effective, some of them have certain disadvantages to limit their uses in this project. Phenol formaldehyde has a strong exothermic reaction combined with shrinkage, which may affect the seal stability. Polyacrylates have doubtful long-term durability. Compressed sodium bentonite may have a bridge problem in the annulus when it is dropped through packer fluid. RTV silicone rubbers, which have to be used with cements to obtain the sufficient strength, are not suitable in our situation after the cements diluent by seawater. The selection is narrowed down to epoxy resin.

The reasons that epoxy-based resins may be the candidate material are:

1. Epoxy resins are generally not miscible with water.

2. Epoxy resins have high compressive and bonding strength after curing.

3. Epoxy resins have good resistance to most chemicals, including carbon dioxide, hydrochloric acid, and seawater components.

4. Both epoxy resin and curing agents are convenient to handle and store.

1.2.3   Epoxy resins

Epoxy resins are one of a host of plastics developed commercially after 1940s. The special properties that have made epoxy resins successful in a competitive market are their high chemical resistance, low shrinkage, excellent adhesive strength to many substrates, heat resistance, very good electrical properties (Lee and Neville, 1986). The epoxy resin is formed from two different chemicals which are referred to as the "resin" and the "curing agent" (sometimes called "hardener"). When the two chemicals are mixed together, the curing agent polymerizes the liquid resin into hard, inert plastic. The properties of the formed plastics depend on the resin type and the choice of curing agent. Liquid resin normally is diluted with a diluent which can decrease the viscosity or modify other properties of the resin.

The applications of epoxy resin in petroleum industry began from 1960s. Treadway et al. (1964) used epoxy resins to consolidate loose sand in producing formations. They injected epoxy resin into sand first followed by a fluid to establish permeability, and then injected a hardener-containing fluid to polymerize the resin. Laboratory tests showed that the loose sand which was placed in a cell and subjected to temperatures up to 200°F and to pressures up to 4,000 psi was consolidated by epoxy resin. The consolidated sand retained about 50% of its original permeability and had high compressive strength even after exposure to brine for one year. The stability of the sand-consolidation resins in hot brine was examined by Rensvold (1983). Several resin systems were tested for durability

in hot (160°F) flowing brine for up to 28 months and in as much as 30 million PV brine. The epoxy resin systems described in the paper were characterized by good strength retention and long term protection against the production of formation sand. Scanning electron microscope (SEM) micrographs of the epoxy resin system showed that the resin system retained high strength after 15 million PV brine flow. The average compressive strength was still good.

Epoxy resins were also used for water control. Gunningham et al. (1992) developed an epoxy resin system which can be used with through-tubing straddle packers to treat intervals selectively. This epoxy resin system was claimed to reduce permeability to water by 99% when used for water shut-off purpose. Rice (1991), Ng and Adisa (1997) introduced the field applications in different oil companies (Tenneco/Chevron and Mobil) using coiled tubing placement method to squeeze epoxy resin into offshore gravelpack production wells for water shut-off. Besides those applications mentioned above, epoxy resin was used as coating material for underwater and wet surface application (Dhanalakshmi et al., 1997), casing repair (Ng, 1994) and plugging wells (Bosma, 2004).

As previously described, curing properties of the epoxy resin system are determined by the type of resin and curing agent. There are two types of resins used in industry commonly, bisphenol-A/epichlorohydrin (BPA resin) and bisphenol-F/epichlorohydrin (BPF) resin, which are synthesized by reacting bisphenol-A or bisphenol-F with epichlorohydrin in presence of a basic catalyst (Lee and Neville, 1986). The BPF resin usually has greater heat and chemical resistance compared to the BPA resin, but also it is more expensive than the BPA one.

Selection of the curing agent plays the major role in determining the properties of the final cured resin system. Curing agents generally base upon amines or amides (Sen, 2000). Some of the most common amines and amides curing agents are listed in **Table 1.2**.

TABLE 1.2–COMMON ANINES AND AMIDES CURING AGENTS		
	Advantage	Disadvantage
Aliphatic Amine	good resistance to heat and chemicals	poor flexibility, reaction with moisture
Cycloalophatic Amine	good resistance to chemicals, solvents and water	short pot life
Aromatic Amine	good physical properties, high resistance to heat and chemicals.	dark color
Polyamide and Amidoamine	excellent adhesion, water resistance and flexibility	low resistance to chemicals, solvents and acids

Besides the resin and the curing agent, the epoxy resin system usually also contains a reactive diluent which is added to decrease the viscosity of the system or to increase load capacity for the fillers (Ng, 1994). The filler can serve to increase the specific gravity of the epoxy resin system or to extend the volume to decrease the cost for some purposes.

Epoxy resins have been used widely in the petroleum industry. When used as plugging material, the epoxy resin systems are usually transported to the suitable position by through-tubing, dump bailer, work string or coiled-tubing methods. The problem addressed in this study is wellbores cannot be accessed by wireline, work string or coiled tubing due to tubing damage at or above mudline. In such cases, accessing the

wellbore may be only through an intervention well, and plugging material may only be placed by bullheading where there is ample opportunity to contact wellbore fluids.

1.3 Objective

The project funded by BORMRE includes several research points, including the curing properties of the epoxy resin, the falling behavior when the resin system drops through wellbore fluids, the effect of weighting material, and the mechanical strength of the cured resin system. In this thesis, we focus on the curing properties of epoxy resin systems. The objective is to determine the optimum epoxy resin system with a suitable curing time which allows the system fall down through wellbore fluids up to 7,000ft and cure properly.

2   EXPERIMENTAL MATERIALS AND PROCEDURES

2.1 Chemical materials

2.1.1   Epoxy resins and curing agents

After literature review and consulting with industrial professional, Dr. Hubert Monteiro, we chose two epoxy resins, BPA resin and BPF resin, and two curing agents to test. All the resins, curing agents, and reactive diluents were provided by Royce International Company. The four systems tested in our project are list in **Table 2.1** and the pictures of the four systems are taken when they are just prepared (**Fig. 2.1**).

TABLE 2.1– FOUR EPOXY RESIN SYSTEMS TESTED IN THIS PROJECT				
	BPA SYSTEM 1	BPA SYSTEM 2	BPF SYSTEM 1	BPF SYTEM 2
EPOXY RESIN	RAR 901	RAR 901	RAR 9281	RAR 9281
CURING AGENT	RAC 9907	RAC 9913	RAC 9907	RAC 9913
DILUENT			RAD 100	RAD 100
	EPOXY:CA*	EPOXY:CA	EPOXY:CA:DILUENT	EPOXY:CA:DILUENT
MIX RATIO	100:35	100:29	100:15:43.5	100:15:36

*:CA=Curing Agent

Two BPA systems are the epoxy resin RAR 901, which is a BPA resin with an epoxide equivalent weight of 180-196 diluted by o-cresyl glycidyl ether (CGE), cured by two different curing agents RAC 9907 and RAC 9913. The BPF systems are the epoxy resin RAR 9281, which is a BPF resin with an epoxide equivalent weight of 165-175, cured by RAC 9907 and RAC 9913. Among the two curing agents, the RAC 9907 is one of the aromatic amine curing agents and the RAC 9913 is one aromatic/cycloalophatic

amine based curing agent. RAD 100 is the o-CGE diluent with the epoxide equivalent weight of 165-185. The basic physical properties of the components of the system could be got from **Table 2.2.**
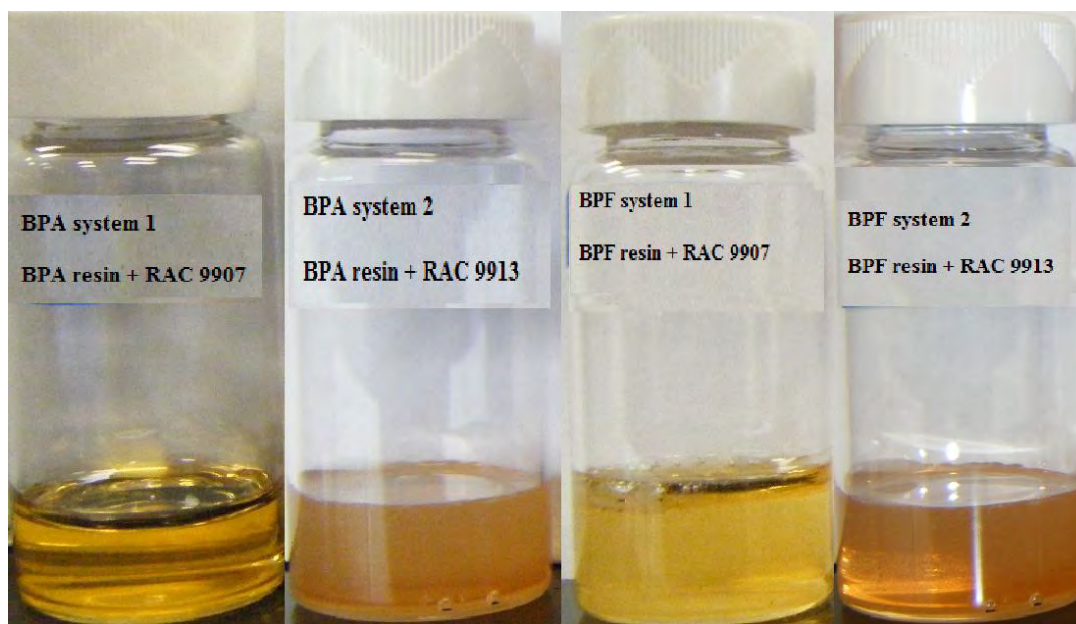
Fig. 2.1—The four epoxy resin systems tested in this project.

TABLE 2.2– PHYSICAL PROPERTIES OF THE COMPONENTS OF THE RESIN SYSTEMS					
	RAR 901	RAR 9281	RAC 9907	RAC 9913	RAD 100
APPEARANCE	Liquid	Liquid	Liquid	Liquid	Liquid
COLOR	Colorless	Pale yellow	Yellow-orange	Yellow-orange	Colorless
TYPE OF ODOR	Faint to slight epoxy odor	Barely perceptible aromatic odor	Perceptible odor	Slight amine odor	Slight characteristic odor
SPECIFIC GRAVITY	1.16	1.20	~1.0	~ 1.0	1.08
VISCOSITY @ 25 °C, cp	450-650	2000-5000	1000-5000	200-300	5-10

2.1.2   Weighting material

There are many weighting materials used in resin industry, such like barite, chalk power and hematite. Considering the price and high density, barite becomes the first choice. We obtained the 4-10 micron barite powder from the drilling lab in the Department of Petroleum Engineering of Texas A&M University. **Table 2.3** shows the physical properties of the barite powder used in this project and **Fig. 2.2** is the picture of the barite powder.

TABLE 2.3 – PHYSICAL PROPERTIES OF THE BARITE	
APPEARANCE	Powder, dust.
COLOR	Tan. To Grey.
ODOR	Odorless or no characteristic odor.
SOLUBILITY DESCRIPTION	Insoluble in water.
SPECIFIC GRAVITY	4.22
DENSITY, PPG	35.21

Fig. 2.2—Barite powder used in this project.

2.2 Experimental conditions

2.2.1 Curing environment

The epoxy resin systems should cure in the tubing and tubing annuli after falling to bottom if they are to be successfully used as the plugging material. We determined model wellbore conditions by investigating the properties of the GOM. Since the likely packer and wellbore fluid are seawater, the properties of the bottom water of the GOM are necessary. **Table 2.4** shows the geochemical compositions of bottom brine in the GOM (Joye, 2005).

TABLE 2.4– GEOCHEMICAL COMPOSITIONS OF BOTTOM BRINE IN THE GOM (AFTER JOYE, 2005.)										
Site ID	Salinity	$[Cl^-]$	$[Na^+]$	$[K^+]$	$[Ca^{2+}]$	$[Mg^{2+}]$	$[SO_4^{2-}]$	$[H_2S]$	$[Fe^{2+}]$	$[NH_4^+]$
Bottom water [b]	34	564	462	43	11	11	29	~0	~0	0.1
Unit: mMol/L										

According to **Table 2.4**, we can calculate the types and amounts of the chemicals used to synthetize seawater. For preparation 500 ml synthetic seawater, the amounts of the chemicals are listed in **Table 2.5.**

TABLE 2.5–COMPONENTS OF SYNTHETIC SEAWATER IN THE PROJECT					
Chemicals	Na_2SO_4	NaCl	KCl	$CaCl_2 \cdot 2H_2O$	$MgCl_2 \cdot 6H_2O$
Concentration, mM	29	404	43	11	11
Molecular Weight	142.04	58.44	74.55	147.01	203.3
Mass Concentration, g/L	4.119	23.61	3.206	1.617	2.236
Amount, g (for 500ml)	2.06	11.81	1.60	0.81	1.12

From **Fig. 2.3**, we can see the temperature/depth plots of the sands below mudline in different fields in the GOM.

(a) West Delta 86 (WD086) Field   (b) Brazos 133A (BA133A) Field
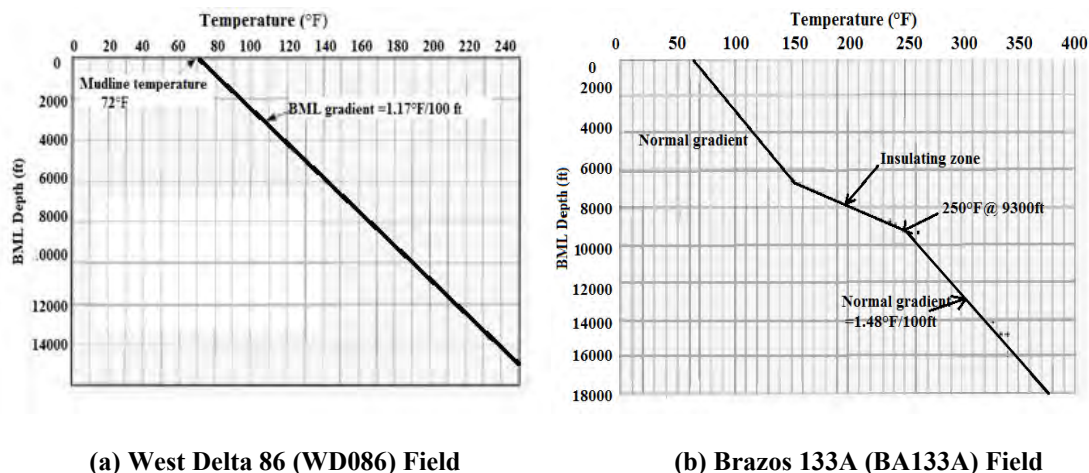
Fig. 2.3—Average temperature/depth plot of sands in two different fields in the GOM, the temperature range at the positions the plugging material placed is from 60°F to 200°F. (After Joye).

The temperature range from mud line to below mudline 8,000 ft is from 60°F to 200°F. Since casing extends from mudline and the packers and completed intervention located in different depths (from mudline to below mudline 8,000 ft), the curing properties of the epoxy resin systems should be tested in the environment with temperature range from 60°F to at least 200°F.

From discussion above, the curing environment condition in the wellbore in the GOM is seawater environment with temperature from 60°F to at least 200°F. To compare with this condition, we also tested the curing properties in air and fresh water environment with same temperatures.

2.2.2 The components of the resin system with/without barite

In this project, we tested curing properties of the resin systems with or without barite to evaluate the weighting material effect. We added different amounts of barite to

get the epoxy resin system with different densities. **Table 2.6** and **Table 2.7** show the components of the BPA and BPF systems with different densities. In our experiments, we added barite to weight the system up to 16.8 ppg.

TABLE 2.6–COMPONENTS OF BPA SYSTEM WITH DIFFERENT DENSITIES				
RAR 901, g	RAC 9907, g	Barite, g	Specific Gravity (water=1)	Density, ppg
4.7	1.6	0	1.108	9.25
4.7	1.6	1.34	1.257	10.49
4.7	1.6	2.80	1.407	11.74
4.7	1.6	5.31	1.578	13.17
4.7	1.6	8.52	1.795	14.98
4.7	1.6	13.51	2.012	16.79

TABLE 2.7– COMPONENTS OF BPF SYSTEM WITH DIFFERENT DENSITIES					
RAR 9281, g	RAC 9907, g	RAD 100, g	Barite, g	Specific Gravity (water=1)	Density, ppg
4.0	1.0	1.73	0	1.096	9.15
4.0	1.0	1.73	1.41	1.257	10.49
4.0	1.0	1.73	2.87	1.407	11.74
4.0	1.0	1.73	4.73	1.578	13.17
4.0	1.0	1.73	7.47	1.795	14.98
4.0	1.0	1.73	10.75	2.012	16.79

2.2.3   The curing time we prefer

According to the previous tests, conducted by Dr. Schubert's group in Petroleum Engineering department of TAMU (EL-Mallawany, 2010), which are about the falling behavior of the epoxy resin systems in the water-filled pipe, the epoxy resin system spreads throughout the water column and then recollects at the bottom of the pipe. **Fig. 2.4** shows the falling resin system in the pipe filled with water. The average falling velocities of the resin systems in a water environment are shown in the **Table 2.8**. From this table, we can read that the average falling velocity of the resin systems in the water environment is about 45 ft/min at the first 25ft. Assuming the resin system falling at this velocity, the falling time for the system falling 7,000ft should less than 3 hours. During the falling process, the temperature of the packer fluid is changed from 40°F at the mudline to around 200°F at the bottom. It means the average pot life of the epoxy resin systems under the changed-temperature conditions should be longer than 3 hours. The pot life mentioned here is the length of time that a catalyzed resin system retains a viscosity low enough to be used in processing. The pot life is an important data which shows the time allowed for the epoxy resin system to fall down through the casing and coalesce into a single mass. At the bottom of the casing annulus, the epoxy resin system also needs about 1-hour time to settle and cure. The discussion above gives us criterion as following to determine the suitable systems:

1. From temperature 40°F to 200°F, the average pot life should be more than 3 hours.

2. At temperature 200°F, the pot life should be at least 1 hour.

Fig. 2.4—The epoxy resin system spreads in the water column during falling down.

TABLE 2.8–AVERAGE VELOCITIES OF EPOXY RESIN SYSTEMS WITH DIFFERENT DENSITIES IN ANNULUS WITH DIFFERENT SIZES		
DENSITIES OF THE SYSTEMS, ppg	ANNULUS SIZES (OD- ID), in	AVERAGE VELOCITIES, ft/min
11.7	6" - 0"	38.44
13.2	6" - 0"	41.00
14.7	6" - 0"	51.25
11.7	6"-1.9"	37.85
13.2	6"-1.9"	42.41
14.7	6"-1.9"	60.00
11.7	6" - 3.5"	36.72
13.2	6" - 3.5"	43.93
14.7	6" - 3.5"	51.25

2.3 Experimental procedures

2.3.1 Seawater preparation

1. Prepare a 500 ml measuring flask and a glass beaker. Make sure the flask and beaker are clean and dry.

2. Measure and add the specific amount of the chemicals listed in **Table 2.5** into the beaker.

3. Add about 100 ml purified water into the beaker and shake the beaker gently until the chemicals dissolved.

4. Pour the water from the beaker into the flask.

5. Add small amount of purified water into the beaker and shake gently, then pour the water into the flask.

6. Repeat step 5 several times.

7. Add purified water into the measuring flask until the liquid is 500 ml. Shake the flash gently to make sure the chemical dissolved evenly.

2.3.2 Resin systems preparation

1. Prepare several beakers and make sure the bakers are clean.

2. Add the epoxy resin into the beakers.

3. Add the reactive diluent if needed into the beakers.

4. Add the barite if the system needed weighting into the beakers.

5. Add the curing agents into the beakers.

6. Stir all the components hardly until the components mixed evenly.

2.3.3 Curing time tests

1. Prepare several clean 20-ml vials.

2. Use pipets to put about 10 ml purified water or seawater prepared in section 2.3.1 if the test curing environment are fresh water or seawater environments.

3. Decide the test temperature and pre-heat the oven to the test temperature.

4. Put the vials prepared in step 2 into the oven to be pre-heated about 10 minutes.

5. Get the vials out of the oven and put the epoxy resin samples prepared in section 2.3.2 into the vials (**Fig. 2.5**). Then put the vials back to oven and record the time.
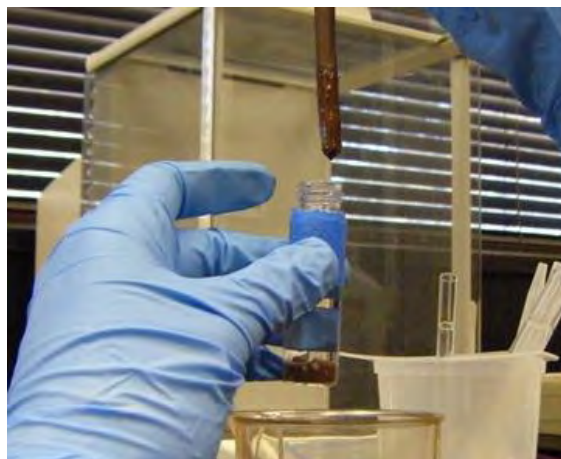
Fig. 2.5 —Use pipet to put the resin sample into the vials.

6. Check the samples every 15 minutes until the epoxy resin system cured completely. Record the pot life and curing time of the system at the set temperature.

2.3.4   Viscosity tests

We used the Brookfield DV-III Ultra Programmable Rheometer (the cone/plate version) to determine the viscosities of these epoxy resins at varying of temperatures. To

protect the viscometer, we only tested the samples without barite because the barite may scratch the spindle. There are two types of the viscosity tests conducted in this project.

A. Test the viscosity changes with increasing temperature:

1. Assemble and level the rheometer.

2. Autozero the rheometer.

3. Select the suitable spindle and enter the spindle number to the rheometer.

4. Attach the spindle to the coupling nut.

5. Use pipet to put sample into the cup and attach the cup to the rheometer. Set the gap between the spindle and cup carefully.

6. Set the temperature the thermostatic water bath system as 30°C and wait for the temperature stable.

7. Measure the viscosity at the speed of rotation of 5, 10, 20, 30, 50, 100, 250RPM.

8. Record the viscosities and the % torque.

9. Increasing the 10°C temperature every time and repeat step7 and 8 until the temperature reach 100°C.

B. Test the viscosity changes with time at the specific temperature:

1. Open the temperature the thermostatic water bath system and set the temperature as the specific test temperature (in our project, the temperature is 96.5°C). Wait for the temperature stable.

2. Autozero the rheometer.

3. Select the suitable spindle and enter the spindle number to the rheometer.

4. Attach the spindle to the coupling nut.

5. Use pipet to put sample into the cup and attach the cup to the rheometer. Set the gap between the spindle and cup carefully.

6. Measure the viscosity at the speed of rotation of 250RPM. Record the time, the viscosity and the % torque.

7. Wait for 5 minutes, repeat step 6 until the viscosity exceed 1000 cp.

8. Get the test sample out of the testing can immediately and use rubbing alcohol to clean the testing can and spindle quickly to avoid the samples cured in the testing can.

3   RESULTS AND DISCUSSIONS

3.1 The viscosity of the Resin Systems

We measured the viscosities of both the BPA resin system and BPF resin system following the procedure described in section 2.3.4. We did those tests just after we mixed the resin and the curing agent together. **Fig. 3.1** shows the viscosity of the BPA system 1 (BPA resin with curing agent RAC 9907) at temperature from 25°C to 97°C. We can see that the viscosity of the resin systems decreases dramatically with increasing temperature.   The viscosities of the other three epoxy resin systems and all the components of those four resin systems have similar behavior.
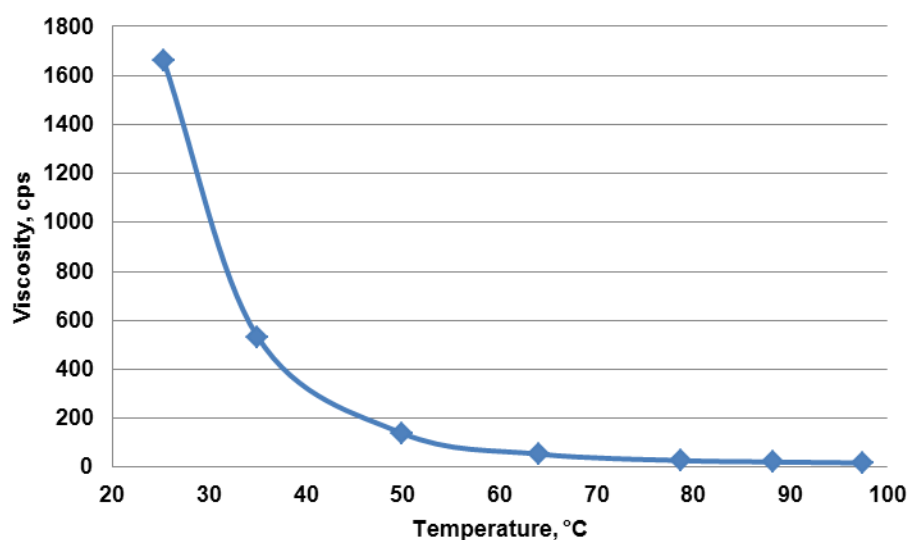
Fig. 3.1—Viscosity of the BPA resin system 1 decreases with increasing temperature.

We also tested the viscosity of the resin system changes with time at 96.5°C. At a specific temperature, after the resin mixed with the curing agent, the viscosity of the

mixture becomes larger and larger with increasing time. We tested the viscosity of the BPA system 1 after the two components mixed together at 96.5°C. **Fig. 3.2** shows the change of the viscosity during the curing process. We stopped the test when the viscosity is more than 1,000 cps because we did not want the epoxy resin cured in the chamber of the viscometer. It is difficult to clean the resins at the end of the curing process.
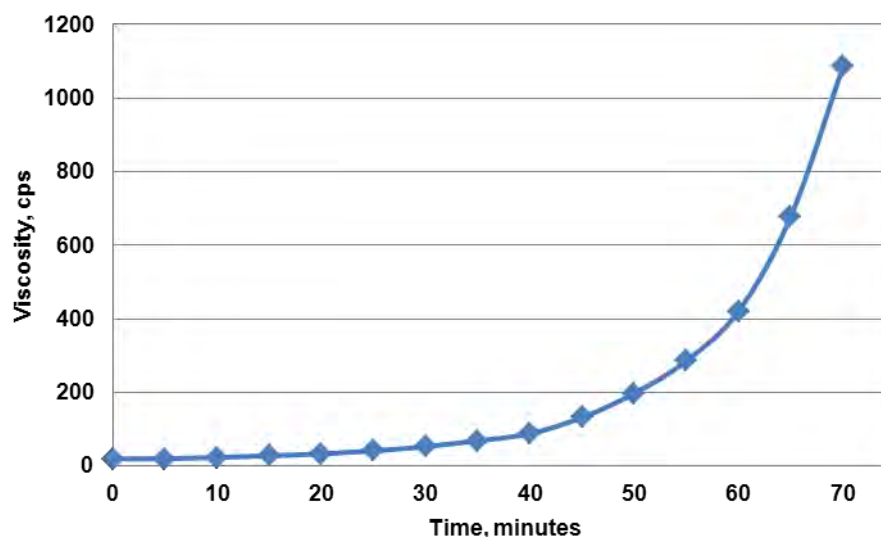
Fig. 3.2—The viscosity change of the BPA system a during the curing process at 96.5°C.

3.2 The curing environments effect

3.2.1 Curing time and pot life are temperature sensitive

We tested the pot life and curing time of the four epoxy resin systems at different temperatures in different curing environments included atmosphere, purified water, and synthesized seawater environment. The results are listed in APPENDIX A.
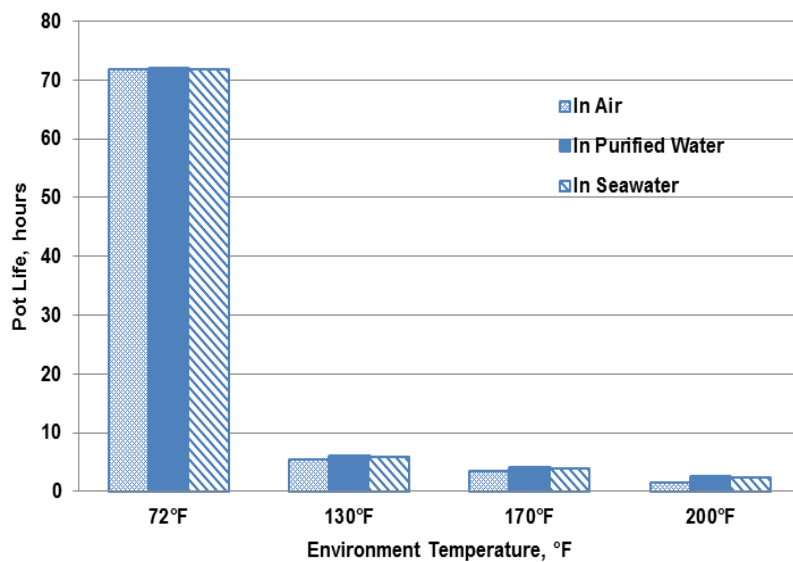
Fig. 3.3—The pot life of the BPA resin cured by RAC 9907 becomes shorter with increasing temperature.
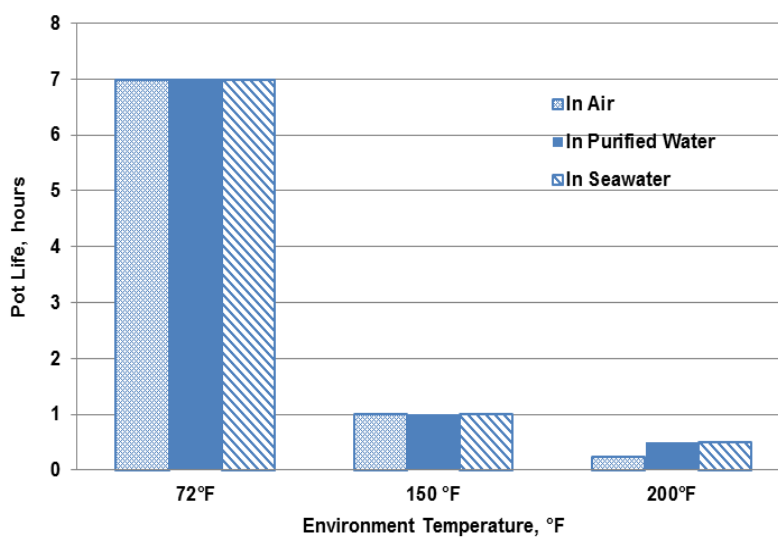
Fig. 3.4—The pot life of the BPA resin cured by RAC 9913 decreases when the temperature increases.

The curing process becomes faster when the system is heated. So the pot life of the system is much shorter when the temperature is higher no matter what kind of curing environment and what kind of curing agent. We could see the tendency clearly from **Fig. 3.3** and **Fig. 3.4**, the pot life of the two BPA systems become shorter when the temperature increases in three different curing environments. The BPF systems also have the same tendency.

3.2.2 The curing time and pot life are determined by the curing agents mainly.

We compared the curing time and pot life of the different epoxy resins cured by the same curing agent at the same condition. The different epoxy resins cured by the same curing agent have similar pot life and curing time. We can get this conclusion clearly from **Fig. 3.5** and **Fig. 3.6**.
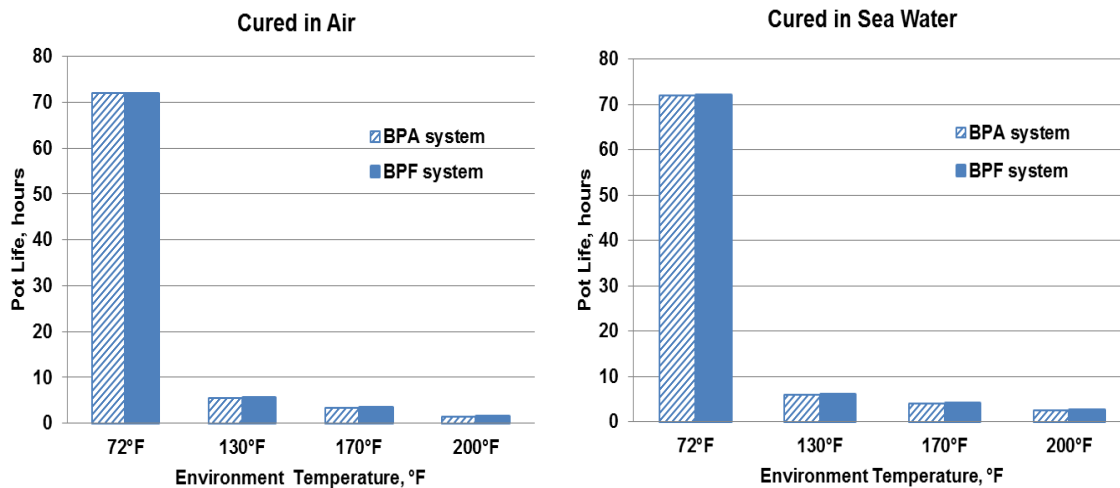
Fig. 3.5—The BPA resin and BPF resin cured by the same curing agent RAC 9907 have the same pot life in various cured conditions.
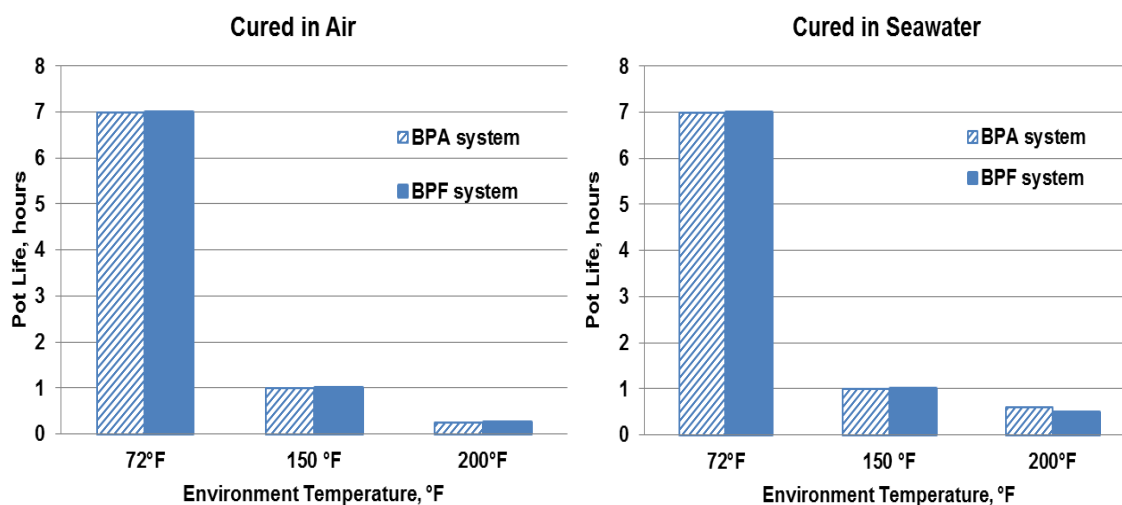
Fig. 3.6—The BPA resin and BPF resin cured by the same curing agent RAC 9913, have similar pot life in various cured conditions.

In **Fig. 3.5,** the BPA System 1 and BPF System 1, which contain the same curing agent RAC 9907, have the exactly same pot life in both air and seawater environment in different temperatures. In **Fig. 3.6**, BPA and BPF system 2, which also contain the same curing agent RAC 9913, have almost same pot life except when cured in seawater at high temperature. From the figures we could get the conclusion that the curing time and pot life were decided by the choice of curing agent mainly. Different epoxy resins cured by the same curing agent have the similar pot life and curing time.

Since the pot life and curing time are determined by the curing agent, we compared the two curing agents we tested to determine the more suitable one. From the **Fig. 3.7**, the systems cured by RAC 9913 have only a few-minute pot life time at high temperature, which is not long enough to meet our requirement which is discussed in section **2.3.3**. Our requirements include at least 3-hours pot life under the environment with temperature changed from 40°F to 200°F and 1-hour settling time under the

reservoir condition. The systems cured by RAC 9907 have a suitable pot life which allows the systems to fall down, coalesce and cure at the bottom of the casing. In the following tests, we would choose RAC 9907 as the curing agent and give up RAC 9913. In the following discussion, we use "BPA system" and "BPF system" instead of the original "BPA system 1" and "BPF system 1" because we would not discuss the "BPA system 2" and "BPF system 2".
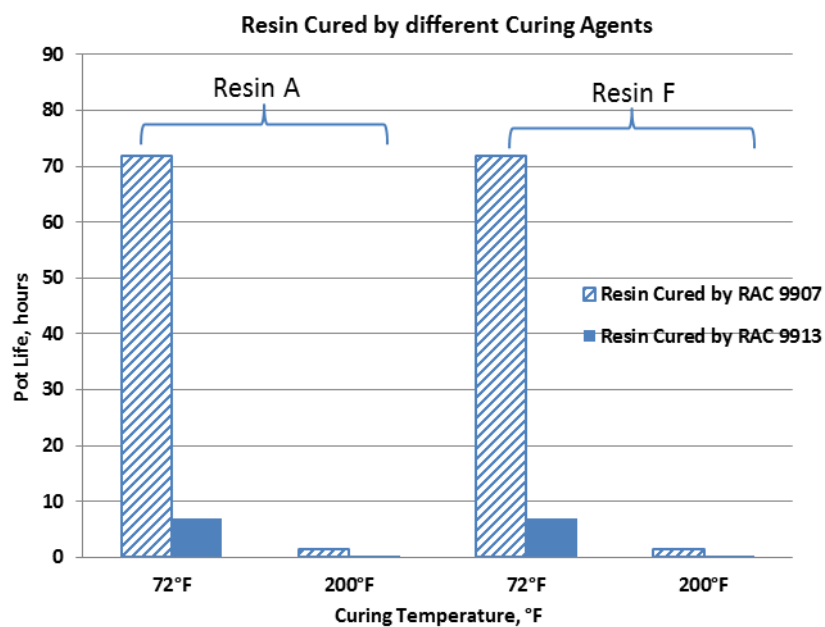
Fig. 3.7—The comparison of the two curing agents, RAC 9913 has too short time to make the system falling and curing.

3.2.3   The curing environment have effects at high temperature

We would like to discuss the effect of the curing environments. For BPA system, we could see from the **Fig. 3.3** at low temperature the system cured in different environments have same pot life. And at high temperature, we could see more clearly from **Fig. 3.8**, the systems cured in the purified water and seawater environments have

same pot life which is longer than the system cured in air environment. The difference is higher when the temperature is higher. The most difference of the pot life between the system cured in air and in water environment is at the highest temperature 200°F, which is about 1 hour difference. Compared with temperature, the curing environment has less effect on the pot life and curing time. **Fig. 3.9** shows the pot life of BPF system in different curing environments. The results are similar with the BPA's. The pot lives are same at room temperature and have 0.5 hours difference at elevated temperatures between the systems cured in the air environment and the underwater environments.
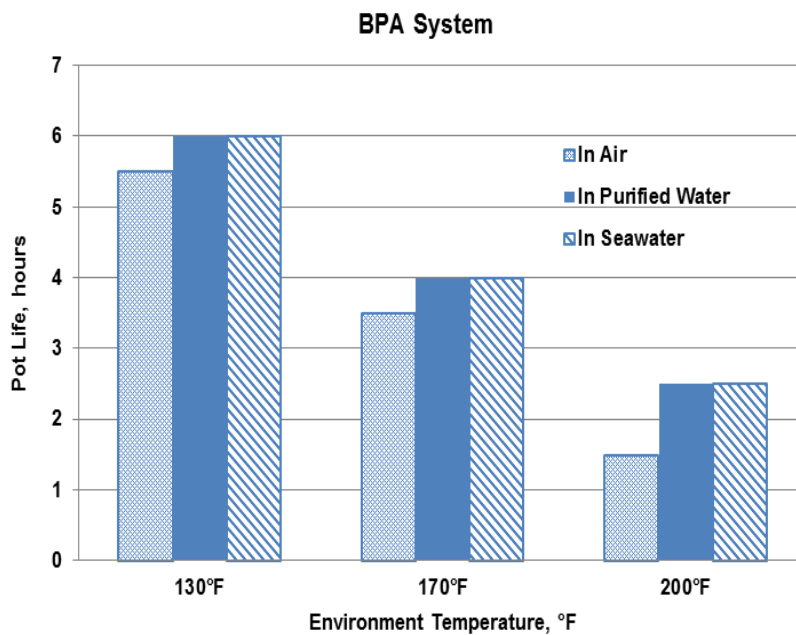
Fig. 3.8—BPA system has longer pot life in water environments compared with cured in air at elevated temperatures.
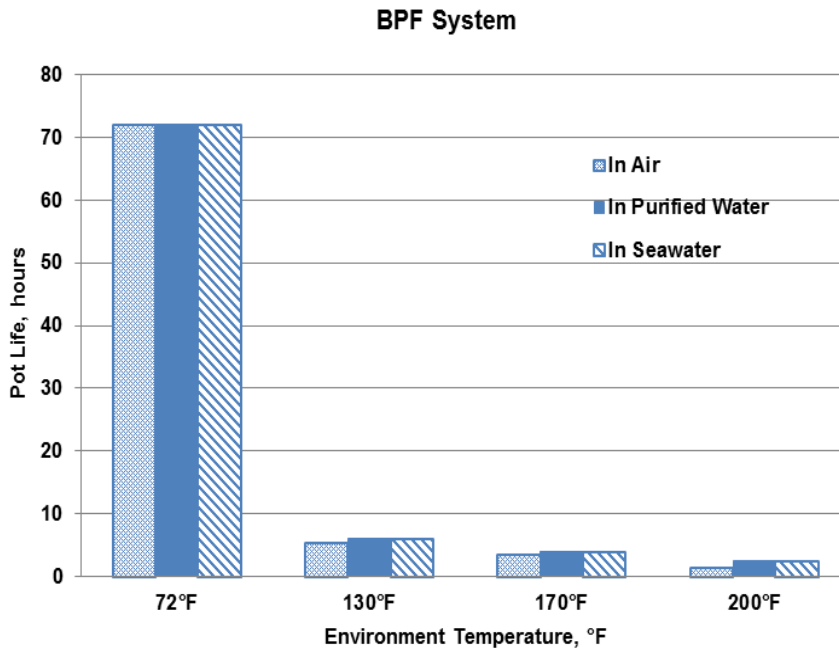
Fig. 3.9—BPF systems cured in different environments have same pot life at low temperature, and have longer pot life in water environments at high temperature.

3.3 The weighting material effect

We already knew the effect of the temperature and the curing environments. In this section, we would discuss the effect of the weighting material barite. The weighting material will increase the falling velocity of the resin system due to the increasing density. In this thesis, we only discuss the effect of weighting material on the curing properties of the systems cured in seawater environment. The pot life and curing time of the epoxy resin systems with barite cured in seawater environment are listed in APPENDIX B.

3.3.1 Weighting material shorten the pot life and curing time

First, we would discuss the effect of the weighting material on the curing time of the epoxy resin system. We could get the effect of the weighting material from the **Fig. 3.10** and **Fig. 3.11**.
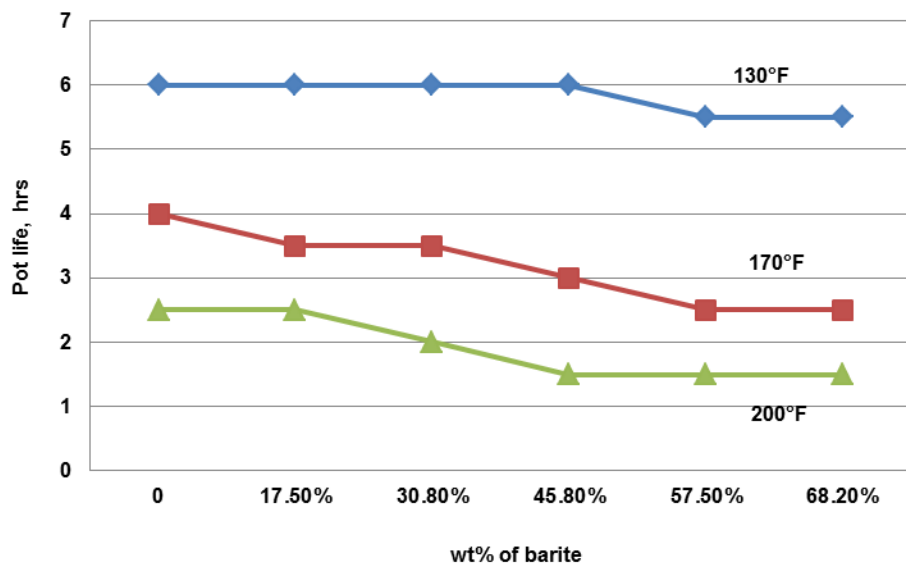
Fig. 3.10—The pot life of the BPA system decreases when the amount of the adding barite increases.
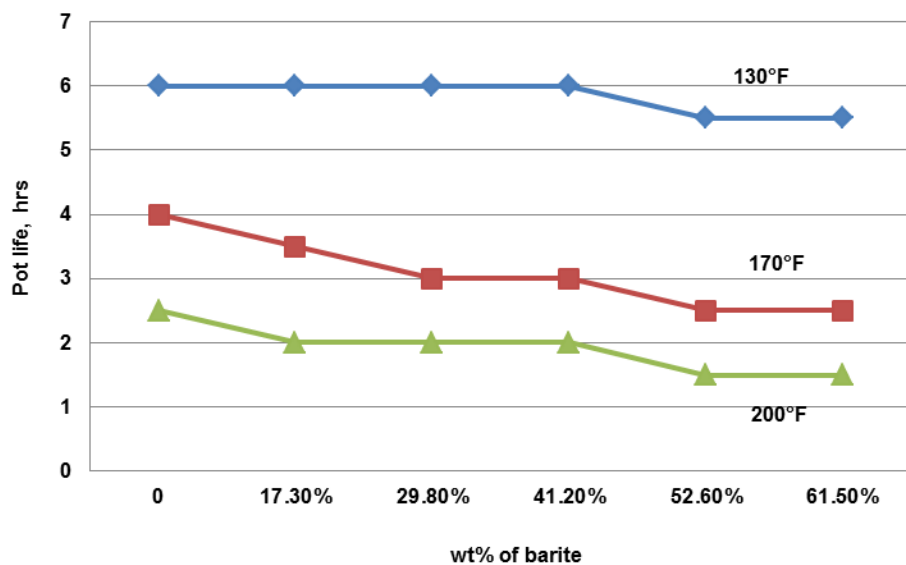
Fig. 3.11—The pot life of the BPF system decreases when the amount of the adding barite increases.

The pot lives of both BPA and BPF systems decrease with increasing amount of the barite when the curing temperature and the curing environment are same. The pot life of the system with barite is about 0.5 hour shorter than the one without any filler at temperature 130°F and below, and more than 1 hour shorter at temperature above 170°F. At temperature 200°F, the pot life of the densest system is 1.5 hours. Although it is shorter than the pure system, from **Table 2.8** the falling time of the denser system is also shorter. Thus, the pot life is still enough to meet our requirements.

Now, we would compare the pot life of BPA and BPF systems with barite. At low temperature, 130°F, the pot lives of those two systems are exactly same. At higher temperatures, 170°F and 200°F, the pot lives have a little difference, which we can see clearly from **Fig. 3.12**. We will discuss other curing properties to decide the better system to meet our requirements.
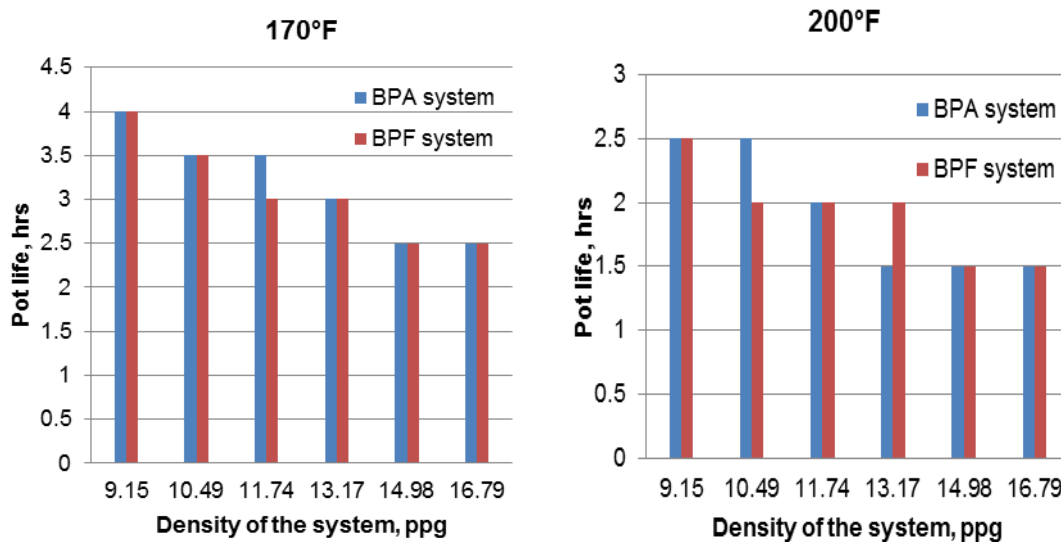
Fig. 3.12—The BPA and BPF systems with barite have a little different pot life at higher temperatures.

3.3.2 Curing properties of the system with barite

The curing time of the BPA system and BPF system with fillers are almost the same. We need to consider other curing properties of those two systems to determine the most suitable one. Now we would like to discuss what happened to those two systems after they are added some barite during the curing process.

From **Fig. 3.13** and **Fig. 3.14**, the barite is distributed evenly in both the BPA and BPF system when they just mixed and stirred into those samples. After the epoxy resin systems are fully cured, the situations are different. The barite came out from the BPA and stay between the cured epoxy resin and the container, which prevents strong bonding between the resin and the bottle. We could easily separate the cured BPA system from the bottle because the bonding is weak meanwhile the bonding between the BPF system and the bottle is much stronger.
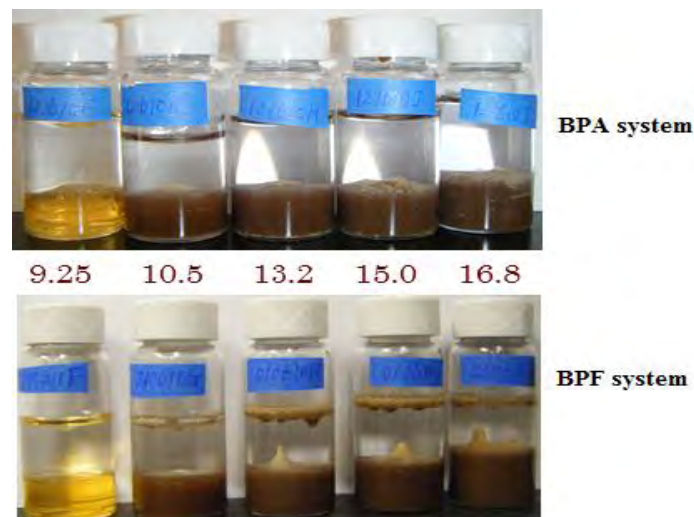
Fig. 3.13—The samples of BPA and BPF systems with barite are just prepared, the barite is evenly distributed in the epoxy resin systems.
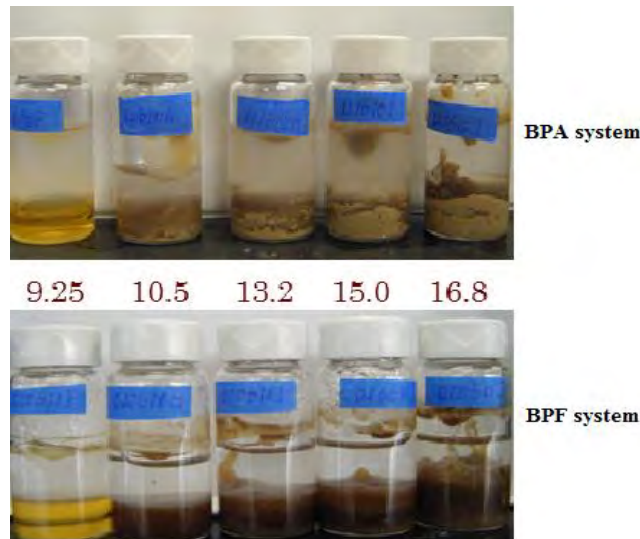
Fig. 3.14—The samples are fully cured. During the curing process, the barite is separated out from BPA system and is still distributed in the BPF system.

From **Fig. 3.13** and **Fig. 3.14**, the barite is distributed evenly in both the BPA and BPF system when they just mixed and stirred into those samples. After the epoxy resin systems are fully cured, the situations are different. The barite came out from the BPA and stay between the cured epoxy resin and the container, which prevents strong bonding between the resin and the bottle. We could easily separate the cured BPA system from the bottle because the bonding is weak meanwhile the bonding between the BPF system and the bottle is much stronger.

Comparison of the barite effects on both BPA and BPF systems, the BPA system could add less than 10%wt of barite and the BPF system could add as much as 60%wt barite.

3.4 Discussions

Through **Table 2.8**, we get the average falling velocities for the epoxy resin systems with different densities. During the falling tests, they only tested three resin systems with density 11.7 ppg, 13.2 ppg and 14.7 ppg respectively. The average falling velocities for these three systems are 37.7 ft/min, 42.4 ft/min and 54.2 ft/min respectively. We assume these three systems falling through the casing annulus and tubing up to 7,000ft with the corresponding falling velocity constantly. For the BPF system with density 14.7 ppg cured in synthetic seawater, the tendency of the pot life changed with temperature is shown in **Fig. 3.15**.

Density of the system 14.7 ppg
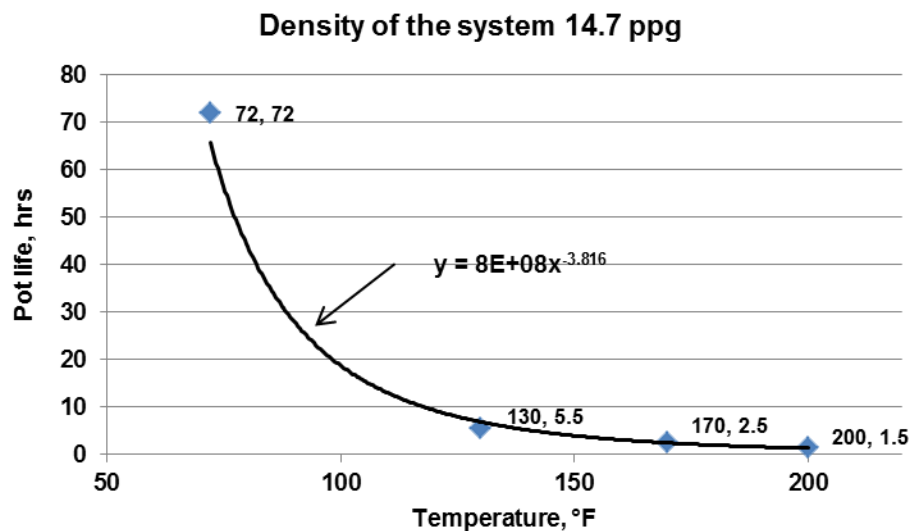
$y = 8E+08x^{-3.816}$

Fig. 3.15—The trendline of the pot life change with temperature for the BPF system with density 14.7 ppg could be described as $y = 8E+08x^{-3.816}$.

Now we discuss about the curing process during the falling. The environment temperature changes during the falling process. We divide the 7,000ft falling distance to 14 even parts while each part has 500ft falling distance. We assume the temperature in

each part is constant, which is the average temperature in this part according to **Fig. 2.3**.
Also we assume the epoxy resin system instantly reaches the environment temperature
present at the given part and we could get the pot life of the system at the given
temperature from the trendline in **Fig. 3.15**. For the BPF system whose density is 14.7
ppg, the falling velocity is 54.2 ft/min, which means the falling time of the system in
each 500ft part is 9.23 minutes, 0.154 hours. We could get fraction of the pot life by
comparing the falling time, 0.154 hours, with the pot life at each 500ft part. We can see
the results clearly from **Table 3.1**. If we assume the epoxy resin system falling through
the casing annulus from depth 500ft to 7,500ft below mudline, the accumulated fraction
of pot life 0.302. It means there is about 70% pot life left when the epoxy resin system
reached the bottom to let the system coalesce. Even the resin system falling from 1,500ft
below mudline to 8,500ft, the fraction of the accumulated pot life is less than 0.50. We
can use the same method to calculate the other two systems whose densities are 11.7 ppg
and 13.2 ppg. We assume they fall from depth 500ft below mudline to 7,500ft. The
results are listed in **Table 3.2**. The weighting material could shorten the pot life of the
epoxy resin system, but it also could shorten the falling time. From **Table 3.2**, the denser
system has less fraction of pot life. It means the overall effect of adding weighting
material is favorable.

TABLE 3.1–FRACTION OF POT LIFE AT EACH 500FT FALLING DISTANCE					
Depth BML, ft	Falling velocity, ft/min	Falling time, hrs	Average temperature, °F	Pot life at given temperature, hrs	Fraction of pot life
0-500	54.2	0.154	77	50.61	0.0030
500-1000	54.2	0.154	81	41.72	0.0037

1000-1500	54.2	0.154	87	31.76	0.0048
1500-2000	54.2	0.154	93	24.62	0.0062
2000-2500	54.2	0.154	99	19.40	0.0079
2500-3000	54.2	0.154	105	15.50	0.0099
3000-3500	54.2	0.154	111	12.54	0.012
3500-4000	54.2	0.154	117	10.25	0.015
4000-4500	54.2	0.154	123	8.47	0.018
4500-5000	54.2	0.154	129	7.06	0.022
5000-5500	54.2	0.154	135	5.94	0.026
5500-6000	54.2	0.154	141	5.03	0.031
6000-6500	54.2	0.154	147	4.29	0.036
6500-7000	54.2	0.154	158	3.26	0.047
7000-7500	54.2	0.154	170	2.46	0.062
7500-8000	54.2	0.154	182	1.90	0.081
8000-8500	54.2	0.154	192	1.55	0.099

TABLE 3.2–THE ACCUMULATED FRACTION OF POT LIFE FOR EACH SYSTEM FALLING FROM 500FT TO 7,500FT BELOW MUDLINE			
System Density, ppg	11.7	13.2	14.7
Accumulated fraction of pot life	0.360	0.357	0.302

4   CONCLUSIONS

The curing properties of the four epoxy resin systems were tested. From all the results and discussions, we draw conclusions as follow:

1. Curing properties of epoxy resin systems are consistent with needs for abandoning wells destroyed by hurricanes.

2. The BPF system which contains the RAR 9281 BPF resin, the RAC 9907 curing agent, and RAD 100 reactive diluent is the optimal system we tested in this project. This system has suitable pot life and curing time and large barite capacity which could weigh the system as much as 16.8 ppg.

3. BPF resin system has superior properties compared with BPA resin system. The BPA system which contains the RAR 901 and the RAC 9907 curing agent has suitable pot life, but the small filler capacity means this system could only be weighed to 10.5 ppg. Considering the lower price compared with BPF system, this BPA system may be used in the cases that require low density.

4. Laboratory verification of shear bond strength properties should lead to field test in test wells.

REFERENCES

1. Abdul-Rahman, R. and Chong, A. 1997. Cementing Multilateral Well with Latex Cement. Paper presented at the SPE/IADC Drilling Conference, Amsterdam, Netherlands. SPE 37623-MS.

2. API, ed. 1993. Environmental Guidance Document: Well Abandonment and Inactive Well Practices for U.S. Exploration and Production Operations.

3. BOEMRE. 2006. Mms Project 549 Final Report-Assessment of Fixed Offshore Platform Performance in Hurricanes Andrew, Lili and Ivan. .

4. BOEMRE. 2007. Mms Project 578 Final Report-Assessment of Fixed Offshore Platform Performance in Hurricanes Katrina and Rita.

5. BOEMRE. 2008. Mms Completes Assessment of Destroyed and Damaged Facilities from Hurricanes Gustav and Ike.

6. BOEMRE. 2010. Mms Project 642 Final Report-Assessment of Damage and Failure Mechanisms for Offshore Structures and Pipelines in Hurricanes Gustav and Ike.

7. Bosma, M.G.R., Cornelissen, E.K., Reijrink, P.M.T. et al. 1998. Development of a Novel Silicone Rubber/Cement Plugging Agent for Cost Effective Thru' Tubing Well Abandonment. Paper presented at the IADC/SPE Drilling Conference, Dallas, Texas. 14. IADC/SPE 39346-MS.

8. Bosma, M.G.R.C., Erik Kerst ; Schwing, Alexander 2004. Method for Plugging a Well with a Resin. United States: Shell Oil Company (Houston, TX).

9. Cowan, K.M. 1996. Remedial Wellbore Sealing with Unsaturated Monomer System. United States: Shell Oil Company (Houston, TX).

10. De Landro, W.V.C. and Attong, D. 1996. Case History: Water Shut-Off Using Plastic Resin in a High Rate Gravel Pack Well. Paper presented at the SPE Latin America/Caribbean Petroleum Engineering Conference, Port-of-Spain, Trinidad. SPE 36125-MS.

11. Dhanalakshmi, M., Maruthan, K., Jayakrishnan, P. et al. 1997. Coatings for Underwater and Wet Surface Application. Anti-Corrosion Methods and Materials 44 (6): 393-398.

12. EL-Mallawany, I. 2010. An Experimental Setup to Study the Fall Rate of Epoxy Based Fluids. MASTER OF SCIENCE, Texas A&M University.

13. Engleharet, J., Wilson, M.J., and Woody, F. 2001. New Abandonment Technology New Materials and Placement Techniques. Paper presented at the SPE/EPA/DOE Exploration and Production Environmental Conference, San Antonio, Texas. SPE 66496.

14. Gunningham, M.C., van Paassen, A.S.W., and Samuel, A.J. 1992. Through-Tubing Remedial Treatments Using a Novel Epoxy Resin System. Paper presented at the European Petroleum Conference, Cannes, France. SPE 24986-MS.

15. Jordan, R. and Head, P. 1995. Cost Effective Well Abandonment. Paper presented at the Offshore Europe, Aberdeen, United Kingdom. 30349. DOI: 10.2118/30349-ms.

16. Joye, S.B. 2005. Geophysical and Geochemical Signatures of Gulf of Mexico Seafloor Brines. Biogeosciences 2 (3): 295-309.

17. Lee, H. and Neville, K. 1986. Handbook of Epoxy Resins. Trans Neville, K. A Mcgraw-Hill Classic Handbook Reissue. New York: McGraw-Hill. Original edition. ISBN.

18. Ng, R.C. and Adisa, O.L. 1997. Coiled Tubing Resin Squeeze to Mitigate Water Production in Offshore Gravelpack Wells. Paper presented at the SPE Annual Technical Conference and Exhibition, San Antonio, Texas. SPE 38836.

19. Ng, R.C.M.I., Thurman W. , Hwang, Myung K. . 1994. Casing Repair Using a Plastic Resin. United States: Mobil Oil Corporation (Fairfax, VA).

20. Olstad, D. and McCormick, J.E. 2011. Case History of Innovative Plug and Abandonment Equipment and Processes for Enhanced Safety and Significant Cost Savings. Paper presented at the SPE/IADC Drilling Conference and Exhibition, Amsterdam, The Netherlands. 140331. DOI: 10.2118/140331-ms.

21. Rensvold, R.F. 1983. Sand-Consolidation Resins - Their Stability in Hot Brine. 23 (2). SPE 10653-pa

22. Rice, R.T. 1991. A Case Study of Plastic Plugbacks on Gravel Packed Wells in the Gulf of Mexico. Paper presented at the SPE Production Operations Symposium, Oklahoma City, Oklahoma. SPE 21671.

23. Sen,   A.   2000.   Chemistry   of   Epoxies.   Accessed http://www.epoxyproducts.com/chemistry.html#part1.

24. Treadway, B.R., Brandt, H., and Parker Jr., P.H. 1964. Laboratory Studies of a Process to Consolidate Oil Sands with Plastics. Paper presented at the Fall Meeting of the Society of Petroleum Engineers of AIME, Houston, Texas. SPE 906.

25. Vaucher, D. and Brooks, R. 2010. Advantages of Inflatable Packer Technology for Temporary or Permanent Well Abandonment in the Gulf of Mexico. Paper presented at the International Oil and Gas Conference and Exhibition in China, Beijing, China. SPE 130270.

APPENDIX A

POT LIFE AND CURING TIMES OF THE FOUR TESTED EPOXY RESIN

SYSTEMS

TABLE A.0.1–CURING TIME OF BPA SYSTEM 1 AT DIFFERENT TEMERATURES					
		72°F	130°F	170°F	200°F
AIR	Pot Life, hr	72	5.5	3.5	1.5
	Cure Time, hr	84	7.5	5.5	2.5
PURIFIED WATE	Pot Life, hr	72	6	4	2.5
	Cure Time, hr	84	8	6	3
SEA WATER	Pot Life, hr	72	6	4	2.5
	Cure Time, hr	84	8	6	3

TABLE A.0.2– CURING TIME OF BPA SYSTEM 2 AT DIFFERENT TEMERATURES				
		72°F	150 °F	200°F
AIR	Pot Life, hr	7	1	0.25
	Cure Time, hr	16	1.5	0.33
PURIFIED WATE	Pot Life, hr	7	1	0.5
	Cure Time, hr	16	1.5	1.2
SEA WATER	Pot Life, hr	7	1	0.5
	Cure Time, hr	16	1.5	1.2

TABLE A.0.3– CURING TIME OF BPF SYSTEM 1 AT DIFFERENT TEMERATURES

		72°F	130°F	170°F	200°F
AIR	Pot Life, hr	72	5.5	3.5	1.5
	Cure Time, hr	84	7.5	5.5	2.5
PURIFIED WATE	Pot Life, hr	72	6	4	2.5
	Cure Time, hr	84	8	6	3
SEA WATER	Pot Life, hr	72	6	4	2.5
	Cure Time, hr	84	8	6	3

TABLE A.0.4– CURING TIME OF BPF SYSTEM 2 AT DIFFERENT TEMERATURES

		72°F	150 °F	200°F
AIR	Pot Life, hr	7	1	0.25
	Cure Time, hr	16	1.5	0.33
PURIFIED WATE	Pot Life, hr	7	1	0.6
	Cure Time, hr	16	1.5	1
SEA WATER	Pot Life, hr	7	1	0.6
	Cure Time, hr	16	1.5	1

APPENDIX B

POT LIFE AND CURING TIME OF THE EPOXY RESIN SYSTEM WITH BARITE

TABLE B.0.1–CURING TIME OF BPA SYSTEM 1 WITH BARITE IN SEAWATER						
Density, ppg	9.25	10.49	11.74	13.17	14.98	16.79
Barite wt%	0	17.5%	30.8%	45.8%	57.5%	68.2%
130°F Pot Life, hrs	6	6	6	6	5.5	5.5
130°F Cure Time, hrs	8	8	7.5	7.5	7	7
170°F Pot Life, hrs	4	3.5	3.5	3	2.5	2.5
170°F Cure Time, hrs	6	6	6	6	5.5	5.5
200°F Pot Life, hrs	2.5	2.5	2	1.5	1.5	1.5
200°F Cure Time, hrs	3	3	3	2.5	2.5	2.5

TABLE B.0.2– CURING TIME OF BPF SYSTEM 1 WITH BARITE IN SEAWATER						
Density, ppg	9.15	10.49	11.74	13.17	14.98	16.79
Barite wt%	0	17.3%	29.8%	41.2%	52.6%	61.5%
130°F Pot Life, hrs	6	6	6	6	5.5	5.5
130°F Cure Time, hrs	8	8	7.5	7.5	7	7
170°F Pot Life, hrs	4	3.5	3	3	2.5	2.5
170°F Cure Time, hrs	6	6	6	5.5	5.5	5.5
200°F Pot Life, hrs	2.5	2	2	2	1.5	1.5
200°F Cure Time, hrs	3	3	3	2.5	2.5	2.5

POTENTIAL OF BARITE-WEIGHTED EPOXY SYSTEMS TO PLUG WELLS

IN THE GULF OF MEXICO

A Thesis

by

ZHUO GAO

Submitted to the Office of Graduate Studies of
Texas A&M University
in partial fulfillment of the requirements for the degree of

MASTER OF SCIENCE

December 2011

Major Subject: Petroleum Engineering

Potential of Barite-Weighted Epoxy Systems to Plug Wells in the Gulf of Mexico

POTENTIAL OF BARITE-WEIGHTED EPOXY SYSTEMS TO PLUG WELLS

IN THE GULF OF MEXICO

A Thesis

by

ZHUO GAO

Submitted to the Office of Graduate Studies of
Texas A&M University
in partial fulfillment of the requirements for the degree of

MASTER OF SCIENCE

Approved by:

Chair of Committee,   Robert Lane
Committee Members,   Jerome Schubert
    Yuefeng Sun
Head of Department,   Steve Holditch

December 2011

Major Subject: Petroleum Engineering

ABSTRACT

Potential of Barite-Weighted Epoxy Systems to Plug Wells in the Gulf of Mexico.

(December 2011)

Zhuo Gao, B.S., China University of Petroleum (East China), P.R.China

Chair of Advisory Committee: Dr. Robert Lane

In the past ten years, there have been 194 hurricane-damaged platforms in the Gulf of Mexico (GOM), each with many wells that have not been permanently abandonment. This could lead to disastrous environmental consequence. The wells where their platforms were destroyed by hurricanes cannot be abandoned by conventional methods. Our research showed that barite-weighted epoxy material could be potentially used for well abandonment for those wells in GOM. Shear bond strength tests showed that between two candidates epoxy systems—the bisphenol A system and the bisphenol F system, the latter was less sensitive to barite weighting material. The shear bond strength of besphenol A system was deteriorated as barite increased, while bisphenol F system showed slightly increasing trend when barite was added. The minimum bond strength given by bisphenol A system appears around 68 wt% of barite, which is around 1290 psi. The maximum value of 2200 psi comes at 0 wt% of barite. And the bisphenol F system can stand a minimum of 1010 psi bond strength at 0 wt% of barite, and a maximum of 1160 psi of bond strength with 70 wt% of barite. Moreover, mixing with seawater did influence the shear bond strength between epoxy system and

low-carbon steel. The influence that seawater has on the F system is less than that of the A system. The time that the epoxy system needs to fully develop the bond is far longer than curing time determined in our parallel research. Bond strength is lower in both seawater environment and at high temperature.

DEDICATION

I dedicate this thesis to my family and friends, especially

to Dad and Mom for instilling the importance of hard work and higher education;

to Yi for her patience and understanding—may you also be motivated and encouraged

to reach your dreams.

ACKNOWLEDGEMENTS

I would like to thank my committee chair, Dr. Lane, and my committee members, Dr. Schubert, Dr. Sun, for their guidance and support throughout the course of this research.

Thanks to John Maldonado and Rodney Inmon for their help to set up and run the experiments.

Thanks to my research partner, Suining Gao for cooperation in the research.

Thanks also to my colleagues, for helping me with the experimental setup and running the experiments.

I also want to extend my gratitude for the following:

BOEMRE: For funding me and the entire project.

Royce International Inc.: For donating all the epoxy the project needed.

Dr. Hubert Monteiro: For generous technical support, guidance with the research.

Finally, thanks to my parents for their encouragement and love.

NOMENCLATURE

HTHP   High Temperature High Pressure

BOEMRE   the Bureau of Ocean Energy Management, Regulation and Enforcement

MMS   Minerals Management Service

GOM   Gulf of Mexico

API   American Petroleum Institute

DOGGR   California Department of Conservation Division of Oil, Gas and

Geothermal Resources

ASTM   American Society for Testing and Materials

FEM   Finite Element Method

AAF   Aqua-Advanced Fabric

EEW   Epoxide Equivalent Weight

AHEW   Amine Hydrogen Equivalent Weight

PHR   Per 100 Parts Resin

BPA   Bisphenol A Type Resin

BPF   Bisphenol F Type Resin

ROR   Reduced-bond-strength/Original-bond-strength Ratio

TABLE OF CONTENTS

LIST OF FIGURES

LIST OF TABLES

CHAPTER I

INTRODUCTION AND LITERATURE REVIEW

1.1 Introduction

In the GOM, approximately 180 offshore platforms were damaged and destroyed by hurricanes in the past several years according to the documents released by the Bureau of Ocean Energy Management, Regulation and Enforcement (BOEMRE). The major hurricanes that passed through the Gulf of Mexico during the last dozen years are Andrew in 1992, Lili in 2002, Ivan in 2004, Katrina and Rita in 2005, and Gustav and Ike in 2008. **Table 1** shows the statistics for hurricanes damaged or destroyed platforms released by BOEMRE in a report of 2006 after hurricane Ivan. From **Fig. 1,** we can see that the major hurricanes pass through dense offshore locations, which leads to the disaster of our offshore industry.

_____

This thesis follows the style of _Society of Petroleum Engineering._

Table 1–HISTORICAL DAMAGE TO OFFSHORE FIXED PLATFORMS FROM HURRICANES IN GOM (BOEMRE, 2010).

No.	Hurricane	Year	Structures Destroyed**	Industry Response or Source
1	Grand Isle	1948	2*	Limited number of platforms in service
2	Carla	1961	3*	
3	Hilda	1964	14*	Several operators start to use a 100 year return period design wave
4	Betsy	1965	8*	
5	Camille	1969	3*	1st ed. API RP2A for fixed platform design
6	Carmen	1974	2*	
7	Frederic	1979	3*	Wave load recipe provided in RP2A
8	Juan	1985	3*	Assess-Inspect-Maintain (AIM) Joint Industry Projects for existing platforms
9	Andrew	1992	28 / 47 / 75	PMB, Andrew JIP, 1996.
10	Lili	2002	8 / 0 /8	Puskar, et.al., OTC 16802, 2004.
11	Ivan	2004	6 /1 / 7	MMS TAR No. 549, Energo, 2006
12	Katrina	2005	45 / 0 / 45	MMS TAR No. 578, Energo, 2007.
13	Rita	2005	56 / 18 / 74	MMS TAR No. 578, Energo, 2007
14	Gustav	2008	1 /0 / 1	MMS New Release November 2008
15	Ike	2008	50 / 9 / 59	MMS News Release November 2008
Total Historical GOM			232 / 75 / 307	

* Platform failures based upon published reports at the time (no data on caissons). Additional failures may have occurred but not reported in literature.
** Data shown as Platforms / Caissons / Total
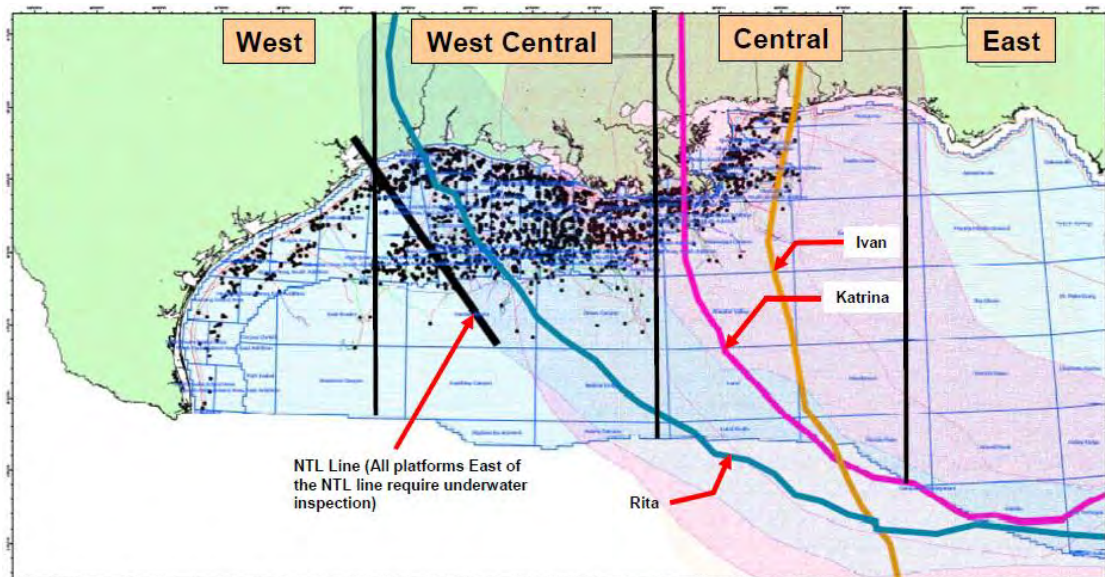
Fig. 1–Path of hurricanes Katrina and Rita and the Gulf of Mexico offshore infrastructure location (BOEMRE, 2007)

The report released by MMS (the former name of BOEMRE) in 2006 said that there were 28 fixed platforms destroyed by Andrew of 1992, 7 by Lili of 2002, and 7 by Ivan hurricane in 2004 (BOEMRE, 2006).

In the report of 2007 shows there are a total of 116 destroyed fixed platforms from Katrina and Rita in 2005 and one floating platform (BOEMRE, 2007). The dots in **Fig. 2** show the location of destroyed platforms after Katrina and Rita. Most of these 116 platforms were either completely toppled to the seafloor with no structure visible above the waterline, or were so severely damaged that it was obvious the structure was destroyed by the hurricanes and could no longer carry out its purpose and had to be removed. Moreover, **Fig. 3** shows how far the platform was moved by hurricanes in sonar image. And **Fig. 4** was a underwater picture of toppled platform. **Fig. 5** shows how the hurricane destroyed platform look like in Gulf of Mexico after Katrina and Rita.
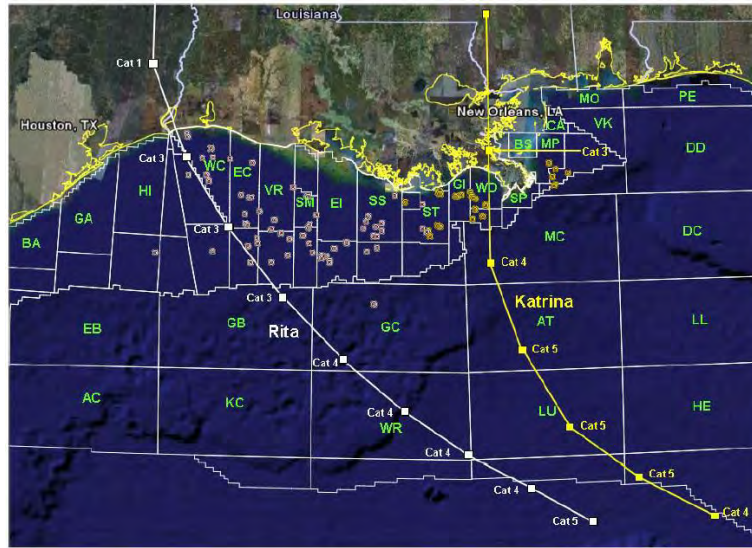
Fig. 2–Location of destroyed platforms in Gulf of Mexico compared to path of hurricane Katrina and Rita (BOEMRE, 2007)
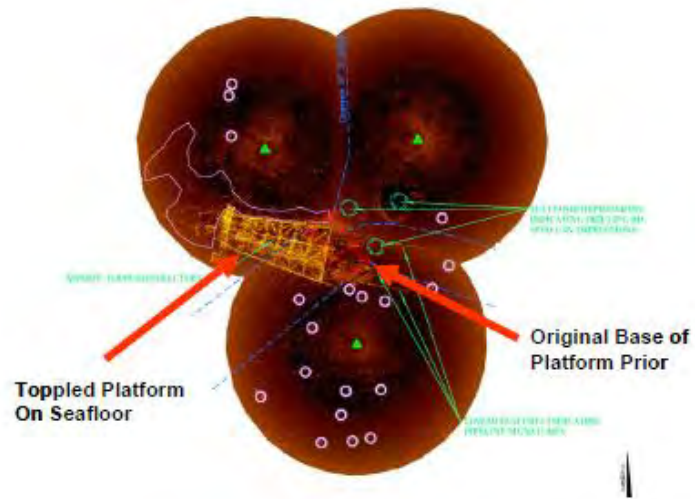
Fig. 3–Sonar image of the toppled platform in the west delta area after Katrina and Rita (BOEMRE, 2007).

Fig. 4–Underwater photo of a toppled platform in the Eugene Island Area (BOEMRE, 2007).

Fig. 5–Destroyed platform in the South Timbalier region after Katrina and Rita in 2005 (BOEMRE, 2007).

Another report officially released in 2010 by BOEMRE presents that there were a total of 60 destroyed fixed platforms in Gustav and Ike in 2008 (BOEMRE, 2010). No floating platforms were reported destroyed in the report. **Fig. 6** shows both the path of hurricanes Gustav and Ike, and the locations of destroyed platforms, which are marked

by red dots. **Fig. 7** shows the typical appearance of a hurricane damaged platform after

Gustav and Ike.
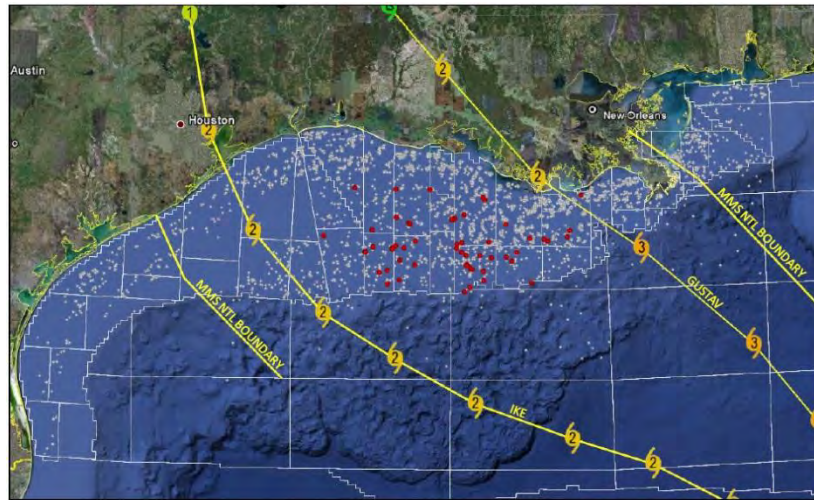
Fig. 6–Location of destroyed platforms compared to path of hurricanes. The red dots indicate destroyed platforms (BOEMRE, 2010).

Fig. 7–Destroyed platform in the Eugene Island Area from Gustav and Ike in 2008 (BOEMRE, 2010).

In cases where platforms have been completely destroyed and toppled, the wells can no longer safely produce oil or gas, and/or have become an environmental hazard. Additionally, such wells cannot be plugged and abandoned by conventional methods. Instead a subsea intersection well may have to be drilled to provide access to the wellbore. Depending on the intersection and the condition of the target well, it may not be possible to circulate or pump cement all the way down to the wellbore. In these cases, a plugging material needs to be spotted at the intersection of the target well, and allowed to fall through the wellbore, and settle at the target plugging zone, which includes annulus and across production interval, and seal the well permanently. **Fig. 8** illustrates a hurricane destroyed well in the Gulf of Mexico. The shadow area in red is the target plugging zone that we proposed to abandon.
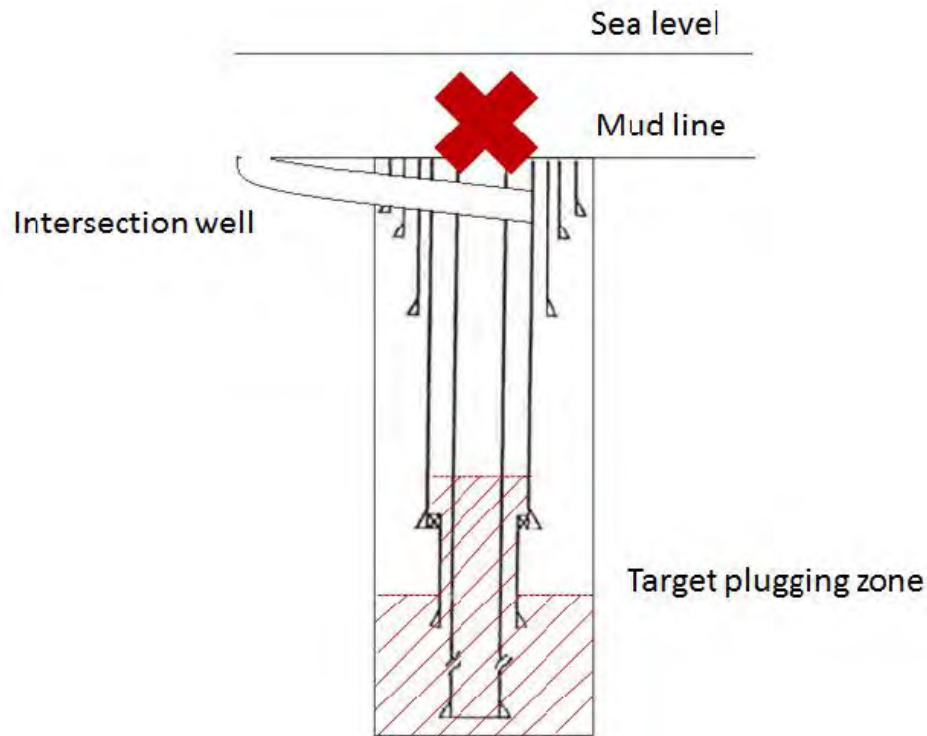
Fig. 8–Schematic of hurricane damaged offshore wellbore

The conventional methods to plug a well offshore include cement slurry plug, inflatable packer, and compressed sodium bentonite (Englehardt et al., 2001). Cement slurry plug is the most commonly used plugging and abandonment material in the oil and gas industry. However, there is a major disadvantage in using it offshore to abandon wells destroyed by hurricanes. Cement is miscibility with seawater and other brine. Such wells are often filled with seawater. Circulation system and mud are the main approach that people onshore use to avoid the contact of cement and unwanted fluid. Secondly, these offshore platforms don't have any circulation system any more, which delivers the high viscosity cement to the spot cannot work with destroyed platform. So as long as cement is applied, mixing with seawater cannot be avoided. Last but not least, in terms of its

particle based structure, the material exhibits relatively poor penetration capabilities in formations and wellbores. Most of the platforms which need to be permanently abandoned had been in service at least a couple of decades before being destroyed. Long time of soaking in the seawater undoubtedly leads to plenty of corrosion and ocean organisms along the wellbore. **Fig. 9** shows the external conductor appearance after hurricanes, which should be similar to what the interior looks like. The disadvantages of cement inhibit itself being applied in this project.
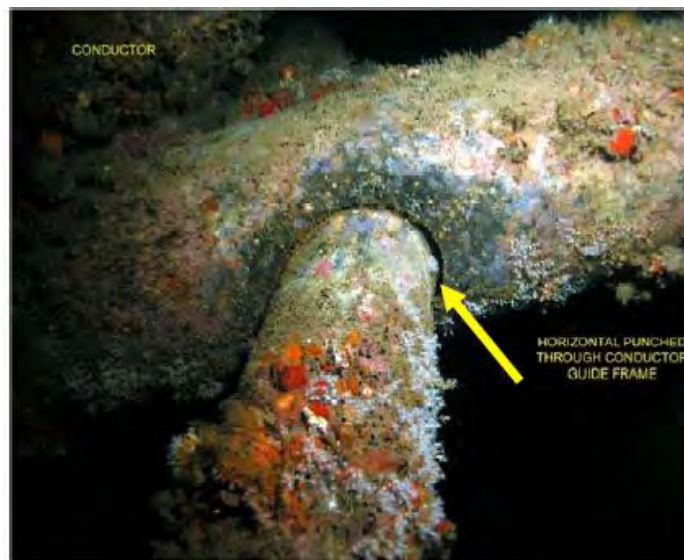
Fig. 9–A underwater picture of conductor surface (BOEMRE, 2006).

Inflatable packer is a promising technology for temporary or permanent well abandonment, which has been successfully applied in the Gulf of Mexico (Vaucher and Brooks, 2010). Basically, it is a smartly designed mechanical tool, containing rubber cover and exposed metal slats. It mostly relies on expansion of rubber cover to seal, and

friction between metal slat and wellbore to locate. The literature states that it's versatile of being conveyed to the depth by threaded tubing, coil tubing, electric wire-line and slick-line or braided line. However, all tubing and wire-line conveying method can only be applied when there is direct access to the wellbore, which is not available for wells on toppled platform where risers have been severely damaged.

Another relatively new abandonment material is compressed sodium bentonite (Englehardt et al., 2001). Both research and field test shows several advantages of compressed sodium bentonite. For example, it can easily fall through the wellbore and be hydrated to form an impermeable plug in oil or gas wells; it can form a plug in seawater and be stable at high temperature; it also can be reentered by using a soft formation drilling facility. Although it can be applied as a weighting material, it is not an adhesive material. So it cannot effectively seal a wellbore. Moreover, its applications are more focusing on onshore abandonment, especially temporary abandonment. No application or research shows that it has been successfully applied in permanent offshore abandonment. In terms of these restricted conditions, conventional plug and abandonment method won't be feasible.

Our research is seeking an alternative method to plug and abandon the well in deep water and particular reservoir condition economically and feasibly. Epoxy-based material popped up in terms of its excellent performance in casing repair, sand consolidating, and well plugging. The epoxy-based material formula generally contains

cross-linkable epoxy, cross-linking agent, and optional filler according to the specific scenarios. The plugging fluid's viscosity should meet the requirement of flowing from the intersection spot and the pot life should be long enough to let the fluid fall all the way down to the top of packer and across the production interval. Also, the bond strength between epoxy system and low-carbon steel should be large enough to stand the relative high temperature and pressure at wellbore.

Permanent plug and abandonment is done with the objective for the well to be sealed and isolated forever. The long-term plugging requirement is one of the principle parameters to measure the success of abandonment. Well abandonment has never received as much attention as reservoir evaluation, drilling procedure and production process. It is a crucial step in a well's life circle especially from an environmental perspective, even though it cannot bring any revenue to the industry. American Petroleum Institute (API) has generated a report entitled, "Environmental Guidance Document: Well Abandonment and Inactive Well Practices for U.S. Exploration and Production Operations". This is considered as the standard in the industry for abandoning the wells environmentally. However, this regulation mainly emphasizes on plugging unwanted zone and onshore abandonment instead of permanent abandonment. Also, their regulation was mostly generated based on cement operation. Besides the regulation of API, California Department of Conservation Division of Oil, Gas and Geothermal Resources (DOGGR), as the lead agency in oil and gas industry in California, also released the requirement of well abandonment in State of California Code of

Regulations, Title 14 Natural Resources, Division 2 Department of Conservation, Chapter 4 Development, Regulation, and Conservation of Oil and Gas Resources, Section 1723 (Harris and Adams, 2007). They have requirement in different operations, such as plugging of oil or gas zones, plugging for freshwater protection, plugging at a casing shoe or the casing stub, and surface plugging. These regulations are also concentrated on onshore abandonment. Even though in some material they mention the regulations in California give the restrictions of offshore well abandonment, it doesn't show quantities requirements and doesn't make engineering work easier either. In general, offshore abandonment is regulated by more strict requirements than that for onshore operation. Unfortunately, BOEMRE hasn't successfully established any regulation on offshore well plugging and abandonment. The strongest one that we can find so far is the one set by the North Sea (Liversidge et al., 2006). The critical criterion is that the plug should pass the test with minimum inflow pressure of 725 psi. In our project, we assume that the BOEMRE will give us the regulation as tight as that in the North Sea. So shear bond strength is the main parameter we tested in our experiment.

BOEMRE is interested in Epoxy-based material application, because it has been used around for decades as an adhesive material, and has been extensively utilized in the whole petroleum industry. The first couple of successful applications in the petroleum industry were in the 1950s. One was as a coating material (Radecke et al., 1959), the other one was as an alternative casing repair material (Kemp, 1964). It quickly won good reputation in terms of its fast reaction and low expense since then. Its first patent in

casing repair was published in 1994 (Ng et al., 1994), which deal with onshore corrosive casing and plugging the thief zone. The well is located at levels in excess of about 5,000 ft, which is often exposed to high temperature, high pressure and corrosive chemicals.

In our project, the operation environment is much tougher than the one mentioned in the patent. The wells are located in deep water of the Gulf of Mexico. The depth of the wells is beyond 5,000ft, whose effective dropping depth might up to 7000ft. The temperature at the bottom of the wellbore might as high as 250 ℉. The falling trail is the casing annuli which is narrow and full of seawater and oceanic organisms attached to the wall. No fluid will be circulated in the system. The only way to abandon a deep-water well with casing completion is pouring the abandonment fluid from intersection and letting it fall through the annuli and set the target plugging zone. To guarantee the falling process, a weighting material—barite is considered to increase the weight of the epoxy system. One reason is that the density of pure epoxy system is quite close to the density of seawater. It might float on the surface or at least be near naturally buoyant instead of falling down. The other reason is that barite is most commonly used filler with low costs in the petroleum industry. Besides low viscosity, relative high specific gravity, the scenarios also require appropriate pot life, acceptable rheology and bond strength.

1.2 Literature review

Epoxy-based material has developed from the 1950s as a coating material for corrosive protection (Radecke et al., 1959). There are several applications, such as coating, casing

repair and sand consolidation, whose advantages of quicker reaction and less expensive operation won reasonable success.

The first application of epoxy as a sealant material in petroleum industry was in 1979 (Cole, 1979). The paper mainly introduced an epoxy sealant-cementing system which performs adhesive and compressive strength, together with chemical resistance superior to Portland and modified Portland type cement. In their research, they tested bisphenol A type epoxy resin with silica fillers. They overcame two serious limitations of epoxy applications by adding nonreactive liquid diluent and fillers to the system. Nonreactive liquid diluent extended latitude pumping time. Inert fillers added strength and reinforcement to the set epoxy sealant allowed more exothermic control than cementing and also reduced the cost of the whole system. Laboratory work showed epoxy adhesive very well to the metal and silica surface. Moreover, the paper mentioned that bisphenol-A type epoxy resin functioned very well in the chemical resistance and bonding strength test. Laboratory tests determining chemical resistance showed that the epoxy could provide suitable protection at temperature up to 60 ℃ from exposure to oilfield brines up to 10%, hydrochloric acid solutions up to 30% and sulfuric acid solutions up to 25% and so on. The bonding strength of the epoxy material was studied in the laboratory as well, which identified that neat epoxy sealant required 3000 psi hydraulic pressure to leakage, and epoxy slurry sealant didn't fail even beyond 500 psi hydraulic pressure added. However the operation process mentioned in the paper was still conventional one using

circulation system. Even though the reservoir condition is not the same as that in our project either, at least it showed the potential being applied in our research.

The use in pipeline coating is quite mature. It also has several problems to be concerned when applying. A paper (Jensen et al., 2000) answered the question, Whether using epoxy to repair pipeline is safe when the environment is complicated and how environment affected the mechanical properties of epoxy-bonded joints for possible use in underwater pipe line repair. They carried out their lab work in testing the interfacial shear strength--three point flexure, scanning electron microscopy, optical microscopy, and X-ray photoelectron spectroscopy to determine the failure of the bonded joints. The result shows that water diffuses through the interface between epoxy and steel resulting in the weaker bond, which is concern in our project. However, the epoxy that they tested is the one without fillers, which is quite different from our formulation. Also, we got to know that surface analysis shows failure always occurs within oxide layer from their research.

One US Patent named "casing repair using a plastic resin" mentioned biophenol-A epichlorohydrin epoxy resin mixed with reactive diluents, a mono-functional glycidyl ether based alkyl groups of C8-C10, could perform rather good seal in salinity and low temperature with specific curing agent. The patent also gives some suggestion in high temperature application, which would replace curing agent from a Mannich base aliphatic polyamine to anhydride. Moreover, the operation method mentioned in the

patent is dump bailer draining, which require the viscosity of the liquid not too high to flow (Ng 1994). In our research, we are looking for pourable liquid epoxy material to abandon the 7000-feet well in temperature up to 250℉. The viscosity should be low enough for flowing. The pot life should be long enough for the liquid to fall. The patent provides good reference in formulation, but improvement is still needed.

A more nearly United States Patent 7886823 filed in 2005 provides a commercial formulation over well plugging material that can be used for both down-hole mixing and applications in brines. (Boyce D Burts et al., 2011). They found the component A and B can react with each other at down-hole form the plugging without any circulation system. However, they improved cement formula to accomplish the objective instead of using epoxy-based material.

 Also, another patent 7748455 from the same author showed another formula of epoxy as a plug component for well remediation. The material in the patent are EPON 862 or 863-RESIN, EPICURE 3046 low-temp hardener, EPICURE W high temp hardener, Heloxy 7-primary reactive diluent, CARDURA E10P-secondary, high-temp diluent. The formulas are presented in Table 2. In generally this patent was designed meet the requirement that the resin component and the activator component are mixed at the surface and then placed in the annulus and allowed to form into a hard impermeable mass. Preferably, epoxy system is heavier than the well fluid to allow gravity flow through the well fluid to the annulus (Boyce D Burts, 2010).

Table 2–FORMULAS OF EACH EPOXY SYSTEM IN PATENT 0133069

Formulation	Resin	Low-temp hardener	High-temp hardener	Primary reactive diluent	Secondary, high-temp diluent	Temperature Range (°F)
	EPON 862/863 (g)	EPICURE 3046 (g)	EPICURE W (g)	Heloxy 7 (g)	CARDURA E10P (g)	
1	100	17-40				50-100
2	100	20-60		20-50		70-125
3	100	10-20	10-20	20-50		125-175
4	100		17-35	0-50		175-250
5	100		15-25	30-50	0-20	250-350

A bio-geosciences paper illustrates the geophysical and geochemical characteristics of Gulf of Mexico, which supply us with the component of bottom seawater in Gulf of Mexico (Joye et al. 2005). We will carry out experiment to evaluate the influence given by seawater.

Even though there is plentiful literature of the application of epoxy-based material, we need to consider the filler effect in our project. A study was developed to see the influence of adhesive thickness and aluminum filler content on the mechanical performance of aluminum joints bonded by aluminum powder filled epoxy (Kahraman et al., 2008). They carried out the research by single-lap shear test that is standardized by American Society for Testing and Materials (ASTM) and Finite Element Method (FEM) simulation. The study showed that adhesive thickness has a negative effect on shear strength which is verified by both lab experiment and FEM. With neat epoxy with no fillers, increase of adhesive thickness from 0.03mm to 1.3mm resulted in a decrease of

about 35-40% in adhesive joint sheer strength. Also the epoxy adhesive retains its adhesion strength even with as much as 50wt% addition of filler. Failure tests showed the failure mostly occurred within adhesive. The shear and Von Mises stresses for various bond thicknesses and various adhesive compositions were analyzed by FEM. Von Mises stress attains maximum at the edges and decrease away from the edges. Adverse effect of adhesive thickness increase in bond strength was observed from comparison between different thickness specimens.

Moreover, epoxy-based adhesion is always exposed to the environment of moisture, freezing and thawing, temperature, and corrosive liquid. So it is quite significant to evaluate the environmental effects on epoxy-based adhesion. The paper published in Construction and Building Material Journal shows the decrease in flexural strength of epoxy-bonded concrete prisms is directly proportional to the adsorbed water content. And corrosive environment with $MgCl_2$ or $MgSO_4$ is not significant to bond stability (Çolak et al., 2009).

A couple of papers on evaluation of material and structural performances gave us an idea to use ASTM standard to carry out our shear bond strength test (Yi et al., 2010)and (Jensen et al., 2000).Their paper shows they did compressive strength, tensile strength test, flexural strength test, thermal expansion test, hardening shrinkage test, and chemical resistance test for Aqua-Advanced Fabric Reinforced Plastic (AAF). Pull-out test showed that failure load increases as the bonded area increased.

CHAPTER II

PROBLEMS

In this project, we will focus on shear bond strength tests. Studies showed that different aspects like fillers added and environment influenced the bond strength of epoxy-bonded material (Çolak et al. 2009) and (Kahraman et al. 2008). Plenty of literature shows the potential of epoxy-base material in aquatic environment. However, so far nothing in the literature has evaluated application of the barite-weighted epoxy system to low-carbon steel with or without the presence of synthetic seawater. We will evaluate the influences of possible aspect on bond strength, such as fillers, aquatic system, and time.

Our project is to determine the shear bond strength of epoxy system as a function of

- Composition

- Filler loading

- Curing in seawater

- Bonding to low-carbon steel

- Time

- Temperature

CHAPTER III

THEORETICAL BACKGROUND

To determine the formulation, we need to consider at least two requirements. One is to be able to applied in seawater environment; the other one is that pot life should be long enough for well operations and falling process.

For the first requirement, our research focused on two most widely used commercial epoxy systems–B47 and XR40 (two commercial products offered by Royce International Company)–to carry out our evaluation tests in our research. B47 is also known as bisphenol A type resin, while XR40 is commonly known as bisphenol F type resin. In order to be able to perform in the tough seawater environment, curing agent K450 (a commercial product offered by Royce International Company) was selected. The curing agent has a successful application history in underwater conditions according to industry expert's suggestion. Also, it is non-MDA curing agent, which is more environmental benign (Norsworthy, 2001).

For the second requirement, theoretical calculations are needed to determine each component that is applied in the formula. To obtain optimal properties with epoxy curing agent and resins, the component are typically used at approximate stoichiometric levels.

Determine the epoxide equivalent weight (EEW) of resin mixture:

$$\text{EEW of mixture} = \frac{\text{total weight}}{\dfrac{\text{wt. A}}{\text{EEW A}} + \dfrac{\text{Wt. B}}{\text{EEW B}} + \dfrac{\text{Wt. C}}{\text{EEW C}}}$$

Determine of amine hydrogen equivalent weight (AHEW) of the curing agent mixture:

$$\text{AHEW of mixture} = \frac{\text{total weight}}{\dfrac{\text{wt. A}}{\text{AHEW A}} + \dfrac{\text{Wt. B}}{\text{AHEW B}} + \dfrac{\text{Wt. C}}{\text{AHEW C}}}$$

Calculate the parts by weight of curing agent per 100 parts resin (PHR) using the following equation:

$$\text{PHR of the curing agent} = \frac{\text{AHEW of Curing Agent}}{\text{EEW of Resin}} \times 100$$

The equations listed above are used to calculation the pure epoxy resin system.

CHAPTER IV

EXPERIMENT AND DISCUSSION

4.1 Comparison of two epoxy system

One of our objects is mainly to see how these two commonly used epoxy system will perform with metal material and seawater when reacting with the curing agent. The other objective is to test properties of barite-weighted epoxy systems instead of the pure epoxy system. So we mixed barite as filler in the epoxy formulation mentioned above. We added barite for bisphenol A type resin up to 72 wt%, which is around 2.1 g/cm^3 (17.5 ppg), and for bisphenol F type resin up to 70 wt%, which is also around 2.1 g/cm^3 (17.5 ppg).

The two formulations visually look quite similar (shown in **Fig. 10**). The recipes and physical properties of each epoxy system are tabulated in **Tables 3** and **4**, respectively. We obtained 4 to 10 micron barite powder from our drilling lab (shown in **Fig. 11**). This is also the commonly used barite in the industry.
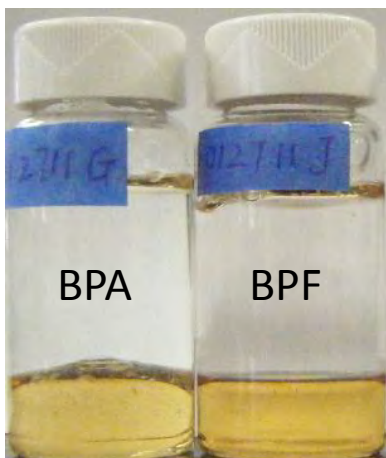
Fig. 10–The pictures of pure formulations of BPA and BPF

Fig. 11–The picture of barite powder applied in our research

Table 3–RECIPES OF EPOXY SYSTEMS

System	Resin, g		Diluent, g		Curing agent, g	
	Product	Amount	Product	Amount	Product	amount
A	B47*	4.7			K450	1.6
F	XR40	4.25	RA100	0.75	K450	1.9

B47* is a resin with diluent premixed in it.

Table 4–PROPERTIES OF EACH EPOXY SYSTEM

Component	Properties
B47	Light yellow liquid; specific gravity of 1.6
XR40	Pale yellow liquid; specific gravity of 1.2
RA100	Colorless; reactive; corrosive
K450	Yellow-orange liquid; crystallization point is around room temperature

4.2 Methodology

To evaluate the bonding effect between our formulation and low carbon steel, we carried out pull-out tests for the formulations attached to low carbon steel. The experiment was guided by ASTM D3164M-03, the "standard test method for strength properties of adhesively bonded plastic lap-shear sandwich joints in shear by tension loading" (ASTM, 2003).

4.2.1 Material

In this project, we selected low carbon steel to make the coupon required in ASTM D3164M-03. The reason for using low carbon steel is that the wells that we are aiming to abandon are offshore wells. In offshore wells, low carbon steel is the first option for most well casings and tubings. The low carbon steel sheet is 0.031 in. with tolerance of +/-0.0015 in. It has been cold-rolled when manufactured. The surface is smooth and not corroded at all.

The epoxy systems that we applied in the test are the same formulation with barite as mentioned above in Table 3.

4.2.2 Pretreatment

Our experiments were carried out in an ideal condition. Real-world applications are likely to be affected by corrosion and ocean organisms. We didn't rough the surface of coupon by either mechanical or chemical methods. The real situation cannot be easily evaluated by just randomly roughing the surface. In terms of those wells that haven't been in use for a long time, casing and tubing might be either severely corroded or covered by aquatic organisms, or both of them. It is hard to find any reference or criteria to rough the surface that could represent the real offshore casing surface. We decided to take the ideal test results as a reference.

4.2.3 Preparation of samples

We cut the low carbon steel sheet into small coupons following the dimensions in ASTM D3164-03. **Fig. 12** shows the schematic of our lap-shear sandwich joint. We modified the preparation according to the material that we could find.
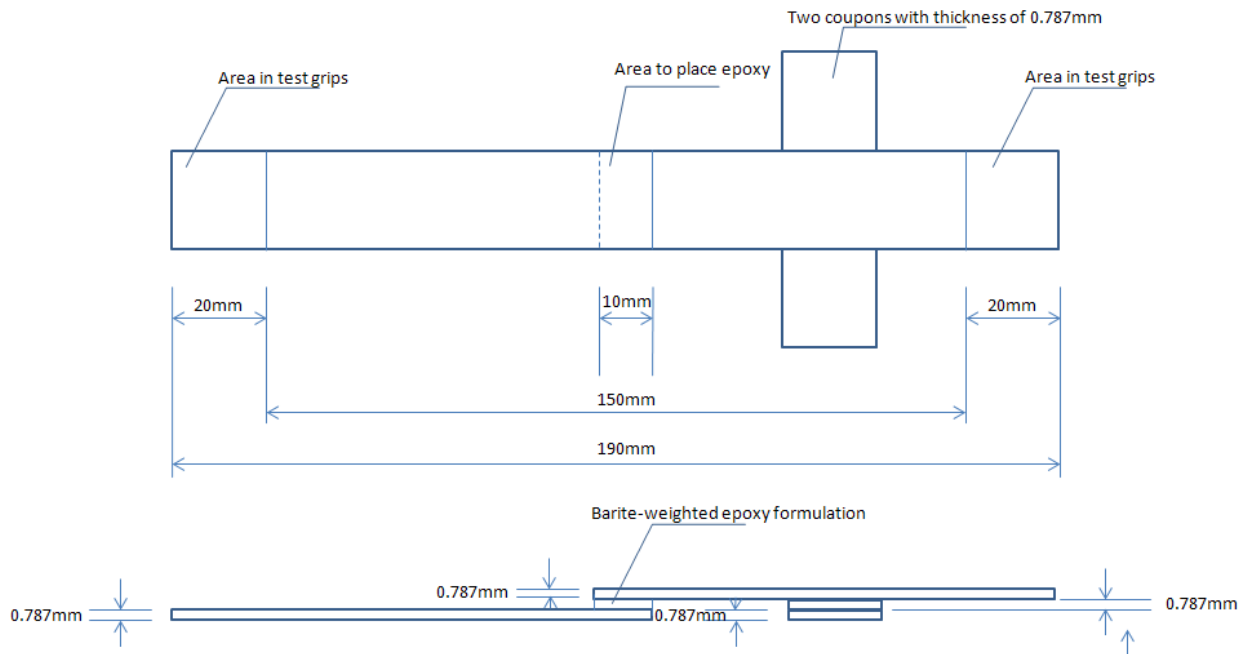
Fig. 12–Schematic and dimension of lap-shear sandwich joint

The main procedure of preparation is:

1. Make specimens that conform to the form and dimensions shown in Fig. 12.

2. Apply the barite-weighted epoxy in the designated area.

3. Place the specimens in the heating oven for certain amount of time before actually doing the shear test

Two coupons below the sandwich joints are used to support the upper coupon and to guarantee the epoxy formulation in between is 0.787 mm thick.

The most difficult part of the preparation is to spread the barite-weighted epoxy formulation on the surface of the coupon in the designated area. Ensuring repeatability of the test depends on exact placement of the epoxy on the coupons. The amount of the epoxy cannot be either too much or too little, which both lead to inaccurate test results. Also, the thickness of the epoxy insert will influence the joint strength obtained in this test due to the added offset. To eliminate the influence as much as possible, we were careful to repeat every step as identically as possible.

Moreover, to eliminate the influence of any nuisance variable, randomizing the order of all the runs in each experiment is extremely important. The experiment is generally a completely randomized single-factor experiment with six levels of the factor for each epoxy system. The levels of the factor are sometimes called treatments, and each treatment has eight observations or replicates. The levels are denoted as A to F, where the amount of barite increases from A to F. Each of these levels is repeated 8 times. Fig. 13 shows the order of preparation in one epoxy system. Experiments are run from A1 to F1, A2 to F2, and An to Fn where n is 8. This order helps to eliminates uncertainty.
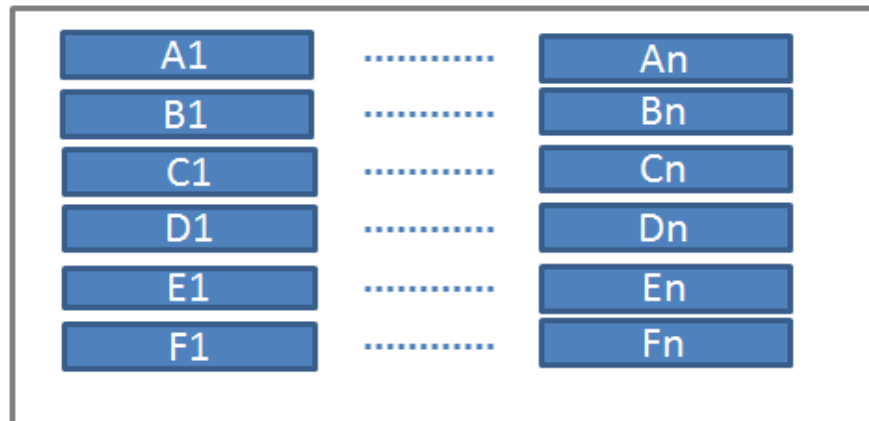
Fig. 13–Schematic of preparation

4.2.4 General information of mechanical tests

The procedures to hook up the equipment and test the specimens are listed as below:

1. Turn on the machine and preheat the heating facility in **Fig. 14** to the target temperature.

2. Take the specimens preheated in the oven in our lab and transport them as quickly as possible to the material test equipment.

3. Hold the specimens by two vertical grips, and set up the software.

4. Following the randomization principle, and do the pull-out test batch by batch.

5. Record the peak load that specimens are able to stand.

We used the MTS Insight^{TM} Electromechanical Testing System, consistent with ASTM D3164-03's requirement. When the heating facility reached the objective temperature, the designed tension load was added to pull the specimens vertically. The load added was set at 160 kgf/min.
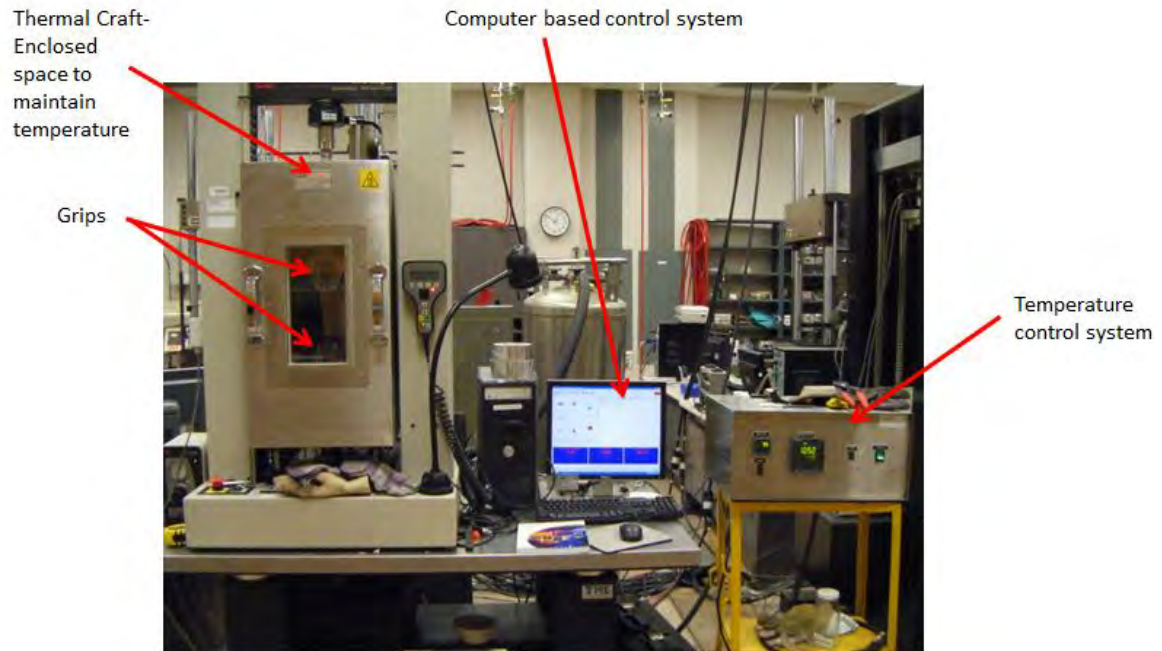
Fig. 14–The equipment for all the shear bond strength tests.

4.3 Filler loading influence on shear bond strength test

We added different amounts of barite into two potential epoxy formulations and generated two epoxy systems. We tested shear bond strength under 200°F, which is a reasonable average reservoir temperature in Gulf of Mexico (Haeberle, 2005) for 24 hours before carrying out the mechanical tests.

The procedures of the mechanical tests were following the general step listed in last chapter.

1. Make specimens that conform to the form and dimensions shown in Fig. 12. The order of making specimens followed Fig. 14.

2. Apply 12 different treatments of the barite-weighted epoxy in the designated area.

3. Place the specimens in the heating oven for 24 hours before actually doing the shear test.

4. Turn on the machine and preheat the heating facility in Fig. 14 to the target temperature 200°F.

5. Take the specimens preheated in the oven in our lab and transport them as quickly as possible to the material test equipment.

6. Hold the specimens by two vertical grips, and set up the software in the computer-based control system.

7. Follow the randomization principle, and do the pull-out test batch by batch.

8. Record the peak load that specimens are able to stand.

The **Table 5** below shows the components of each formulation/treatment.

Table 5–COMPONENTS OF EACH FORMULATION					
Barite added to the formulation, g					
Aa	Ab	Ac	Ad	Ae	Af
0	1.3	5.3	8.5	13.5	16
Barite, wt%					
0	17	46	57	68	72
Barite added to the formulation, g					
Fa	Fb	Fc	Fd	Fe	Ff
0	1.3	5.3	8.5	13.5	16
Barite, wt%					
0	16	44	55	66	70

(Bisphenol A system — rows 1–4; Bisphenol F system — rows 5–8)

For each barite-weighted epoxy formulation, we made and tested eight identical specimens under same conditions. However, whether the specimens prepared are good or not cannot be evaluated until the pull tests are finished. The wettability, viscosity and density, all influence the thin film spread covering the designated area. The quality also might change after they were placed into the heating oven. This is mainly because of viscosity change when being heated. The epoxy formulations were not able to stand in between the two coupons when it became less viscous. To eliminate the variables' influence, we recorded all the data from the tests and eliminated the ones that didn't visually look fabricated well (Seen the samples on the right of **Fig. 15**). When extrapolating the data, we did the average for the rest of values. Fig. 15 shows how the elimination work was done. The samples on the left are those meeting the requirements of ASTM D3164-03, while the ones on the right are failure samples than cannot be accounted into our data extrapolation.

Fig. 15–Screening qualified samples for the test. The samples on the left are those well fabricated, with which we extrapolated the data. The samples on the right are the examples being eliminated.

According to the data recorded by the computer system (Seen in appendix Table A), we generated the trends in **Fig. 16**. For bisphenol A system, shear bond strength was deteriorated as barite weight percentage increases up to 72 wt%. According to the data that we had in our research, it has a minimum bond strength value, which comes at around 68 wt%. Compared to the bisphenol A system, the bisphenol F system data shows better stability in the data collected in Fig. 16. Also it shows that shear bond strength was very slightly increased by filler weight percentage increasing up to 70 wt%. The figure below also tells us that bisphenol A system is more filler sensitive compared to that of bisphenol F system.
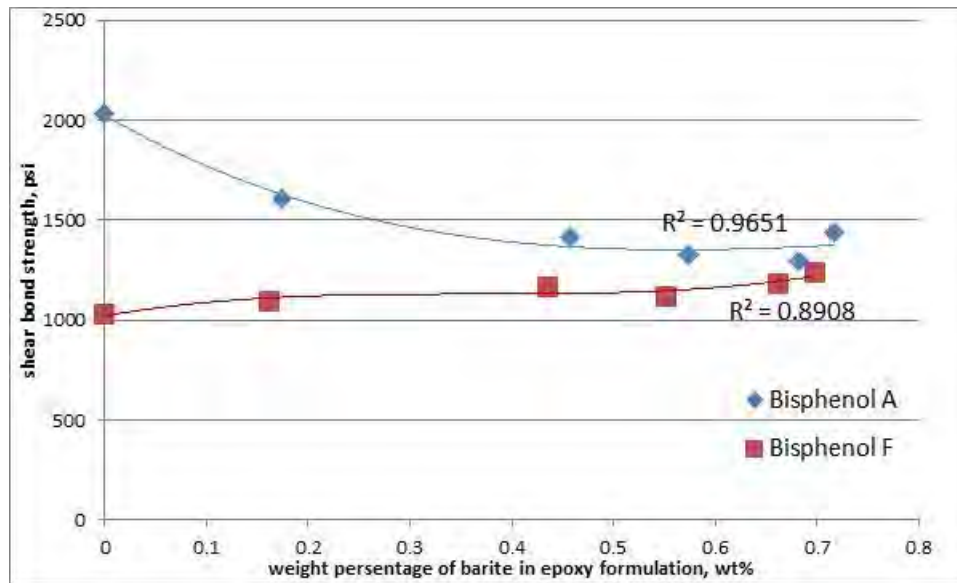
Fig. 16–Bond strength of bisphenol A system was deteriorated as fillers increase. Bond strength of bisphenol F system stays stable as fillers increase.

4.4 Simulated environmental tests

Our simulated environmental tests showed that when epoxy contacts steel in the presence of synthetic seawater, the epoxy/steel bond strength is decreased.

In our simulated environmental tests, we placed both systems in synthetic seawater for one hour before spreading it on the coupon, and then heated the specimens for 24 hours before the shear bond strength tests. We chose to test three treatments for each epoxy system. 6 observations were recorded by each treatment. For all the barite-weighted epoxy formulations, we did the same elimination as the previous tests, and extrapolated the data by doing an average for each formulation.

The procedures of the specific experiment are listed below:

1. Prepare the mixture with barite. Three different treatments for each epoxy system. So there are overall six treatments.

2. Prepare the synthetic seawater according to the geophysical and geochemical signatures research of the Gulf of Mexico (Joye et al., 2005). The synthetic seawater components are listed in **Table 6**.

3. Dump half of the mixture into the vials which contain the synthetic seawater and soak them for one hour as shown in **Fig. 17**. The vials were shaken some to increase the contact with the synthetic seawater, which is also shown in Fig. 17.

4. Dispose of the synthetic seawater, take the mixture out of the vial and spread it on the designated area on the coupon, which is shown in **Fig. 18**. Make specimens that conform to the form and dimensions shown in Fig. 12. The order of making specimens followed Fig. 14.

5. Place the specimens in the heating oven for 24 hours before actually doing the shear test.

6. Turn on the machine and preheat the heating facility in Fig. 14 to the target temperature 200°F.

7. Take the specimens preheated in the oven in our lab and transport them as quickly as possible to the material test equipment.

8. Hold the specimens by two vertical grips, and set up the software in the computer-based control system.

9. Follow the randomization principle, and do the pull-out test batch by batch.

10. Record the peak load that specimens are able to stand.

Table 6–SYNTHETIC SEAWATER FORMULA

Component	Amount, g/l
$MgCl_2 \cdot 6H_2O$	2.2
$CaCl_2 \cdot 2H_2O$	1.6
KCl	3.2
Na_2SO_4	4.1
NaCl	23.6

The density of the synthetic seawater is 8.31 ppg.

Fig. 17–We soaked and shaked the samples in synthetic seawater for one hour before pull-out tests. The upper one is shown what samples look like before shaking. The lower one tells barite in A epoxy system is easier to come out after shaking.

Fig. 18–After one hours of being soaked in synthetic seawater, the epoxy was mixed with synthetic seawater. The left three samples are for A epoxy system. The right three are F epoxy system's samples

The results show the significant decrease of bond strength when introducing the synthetic seawater into the formulation. The data obtained from our shear bond strength test are presented in Table 7 and **Fig. 19**. The solid bars in Fig. 19 represent the original test results without being soaked in the synthetic seawater. The no-fill bars show the results with treatment in the synthetic seawater. All the bond strength was reduced significantly by introduction of the synthetic seawater. Most of reduced data are less than the North Sea criteria—725 psi, except one treatment of BPA with 17 wt% barite. The 725 psi-criteria is given by the Netherland. The UK Offshore Operation Association has the similar criteria, which is given as 500 psi (dash line in Fig.19). If we use the UK's criteria, most of the treatment after simulated environmental test can meet the requirement. The original result listed in appendix Table B shows that the data of BPA

looks quite erratic, while data of BPF are consistently stable. It also verifies our conclusion in previous test that the BPA is more barite sensitive than BPF system.

Table 7–SIMULATED ENVIRONMENTAL TEST DATA AT 200°F

Name of system	Barite, wt%	Soaked	Average bond strength, psi
BPA	72	N	1527
BPA	72	Y	560
Difference			967
BPF	70	N	1163
BPF	70	Y	322
Difference			841
BPA	57	N	1320
BPA	57	Y	551
Difference			769
BPF	55	N	1126
BPF	55	Y	615
Difference			511
BPA	17	N	1544
BPA	17	Y	875
Difference			669
BPF	16	N	1113
BPF	16	Y	565
Difference			548
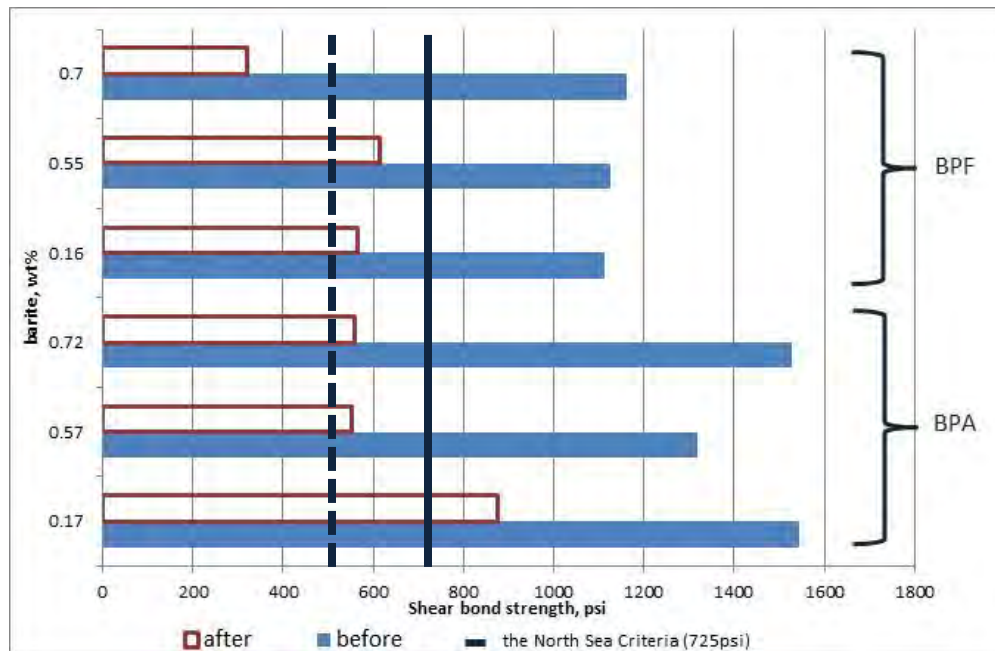
Fig. 19–Two formulations with different weight percentage of barite show the same results. Shear bond strength decrease with the introduction of the synthetic seawater into the epoxy system

In order to analyze the reasons why this phenomenon happens, we looked into the observations during the simulated environmental test. The **Fig. 20** shows the difference between samples with and without being soaked in the synthetic seawater. The upper one is a sample mixed with the synthetic seawater, while the bottom one is pure formulation with the same amount of barite which was not experienced simulated environmental treatment. The upper one shows the uneven surface and different reflection which is caused by the introduction of the synthetic seawater. The light colored part in Fig. 18 shows what the barite looks contacting with the synthetic water. The light colored areas of BPA system are definitely larger than that in BPF system. The barite separation of BPA is more obvious than that in BPF in Fig. 17. So larger light

colored areas are most likely attributed to that more synthetic seawater was introduced into the system, which leads to the greater reduced-bond-strength/original-bond-strength ratio (ROR). The ROR values can be calculated by the equation below. The **Fig.** 21 and the **Fig. 22** show the comparison of what samples look like after pull-out test with or without being placed in the synthetic seawater. From the pictures of both BPA and BPF systems, the introduction of the synthetic seawater into the formulation, leads to not only loose texture, but also the reduction in contact area of epoxy and low carbon steel. This can be applied to illustrate the deterioration of bond strength when the synthetic seawater was introduced into the system.

$$\text{ROR} = \frac{\text{original bond strength} - \text{bond strength in stimulated test}}{\text{orignial bond strength}}$$

Fig. 20–Formulations mixed with/without the synthetic seawater were placed on the coupons.
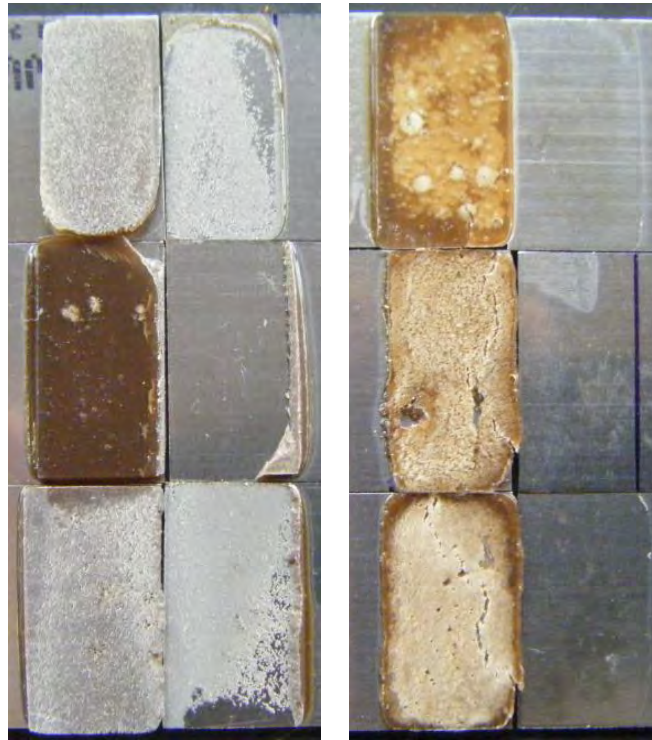
BPA without being soaked by the
synthetic seawater

BPA with being soaked by the
synthetic seawater

Fig. 21– After shear bond strength at 200 °F, for BPA system, the texture on the right look looser and the contact area seems less than the ones on the left.

BPF without being soaked in the
synthetic seawater

BPF with being soaked in the
synthetic seawater

Fig. 22– After shear bond strength at 200 °F, for BPF system, the texture on the right look looser and the contact area seems less than the ones on the left.

Comparing all the six treatments, we put the reduced-bond-strength/original-bond-strength ratio (ROR) into **Fig. 23** to show the difference. And it is generated to evaluate the influence of the synthetic seawater in bond strength. The smaller the ratio is the better quality that the material has. The Fig. 23 shows the ratio varies between two systems. The ROR of BPA system increases as the barite is increasingly added, while ROR of BPA has a minimum value which comes at around 50 wt% barite. Based on the ROR, we would like to have the formulations with low ROR value, which is circled in Fig. 23. For BPA, low barite weight is recommended. For BPF, around 50 wt% of barite

is recommended. While if economic factor is taken into consideration, the more barite we will use, the less expensive it will cost. So the BPF should be more economic at this point. Moreover, at most of barite weight percentage, ROR of BPF is smaller than that of BPA. It verifies our previous conclusion that BPA system is more seawater sensitive compared to BPF system one more time. However, if combined with the North Sea criteria, the BPF recipe still need some improvements to strengthen the bond strength.
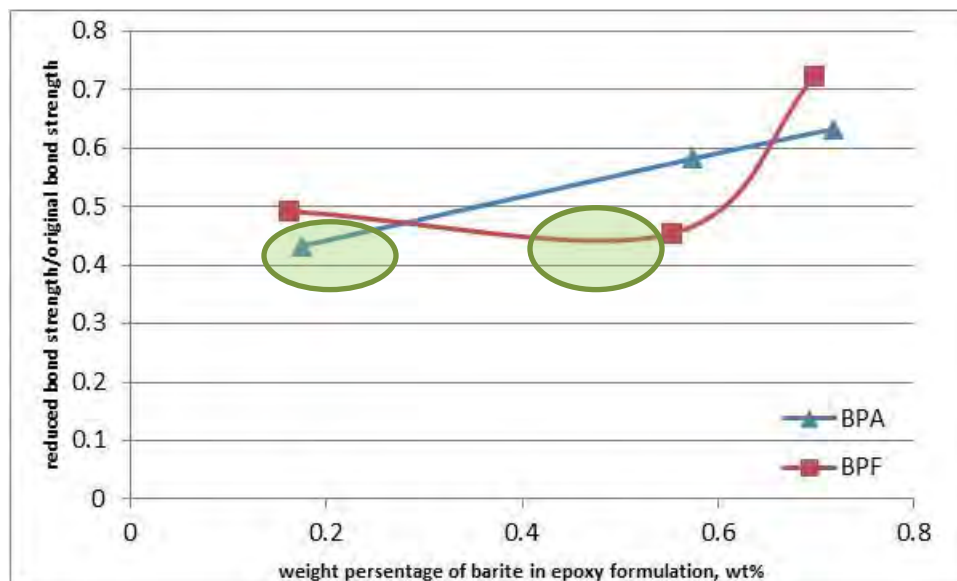
Fig. 23–Reduced-bond-strength/ original-bond-strength ratio varies between two systems at 200 °F-shear-bond-strength test.

Let's assume we'll set a plugging at a casing 1 ft long with inside diameter of 5 inches applying BPF formulation. We did calculation to see what the North Sea criteria-725 psi means to us quantitatively.

The surface area of inside tubing is

$$A_{in} = \pi Dh = 3.14 \times 5\text{in} \times 12\text{in} = 188 \ in^2$$

The pounds of force A_{in} can withstand

$$F_{in} = A_{in}P = 188.4in^2 \times 725psi = 137000 \ pound$$

The cross-section area of the tubing is

$$A_{cs} = \pi\frac{D^2}{4} = 3.14 \times \frac{5in \times 5in}{4} = 19.6 \ in^2$$

The pounds of force exerted on the end of the plug

$$F_{cs} = A_{cs}P = 19.6 \ in^2 \times 725psi = 14200 \ pound$$

Comparing the F_{in} and F_{cs}, if the bond strength of BPF/barite system bonded to steel is 725 psi, then a one-foot length in the wellbore will hold nearly ten times the force of a delta p of 725 psi in a five inch casing. So even if the strength is even further degraded, there is very large margin for error.

To conclude the simulated environmental tests, mixing with synthetic seawater did deteriorate the bond strength between barite-weighted epoxy and low carbon steel. However, the influence varies among different treatments. The more barite sensitive, the more reduction in bond strength it will cause. BPF performs more stable, economic in retaining bond strength after simulated environmental treatment.

4.5 Bond strength development tests

We did bond strength tests to see what influence the time will have on the bisphenol F system. The results show that epoxy/steel shear bond strength continues developing over the next 6 days, even though the resin hardening time (curing time) is far shorter than that.

In our previous research, we determined the relationship of the epoxy formulation with different weight percentage of barite and curing time (hardening time). Our laboratory work shows curing time is not equal to the time that the formulation needs to develop complete bond strength.

We prepared all the specimens same as that shown in Fig. 12 and carried out the pull-out tests by the same equipment in Fig. 14, and then did average calculation to analyze the data. All the original lab data can be found in appendix C.

Compared to the 2 hours curing time we obtained for the formulation with 66 wt% of barite, the bond strength keep developing for the next 6 days (see in **Fig. 24**). To reach the maximum based on our one-week test, the forecast in Fig. 24 shows it might need more than 6 days. Also, from the Fig. 24, it shows the bond strength can reach 725 psi of the North Sea Criteria around 10 hours, which is far shorter than 24 hours of cement hardening time (Kenneth et al. 2010).
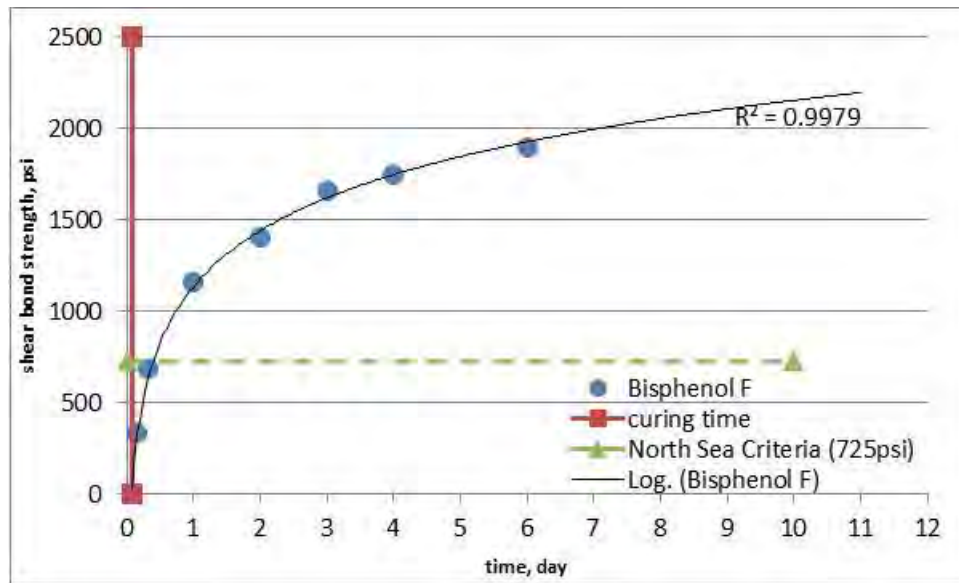
Fig. 24–The bond strength continues developing even after hardening time at 200 °F.

4.6 High temperature tests

We also carried out high temperature test to see the performance of epoxy material in high temperature, in case there are some wells located in high temperature formation. 200°F is a reasonable average reservoir temperature in Gulf of Mexico (Haeberle, 2005). The BPF does give us really excellent bond strength at 200°F. However, when increased the experiment temperature, the shear bond strength decreased significantly.

We did the high temperature test followed the procedure below:

1. Mix the F epoxy formulation with 13.5g barite.

2. Prepare all the samples in room temperature

3. Fabricate all the samples in heating oven either at 250°F or 300°F

4. Preheat the material test system shown in Fig. 14 at target temperature and transport the samples as quickly as possible to the material test equipment.

5. Hold the specimens by two vertical grips, and set up the software.

6. Following the randomization principle, do the pull-out test one by one.

7. Record the peak load that specimens are able to stand.

The results can be found in appendix D. The average values are shown in **Fig. 25.** The bond strength peak load at 250°F reduced 66% of bond strength compared to the one at 200°F. And the peak load at 300°F is only 18% of the bond strength at 200°F. The bond strength degradation is consistent with literature published by Benjamin J (2011). However, the reduction extent in other literature shows less than what we had in our experiment (Adamvalli and Parameswaran, 2008). There are some equipment limitations in our experiment that we cannot avoid. Take an example, we cannot not fabricate samples and pull out tests in the same heating facility. The interval to transport the samples might change the thermal history. The slight change in thermal history has influence on thermal expansion character. After a cooling down and heating up process, it is most likely to reduce the bond strength. Especially, when the fabricating temperature is high, the influence is much greater. The transportation interval for samples at 200°F experienced an around-100°F-temperature-drop process. While, for the one at 250°F experienced an around-150°F-temperature-drop process. And for the one at 300°F, it was a 200°F temperature-drop. The temperature factor at high temperature has greater influence on bond strength. So the higher temperature value might be

underestimated in this way. Also, in Benjamin J's paper, they proved that high temperature could cause weight adhesion loss as a result of aging and degradation. Their tests were carried out at temperature at 220 ℃ and plus, which is even higher than the temperature requirement in our proposal. All in all, one thing is undoubted that the bond strength is turning weak when the temperature goes up.
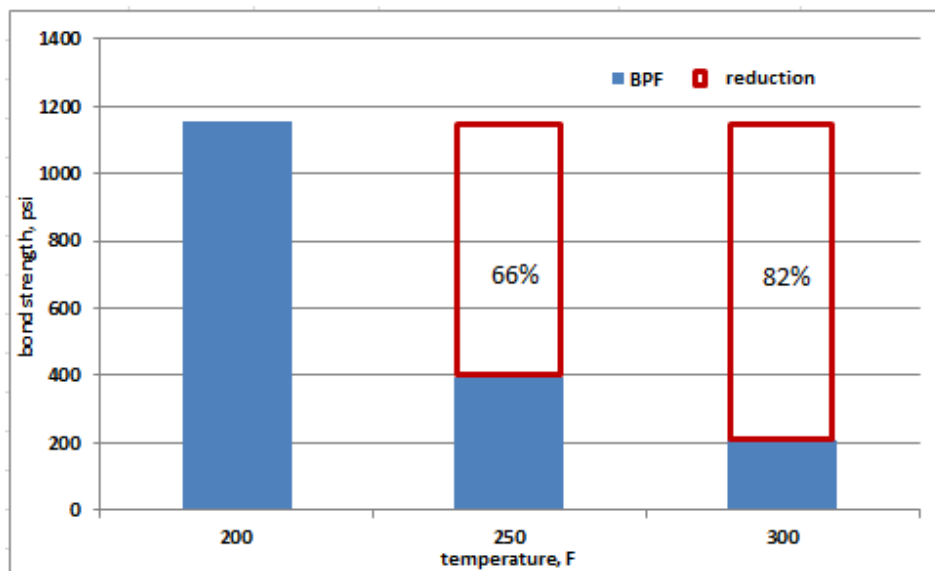
Fig. 25–Bond strength of F epoxy decreases as temperature goes up.

4.7 Discussion

As our research progressed, it became clear that the bisphenol A system had some undesirable characteristics that we would not like to see. Besides BPA's bond strength sensitivity to barite, which has been discussed in previous portions, the flow-ability at higher barite loadings was worse for BPA.

When they were shaken for the simulated environmental test, we could see the ability of flow-ability for the bisphenol A system is worse than that of the bisphenol F system, especially when barite addition is increased. When gathering all the simulated pictures together in Fig. 26, we can easily figure out that the difference of flow-ability in the bottom vials is obvious. It's more difficult for BPA with 71 wt% barite to flow as BPF did. The formulations in the vials with yellow and red sticker are hard to tell the flow-ability difference.

BPA VS BPF
16.5 wt% barite

BPA VS BPF
55 wt% barite

BPA VS BPF
71 wt% barite
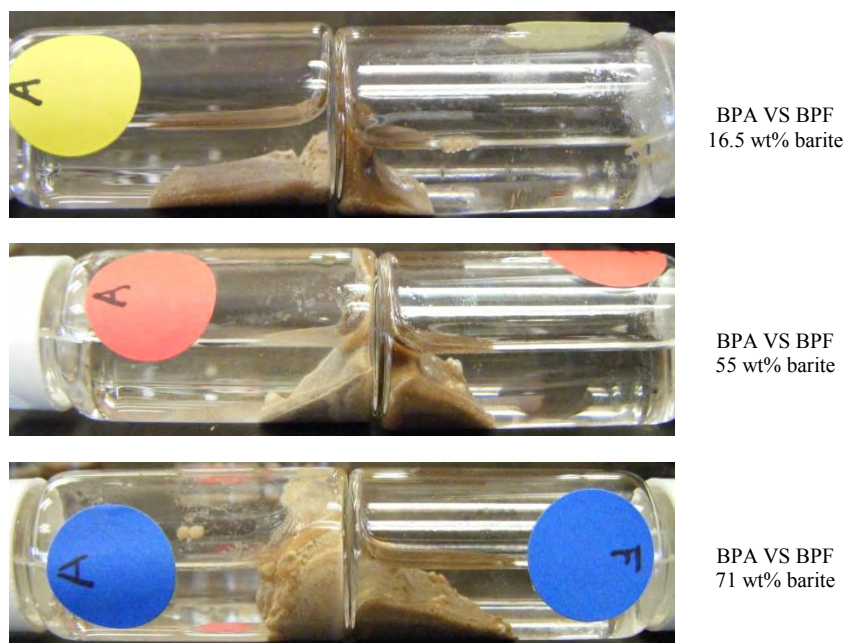
Fig. 26–The picture of flow-ability comparison among different treatments.

According to regulation established by The Netherland sector in Dutch mining authority guidelines, a plug on the borehole had to be tested with pressure min 725 psi inflow test (Liversidge et al., 2006). In our research, our laboratory results give us average bond

strength of the bisphenol F formulation from 1010 psi to 1160 psi as barite increased from 0 up to 70 wt% barites. The average bond strength of the bisphenol A formulation has minimum value of 1290 psi with 68 wt% barite, and maximum value of 2140 psi which appears at 0 gram of barite added. Both epoxy system meet the requirement. However, the BPF system is stable at bond strength both with and without the synthetic seawater treatment, while BPA system is much filler sensitive than BPF system. Also, in the simulated bond strength tests, formulations of BPF didn't meet the North Sea criteria. So improvement in the formulation might be needed in the future.

4.8 Limitations

Our tests were carried out in an ideal condition. In the real world, applications are likely to be affected by corrosion and organisms along the wall. In our tests, we didn't do any pretreatment on the surface of low carbon steel, either mechanically or chemically. Tubings and casings in the real world are not as smooth as what we had in our tests. Corrosion and organisms along the casing can increase the contact area which contributes to increase fictions and bond strength as well. At this point, corrosion and organisms might be something that we could take advantages of. Epoxy might not be the only material that we are going to apply in abandoned offshore wells in the GOM. Bentonite is also being considered. With bentonite, or any other heavier materials placed on the top of epoxy formulation, it would help epoxy to withstand more pressure differential than the value obtained in our pull-out tests.

Also, if we combine moisture and high temperature influence onto this barite-weighted epoxy system, the bond strength might be weaken more severely. One paper showed the temperature increasing might activate the process of absorbing moisture into the reinforced epoxy system, which leads to adhesion loss and bond strength reduction (B.C, 2006). Their experiments were actually tested in room temperature. We are also limited by our laboratory equipment and cannot carry out this complex effect experiment either. However, based on our previous work, we can have a general prediction that combining both moisture and high temperature weakens the bond strength. The extent need to be evaluated.

CHAPTER V

CONCLUSIONS

Previous research in our lab has shown resin hardening time increased with the amount of barite added, which is good to give sufficient time to complete the abandonment work. Tests in this project were carried out in ideal conditions. Real world applications are likely to be affected by corrosion etc. Shear bond strength tests in this study showed further properties of epoxy systems:

1. A large number of mechanical tests verified that the shear bond strength of bisphenol F type epoxy bonded to low carbon steel remained stable when barite filler was added to the formulation.

2. Simulated environmental tests demonstrated that when epoxy contacts steel in the presence of synthetic seawater, shear bond strength decreases. We suspect that the strength decrease is due to the epoxy-steel contact area being decreased and the bond thus weakened due to some capture of some seawater between epoxy, steel, and epoxy, barite.

3. Even though strength reduction must be accounted for in determining pressure differential that the epoxy-steel bond can withstand, bisphenol F system with barite bonded to low carbon steel retains sufficient shear bond strength to exceed all established regulations.

4. Epoxy-Steel shear bond strength continues developing for six days, much longer than hardening time and reaches 725 psi more rapidly than cement formulations.

5. Increasing temperature weakens the bond strength of the barite-weighted epoxy with the low carbon steel. At least a portion of the observed weakening is due to unavoidable temperature cycling caused by the necessity of curing the samples in a separate oven from the testing device oven.

6. Even with weakening at high temperature, the shear bond strength of BPF/barite system bonded to low carbon steel is strong enough so that even a short length of plug in a wellbore will meet the most stringent regulatory criteria.

7. The BPF/barite system should be evaluated in a test wellbore where the epoxy system must drop through several thousand feet of synthetic seawater and bond to a section of steel casing in order to demonstrate strength of the bond under more realistic conditions.

REFERENCES

Adamvalli, M. and Parameswaran, V. 2008. Dynamic Strength of Adhesive Single Lap Joints at High Temperature. *International Journal of Adhesion and Adhesives* 28 (6): 321-327. DOI: http://dx.doi.org/10.1016/j.ijadhadh.2007.10.005

ASTM. 2003. Test Method for Strength Properties of Adhesively Bonded Plastic Lap-Shear Sandwich Joints in Shear by Tension Loading [Metric]. In, CONTAINED IN VOL. 15.06, 2009 Specifies test method to complement Test Method D 1002 and D 3163 and extend its application to single-lap-shear adhesive joints employing plastic adherends.:4.

Benjamin J, A. 2011. Thermal Stability of High Temperature Epoxy Adhesives by Thermogravimetric and Adhesive Strength Measurements. *Polymer Degradation and Stability* 96 (10): 1874-1881. DOI: http://dx.doi.org/10.1016/j.polymdegradstab.2011.07.010

BOEMRE. 2006. *Assessment of Fixed Offshore Platform Performance in Hurricanes Andrew, Lili and Ivan*, by BOEMRE, E.E. Doc. MMS Project No.549, pt.

BOEMRE. 2007. *Assessment of Fixed Offshore Platform Performance in Hurricanes Katrina and Rita*, by BOEMRE, E.E. Doc. MMS Project No. 578, pt.

BOEMRE. 2010. *Assessment of Damage and Failure Mechanisms for Offshore Structures and Pipelines in Hurricanes Gustav and Ike*, by BOEMRE, E.E. Doc. MMS TAR No.642, pt.

Boyce D Burts, J., Boyce Donald Burts, I., Sabins, F.L. et al. 2011. *Well Remediation Using Downhole Mixing of Encapsulated Plug Components*. Doc. 7,886,823 B1, pt.

Boyce D Burts, J.B.D.B., III; Freddie L. Sabins; Larry Watters. 2010. *Surfaced Mixed Epoxy Method For*. Doc. 7,748,455 B2, pt.

Çolak, A., Çosgun, T., and Bakırcı, A.E. 2009. Effects of Environmental Factors on the Adhesion and Durability Characteristics of Epoxy-Bonded Concrete Prisms. *Construction and Building Materials* 23 (2): 758-767. DOI: http://dx.doi.org/10.1016/j.conbuildmat.2008.02.013

Cole, R.C. 1979. Epoxy Sealant for Combating Well Corrosion. Paper presented at the SPE Oilfield and Geothermal Chemistry Symposium, Houston, Texas. SPE-7874.

Cowan, K.M. 2010. *Geosynthetic Composite for Borehole Strengthening*. Doc. 7,741,249 B2, pt.: Shell Oil Company.

Englehardt, J., Wilson, M.J., and Woody, F. 2001. New Abandonment Technology New Materials and Placement Techniques. Paper presented at the SPE/EPA/DOE Exploration and Production Environmental Conference, San Antonio, Texas. SPE-66496. DOI:http://dx.doi.org/ 10.2118/66496-ms.

Haeberle, F.R. 2005. Gulf of Mexico Reservoir Properties Are Helpful Parameters for Explorers. *Oil&Gas Journal*.

Harris, D. and Adams, P.G. 2007. A New Offshore Rigless Intervention System. Paper presented at the SPE/IADC Drilling Conference, Amsterdam, The Netherlands. SPE-104747.

Jensen, M.K., Love, B.J., Grant, J.W. et al. 2000. Comparison Study of Dicyandiamide-Cured Epoxy Bonded Steel Joints and Polyamidoamine-Cured Epoxy Bonded Steel Joints. *International Journal of Adhesion and Adhesives* 20 (6): 437-444. DOI: http://dx.doi.org/10.1016/s0143-7496(00)00014-2

Joye, S.B., MacDonald, I.R., Montoya, J.P. et al. 2005. *Geophysical and Geochemical Signatures of Gulf of Mexico Seafloor Brines*: Biogeosciences. 2(3) (pp 295-309), 2005. Date of Publication: 2005. Original edition. ISBN.

Kahraman, R., Sunar, M., and Yilbas, B. 2008. Influence of Adhesive Thickness and Filler Content on the Mechanical Performance of Aluminum Single-Lap Joints Bonded with Aluminum Powder Filled Epoxy Adhesive. *Journal of Materials Processing Technology* 205 (1-3): 183-189. DOI: http://dx.doi.org/10.1016/j.jmatprotec.2007.11.121

Kemp, G. 1964. Field Results of the Stressed Steel Liner Casing Patch. *SPE Journal of Petroleum Technology* 16 (2). SPE-664. DOI: http://dx.doi.org/10.2118/663-pa

Liversidge, D., Taoutaou, S., and Agarwal, S. 2006. Permanent Plug and Abandonment Solution for the North Sea. Paper presented at the SPE Asia Pacific Oil & Gas Conference and Exhibition, Adelaide, Australia. SPE-100771.

Ng, R.C., Thurman W. Mc Pherson, I., and Hwang, M.K. 1994. *Casing Repair Using a Plastic Resin*. Doc. 5,295,541, pt. US: Mobil Oil Corporation.

Norsworthy, R. 2001. Test Results of Epoxy System Applied to Wet Pipe Surfaces. Paper presented at the CORROSION 2001, Houston, Tx. NACE International 01611.

Radecke, W., Scheibli, P.R., Wildschut, A.J. et al. 1959. 10. Epoxy Resin Coatings in the Oil Industry. Paper presented at the 5th World Petroleum Congress, New York, USA. World Petroleum Congress 8610.

Vaucher, D. and Brooks, R. 2010. Advantages of Inflatable Packer Technology for Temporary or Permanent Well Abandonment in the Gulf of Mexico. Paper presented at the SPE EUROPEC/EAGE Annual Conference and Exhibition, Barcelona, Spain. SPE-130271. DOI:http://dx.doi.org/ 10.2118/130271-ms.

Yi, N.H., Nam, J.W., Kim, S.B. et al. 2010. Evaluation of Material and Structural Performances of Developed Aqua-Advanced-Frp for Retrofitting of Underwater Concrete Structural Members. *Construction and Building Materials* 24 (4): 566-576. DOI:http://dx.doi.org/ 10.1016/j.conbuildmat.2009.09.008

APPENDIX A

Table A–Shear bond strength of different treatments, kgf$/$cm^2

Barite,g	Observations of BPA								Average, kgf/cm2
	1	2	3	4	5	6	7	8	
0		133.74	327.03	315.17	312.10	362.93	333.02	215.9	142.85
2.8	259.81	362.90	283.33	218.89	133.63		129.59	190.41	112.75
5.3	262.57	226.38	151.28	252.46	151.28	252.46	134.00	157.04	99.58
8.5	239.99	186.94	193.22	221.80		140.64	136.80		93.28
13.5	158.59	144.61	221.96		124.96	194.44	238.59	188.21	90.81
16	284.56	112.84	135.64	267.51	157.76	188.65	180.31	288.77	101.00
	Observations of BPF								
0	172.22	207.61	145.31	128.21	125.95	121.54	142.53	109.31	72.04
2.8	195.61	147.95	111.86	205.66	168.99	152.10	136.13	113.16	76.97
5.3	191.05	173.73	141.98		111.071		186.90	179.79	82.04
8.5	157.53	176.16	183.33	122.26	125.40	155.82	176.95	158.37	78.39
13.5	162.38	153.63	159.03	187.29	151.56	145.49	206.86	162.68	83.03
16	129.54	163.96	188.13	185.29	183.32	165.07	191.39	184.67	86.96

Table B–Shear bond strength data from simulated environmental tests, kgf/cm^2

Name of system	Barite, wt%	1	2	3	4	5	6	Average bond strength, kg/cm2
BPA	72	101.22	85.49	76.56	84.08	87.57	37.75	78.78
BPA	57	38.212	35.19	40.06	68.03	170.58	112.89	77.49
BPA	17	93.73	120.81	90.73	94.32	162.44	176.59	123.10
BPF	70	40.80	44.92	51.70	38.19	44.18	51.78	1278.99
BPF	55	90.22	93.84	77.25	96.92	81.12	79.54	300.21
BPF	16	62.81	67.21	63.49	78.94	98.26	106.17	978.78

Table C—Shear bond strength after different fabrication time, kgf/cm^2

Time, hr	1	2	3	4	Average, kg/cm2
2 hr	0	0	0	0	0
4hr	52.04	58.56	37.39	41.825	47.45
8hr	92.67	86.38	107.25	97.82	96.03
48hr	265.89	142.33	179.50	200.57	197.07
72hr	219.45	263.30	217.00	140.58	210.08
96hr	278.71	248.08	243.94	215.01	246.43
144hr	230.24	270.89	280.11	282.68	265.98

Table D–Shear bond strength at high temperature, kgf/cm^2

Temperature, F	1	2	3	4	5	6	7	8	Average, kg/cm2
200	162.38	153.63	159.03	187.29	151.56	145.49	206.86	162.68	162.68
250	43.27	54.72	55.84	50.62	54.46	59.88	61.54	55.517	392.37
300	28.63	25.58	28.76	29.61	32.95	30.06	28.65		207.23

VITA

Name: Zhuo Gao

                C/O Dr. Robert Lane

Address: Department of Petroleum Engineering

                Texas A&M University

                3116 TAMU - 501 Richardson Building

                College Station, TX, 77843-3116

Education: B.S., Oil&Gas Storage and Transportation Engineering,

                China University of Petroleum (East China). 2008

                M.S., Petroleum Engineering, Texas A&M University. 2011

Email Address: peggysayhi@gmail.com

THE EVALUATION OF THE MECHANICAL STRENGTH OF EPOXY-BASED RESIN AS A PLUGGING MATERIAL, AND THE DEVELOPMENT OF A NOVEL PLUG AND ABANDON TECHNIQUE USING VITRIFIED SOLID EPOXY-BASED RESIN BEADS.

A Thesis

by

AHMED RAMI ABUELAISH

Submitted to the Office of Graduate Studies of

Texas A&M University

in partial fulfillment of the requirements for the degree of

MASTERS IN SCIENCE

May 2012

Major Subject: **Petroleum Engineering**

THE EVALUATION OF THE MECHANICAL STRENGTH OF EPOXY-BASED

RESIN AS A PLUGGING MATERIAL, AND THE DEVELOPMENT OF A NOVEL

PLUG AND ABANDON TECHNIQUE USING VITRIFIED SOLID EPOXY-BASED

RESIN BEADS.

THE EVALUATION OF THE MECHANICAL STRENGTH OF EPOXY-BASED RESIN AS A PLUGGING MATERIAL, AND THE DEVELOPMENT OF A NOVEL PLUG AND ABANDON TECHNIQUE USING VITRIFIED SOLID EPOXY-BASED RESIN BEADS.

A Thesis

by

AHMED RAMI ABUELAISH

Submitted to the Office of Graduate Studies of

Texas A&M University

in partial fulfillment of the requirements for the degree of

MASTERS IN SCIENCE

Approved by:

Chair of Committee,	**Dr. Hisham Nasr-El-Din**
Committee Members,	**Dr. Jerome Schubert**
	Dr. Mahmoud El-Halwagi
Head of Department,	**Dr. Stephen Holditch**

May 2012

Major Subject: **Petroleum Engineering**

ABSTRACT

The Evaluation Of The Mechanical Strength Of Epoxy-Based Resin As A Plugging Material, And The Development Of A Novel Plug And Abandon Technique Using Vitrified Solid Epoxy-Based Resin Beads (May 2012). Ahmed Rami Abuelaish, B.Sc., Mechanical Engineering, Texas A&M University

Chair of Advisory Committee: Dr. Hisham Nasr-El-Din

Over the past several years, some of the platforms in the Gulf of Mexico have been damaged completely, such that conventional P&A operations may not be possible. In these cases, plugging fluid needs to be pumped through an intervention well and dropped several thousand feet in water to settle above a packer and seal the well.

The current P&A material of choice is cement, but cement is miscible in water, which dilutes and contaminates the cement. Therefore, alternate plugging materials need to be used for these operations. This paper discusses the development of a cost-effective Epoxy P&A method and the challenges of using Epoxy. First, the impact of seawater, oil, and pipe dope on the curing process remains unknown. Secondly, the yield strength of Epoxy with and without the contaminating chemicals must be equal to or better than cement. Finally, previous tests have shown significant losses of Epoxy to the walls of the wellbore during the 7,000-ft drop.

High temperature curing and compression tests were performed on contaminated epoxy samples to determine the effectiveness of the epoxy plug. To reduce material losses, an improved method for introducing the epoxy into the target zone was developed. This method takes advantage of a narrow window in the cure process where the curing process can be suspended by quenching the partially cured liquid epoxy in water at room temperature, thereby changing the liquid epoxy into solid beads. The beads can then be pumped into the wellbore, where they liquefy at wellbore temperature, 200°F, then cure into a solid plug.

Seawater was found to accelerate the cure time, while all contaminants tested reduced the fracture strength by more than 25% compared to pure resin. The yield strengths of contaminant mixtures, however, remained relatively constant, with the greatest drop being only 11%. The use of solid epoxy beads was found to have a compressive strength 50% greater than Portland cements I&II. In addition, the application mentioned herein eliminates the need to prepare the plug material on site. These advantages greatly contribute to reducing the costs of an epoxy P&A operation, to potentially being USD 0.7 million cheaper than a Portland cement operation.

ACKNOWLEDGEMENTS

I would like to thank my committee chair, Dr. Nasr-El-Din, and my committee members, Dr. Schubert, and Dr. El-Halwagi, for their guidance and support throughout the course of this research.

Thanks also go to my friends and colleagues and the department faculty and staff for making my time at Texas A&M University a great experience. I also want to extend my gratitude to the BOEMRE for funding this research, Professional Fluids Systems for providing me with all the resin I needed for the experiments, and Best-o-life for providing me with all the pipe dope material I needed.

Finally, thanks to my mother and father for their encouragement and support.

NOMENCLATURE

bbl/bbls	barrel/barrels
BOEMRE	The Bureau of Ocean Energy Management, Regulation & Enforcement
deg	degrees
ft	foot/feet
g	gram
gal	gallons
GOM	Gulf of Mexico
ID	inner diameter
in	inch
lb/lbs	pound/pounds
min	minutes
mL	milliliters
MMS	Mineral Management Services
O&G	Oil and Gas
OD	outer diameter
P&A	Plug and Abandon
PFS	Professional Fluid Services
ppg	pounds per gallon
PVC	Polyvinyl chloride

sec/secs	second/seconds
TETA	tri-ethylene-tetra-amine
TTT	time-temperature-transformation diagram
TVD	True Vertical Depth
TVDSS	True Vertical Depth Subsea
WOC	Wait on Cement
WGSO	Water/Gas Shutoff
vs.	versus

TABLE OF CONTENTS

LIST OF FIGURES

LIST OF TABLES

CHAPTER I: INTRODUCTION

There are currently approximately 80 producing offshore rigs in the Gulf of

Mexico, each with one or more drilled wells, all of which will eventually need to be

plugged either temporarily or permanently once they are no longer needed. One major

factor for abandoning a well is weather conditions, especially with the turbulent

hurricane weather that's common in the Gulf of Mexico. Over the past several years the

Bureau of Ocean Energy Management, Regulations and Enforcement (BEOMRE)

reported 9 jack-up rigs and 19 moored rigs were either toppled or torn from their

mooring systems by hurricanes Ivan, Katrina, and Rita. 61 platforms were destroyed as a

result of hurricanes Gustav and Ike in 2008, totaling 180 destroyed and 178 damaged

offshore oil and gas producing platforms between 2004 and 2008 (BOEMRE 2011). As

a result of this damage, many wells can no longer produce oil and gas safely, and/or

have become an environmental hazard, requiring them to be plugged and abandoned.

Standard procedures in the oil and gas industry involve using Portland cement

(ASTM types I and II, or API Classes A, C, G, or H) as the plugging material. Plugs are

typically placed across perforations, across certain intervals to isolate critical zones, or in

the wellbore and annulus to plug and isolate the well from the surface (Kelm and Faul

1999). These procedures typically involve using a workover rig and placing the cement

_____

This thesis follows the style of *Society of Petroleum Engineers*

through tubing, drillpipe, or coil tubing at the target zone (Barclay et al. 2004; Chong et al. 2000; Tettero et al. 2004). These cement plug systems may or may not be balanced between the inside and outside volumes of the pipe which may cause the plug to contaminate and dilute, due to contact with wellbore fluids (Calvert and Smith 1994). Contaminated and diluted cement often requires the plug to be redone.

Some of the hurricane damaged platforms may have been toppled completely and destroyed, their riser damaged, or well equipment and casing damaged due to mudflow at the seabed (BOEMRE 2011). Some of these wells may still be plugged by conventional methods, but for most wells, access through the wellhead may be blocked. In this case, an offset well needs to be drilled to access the wellbore, and plugging material be allowed to drop down the well to settle on top of a packer, as displayed in **Fig. 1**. While cement is significantly cheaper than other plugging materials such as epoxy resin, it is miscible, and dilutes, in seawater and brines used as packing fluids in the Gulf of Mexico, causing it to lose its mechanical strength. To successfully place the cement plug at the target zone would require the offset well to be drilled to the target zone and cement placed using conventional methods. At a target zone depth of 7,000 ft, the time and cost of such an operation may be substantial and would cancel the competitive price advantage of cement over alternative plugging fluids.
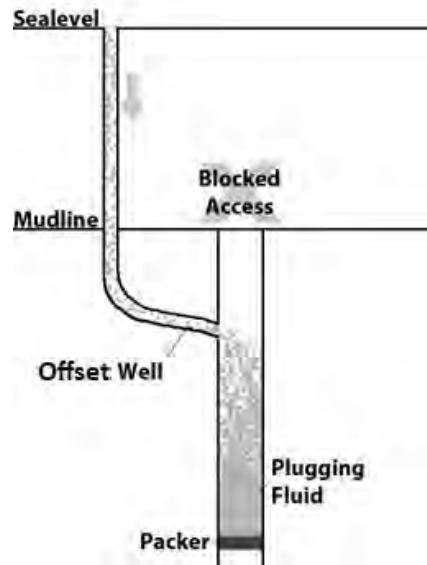
Fig. 1—Using an offset well to gain access to the wellbore.

During the drop in the wellbore, the plugging fluid will be in contact with any fluid or solids that are present in the well; as a result, contamination may occur. Many studies have been conducted to identify the quantity and type of contaminants in well tubulars (Holub et al. 1974; Jr. 1984; Maly 1976; McLeod Jr. et al. 1983). It was found that one of the most prominent contaminants in production tubing or an annulus is pipe dope in addition to hydrocarbons, sand, and debris (Gougler Jr. et al. 1985; Loewen et al. 1990; Nasr-El-Din et al. 2002). If the contaminants have a deteriorating effect on the curing time of epoxy resin, it may affect the plugging effectiveness of the fluid. The contaminants may reduce the maximum compressive strength or yield strength of the plug causing the onset of crack propagation leading to a leaking plug. There is a need to study the effect of contaminants on epoxy resin, whether curing in the presence of

contaminants, or mixing with contaminants during the drop then curing to determine the applicability of these fluids.

This thesis is part of a research effort funded by the MMS (now known as BOEMRE) which aims to investigate the applicability of epoxy-based resins or other non-cement materials as plugging fluids for hurricane damaged wells in the Gulf of Mexico, as mentioned herein. The materials in question have only been used in limited permanent plug applications, and the applicability of the materials has not been sufficiently studied. The MMS aims to develop on the following points:

1) Comparing epoxy-based materials against cement abandonments and other potential plugging materials

2) Determining whether epoxy material can effectively drop 7,000 ft through a casing annuli and accumulate on top of the packer

3) Determining how long material takes to travel to the bottom of casing annuli and cure

4) Determining how material performs over time

5) Determining how weighting of this material with $BaSO_4$ affects the compressive and bond strength of the material

6) Determining whether there are other weighting materials which may perform better than $BaSO_4$

7) Ranking various resin and hardener chemical systems for best performance in the field

8)   Evaluating the effects of various liquids such as calcium chloride, sea water, and formation hydrocarbons on the resin chemical systems

The research done for this thesis covers points 1 and 8 above. In addition, it addresses concerns raised by El-Mallawany regarding point 2. The work done focuses on the cure process of epoxy-based resins during the settling and curing of the plugging fluid. This thesis covers the effect of wellbore chemicals on the cure process of epoxy during the fall, where the fluids are constantly being mixed until the plugging fluid settles on top of the packer and cures at bottomhole temperature. The yield and maximum compressive strength of the solid plugs were analyzed to note any deterioration on mechanical strength by contamination. To address the effectiveness of dropping 7,000 ft in casing annulus, a new method was analytically and experimentally studied as an attempt to reduce the material losses during the fall. The method required studying the vitrification point of the epoxy to allow the formation of solid beads that liquefy at bottomhole temperature.

CHAPTER II: LITERATURE REVIEW

Epoxy-based resins are not new to the petroleum industry; they have been used for sand consolidation, resin coated proppants, remedial casing procedures, formation plugging and many other applications. For example, Kabir et al. discuss the use of resins and elastomers in water and gas shutoff applications. Thermosetting resins and elastomers are used because they have sufficient physical strength to seal fractures, perforations, and channels. Among resins, phenolic and epoxy resins are two of the types used. Conventional phenolic resin, or phenol-formaldehyde resin, may be formed by step-polymerization of phenol and formaldehyde forming a Resole as shown in **Fig. 2** (Peng and Riedl 1995). This reaction can be assisted by heating, but is slow and can be considered stable at room temperature. An acid or base catalyst is added before pumping which accelerates the reaction in the liquid and allows it to solidify at bottomhole temperature. Bottomhole temperature and pumping time should be known, to avoid polymerization of the fluid too soon or occurring too slowly (Kabir 2001). Epoxy resins are another type of thermosetting resin, especially popular in the aircraft industry. Epoxies are also common in construction and in the manufacture of composite materials with fiberglass and carbon-fiber. It consists of an epoxy group and a hardener. The hardener reacts with the epoxy, causing it to polymerize into a hard, inert plastic. Typically, epoxy is a product of the reaction between epichlorohydrin and bisphenol A, as represented in **Fig. 3**, and a common hardener is diethylenetriamine (Kabir 2001).
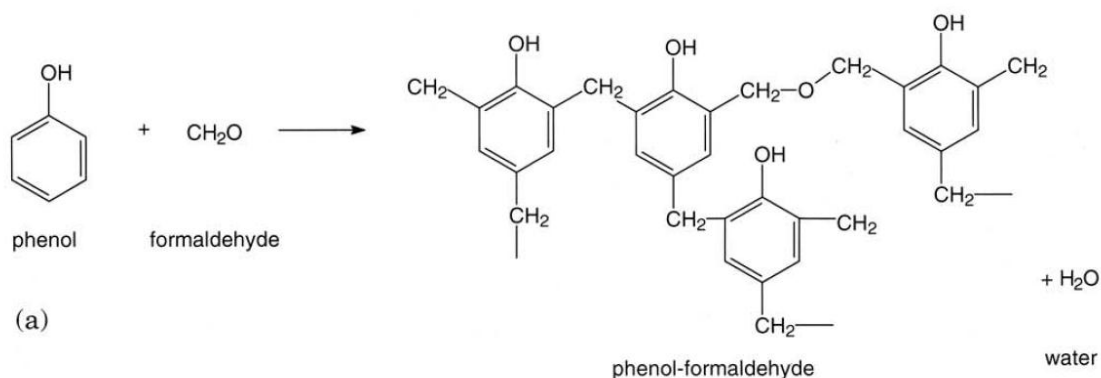
Fig. 2—The structure of a phenol-formaldehyde (Peng and Riedl 1995)
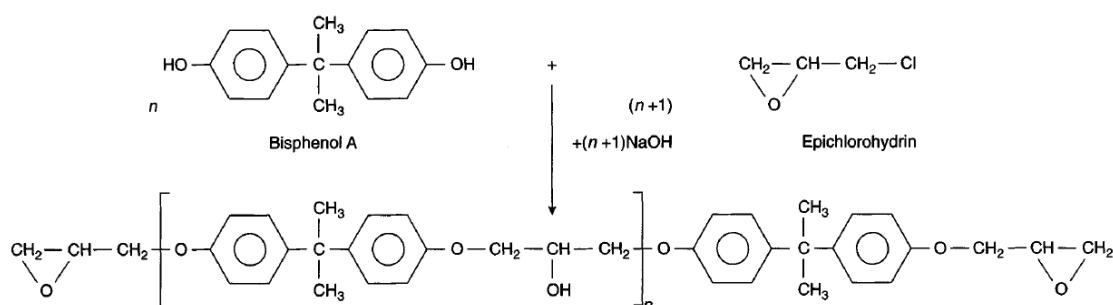
Fig. 3—Synthesis of a Bisphenol A based epoxy resin (Irfan 1998)

A patent by Ng et al. discusses the use of epoxy resin used to repair casing when it is damaged or corroded by wellbore fluids. The process described in the patent involves under-reaming the damaged section of casing and placing a retrievable packer right under the target zone, to create a surface for the epoxy to settle on. The epoxy resin mixture with hardener is then placed on top of the packer and flows into the thief zone, then forms a hardened solid underwater. The resin is typically placed with a dump bailer or through tubing squeeze in the target zone, both of these placement methods are not

suitable for the application intended herein. The solid plug formed can then be milled out to the same diameter as the casing, to form a resinous casing, as shown in **Fig. 4**. The patent explains that in wellbores at depths in excess of 5,000 ft, an environment of high temperature, high pressure, and corrosive chemicals will be encountered, which necessitates the repair in this manner. Often the wellbore is filled with materials, or brines, which deteriorate the integrity of most zonal isolation fluids. Hydrocarbons, water, saltwater, and other materials such as pipe dope, can cause the plugging fluid to deteriorate and lose effectiveness. In addition, during the time these plugging fluids are being pumped, the fluid will begin to harden during the operation such that the zonal isolation operation cannot be completed (Ng 1995). It is important to understand the cure process of the fluid in question and the effect of wellbore chemicals on the effectiveness of the plug.
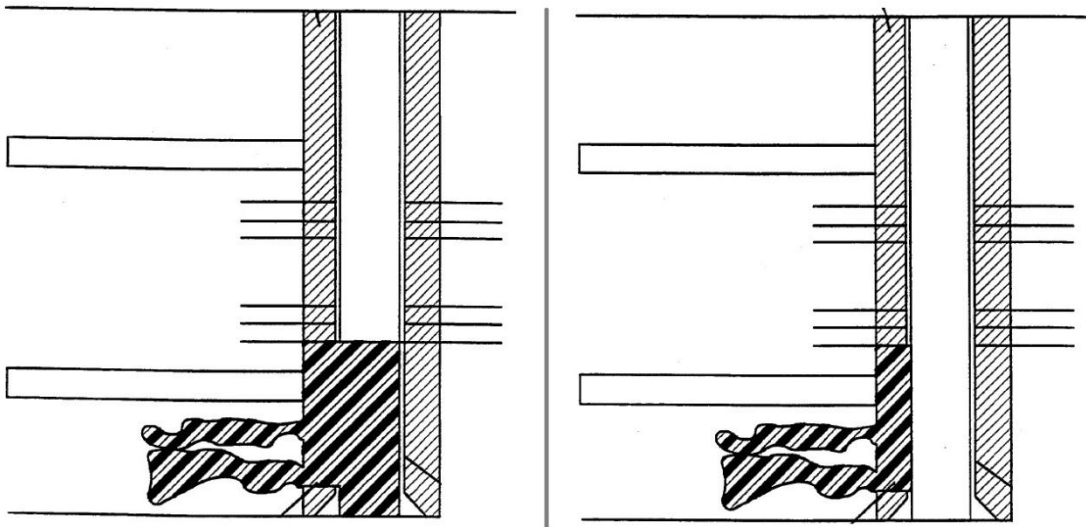
Fig. 4—Placing the epoxy resin in the thief zone and allowing it to cure, then milling out the hardened solid to the same inner diameter of the casing (Ng 1995).

ULTRA SEAL®-R, by Professional Fluid Services, is an epoxy-based resin that has been used in applications similar to the application discussed in this thesis and is the main material used for this research. In June of 2005, ULTRA SEAL®-R was used on Chevron's Vermillion 31 platform, to seal a leaking packer in an offshore production well without the use of a rig. The fluid was required to fall several feet in seawater and settle on top of the packer. 168 gallons of the fluid were loaded into the annulus along with 9 bbls of seawater. After 14 hours of settling time and 24 hours of curing time the plug was tested at 1,000 psi without pressure losses. PFS has applied ULTRA SEAL®-R in several other wells in the Gulf of Mexico, one of these was W&T Offshore-Ship Shoal 349, Well A7. The objective of the operation was to seal micro annular gas migration. To achieve the objective, two plugs were required. Prior to pumping Liquid Bridge Plug® (another name for ULTRA SEAL®-R), the well was cleaned by circulating

it with seawater. Prior to pumping the first plug, 15 ft of sand were pumped to the bottom then 7 bbls of Liquid Bridge Plug® were circulated down on top of the sand. The well was tested to 600 psi with no pressure loss over 24 hours. 12 bbls of Liquid Bridge Plug® were circulated to form the second plug and the well was tested to 800 psi with no pressure loss over 48 hours (P.F.S 2007).

Table 1—EPOXY FALL RATE IN 30 FT OF WATER (After El-Mallawany 2011).				
Annulus	Epoxy Density, ppg	Angle, degrees	Fall Rate, ft/min	Material Loss, %
6" - 0"	11.5	0	39.46	18.8
6" - 0"	13.2	0	41.71	19.3
6" - 0"	13.2	0	41.71	16.4
6" - 0"	14.7	0	50.34	28.4
6" - 0"	13.2	30	91.25	21.9
6" - 0"	13.2	45	85.88	27.7
6"-1.9"	11.5	0	36.5	24.9
6"-1.9"	13.2	0	42.94	25.8
6"-1.9"	14.7	0	60.83	31.4
6" - 3.5"	11.5	0	36.5	25.9
6" - 3.5"	13.2	0	44.24	26.3
6" - 3.5"	14.7	0	56.15	32.3

El-Mallawany developed an experimental apparatus to determine the fall rate of epoxy in a column of water, and measure the material losses during the fall. The apparatus involved a 30-ft column of clear PVC pipe mounted on a metal support structure. The structure is hinged and can be tilted at any angle between vertical and horizontal. Epoxy was dumped into the top of the pipe and collected at the bottom. The results of the experiments are presented in **Table 1** above, which shows significant trends in terms of annulus size, inclination, density, and material loss. It was found that the size of the annulus had no effect on the terminal velocity, where it averaged around

37.5-, 41.7-, and 55.8-ft/min for 11.5-, 13.2-, and 14.7-ppg formulations, respectively. On the other hand, a smaller annulus caused more material buildup on the walls, resulting in losses of up to 32.3%. It was also noted that in sloping columns, both fall rate and material losses increase, compared to a vertical column. **Fig. 5** shows the behavior of the epoxy as it falls through the water column. The fluid broke down into smaller droplets and spread through the water, but, due to the difference in densities, the epoxy fell to the bottom of the pipe and settled as one mass (El-Mallawany 2011).

Fig. 5—Epoxy breaking down into smaller droplets and spreading in a column of water (El-Mallawany 2011)

CHAPTER III: PRIMARY OBJECTIVES

1. Determine if there is a reduction in yield strength, fracture strength, or ultimate strength of cured epoxy-based resin as a result of being mixed for one hour with seawater, oil, or pipe dope during the 7,000-ft fall in the contaminant. Determine if any of the contaminants deteriorate the resin's integrity, to the extent of causing a 25% reduction in fracture strength compared to pure epoxy-based resin.

2. The application discussed in this thesis requires the resin to cure in the presence of wellbore chemicals. It is important to study the cure process of epoxy resin in the presence of seawater, oil, and pipe dope, to understand the changes in terms of cure time and level of gelation relative to pure resin. During a 6-hour cure time, the criteria for defining a significant change from the cure process of pure resin are a difference of 2 hours in the cure time, or a reduced level of gelation of 4 at 6 hours.

3. Determine whether the vitrification point of epoxy resins successfully allows the formation of solid beads without gelation. Secondly, determine whether the vitrified solid beads can be stored for a period of time greater than double the 6-hour cure period of the resin. Finally, determine whether the solid beads can be devitrified at wellbore temperature and reconsolidate into one mass and cure.

4. Determine if the compressive strength of the reconsolidated resin solid to can be an improvement over Portland cement, specifically creating an increase in strength of up to 50%.

5. Analyze the operational cost savings by comparing the use of vitrified resin beads to conventional cement. Determine cost savings created by reducing the material losses, due to using vitrified epoxy resin beads in place of pumping liquid epoxy in a 7,000-ft application.

CHAPTER IV: MECHANICAL STRENGTH TESTS

BACKGROUND

Epoxy-Based Resin

Epoxy resins are compounds with more than one ethylene oxide. These resins are called "thermosetting" resins, due to their ability to harden, or cure, with increasing temperature. Typical construction applications for epoxies require the resin to be mixed with other compounds or resins to achieve the desired characteristics of the thermoset (Irfan 1998). In some cases these resins are mixed with phenol-formaldehyde based resins.

The resin used in this thesis consists of Part A, Part B, and a diluent mixed in the ratios shown in **Table 2**. The content of Part A includes phenol-formaldehyde, Diglycidyesther and 1-chloro-2,3-epoxypropane, also known as epichlorohydrin. Phenol-formaldehyde is stable at room temperature, until it reacts at 200°F. The reaction is a step-growth polymerization, where phenol reacts with formaldehyde and forms a hydroxymethyl phenol. The hydroxymethyl group can react with another phenol and create a methylene bridge, or react with another hydroxymethyl group to form a diphenol, called bisphenol F. Bisphenol F is an important monomer that is present in epoxy resins, and it can further react with itself to create larger phenol oligomers. Diglycidyesther and epichlorohydrin, are epoxy resin components that react with the hardener triethylenetetramine, TETA, from part B causing it to polymerize into a hard, inert plastic (Kelland 2009).

Table 2—MIX RATIOS FOR ULTRA SEAL-R				
Component	**Weight**	**Volume**	**Density**	
	g	mL	g/mL	ppg
Part A	2.89	2.42	1.19	9.97
Diluent	0.29	0.3	0.97	8.07
Part B	0.87	0.91	0.96	7.98

Pipe Dope

Pipe dope is used as a thread lubricant, and thread sealing compound for casing and tubing threads. The main use is to make a joint leak-proof and pressure-tight. While most pipe threads are machined to form an interference fit with proper assembly, some machining and finishing variances will result in a less than 100% fit. Pipe dope is applied to all casing and tubing joints prior to assembly, to ensure minor gaps will be filled and any potential leaks blocked. As a result of the frequent use in the assembly of casing and tubing, pipe dope is one of the most prominent materials in production tubing and annuli (Gougler Jr. et al. 1985; Loewen et al. 1990; Nasr-El-Din et al. 2002). All the pipe dope compounds used in these experiments are products of Bestolife Corporation and conform to API RP 5A3 with the exception of "ZN 18", a zinc-based nonmetal compound. "ZN 18" was recommended for testing by the company representatives because of its popularity in the industry as a thread compound suitable for storage and light duty use. The main components of the pipe dope compounds are a petroleum grease mixture and either metallic or nonmetallic particles. "OCTG" is a black-copper compound which contains zinc, graphite, copper and other nonmetallic additives. "2000"

is a black-copper colored compound with lime, inert nonmetallic solids, and less than 4 wt % copper. "API Modified" is a black-copper colored compound with powdered graphite, copper flakes, lead powder, and zinc dust. "4010 NM" is a gray compound with graphite, calcium compounds, talc, and titanium dioxide. "Metal Free" is a black compound with synthetic and amorphous graphite, Teflon®, and other nonmetallic additives. The composition of the mentioned pipe dope compounds is presented in **Table 3**.

Table 3—6 TYPES OF "BESTOLIFE" PIPE DOPE	
Pipe dope	**Composition (with petroleum grease mixture)**
OCTG	Zinc, graphite, copper, & nonmetallic additives
2000	Lime, inert nonmetallic additives, & copper
API Modified	Graphite, zinc, copper, lead, & lime
4010 NM	Graphite, talc, calcium compounds, titanium dioxide
ZN18	Zinc
Metal Free	Synthetic and amorphous graphite, Teflon®, nonmetallic additives

Properties of Wells in the Gulf of Mexico

This research focuses on wells in the Gulf of Mexico; therefore it is necessary to perform all experiments in similar conditions. In offshore wells, seawater is present in abundance. The seawater mixture used in the experiments in this thesis, included, in decreasing weight percent: sodium chloride, magnesium chloride hexahydrate, sodium sulfate, calcium chloride dihydrate, and sodium bicarbonate, as listed in **Table 4**. Model wells will be chosen with a packer depth of approximately 7,000 ft TVDSS. At this depth the temperature is approximately 200°F based on the upper end of the temperature gradient scope which ranges between 0.8°F/ft and 1.9°F/ft as shown in **Fig. 6** (API 1999).

Table 4—COMPOSITION OF SEAWATER	
Salt	g/100mL of H2O
NaCl	3.839
CaCl2.2H2O	0.244
MgCl2.6H2O	1.906
Na2SO4	0.526
NaHCO3	0.027
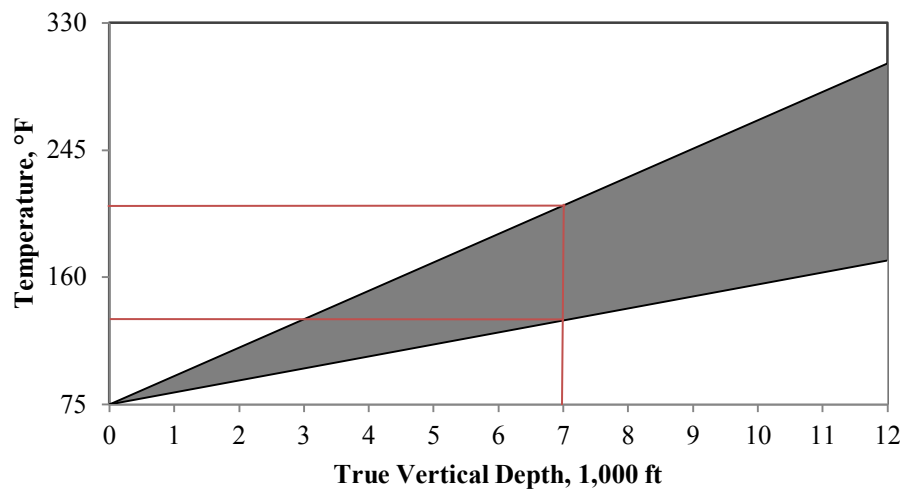
Fig. 6—The approximate temperature increase per 1,000 ft True Vertical Depth Subsea based on a 0.8 °F/100ft and 1.9 °F/100ft rate (data from API 1999)

Mechanical Strength

Hooke's Law

Hooke's Law of Elasticity states that the extension (or contraction) of a spring is directly proportional to the load applied on it. Many materials obey this law, as long as the load does not exceed the material's elastic limit. Hooke's Law is represented by

$$F = kx$$

where F is the applied load, x is the extension or contraction, and k is the proportionality constant.

Stress-Strain Curves

The mechanical strength of a material is largely defined by its internal stresses in the material. Knowledge of these stresses is essential in a safe design. When compressive or tensile tests are carried out on cylindrical specimens with different cross-sections of the same material, the breaking loads are found to be proportional to the cross-sectional area A of the specimen. This is because the strength of the material is determined by the intensity of the force on the normal cross-section, and not on the net force P. This intensity is known as the compressive stress σ, in the case of compressive loading. The compressive stress of a cylindrical specimen is defined as

$$\sigma = \frac{P}{A}$$

where P is the net axial force applied on the normal cross-sectional area A of the cylinder, as shown in **Fig. 7**.
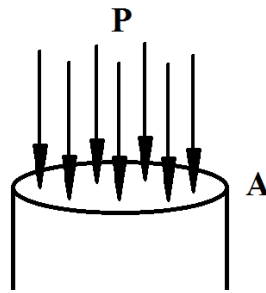
Fig. 7—Applied axial compression force *P* on the normal cross-sectional area *A* of a cylindrical specimen.

Strain, by definition, is a measure of the distortion of the material under a compressive or tensile load. The compressive strain is a non-dimensional quantity, and is the ratio of the contraction of the material *l* to the original length L_0 of the specimen; the compressive strain ε is defined as

$$\varepsilon = \frac{l}{l_0}$$

Many characteristics can be deduced from a compression test by creating a stress-strain curve. These characteristics are a more convenient method of comparing materials, than using loads and contractions. Typically, different brittle materials follow the same general trend, shown in the stress-strain curve in **Fig. 8**. The initial portion of the stress-strain curve is linear, where the material acts elastically obeying Hooke's law, and no permanent distortion occurs if the load is removed during this period. With increasing loads, the material begins to deform plastically up to the breaking point (Case et al. 1999).
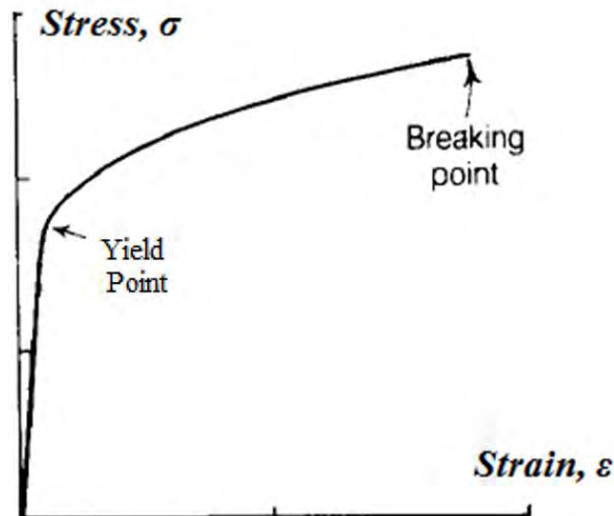
Fig. 8—Stress-Strain curve for a brittle material (after Case et al. 1999)

Brittle materials are classified as materials that exhibit relatively little contraction at failure. In contrast, materials such as mild steel and synthetic polymers show significant deformation before failure. These materials are classified as ductile materials. Ductile materials have the same general trend as brittle materials on a stress-strain curve but differ in some key characteristics. The stress-strain curve, in **Fig. 9**, obeys Hooke's law where the slope is linear and elastic up to a point called the yield point. Loading the specimen past this point exhibits a drastic decrease in the slope of the curve, where the stress decreases then remains constant while strain continues to increase. The material becomes strain-hardened, and the stress again begins to increase until failure. The point of highest stress, the ultimate stress, may be reached before or at fracture.
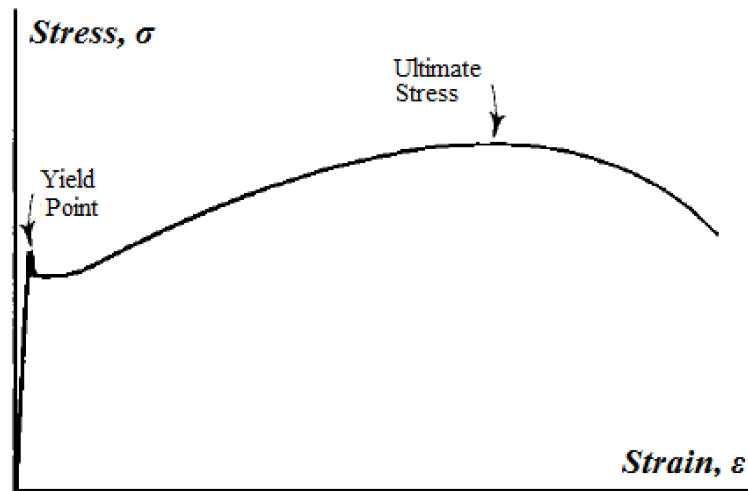
Fig. 9—Stress-Strain curve for a ductile material (after Case et al. 1999)

In certain cases, a material fractures at the yield point but continues to deform while maintaining a constant stress level. Wei et al. describe such materials as having crack tolerance. The residual stress due to crack tolerance allows the material to withstand the load until it eventually fails completely at the rupture point (Wei 2010). The rupture point is defined on a stress-strain graph by a sudden drop in stress.

Failure Modes

Ductile and brittle materials fracture in different manners. Brittle materials tend to fail with a fracture that extends in a diagonal plane in the specimen, as shown in **Fig. 10**, or crumble into smaller pieces.
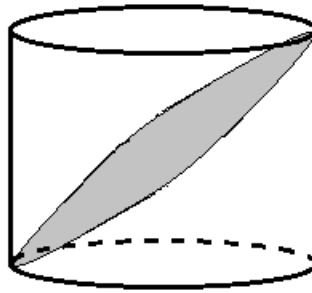
Fig. 10—Failure showing a fracture in a diagonal plane due to compressive loading on a specimen of a brittle material.

On the other hand, ductile materials experience greater contraction accompanied by radial expansion along the specimen resulting in a barrel-like shape as shown in **Fig. 11**.
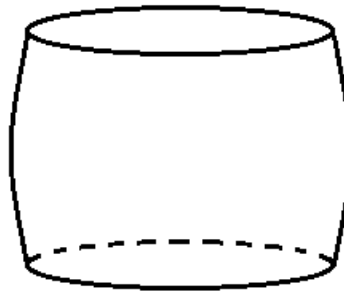
Fig. 11—Barrel-like failure due to compression on a specimen of ductile material.

OBJECTIVES

Determine if there is a reduction in yield strength, fracture Strength, or ultimate strength of cured epoxy-based resin, as a result of being mixed for one hour with seawater, oil, or pipe dope during the 7,000 ft fall in the contaminant. Determine if any

of the contaminants deteriorate the resin's integrity to the extent of causing a 25%

reduction in fracture strength compared to pure epoxy-based resin.

PROCEDURE

The parts of epoxy-based resin were mixed and allowed to cure in an oven under

a simulation of the plugging fluid falling 7,000 ft in the wellbore. This was carried out

by mixing the resin with each contaminant at wellbore conditions before allowing it to

settle and cure in the oven. The resin was prepared following the steps mentioned below:

1. Set the oven temperature to 200°F and allow it to reach steady state.

2. Prepare the first portion of the resin formulation by thoroughly mixing the

   Part A resin and diluent in a beaker based on the ratios in Table 2 above.

3. Mix in Part B of the resin formulation based on the ratios in Table 2

   above.

The samples simulating the 7,000 foot drop in the wellbore require the resin to be

mixed with the contaminant for a certain time period under certain temperatures to

replicate wellbore conditions. Preparation of the mixture requires the use of a heat-plate

magnetic stirrer, for the setup of a water bath and to create turbulence in the beaker. The

temperature in the water bath is linearly increased from 80°F to the bottom-hole

temperature, 200°F, for one hour, roughly matching the fall rate of the resin. The

procedure followed to prepare samples of resin mixed with contaminants is listed below:

4. Prepare a 150-mL batch of resin.

5. Set up a hot water bath by placing a 5,000-mL glass container on a magnetic stirrer/hot plate combination device.

6. Fill up approximately 400 mL of water and heat the water to 80°F.

7. Place the beaker of resin in the hot water.

8. Mix in the contaminant using a magnetic stirrer rod. Use quantities of contaminants based on **Table 5**.

9. Cover the large glass container and allow the fluid to mix for one hour while ramping the temperature of the water bath from 80°F to 200°F

10. Distribute the fluid into 50-mL Ultra-High Performance Centrifuge Tubes with 45 mL of fluid per tube.

Table 5—MIX RATIOS OF CONTAMINANTS IN RESIN			
	Mass of Resin, g	Mass of Contaminant, g	wt % Contaminant
Seawater	111	102	91.9%
ZN18	167	10	5.7%
API	167	9	5.6%
2000	167	10	6.0%
OCTG	167	10	6.2%
Metal Free	167	11	6.4%
4010NM	167	11	6.7%
Oil	80	57	72.0%

The strength of a material is a relation of the load and dimension of the sample. If the ratio of height to diameter of the specimen is equal to or less than 1.75, then the correction factor in **Table 6** must be applied to the stress values obtained (ASTM). It is important for uniaxial compression tests to maintain a load vector parallel to the axis of the sample being tested. As a result, the samples are required to have ends that are

parallel to each other and the surfaces of the compression machine. The ends are also required to be square with the sides of the cylinder to ensure uniform loading and deformation. The following list describes the steps necessary to achieve these requirements:

11. Remove the cured solid samples from the 50-mL Ultra-High Performance Centrifuge Tubes.

12. Use a band-saw to cut off the conical end of the sample and to cut the samples into two 1-inch long cylinders.

13. Sand the ends of the samples on a disc sander to ensure parallel ends to the sample as well as to smooth off the surface for an adequate compression test surface.

14. Measure the height and average diameter of each specimen.

15. Check each sample for its conformance to the requirement of parallel top and bottom ends. Any sample that does not meet the specifications is unsuitable for testing.

Table 6—CORRECTION FACTOR(ASTM)	
L/D	k, correction factor
1.75	0.98
1.5	0.96
1.25	0.93
1	0.87

The compression tests were run using an Instron 4206, **Fig. 12**, connected to a computer running a Labview data acquisition program. For each run, the machine was

allowed to apply a load on the sample until the sample failed or the load reached the load limit of 30,000-psi. A sample failing is indicated by a sudden drop in the measured load. The following steps list the directions used to run the compression tests and collect the data points:

Fig. 12—The Instron 4206 used for compression tests with a load limit up to 30,000 psi.

16. Turn on the Instron 4206.

17. On the control panel displayed in **Fig. 13**, hit "Load Cal" then "Enter"

18. Hit "Load Bal" then "Enter"

19. Hit "GL reset"

20. Hit "Speed" and set it to 0.2 inches per minute.

21. Launch the Labview program.

22. Start data acquisition by running the Labview program.

23. Hit the "Down" button to start the Instron.

24. Stop the machine when the sample fails or reaches the load limit of 30,000-psi.

Fig. 13—The control panel for the Instron 4206.

RESULTS & DISCUSSION

Pure Epoxy-Based Resin

The compression tests on samples of pure epoxy resin produced the expected stress-strain graph of a ductile material as shown in **Fig. 14**. The slope of the curve increases linearly up to, approximately, 13,900 psi and a strain of 0.11, where the stress dropped and remained relatively constant then gradually increased. Every specimen of pure resin experienced a gradual increase in stress until failure. The point of failure is the point of maximum stress, or ultimate stress, and averaged at 19,800 psi.
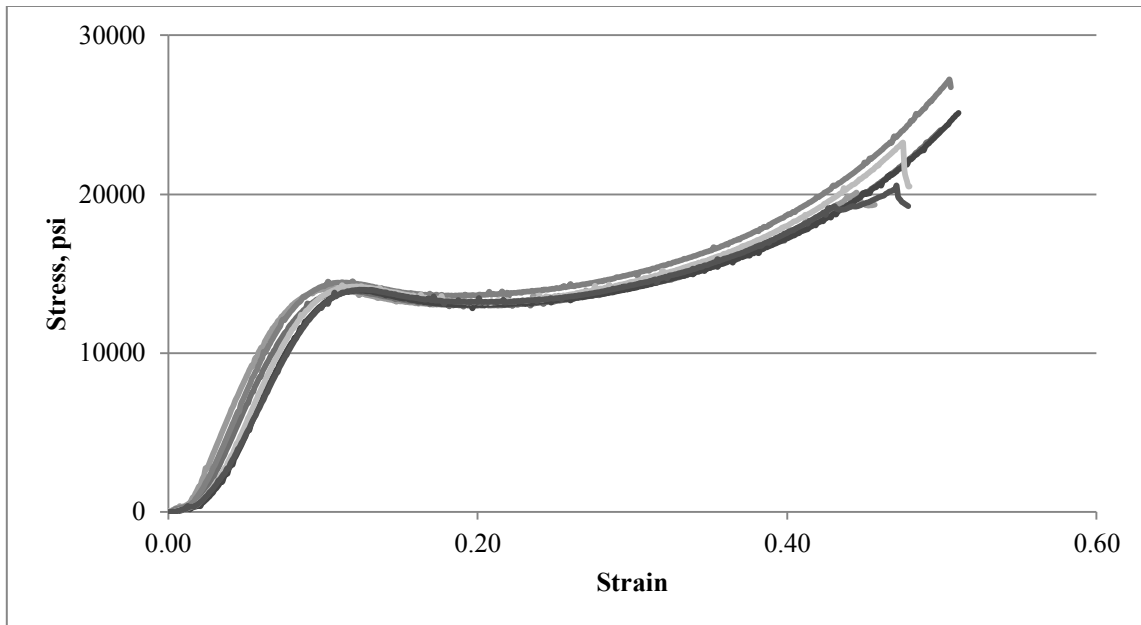
Fig. 14—The stress-strain curve from 6 experiment runs for pure epoxy-based resin, tested under compression until failure.

The resin specimens were clear, yellow solid cylinders, as shown in **Fig. 15**. Barreling of the specimen was initiated at the yield point. It then continued to withstand loads until the first crack propagated at the ultimate stress point. Once cracks formed, the specimen lost its integrity and lost its ability to withstand loads resulting in the crack pattern in Fig. 15.

Fig. 15—A specimen of pure epoxy-based resin before and after the compression test.

Seawater Brine

The resin was mixed with seawater for one hour, as described in the procedure section above. Before mixing the two fluids it was obvious the fluids were not miscible, as can be seen in the clear separation in **Fig. 16**.

Fig. 16—The separation of resin and seawater brine is apparent due to the fluids being immiscible.

After mixing the fluids for an hour and linearly increasing the temperature up from 80°F to 200°F, the resin and brine fluids formed an emulsion as can be seen in **Fig. 17**.

Fig. 17—An emulsion of resin droplets in seawater brine during and after mixing for one hour prior to curing.

Once the mixture was prepared and ready to be transferred to the oven to cure, the fluid was distributed among the centrifuge tubes. The epoxy resin droplets began separating out of the emulsion and a separation between the two fluids was again appearing, but only when settled in the oven for more than 15 minutes. The separation can be seen in **Fig. 18**. Over the first hour, the resin had settled at the bottom of the tubes and continued the cure process until fully cured.

Fig. 18—Epoxy and seawater brine mixture after being mixed for an hour then settling for approximately 15 minutes in a 200 °F oven.

Once the samples were fully cured, the compression tests were performed as described in the procedure section. The compression tests on samples of epoxy-resin mixed with seawater produced a stress-strain graph of a ductile material, as shown in **Fig. 19**. Initially, the slope of the curve increased linearly then decreased at the yield point, as it did for pure epoxy resin. Similar to pure epoxy resin, the yield strength and maximum compressive strength were two distinct points on the stress-strain graph. In addition, the maximum compressive strength corresponded to the fracture strength of the specimens. After the yield point, the stress dropped slightly then gradually increased. The specimens continued to deform until fractures propagated through the samples and resulted in the fracture pattern shown in **Fig. 20**.
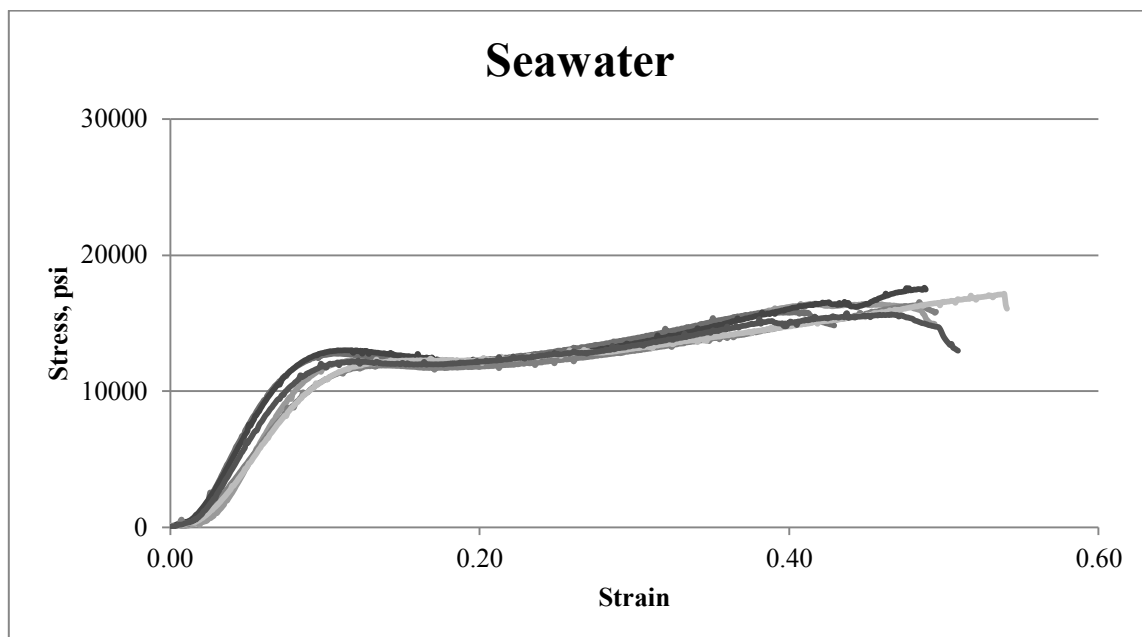
Fig. 19—The stress-strain curve from different experiment runs for epoxy-based resin with seawater brine, tested under compression until failure.

Fig. 20—A specimen of fully cured resin mixed with seawater brine before and after the compression test.

Pipe Dope

The different types of pipe dope were mixed in with the resin as described in the procedure section above. Initially, the pipe dope added to the solution settled at the bottom of the beaker, due to its greater density. Through mixing and heating, the liquid portion of the pipe dope mixed with the resin, and the solid particles were suspended in the fluid due to the turbulence of mixing. After the preparation stage, the samples were distributed over the centrifuge tubes and allowed to cure in the oven. By remaining stationary in the oven, the solid particles settled to the bottom of the tubes while the liquid portion of the pipe dope remained in the mixture.

ZN18

ZN 18 is a zinc-based nonmetal compound popular in the industry for storage and light duty use, despite not being rated per API RP 5A3. The ZN18 thread compound, shown in **Fig. 21,** is a grey compound of fine grey zinc dust held together by the organic grease having a yellow-green appearance. The fully cured mixture in **Fig. 22** shows the zinc particles collected at the bottom of the tube while the grease component of ZN18 pipe dope remained in the mixture.

Fig. 21—ZN18 thread compound

Fig. 22—The fully cured sample of resin mixed with ZN18 pipe dope.

Once the samples were fully cured, the compression tests were performed as described in the procedure section. The compression tests on samples of epoxy resin mixed with ZN18 pipe dope produced the stress-strain graph shown in **Fig. 23**. Initially, the slope of the curve increased linearly then the slope decreased at the yield point. It is important to note that, unlike the pure resin samples, these samples fractured at the yield point, but maintained a constant stress after the yield point while the sample continued to deform. The samples displayed the barreling effect at the yield point, which is an effect definitive of ductile failure, and formed the fracture pattern shown in **Fig. 24**.
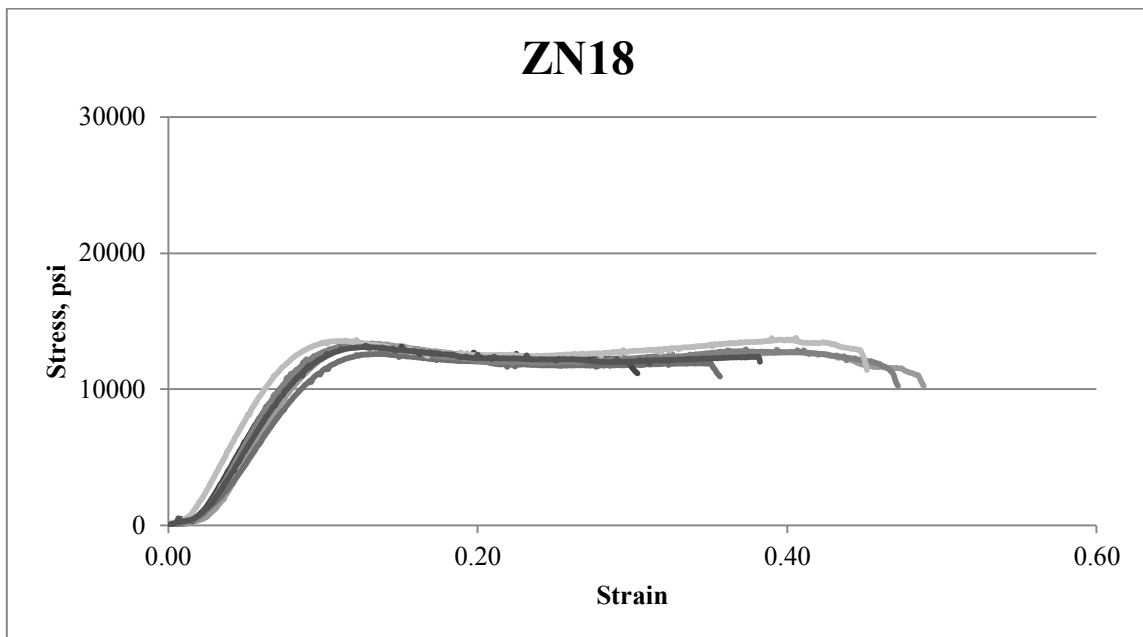
Fig. 23—The stress-strain curve from different experiment runs for epoxy-based resin with ZN18 pipe dope, tested under compression until failure.

Fig. 24—A specimen of fully cured resin mixed with ZN18 pipe dope before and after the compression test

API-Modified

API-Modified is a black-copper colored compound with powdered graphite, copper flakes, lead powder, and zinc dust which is rated per API RP 5A3. The API-Modified compound shown in **Fig. 25** is a dark brown/copper colored compound, held together by organic grease having a yellow-green appearance. The fully cured mixture in **Fig. 26** shows the grease component of API-Modified pipe dope mixed with the resin, and distributed solid flakes throughout the length of the sample.

Fig. 25—API-Modified pipe dope compound

Fig. 26—The fully cured sample of resin mixed with API-Modified pipe dope.

Once the samples were fully cured, the compression tests were performed as described in the procedure section. The compression tests on samples of epoxy resin mixed with API-Modified pipe dope produced the stress-strain graph shown in **Fig. 27**. Initially, the slope of the curve increased linearly then the slope decreased at the yield point. Similar to ZN18 samples, these samples fractured at the yield point and maintained a constant stress after the yield point while the sample continued to deform. The samples displayed the barreling effect at the yield point, which is an effect definitive of ductile failure, and formed the fracture pattern shown in **Fig. 28**.
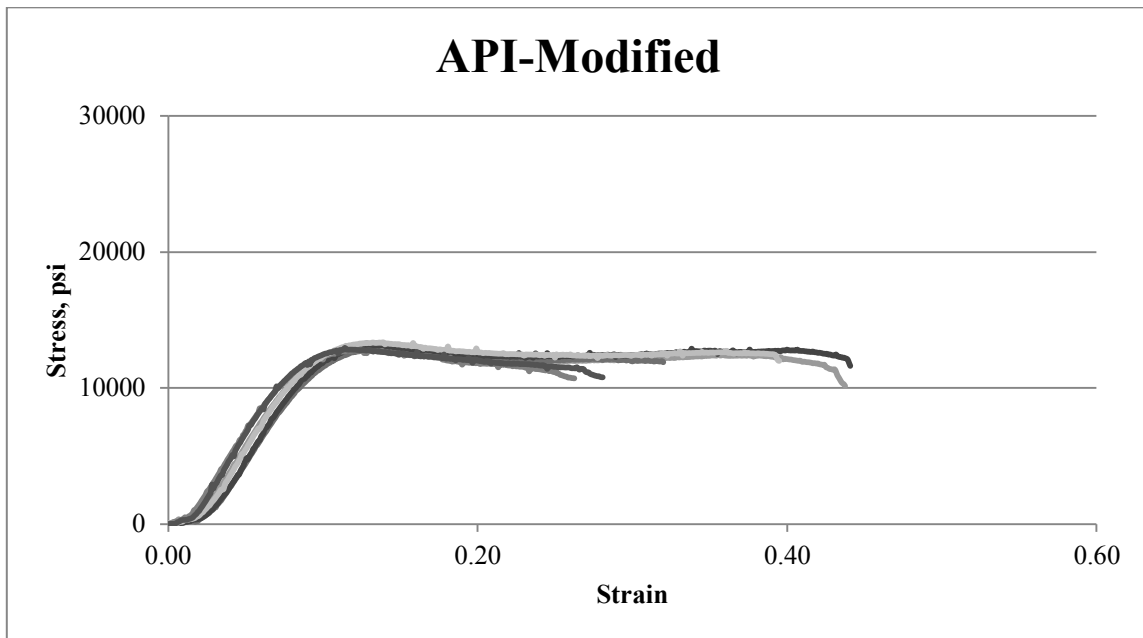
Fig. 27—The stress-strain curve from different experiment runs for epoxy-based resin with API-Modified pipe dope, tested under compression until failure.
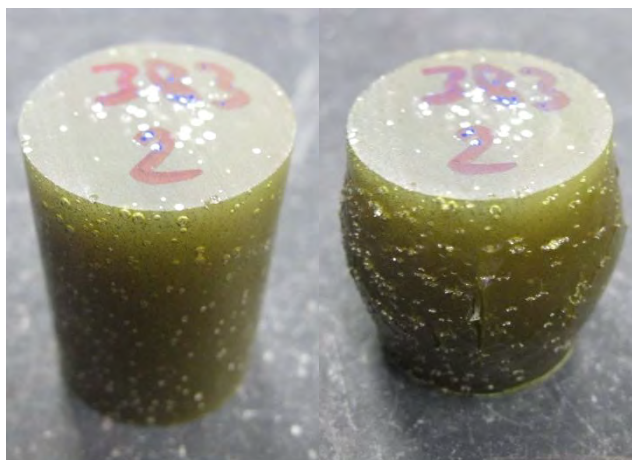
Fig. 28—A specimen of fully cured resin mixed with API-Modified pipe dope before and after the compression test

2000

2000, rated per API RP 5A3, is a black-copper colored compound, as shown in **Fig. 29**, with lime, inert nonmetallic solids, and less than 4 wt % copper. The solid particles of 2000 compound are held together by organic grease having a yellow appearance. The fully cured mixture in **Fig. 30** shows the grease component of 2000 pipe dope mixed in with the resin and distributed black solid flakes throughout the length of the sample.

Fig. 29—2000 pipe dope compound

Fig. 30—The fully cured sample of resin mixed with 2000 pipe dope.

Once the samples were fully cured, the compression tests were performed. The compression tests on samples of epoxy resin mixed with 2000 pipe dope produced the stress-strain graph shown in **Fig. 31**. These samples fractured at the yield point, and maintained a constant stress after the yield point while the sample continued to deform. The samples displayed the barreling effect at the yield point, which is an effect definitive of ductile failure, and formed the fracture pattern shown in **Fig. 32**.
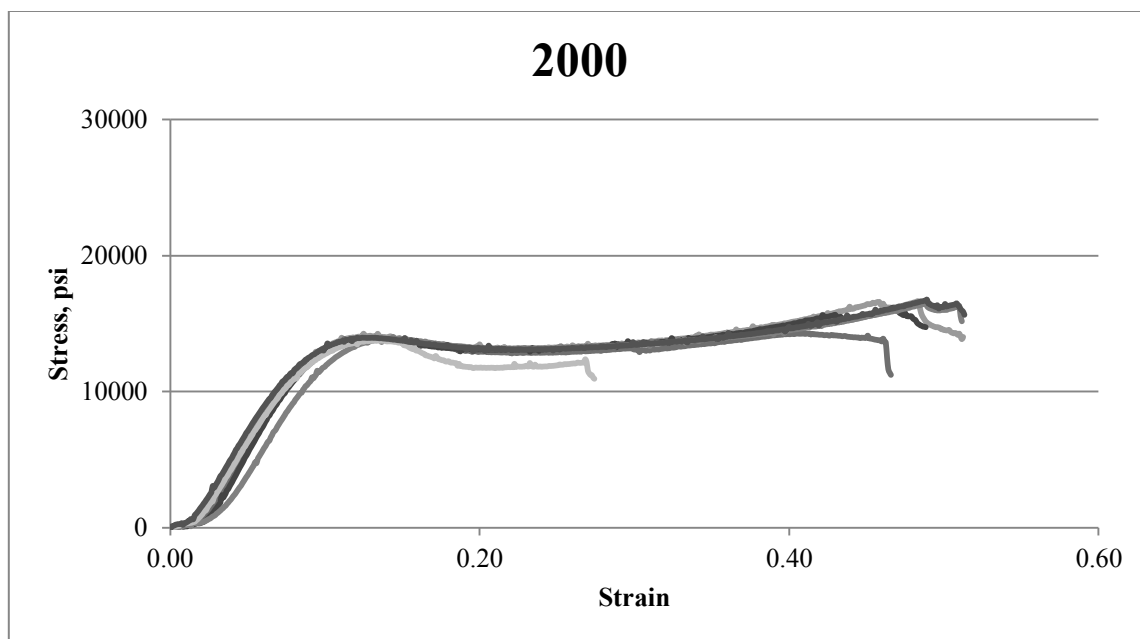
Fig. 31—The stress-strain curve from different experiment runs for epoxy-based resin with 2000 pipe dope, tested under compression until failure.

Fig. 32—A specimen of fully cured resin mixed with 2000 pipe dope before and after the compression test

OCTG

OCTG, rated per API RP 5A3, is a black-copper compound, as shown in **Fig. 33**, which contains zinc, graphite, copper and other nonmetallic additives. The fully cured mixture in **Fig. 34,** shows the grease component of OCTG pipe dope mixed in with the resin while solid particles in the compound settled out of solution to the bottom of the tubes.

Fig. 33—OCTG pipe dope compound

Fig. 34—The fully cured sample of resin mixed with OCTG pipe dope.

The compression tests were performed on the fully cured samples of epoxy resin mixed with 2000 pipe dope, and produced the stress-strain graph shown in **Fig. 35**. These samples fractured at the yield point and also started barreling at the yield point. The barreling effect and the fracture pattern on the specimen are shown in **Fig. 36**.
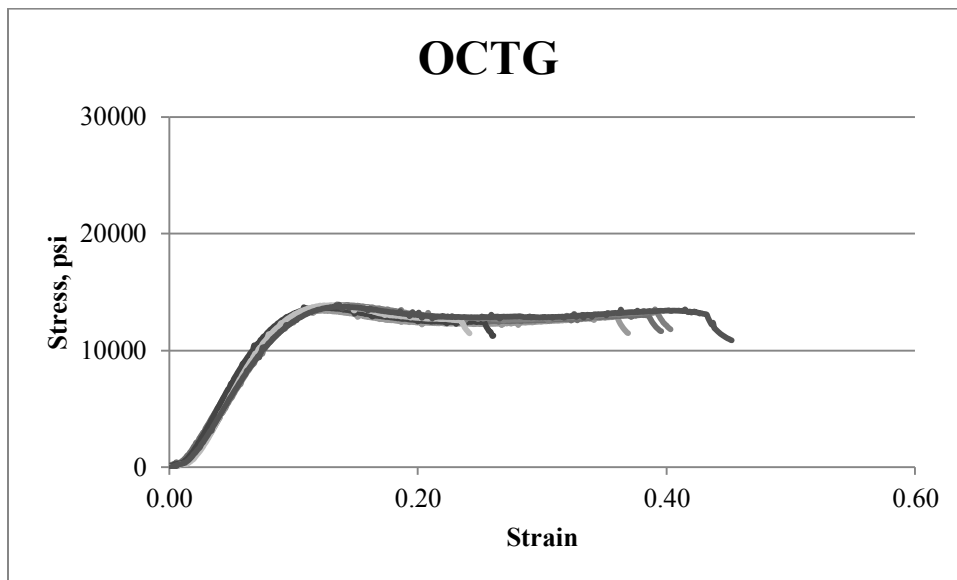
Fig. 35—The stress-strain curve from different experiment runs for epoxy-based resin with OCTG pipe dope, tested under compression until failure.

Fig. 36—A specimen of fully cured resin mixed with OCTG pipe dope before and after the compression test

Metal Free

Metal Free, rated per API RP 5A3, is a black compound, as shown in **Fig. 37**, with synthetic and amorphous graphite, Teflon®, and other nonmetallic additives. The fully cured mixture in **Fig. 38** shows the green grease component of Metal-free pipe dope mixed in with the resin, while the fine solid particles in the compound settled out of solution to the bottom of the tubes.

Fig. 37—Metal-free pipe dope compound

Fig. 38—The fully cured sample of resin mixed with Metal-free pipe dope.

The compression tests were performed on fully cured samples of epoxy resin mixed with Metal-free pipe dope, and produced the stress-strain graph shown in **Fig. 39**. The stress-strain graph displays a yield stress and ultimate stress, but samples were observed to fracture at the yield point, an effect in brittle materials. The samples

deformed elastically by barreling at the yield point, producing the fracture pattern shown

in **Fig. 44**, then continued deforming and strain hardening, despite the present fractures.
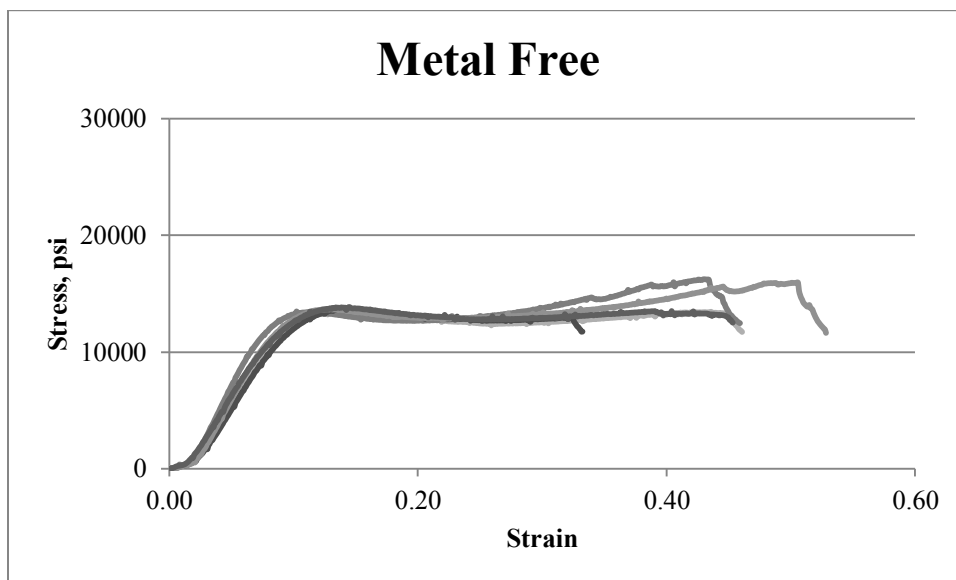
Fig. 39—The stress-strain curve from different experiment runs for epoxy-based

resin with Metal-free pipe dope, tested under compression until failure.

Fig. 40—A specimen of fully cured resin mixed with Metal-free pipe dope before

and after the compression test

4010NM

4010NM is a gray compound, rated per API RP 5A3, containing graphite, calcium compounds, talc, and titanium dioxide. The compound in **Fig. 41** shows a grey compound held together by the organic grease having a yellow appearance. The fully cured mixture in **Fig. 42,** shows the fine particles collected at the bottom of the tube while the grease component of 4010NM pipe dope remained in the mixture.

Fig. 41—4010NM pipe dope compound

Fig. 42—The fully cured sample of resin mixed with 4010NM pipe dope.

The compression tests we performed on fully cured samples of epoxy resin mixed with 4010NM pipe dope, and produced the stress-strain graph shown in **Fig. 43**. The samples deformed by barreling at the yield point, producing the fracture pattern

shown in **Fig. 44**, then continued deforming and strain hardening, despite the present

fractures. The fracture strength in this case is at the yield point of the stress-strain graph.
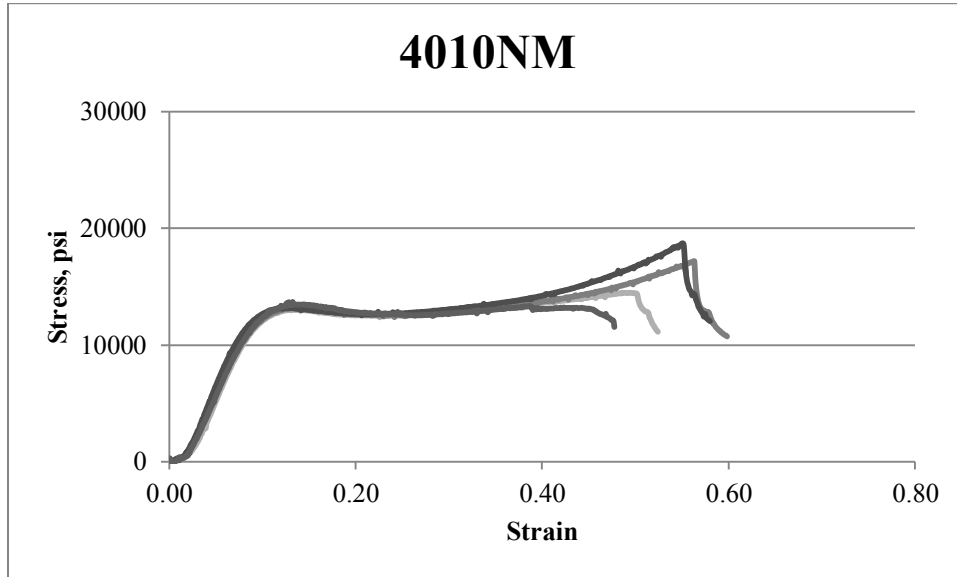
Fig. 43—The stress-strain curve from different experiment runs for epoxy-based resin with 4010NM pipe dope, tested under compression until failure.
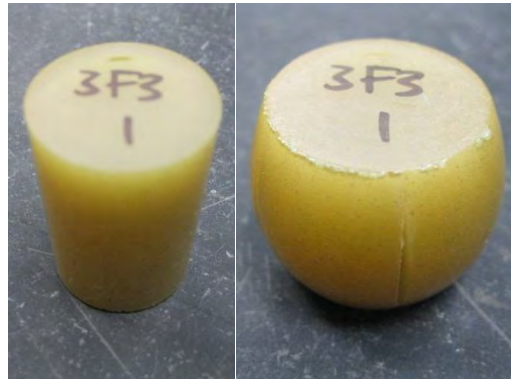
Fig. 44—A specimen of fully cured resin mixed with 4010NM pipe dope before and after the compression test

Sour Oil

Sour oil was mixed with the resin for one hour while linearly increasing the temperature from 80 °F to 200 °F as described in the procedure section above. The resin was miscible in oil, therefore, mixing the two fluids resulted in one homogeneous fluid which was distributed over the centrifuge tubes and allowed to cure in the oven. The fully cured sample was a dark brown/black opaque solid as shown in **Fig. 45**.

Fig. 45—The fully cured sample of resin mixed with sour oil.

Once the samples were fully cured, the compression tests were performed to produce the stress-strain graph shown in **Fig. 46**. The stress-strain was similar to that of pure resin, with distinct yield and maximum compressive strengths. In addition, the maximum compressive strength of these mixtures corresponded to the samples' fracture strength. At the yield point on the stress-strain graph, the samples experienced barreling then continued deformation while not forming any fractures. At the fracture point the specimens developed the shape and fracture pattern shown in **Fig. 47**.
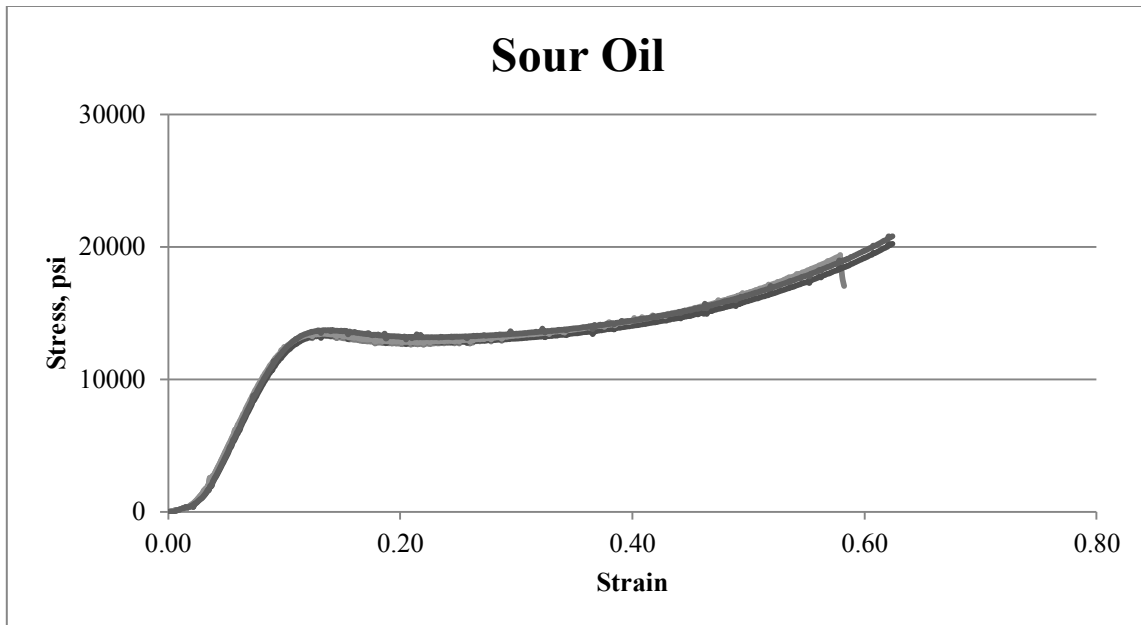
Fig. 46—The stress-strain curve from different experiment runs for epoxy-based resin with Sour Oil, tested under compression until failure.

Fig. 47—A specimen of fully cured resin mixed with oil before and after the compression test

Fracture Strength

The compression test results displayed a clear reduction in the yield and ultimate compressive strengths of the resin, as a result of mixing with contaminants. While it is typical for ductile materials to fracture at the ultimate compressive strength, the pipe dope samples experienced fracture propagation at the yield strength. The constant stress after the yield point, or the slight increase in stress after the yield point, is the result of crack tolerance and the samples maintaining residual strength. The highest yield stress was that of pure resin at 13,940 psi, as shown in **Table 7**, followed by the pipe dope compositions of 2000, Metal-free, and OCTG with less than a 1% drop in yield strength each. The pipe dope composition of 4010NM and ZN18, and sour oil resulted in a 3% to 6% drop in yield strength. While API-modified and seawater caused the largest drop in yield strength of 10% to 11% or approximately 1,400 psi to 1,500 psi.

Table 7—AVERAGE YIELD STRENGTH		
	Average Yield Strength, psi	**% Drop**
Pure	13,940	0%
2000	13,920	0%
Metal free	13,810	1%
OCTG	13,810	1%
4010NM	13,510	3%
Oil	13,510	3%
ZN18	13,170	6%
API modified	12,520	10%
Seawater	12,470	11%

The majority of the samples tested had only one value that corresponded to both the yield strength and the fracture strength. Only two mixtures, other than pure resin,

maintained fracture strength greater than their yield strength. These mixtures were sour oil, and seawater, as shown in **Fig. 48**. The pure samples, oil samples, and seawater samples had yield strengths that were 58%, 63%, and 75% less than their ultimate strengths, respectively.
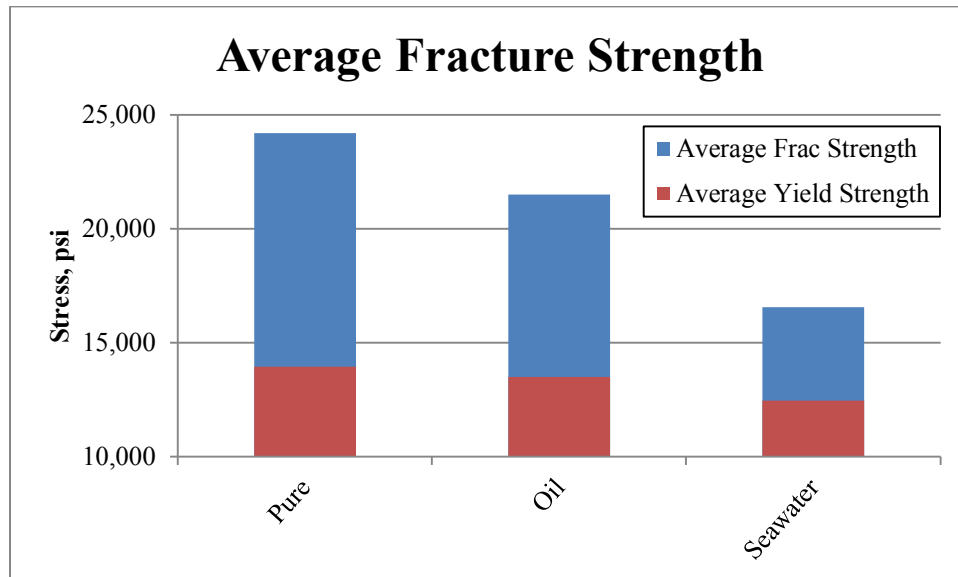
Fig. 48—The average fracture strengths of samples in comparison to their average yield strengths

The average fracture strengths of the oil and seawater samples were decreased by 11% and 32%, respectively, compared to pure resin. In comparison, the fracture strengths of the pipe dope mixtures resulted in a drop between 35% and 48% of the fracture strength of pure resin.

Table 8—AVERAGE FRACTURE STRESS

	Average Fracture Stress, psi	% Drop
Pure	24,190	0%
Oil	21,500	11%
Seawater	16,550	32%
2000	15,670	35%
Metal free	13,820	43%
OCTG	13,810	43%
4010NM	13,510	44%
ZN18	13,170	46%
API modified	12,520	48%

As shown in the results above, the addition of contaminants to pure epoxy resin reduced the maximum compressive strength and yield strength of the mixtures. The fracture strength corresponds to the maximum compressive strength for pure epoxy resin, the oil mixtures, and the seawater mixtures, but it corresponded to the yield strength for all pipe dope samples. The difference in fracture strengths between the samples tested was significantly greater than a 25% drop, while the yield strengths of all the samples remained relatively constant with the largest drop being as little as 11%.

CHAPTER V: EVALUATING THE EFFECT OF CONTAMINANTS ON THE CURE PROCESS OF EPOXY RESIN

OBJECTIVE

The application discussed in this thesis requires the resin to cure in the presence of wellbore chemicals. It is important to study the cure process of Epoxy Resin in the presence of seawater, oil, and pipe dope to understand the changes in terms of cure time and level of gelation relative to pure resin. During a 6 hour cure time, the criteria for defining a significant change from the cure process of pure resin, are a difference of 2 hours in the cure time or a reduced level of gelation of 4 at 6 hours.

PROCEDURE

The experimental procedure to test the cure process included an oven to simulate the temperature in the wellbore. The resin was cured in 10-mL or 30-mL screw-cap glass vials, or 50-mL Ultra-High Performance Centrifuge Tubes. The experiments discussed in this chapter were performed following the steps described below:

1. Set the oven temperature to 200°F and allow it to reach steady state.

2. Prepare the first portion of the resin formulation by thoroughly mixing Part A resin and diluent in a beaker based on the ratios in Table 2 above.

3. Mix in Part B of the resin formulation based on the ratios in Table 2 above.

4. Fill the glass vials with seawater brine, sour oil, or pipe dope according to the proportions in **Table 9** to create 10, 20, 30, 40, and 50 wt % contaminant in resin mixtures.

5. Fill each of the 10-mL glass vials with resin for a total of 4.00 g of mixture.

6. Place the vials in the 200°F oven.

7. At 1 hour intervals, measure the level of gelation of the samples based on the qualitative test method in **Table 10** until they are fully cured.

8. Record the cure time for each sample.

Table 9—COMPOSITION OF 4.00 GRAM SAMPLES						
	0 wt %	10 wt %	20 wt %	30 wt %	40 wt %	50 wt %
Mass of Resin, g	4.00	3.60	3.20	2.80	2.40	2.00
Mass of Contaminant, g	0.00	0.40	0.80	1.20	1.60	2.00

For each experiment cycle, 44 samples were prepared: five samples of 10, 20, 30, 40, and 50 wt % seawater brine, five samples of 10, 20, 30, 40, and 50 wt % Sour Oil, two samples for each of the 5 salts in seawater brine shown in Table 4, and 2 samples of 33 wt % of each of the 6 types of pipe dope shown in Table 3. In addition, for each run, at least two samples of resin without any contaminants were used with each test as the control. The samples were placed in the oven and analyzed at 1-hour intervals up to 7 hours. The experiments were repeated three times to confirm the results.

Level of Gelation

The level of gelation was determined qualitatively by a simple 0-5 qualitative test method. 0 indicates a resin with a water-like viscosity. 1 represents a resin with the same viscosity as the stable unreacted Part A fluid at room temperature. A level of gelation of 2 indicates a gel that moves or shakes when the vial is tilted or agitated. At a level of gelation of 3, the resin appears to be a solid but applying pressure on the surface when a 3-mm metal rod, shown in **Fig. 49**, easily penetrates the surface. At 4, the resin appears to be solid and applying pressure on the surface with a 3-mm metal rod creates a minor indentation but does not penetrate the surface. A level of gelation of 5 indicates a fully cured solid with no apparent indentation caused by pressure from the metal rod. The qualitative test method is listed in Table 10 below.

Fig. 49—The 3mm metal rod used in the qualitative level of gelation test

Table 10—THE LEVEL OF GELATION	
Level of Gelation	**Description**
0	Water-like viscosity
1	Thick liquid
2	Gel moves
3	Visually cured but applying pressure penetrates the surface
4	Cured but applying pressure creates minor indentation
5	Fully cured with no indentation when pressure is applied

RESULTS AND DISCUSSION

Pure Epoxy-Based Resin

The pure epoxy-based resin was prepared following the procedure mentioned in the section above to form a clear orange colored viscous liquid, as shown in **Fig. 50**. The initial state of the resin was a thick liquid with a level of Gelation of 1. After the first hour in the 200°F oven, the viscosity of the resin decreased to a level of Gelation of 0.5. Hourly testing showed a gradual increase in the level of Gelation of the samples until full cure at 6 hours, as shown in **Fig. 51.**

Fig. 50—Thick, clear, orange colored, viscous epoxy resin.
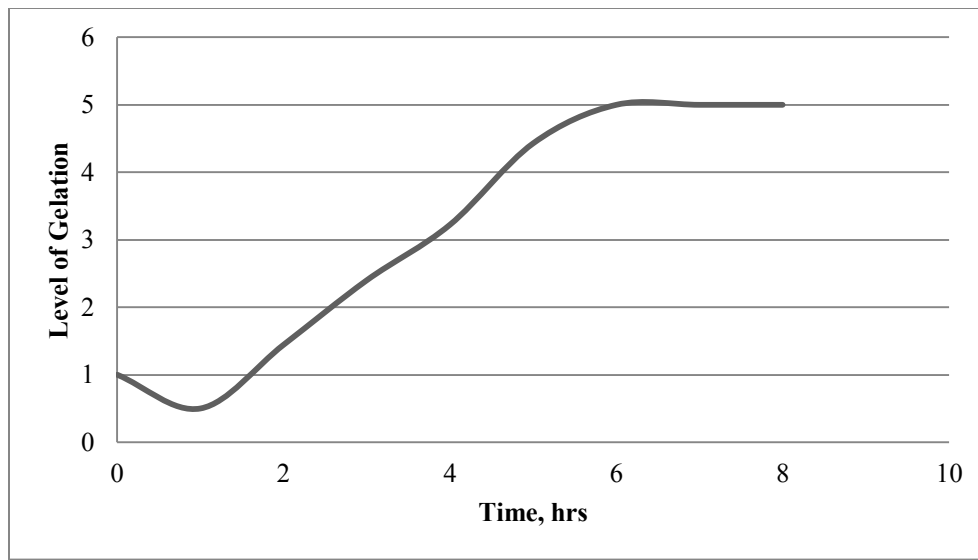
Fig. 51—The curing trend for pure epoxy-based resin which shows a decrease in the level of Gelation during the first hour, then a gradual increase until full cure at 6 hours.

Seawater Brine

The presence of seawater brine in the mixture increased the rate of the cure process, starting from the first hour into the experiment. At 1 hour, the resin's viscosity had increased to a level of Gelation of 1.5, as opposed to the expected result of a decreased viscosity and 0.5 level of Gelation. The samples reached full cure in as little as 3 hours, compared to the 6 hours for pure resin. The results for the cure process tests of epoxy-based resin cured in the presence of seawater brine are shown in **Fig. 52**.
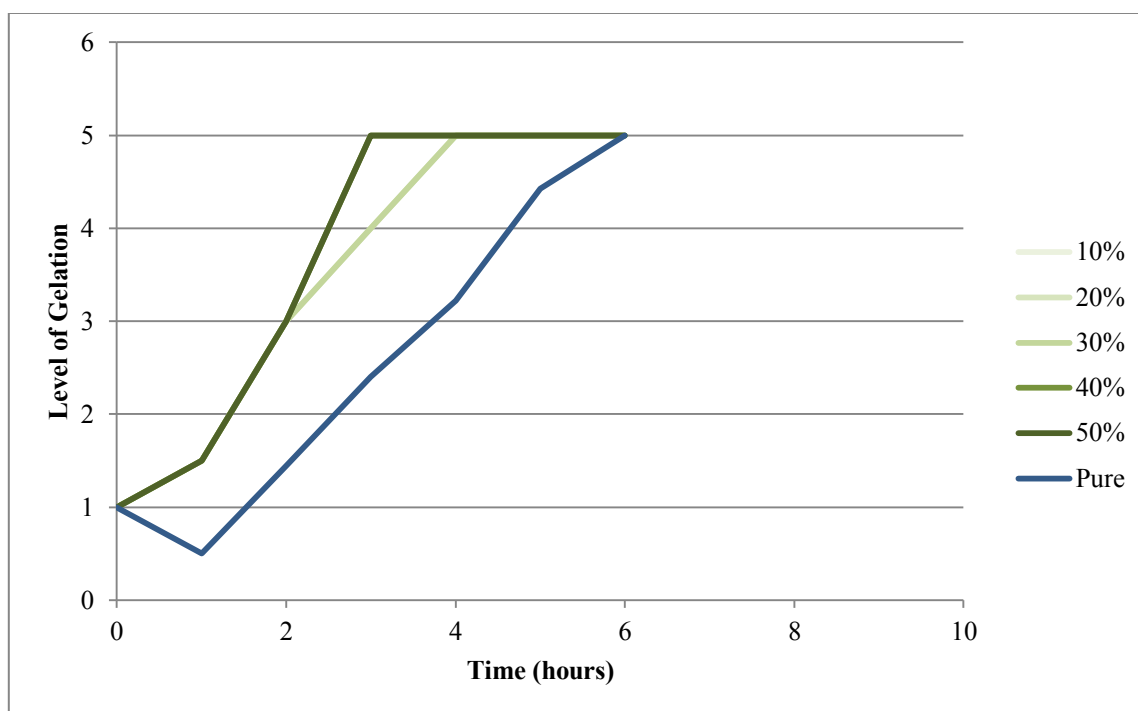
Fig. 52—The curing trend for epoxy-based resin in the presence of seawater brine at 10, 20, 30, 40, and 50 wt % seawater.

Samples of each of the five salts of seawater brine were tested separately with epoxy-based resin to determine the effect of each salt. The resin was allowed to cure in the presence of ten different brines. Each salt brine was prepared with only one salt, and for each salt, two brines were prepared with a "High" and "Low" concentration as listed in **Table 11.**

Table 11—COMPOSITION AND CONCENTRATIONS OF 5 BRINES

Salt	Name	Concentration, M
$NaCl$	High	0.86
	Low	0.44
$CaCl_2.H_2O$	High	0.34
	Low	0.14
$MgCl_2.6H_2O$	High	0.25
	Low	0.14
Na_2SO_4	High	0.35
	Low	0.22
$NaHCO_3$	High	0.60
	Low	0.43

Each sample was mixed in a 1:1 (by weight) ratio of brine to resin, and the cure process was analyzed following the procedure above. The cure trend of the ten brines followed similar trends to that of seawater brine. The cure process was accelerated for all ten brines. All the high concentration brines were fully cured by 3 hours, similar to seawater brine but the high concentration mixtures with NaCl were fully cured in as little as 2 hours. For each salt solution, the high concentration mixtures showed accelerated curing trends than the corresponding low concentrations and a shorter cure period, as shown in **Fig. 53**.
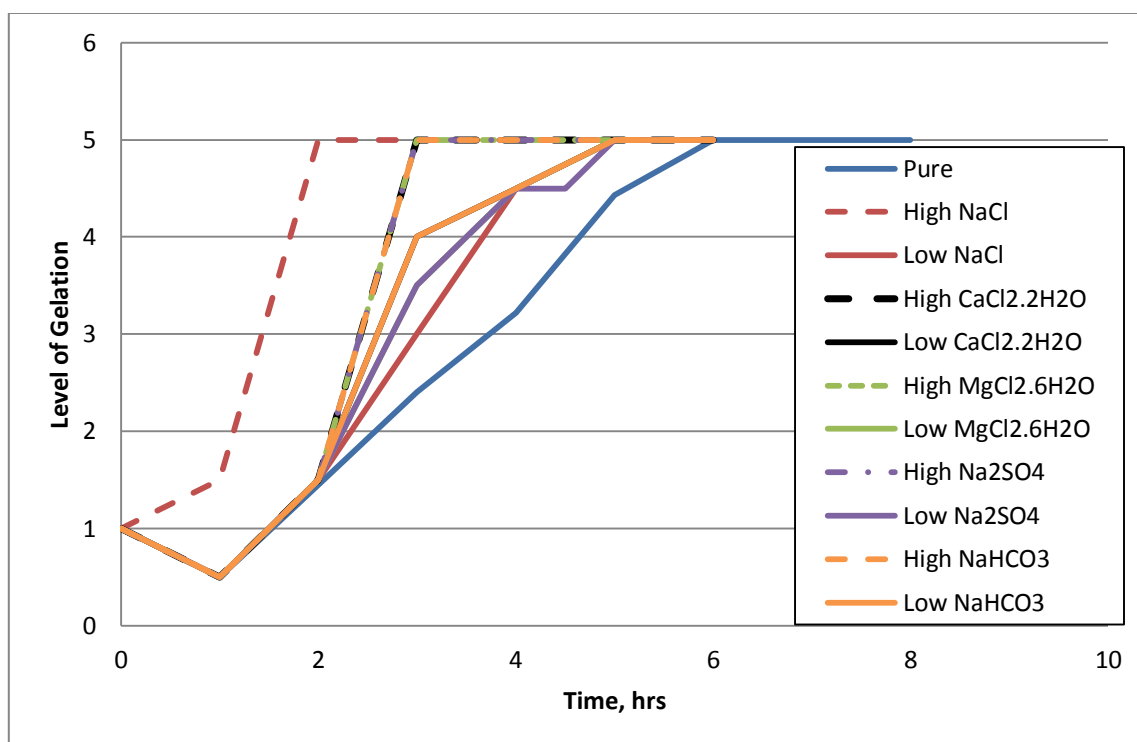
Fig. 53— The curing trend for epoxy-based resin in the presence of 50 wt % of 5 brines at 2 different concentrations.

Sour Oil

For each test run, five different mixtures of epoxy-based resin with 10, 20, 30, 40, and 50 wt % sour oil were tested. The presence of sour oil in the mixtures did not significantly affect the rate of the cure process, compared to pure epoxy-based resin, as shown in **Fig. 54**. Several samples removed from the oven at 3 hours began showing effects of vitrification, as will be discussed in a later chapter. The phase change due to vitrification was recognized by the sudden rise in the level of Gelation as the sample cooled. This highlighted the importance of testing all the samples at the oven's 200°F to get more accurate bottomhole trends. The phase change with sour oil was accompanied

by a change in color of the mixtures from a clear black-brown color to an opaque light

brown color as shown in **Fig. 55**.
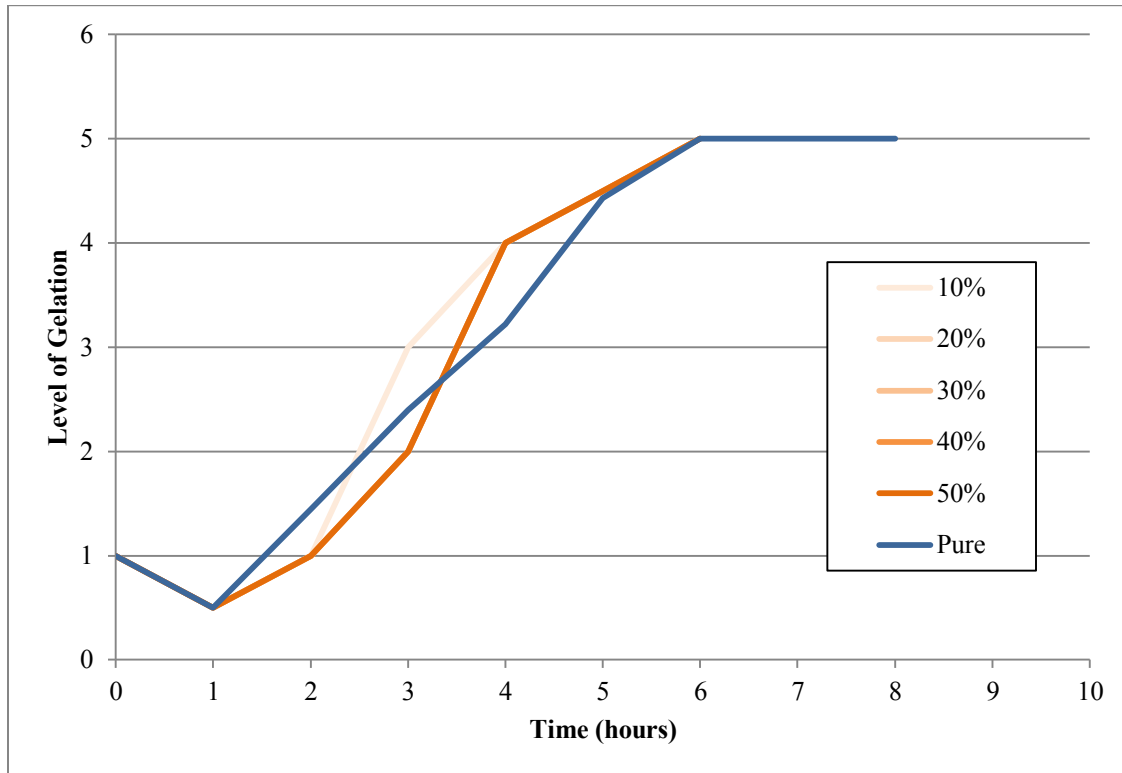
Fig. 54—The curing trend for epoxy-based resin in the presence of sour oil at 10,

20, 30, 40, and 50 wt % sour oil.
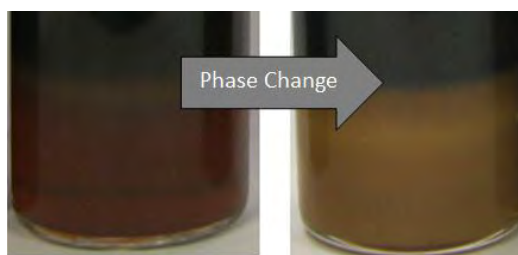
Fig. 55—The difference in color due to the phase change of resin mixed with sour-

oil caused by the change in temperature from 200 °F to room temperature.

Pipe Dope

Separate samples were prepared for each of the 6 types of pipe dope. Pipe dope is typically composed of organic grease and a mixture of inorganic materials. In these experiments, the samples all remained heterogeneous, where the inorganic material dropped out of solution and the organic material was mixed in with the resin. The samples exhibited altered curing trends. OCTG, 2000, and API-modified exhibited elastic properties at 4 hours, where applying pressure on the surface created an indentation but did not penetrate the surface. At 6.5 hours, these three mixtures maintained hard rubber properties. 4010NM, ZN18, and "Metal Free" remained at a level of Gelation below 3 up to 4 hours and "Metal Free" displayed an increased tackiness compared to pure resin. By 6.5 hours, the OCTG, 2000, API-modified, ZN18, and "Metal Free" maintained a hard rubber texture, but had not fully cured. 4010NM, on the other hand, had separated at 4 hours into 3 phases. The topmost phase was a water-like liquid, a low viscosity resin in the middle, and the inorganic material at the bottom. At 5 hours it remained very soft and tacky with a level of Gelation of 3, then at 6.5 it became a soft elastic material with a level of Gelation less than 4, as shown in **Fig. 56**. In less than 24 hours all samples had fully cured, but maintained heterogeneity in the mixture which affected the mechanical strength of the sample.
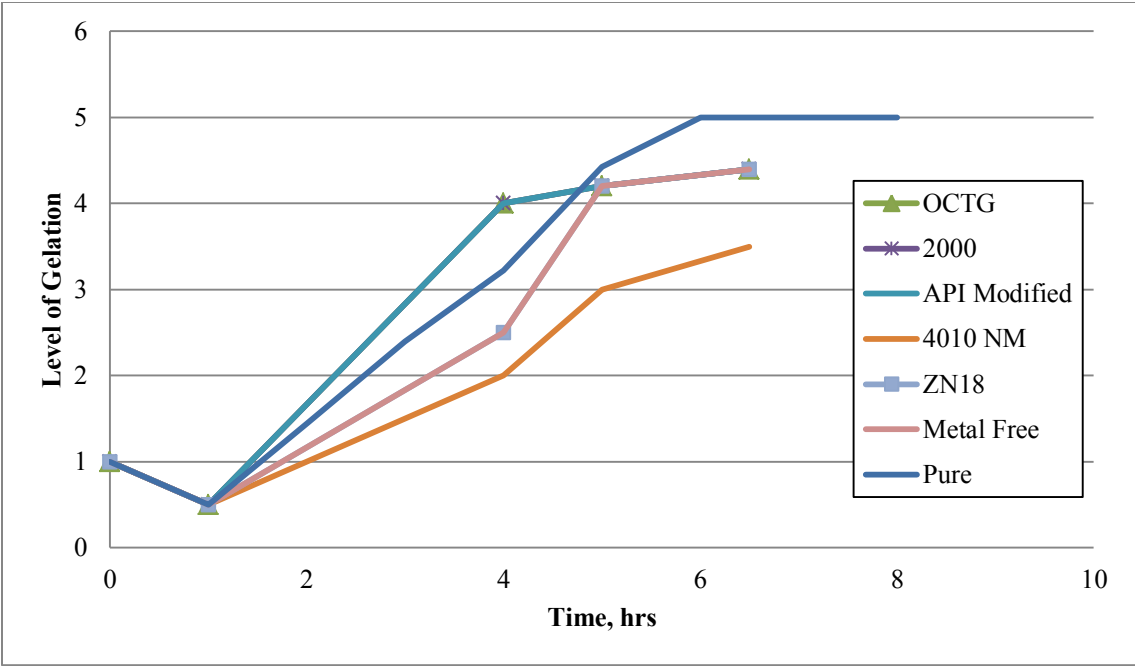
Fig. 56—The curing trend for epoxy-based resin in the presence of the 6 types of

Best-o-life pipe dopes: OCTG, 2000, API modified, 4010NM, ZN18, and Metal Free

CHAPTER VI: EVALUATING THE USE OF SOLID EPOXY RESIN BEADS AS A PLACEMENT METHOD

BACKGROUND

Vitrification and Gelation

A time-temperature-transformation (TTT) isothermal cure diagram, shown in **Fig. 57**, can be used for understanding the cure properties of thermosetting systems (Dawkins 1986; Gillham 1985). The main events of such a diagram include the onset of gelation, vitrification, and full-cure. Gelation corresponds to the formation of an infinite molecular network, according to Flory's theory of gelation (Flory 1953). Vitrification, a completely distinct phenomenon from gelation, can occur at any stage during the reaction to form either an ungelled glass or a gelled glass. In the glassy state, the rate of reaction undergoes a significant decrease but is not zero. Unlike gelation, vitrification is reversible by heating, and the cure process may be reestablished by heating to devitrify the partially cured Epoxy (Menczel 2009).

During the cure process, the system follows the isothermal line labeled as "Cure Process" in Fig. 57 where the resin goes through gelation, vitrification, and eventually full cure. Interrupting the cure process at a time, t, by reducing the temperature of the resin, will cause the resin to vitrify into an ungelled glass and significantly decrease the reaction rate. The time at the point of gelation is assumed to be the cure time, then, according to Fig. 57, the point of vitrification at T_{gel} is greater than the cure time. Assuming time t is a fraction of the cure time, then time t corresponds to the point at

which the ratio of t to the cure time at T_{gel} is equal to or greater than the ratio of the time

to vitrification over the cure time at room temperature.
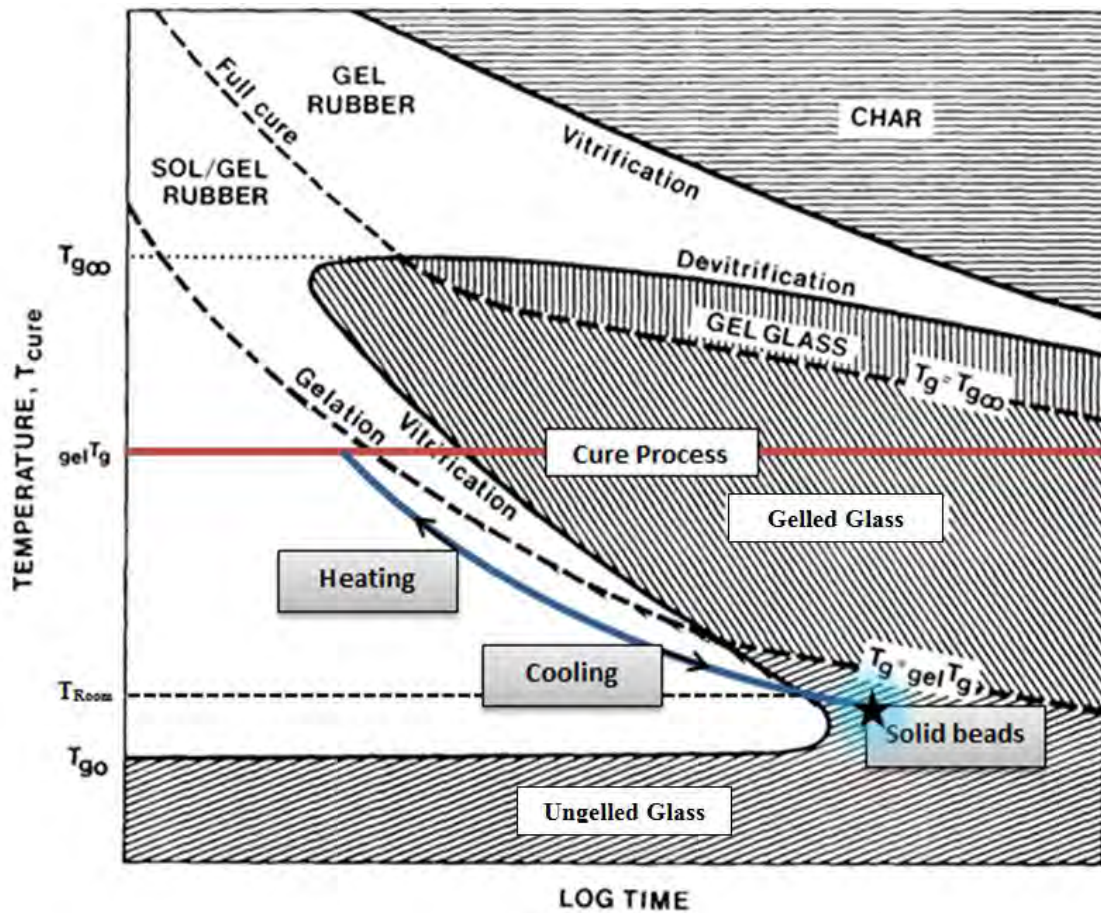
Fig. 57—An isothermal time-temperature-transformation (TTT) diagram showing the onset of gelation, vitrification, and full cure for a thermosetting epoxy (after Gillham 1985)

Portland Cement

Standard procedures in the oil and gas industry involve using Portland cement, ASTM types I and II, as the plugging material. ASTM standards define the properties of these cement mixtures; ten such mixtures are defined in ASTM C150/C150M with compressive strengths included and listed in **Table 12** below (ASTM). The compressive strength values defined in ASTM C150/C150M are based on uniaxial compressive tests performed on 2-in cement cube specimens as defined in ASTM C109/C109M (ASTM). Cube specimens are always stronger than cylinders due to cubes having an overlapped restrained zone towards the corners while testing under uniaxial compression, hence, a zone of triaxial compression develops.

Table 12—PORTLAND CEMENT COMPRESSIVE STRENGTHS(Data from ASTM C150/C150M)

Cement Type	Compressive Strength, psi
I	4080
IA	4080
II	3190
IIA	3190
II(MH)	4060
II(MH)A	3190
III	3480
IIIA	2760
IV	2470
V	3050

OBJECTIVES

1. Determine whether the vitrification point of epoxy resins successfully allows the formation of solid beads without gelation. Secondly, determine whether

the vitrified solid beads can be stored for a period of time greater than double

the 6-hour cure period of the resin. Finally, determine whether the solid beads

can be devitrified at wellbore temperature and reconsolidate into one mass

and cure.

2. Determine if the compressive strength of the reconsolidated resin solid can be

   an improvement over Portland cement, specifically creating an increase in

   strength of up to 50%.

3. Analyze the operational cost savings by comparing the use of vitrified resin

   beads to conventional cement. Determine cost savings created by reducing

   the material losses due to using vitrified epoxy resin beads in place of

   pumping liquid epoxy in a 7,000-ft application.

PROCEDURE

The parts of epoxy-based resin were mixed and allowed to partially cure in an

oven. Before gelation occurs at high temperature, the resin was removed and solid beads

were formed by cooling the fluid. The resin was stored then returned to the oven to

continue the curing process. The resin was prepared following the steps mentioned

below:

1. Set the oven temperature to 200°F and allow it to reach steady state.

2. Prepare the first portion of the resin formulation by thoroughly mixing the

   Part A resin and diluent in a beaker based on the ratios in Table 2 above.

3. Mix in Part B of the resin formulation based on the ratios in Table 2 above.

4. Mix in 50% (by weight) of oil.

To be able to create vitrified solid resin beads at any time, t, the fluid should be in liquid form at 200°F and in solid form at 39°F, at the same time t. At 200°F, the resin must maintain a low enough viscosity to be transported with a syringe. While at 39°F, the solid beads must be capable of maintaining their shape and must not exhibit a tacky surface that adheres to surfaces or other beads. To test these two conditions requires the use of two qualitative test methods that will be described below. The following list describes the steps required to find time t at which solid beads can be formed:

5. Separate the resin-oil mixture into two equal batches, called Batch A and Batch B

6. Divide each batch into 5-mL samples over eight 10-mL glass vials.

7. Place all 16 glass vials upright in the oven at 200°F

8. At 1-hour intervals

   a. Remove 1 glass vial from Batch A from the oven and allow it to cool to room temperature. Ensure the glass vial remains upright.

   b. Turn 1 glass vial from Batch B onto its side so it is lying horizontally in the 200°F oven.

9. After 12 hours from the initiation of the experiment

a. Measure the level of Gelation of Batch A samples based on the qualitative test method of Table 10.

b. Classify Batch B samples based on the Sydansk qualitative test method listed in **Table 13**

10. Determine time, *t,* at which the resin formulation in question can be transformed from a liquid to a solid by a sudden drop in temperature from 200°F to 39°F.

	Table 13—GEL STRENGTH CODE (Sydansk 1989)
A	No detectable gel formed: the bulk of the system has the same viscosity as the polymer solution
B	High flow gel: slightly more viscous than the polymer solution
C	Flowing gel: most of the gel flows to the bottle cap upon inversion
D	Moderately flowing gel: only a portion of the gel (~5-10%) does not flow to the bottle cap
E	Barely flowing gel: gel can barely flow to the bottle cap and/or a significant portion (>15%) does not flow to the cap
F	Highly deformable nonflowing gel: gel does not flow to the cap
G	Moderately deformable nonflowing gel: gel deforms about half way down the bottle upon inversion
H	Slightly deformable nonflowing gel: only the gel surface slightly deforms upon inversion
I	Rigid gel: no gel surface formation by gravity upon inversion
J	Ringing rigid gel: a tuning fork-like mechanical vibration can be felt upon tapping the bottle

The Sydansk test method is used to examine Batch B samples once the experiment is over. The purpose of turning the vials on their side is to allow any liquid resin to flow along the walls of the vial. By keeping the vials in the oven, it ensures that the amount of resin that flowed along the walls will cure and allow the examiner to determine the gel strength code of that specimen. An uncured sample will have the bulk of the resin along the wall of the vial up to the lid, while a cured sampled will have the bulk of the resin at the base of the vial with no lip on the wall.

The resin mixture at 200°F continues to cure, as long as the temperature of the mixture remains at 200°F. Solid beads can be formed by allowing the resin to cool to room temperature, but quenching the mixture in 39 °F water allows a faster solidification and ensures the curing process has been suspended. The following steps describe the process of forming the solid beads:

11. Repeat steps 1 to 4

12. Place the mixture in the 200°F oven until time t.

13. Use a syringe to inject droplets of the resin mixture into 39°F water to quench the resin and form solid beads.

14. Store the solid beads at 39°F to maintain long shelf life

When the solid beads are needed to be tested, they can be placed at 200°F, where they liquefy then continue the cure process to form one solid mass. It is important to note that the cure process does not stop completely during storage; it is simply slowed down significantly.

15. Place solid beads in 50-mL Ultra-High Performance Centrifuge Tubes and place them in the 200°F oven until the beads have liquefied then fully cured.

16. Removed the cured samples from the 50-mL Ultra-High Performance Centrifuge Tubes.

It is important for uniaxial compression tests to maintain a load vector parallel to the axis of the sample being tested. As a result, the samples are required to have ends that are parallel to each other and the surfaces of the compression machine. The ends are also required to be square with the sides of the cylinder to ensure uniform loading and deformation. The following list describes the steps necessary to achieve these requirements:

1. Remove the cured solid samples from the 50-mL Ultra-High Performance Centrifuge Tubes.

2. Use a band-saw to cut off the conical end of the sample and to cut the samples into two 1-inch long cylinders.

3. Sand the ends of the samples on a disc sander to ensure parallel ends to the sample as well as to smooth off the surface for an adequate compression test surface.

4. Measure the height and average diameter of each specimen.

5. Check each sample for its conformance to the requirement of parallel top and bottom ends. Any sample that does not meet the specifications is unsuitable for testing.

The compression tests were run using an Instron 4206 connected to a computer running a Labview data acquisition program. For each run, the machine was allowed to apply a load on the sample, until the sample failed or the load reached the load limit of 30,000 psi. A sample failing is indicated by a sudden drop in the measured load. The

following steps list the directions used to run the compression tests and collect the data

points:

6. Turn on the Instron 4206.

7. On the control panel hit "Load Cal" then "Enter"

8. Hit "Load Bal" then "Enter"

9. Hit "GL reset"

10. Hit "Speed" and set it to 0.2 inches per minute.

11. Launch the Labview program.

12. Start data acquisition by running the Labview program.

13. Hit the "Down" button to start the Instron.

14. Stop the machine when the sample fails or reaches the load limit of

    30,000 psi.

RESULTS AND DISCUSSION

The Batch B samples were turned on their side every hour, as mentioned above and kept in the oven. Once the time of the experiment was completed the samples were removed and examined. The samples from the first 4 hours, in **Fig. 58**, show the resin flowed to the lid of the vials while the vials were horizontal. The black fluid at the base of the vials in the images of this section, is the residual oil portion of the mixture, while the brown fluid/solid is the thermosetting portion of the mixture.
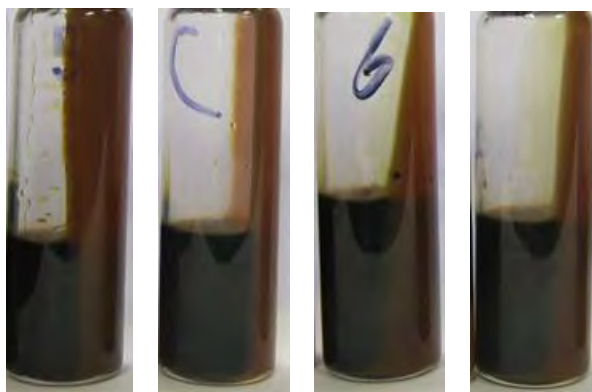
Fig. 58—The 1-hour, 2-hour, 3-hour, and 4-hour samples of Batch B repositioned and kept in the 200°F oven.

At the 5-hour sample, signs of gelation began to appear. The majority of the resin remained at the base of the vial, but a portion created a lip halfway up to the lid of the vial, as seen in **Fig. 59.**
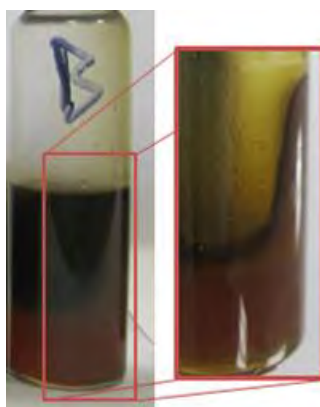
Fig. 59—The 5-hour samples of Batch B repositioned and kept in the 200°F oven.

The 6-hour, 7-hour, and 8-hour samples showed no movement in the resin, as seen in **Fig. 60**, indicating that the resin at this point will maintain its shape until fully cured.
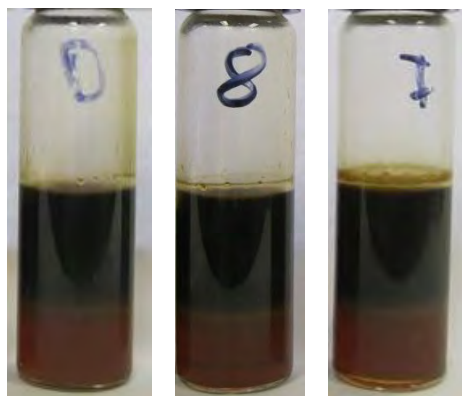
Fig. 60—The 6-hour, 7-hour, and 8-hour samples of Batch B repositioned and kept in the 200°F oven.

One sample from Batch A was removed from the oven every 1 hour, and allowed to cool to room temperature. Each sample was tested using the qualitative test in Table 10 after the first 12 hours had passed. The results displayed a progressively hardening trend, starting from the 2-hour sample at a level of gelation of 1, to the 6-hour

sample at a level of gelation of 5. **Fig. 61** shows the hardening trend of Batch A compared to the results from Batch B. It is apparent that Batch B at 200°F, had a 2-hour delay in the onset of gelation compared to Batch A. At 4 hours, Batch B samples remained a flowing liquid while Batch A had a level of Gelation of 3, corresponding to a resin that is visually cured but applying pressure penetrates the surface. Therefore, to create the vitrified solid resin beads the time, t, at which the cure process should be stopped, is 4 hours.
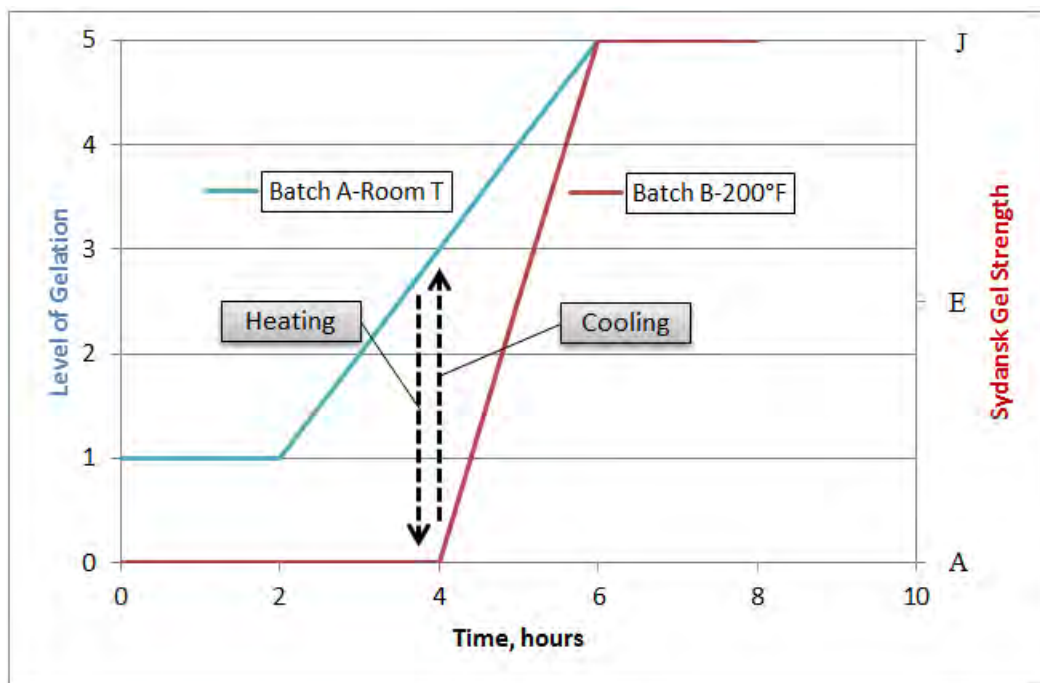
Fig. 61—The trends of Batch A and Batch B samples showing the effect of temperature on gel strength

At 3.5 to 4 hours the resin can be removed from the oven at 200°F and cooled down rapidly to 39°F to instantly form solids, shown in **Fig. 62**. This was done using a

syringe to remove the resin from the vial and place it, as droplets, in ice water. Once the droplets were solidified they would then be placed in a beaker and put in a refrigerator.

Fig. 62—Vitrified resin droplets that were formed by quenching droplets of resin in 39°F water 3.5 hours into the cure process.

Once the beads are needed, they can be placed back in the oven. The vitrified resin beads began devitrification at approximately 130°F. Once in liquid form, the material reconsolidated and continued the cure process in the 50-mL Ultra-High Performance Centrifuge Tubes until fully cured. The resin mixture cured to one consolidated solid, but bubbles were observed in the material, as seen in **Fig. 63**, due mainly to the fact that when the beads liquefy, the viscosity is greater than that of the pure liquid epoxy resin, resulting in slower bubble release and heterogeniety in the final solid.

Fig. 63—A specimen of fully-cured reconsolidated epoxy-resin beads before and after the compression test

The cured solid was removed from the centrifuge tubes, machined, and sanded in preparation for a compression test. The stress-strain curve produced from the compression tests are shown in **Fig. 64**. As the load increases beyond the yield point, pore collapse causes the strain to increase until, eventually, the specimen fractures and fails completely. The fracture strength, in this case, has the same value as the yield strength of the specimens. These samples did not exhibit any barreling; instead they deformed axially then broke into several pieces as seen in Fig. 63 above. The average fracture strength was found to be 7,717 psi, which is 89% more than the compressive strength value of Portland cements I & II in Table 12, but also corresponds to a 45% drop from the yield strength of pure resin. The heterogeneity in the solid is the largest contributor to the drop in fracture strength, due to the bubbles aiding in crack initiation and propagation.
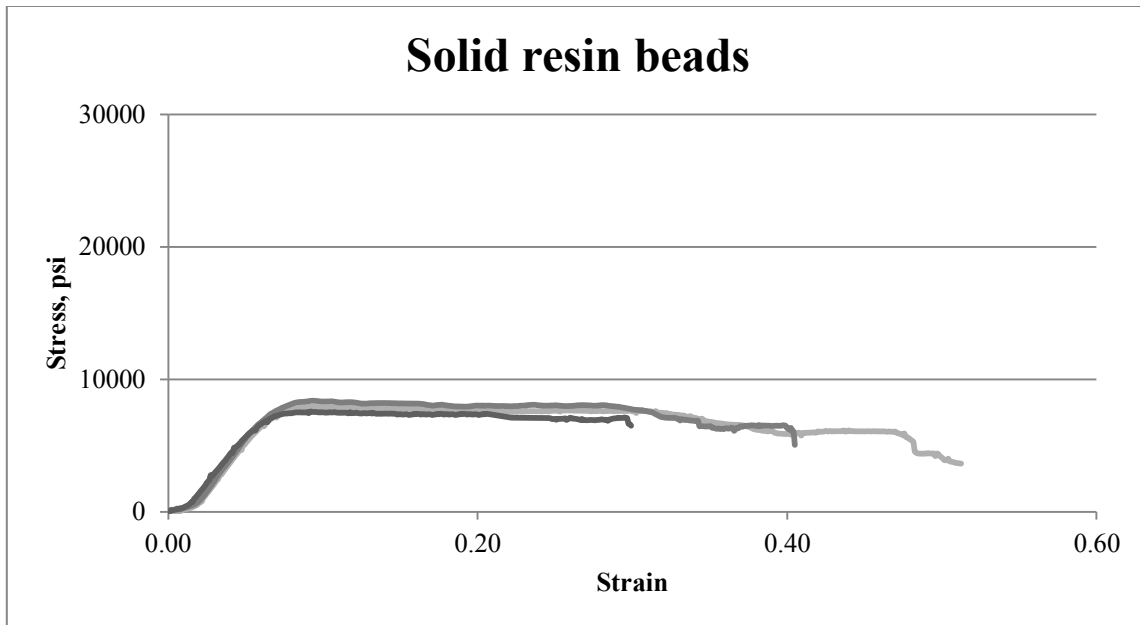
Fig. 64—The stress-strain curve for reconsolidated epoxy resin beads tested under compression until failure.

Cost Analysis

A cost comparison between two P&A operations was performed to determine the cost benefits to using vitrified solid resin beads over conventional Portland cement. In the first case, with the resin beads, an offset well was drilled to a depth of 1,000-ft below the mudline, where the beads were pumped and allowed to drop in the annulus and settle for 6,000 ft to the top of the packer. The second case, with Portland cement, the offset well was drilled 7,000 ft below the mudline, and cement was spotted in place. The cost comparison for the two cases is shown in **Table 14**.

Table 14—COST COMPARISON FOR P&A		
	Resin Beads	**Portland Cement**
Material Cost	$190,000[a]	$23,800[b]
Drilling Cost	$143,700[c]	$1,005,800[d]
Total	**$333,700**	**$1,029,600**

a) Approximated based on the cost of UltraSeal at $10,000/bbl and a plug height of 550 ft in 6-in tubing
b) Approximated based on the cost of Portland Cement at $1,250/bbl and a plug height of 550 ft in 6-in tubing
c) Approximate drilling cost for 1,000-ft at a rate of 116 ft/min and a $400,000/day equipment cost (Kaiser M.J 2008)
d) Approximate drilling cost for 7,000-ft at a rate of 116 ft/min and a $400,000/day equipment cost (Kaiser M.J 2008)

While the cost of UltraSeal is approximately 8 times the cost of Portland cement, the time required to drill the offset well and apply the resin beads is significantly reduced, and subsequently the cost is reduced. There is a potential for USD 0.7 million in savings using this system, based on the assumptions made in this section. In addition, using resin beads reduces the amount of material loss on the walls of the well. According to El-Mallawany, up to 32% of material can potentially adhere to the casing and not settle on the packer (El-Mallawany 2011). 32% of the cost of epoxy required for the application is approximately USD 60 thousand for a 7,000-ft application with a 550-ft plug height.

CHAPTER VII: CONCLUSIONS

1. Mixing the resin with seawater, oil, or pipe dope will reduce the ultimate strength and fracture strengths of the mixtures compared to the strengths of pure resin. The ultimate strength of contaminated resin will most likely drop to the value of the yield strength, and should be designed with that in mind. The fracture strengths of contaminated resin will experience a drop greater than a 25% compared to pure resin, while the yield strength, on the other hand, can remain relatively unaltered.

2. During a 6-hour cure, the cure process of resin mixed in with seawater can be accelerated by more than 2 hours compared to pure resin, while oil has no apparent effect on the cure process.

3. Quenching droplets of epoxy resin in 39°F diluted water before the initiation of gelation during the cure process was found to form solid beads through the reversible physical process of vitrification; using this effect as a plugging application can be successful.

4. The average fracture strength of reconsolidated epoxy resin beads was found to be 7,717 psi, indicating that an application utilizing solid resin beads, as discussed in this thesis, can be up to 89% stronger than the ASTM compressive strength values for Portland cements I & II.

5. From an operational cost standpoint, using vitrified epoxy resin beads has the potential to create up to USD 0.7 million in savings compared to conventional

cement costs for cases similar to the one discussed herein. In Addition, using vitrified epoxy resin beads in place of pumping liquid epoxy resin could eliminate the 32% of material lost during settling, thus creating savings of approximately USD 60 thousand for a 7,000-ft application with a 550-ft plug height.

REFERENCES

API. 1999. 10tr3 - Technical Report on Temperatures for API Cement Operating Thickening Time Tests. In: American Petroleum Institute. API TR 10TR3

ASTM. C42/C42m Test Method for Obtaining and Testing Drilled Cores and Sawed Beams of Concrete. In: ASTM International.

ASTM. C109/C109m Test Method for Compressive Strength of Hydraulic Mortars. In.

ASTM. C150/C150m Specification for Portland Cement. In: ASTM International.

Barclay, I.S., Johnson, C.R., Staal, T.W. et al. 2004. Utilizing Innovative Flexible Sealant Technology in Rigless Plug and Abandonment. Paper presented at the SPE/ICoTA Coiled Tubing Conference and Exhibition, Houston, Texas. 89622. DOI: 10.2118/89622-ms.

BOEMRE. 2011. *Gulf of Mexico OCS Oil and Gas Lease Sale: 2011*. New Orleans.

Calvert, D.G. and Smith, D.K. 1994. Issues and Techniques of Plugging and Abandonment of Oil and Gas Wells. Paper presented at the SPE Annual Technical Conference and Exhibition, New Orleans, Louisiana. 28349. DOI: 10.2118/28349-ms.

Case, J., Chilver, L., and Ross, C.T.F. 1999. *Strength of Materials and Structures*: Elsevier. Original edition. ISBN 978-0-340-71920-6.

Chong, K.K., Charles A. Butterfield, J., and Conwell, R.P. 2000. Novel Technique for Openhole Abandonment Saves Rig Time-a Case History. Paper presented at the SPE Asia Pacific Oil and Gas Conference and Exhibition, Brisbane, Australia. 64481. DOI: 10.2118/64481-ms.

Dawkins, J.V. 1986. *Developments in Polymer Characterisation*: Elsevier Applied Science Publishers. Original edition. ISBN 978-0-8533-4401-8.

El-Mallawany, I.I. 2011. An Experimental Setup to Study the Settling Behavior of Epoxy Based Fluids. Masters of Science, Texas A&M University.

Flory, P.J. 1953. *Principles of Polymer Chemistry*: Cornell University Press. Original edition. ISBN 978-0-8014-0134-3.

Gillham, J.K. 1985. Cure and Properties of Thermosetting Systems. *British Polymer Journal* **17** (2): 224-226. DOI: 10.1002/pi.4980170225

Gougler Jr., P.D., Hendrick, J.E., and Coulter, A.W. 1985. Field Investigation Identifies Source and Magnitude of Iron Problems. Paper presented at the SPE Production Operations Symposium, Oklahoma City, Oklahoma. 13812. DOI: 10.2118/13812-ms.

Holub, R.W., Noel, R.P., and Weinbrandt, R.M. 1974. Scanning Electron Microscope Pictures of Reservoir Rocks Reveal Ways to Increase Oil Production. Paper presented at the SPE Symposium on Formation Damage Control, New Orleans, Louisiana. 4787. DOI: 10.2118/4787-ms.

Irfan, M.H. 1998. *Chemistry and Technology of Thermosetting Polymers in Construction Applications*: Springer - Verlag. Original edition. ISBN 978-0-7514-0428-9.

Jr., H.O.M. 1984. Matrix Acidizing. *SPE Journal of Petroleum Technology* (12). DOI: 10.2118/13752-pa

Kabir, A.H. 2001. Chemical Water & Gas Shutoff Technology - an Overview. Paper presented at the SPE Asia Pacific Improved Oil Recovery Conference, Kuala Lumpur, Malaysia. 72119. DOI: 10.2118/72119-ms.

Kelland, M.A. 2009. *Production Chemicals for the Oil and Gas Industry*: CRC Press. Original edition. ISBN 978-1-4200-9290-5.

Kelm, C.H. and Faul, R.R. 1999. Well Abandonment- a "Best Practices" Approach Can Reduce Environmental Risk. Paper presented at the SPE Asia Pacific Oil and Gas Conference and Exhibition, Jakarta, Indonesia. 54344. DOI: 10.2118/54344-ms.

Loewen, K., Chan, K.S., Fraser, M. et al. 1990. A Well Stimulation Acid Tube Clean Methodology. Paper presented at the Annual Technical Meeting, Calgary, Alberta. 90-47. DOI: 10.2118/90-47.

Maly, G.P. 1976. Close Attention to the Smallest Job Details Vital for Minimizing Formation Damage. Paper presented at the SPE Symposium on Formation Damage Control, Houston, Texas. 5702. DOI: 10.2118/5702-ms.

Mcleod Jr., H.O., Ledlow, L.B., and Till, M.V. 1983. The Planning, Execution, and Evaluation of Acid Treatments in Sandstone Formations. Paper presented at the SPE Annual Technical Conference and Exhibition, San Francisco, California. 11931. DOI: 10.2118/11931-ms.

Menczel, J.D., Prime, R. Bruce. 2009. *Thermal Analysis of Polymers :Fundamentals and Applications*. Trans Menczel, J.D., Prime, R. Bruce. Hoboken, N.J.: John Wiley & Sons. Original edition. ISBN 978-0-4717-6917-0.

Nasr-El-Din, H.A., Al-Mutairi, S.H., and Al-Driweesh, S.M. 2002. Lessons Learned from Acid Pickle Treatments of Deep/Sour Gas Wells. Paper presented at the International Symposium and Exhibition on Formation Damage Control, Lafayette, Louisiana. 73706. DOI: 0.2118/73706-ms.

Ng, R.C. 1995. *Low Temperature Epoxy System for through Tubing Squeeze in Profile Modification, Remedial Cementing, and Casing Repair*. Doc. 5,377,757, pt. United States: Mobil Oil Corporation.

P.F.S. 2007. Liquid Bridge Plug/ Ultra Seal R Micro Annular Gas Migration Shut Off. In: Professional Fluids Services, LLC.

Peng, W. and Riedl, B. 1995. Thermosetting Resins. *Journal of Chemical Education* **72** (7): 587. DOI: 10.1021/ed072p587

Sydansk, R.D. 1989. *Delayed in Situ Crosslinking of Acrylamide Polymers for Oil Recovery Applications in High-Temperature Formations*. Doc. US 4844168, pt.

Tettero, F., Barclay, I., and Staal, T. 2004. Optimizing Integrated Rigless Plug and Abandonment - a 60 Well Case Study. Paper presented at the SPE/ICoTA Coiled Tubing Conference and Exhibition, Houston, Texas. 89636. DOI: 10.2118/89636-ms.

Wei, R.P. 2010. *Fracture Mechanics - Integration of Mechanics, Materials Science, and Chemistry*: Cambridge University Press. Original edition. ISBN 978-0-521-19489-1.

VITA

Name: Ahmed Rami Abuelaish

Address: Harold Vance Department of Petroleum Engineering

Texas A&M University

3116 TAMU - 507 Richardson Building

College Station, TX 77843-3116

Email Address: ahmed.abuelaish@pe.tamu.edu

Education: B.S., Mechanical Engineering, Texas A&M University, 2009

AN EXPERIMENTAL SETUP TO STUDY THE FALL RATE OF EPOXY BASED
FLUIDS

A Thesis

By

IBRAHIM EL-MALLAWANY

Submitted to the Office of Graduate Studies of
Texas A&M University
in partial fulfillment of the requirements for the degree of

MASTER OF SCIENCE

December 2010

Major Subject: Petroleum Engineering

AN EXPERIMENTAL SETUP TO STUDY THE FALL RATE OF EPOXY BASED
FLUIDS

ABSTRACT

This thesis is part of a project funded by MMS to study the use of epoxy (or any cement alternative) to plug hurricane damaged wells. Some of the wells destroyed by hurricanes are damaged to an extent that vertical intervention from the original wellhead is not possible. The means to plug such wells, as sought by this project, is to drill an offset well and intersect the original at the very top and spot some epoxy (or any suitable non-cement plugging material) in the original well. The epoxy will then fall by gravity all the way until it reaches the packer and then set on top of the packer to plug the annulus of the well permanently.

One of the most important factors in this process is to be able to predict the settling velocity of the epoxy to be able to determine the required setting time of the epoxy so that the epoxy does not set prematurely. This thesis aims to design, build and run an experimental setup that would help develop a model to estimate settling velocities of different epoxies. The model itself will be part of a different dissertation. Part of this thesis is to also investigate how much epoxy will adhere to the pipe walls to be able to account for epoxy lost on the journey towards the packer. The thesis will also investigate whether weighting materials such as barite would separate from the epoxy when freefalling through water.

DEDICATION

ACKNOWLEDGMENTS

I would like to thank my committee chair, Dr. Jerome Schubert, my committee co-chair Dr. Hisham Nasr El-Din and my committee member, Dr. Mahmoud El-Halwagi for their guidance and support throughout the course of this research.

Thanks to John Maldonado for his help to build and run the experiments.

Thanks also to my colleagues, Arash Haghshenas, Tinlee Tilton and Salvador Lopez, for helping me with the experimental setup and running the experiments.

I also want to extend my gratitude for the following:

MMS: For funding me and the entire project.

PFS: For donating all the epoxy the project needed.

Dr. Mikael Olsen and the University's physical plant: For their help and guidance with the experimental setup.

David from Industrial Machines: For building the experimental setup.

TABLE OF CONTENTS

LIST OF FIGURES

LIST OF TABLES

1. INTRODUCTION

In the past years many oil platforms have been either completely destroyed or extremely damaged by hurricanes. **Table1** shows the number of destroyed or extremely damaged platforms according to the MMS released documents. (Ref 1, 2, 3 & 4)

Hurricane	No. Destroyed	No. Extremely Damaged
Rita & Katrina	113	144
Ike & Gustav	60	31
Ivan, Andrew & Lily	18	

Table1. Number of wells damaged or destroyed by hurricanes.

Table1 shows that the total number of destroyed or damaged platforms exceeds 350. All these wells need to be plugged and abandoned. Some of these wells will enable plugging by conventional means using cement. However, others will have been destroyed to a point that reentering the well is impossible for example the casing may be buckled at or below mudline or the wellhead might be buried with seafloor mud. This will prevent wire line operations via tubing to set plugs near the packer or punch the tubing to circulate cement into the casing. Cement is mixed with water and therefore is miscible with seawater and brines which are the main packer fluids found in the Gulf of Mexico. Long interaction with these fluids can be devastating causing dilution or contamination of the cement mix which in turn cause it not to cure or lose its compressive or bonding strength. Therefore, for these latter wells the use of cement is not suitable because cement needs to be delivered to the point of application with minimum or no interaction with water and the only way this would be possible for these wells is that an intersection well be drilled and intersects at or near the packer meaning that it has to be drilled to full depth. This of course would be very costly and time consuming offsetting the competitive price advantage of cement over other plugging materials. An alternative means to plug these wells is have an intersection well that

intersects the original wellbore at the very top through perforations between the wells. Then epoxy would be spotted inside the original wellbore. The epoxy would then settle by gravity all the way down to the packer. Of course, for this to work the well must not be flowing at the time. Epoxy in this situation is an excellent choice because generally they do not mix with water or brines and could reach the packer without being diluted or contaminated.

This thesis is part of a project funded by MMS which aims to investigate the applicability of epoxy or another non cement plugging material to plug hurricane damaged wells described in the previous paragraph. The current limitations of the use of epoxy based materials as a permanent plug is that these materials have very rarely been used for plugging and abandonment applications and the applicability of using such materials has not been adequately studied. The MMS project will include the following research points.

1) Comparing epoxy-based materials against cement abandonments and other potential plugging materials

2) Determining whether epoxy material can effectively drop 7000 feet through a casing annuli and accumulate on top of the packer

3) Determining how long material takes to travel to the bottom of a casing annuli and cure

4) Determining how material performs over time

5) Determining how weighting of this material with BaSO4 affects the compressive and bond strength of the material

6) Determining whether there are other weighting materials which may perform better than BaSO4

7) Ranking various resin and hardener chemical systems for best performance in the field

8) Evaluating the effects of various liquids such as calcium chloride, sea water, and formation hydrocarbons on the resin chemical systems

The work discussed in this thesis is aimed to help study points 2 & 3. It is about designing, building and running an experimental setup that will provide experimental data to help develop a model that could predict the time it takes for epoxy to drop a certain distance from the injection point to the packer. The thesis will also try to investigate how much epoxy will adhere to the walls of the pipe before it reaches the packer so excess epoxy can be injected to overcome this. Another point that will be discussed is whether weighting materials such as barite will be able to hold inside the epoxy without separating during or after it falls through the wellbore.

2. LITERATURE REVIEW

Historically in the oil industry epoxy has been used for sand consolidation, resin coated proppants, remedial casing procedures, formation plugging and many other applications. For example US patent 5,295,541 by Ng et al discusses using epoxy to repair corroded casing in the wellbore. The idea of this patent is that when a part of the casing is corroded, that part gets milled off. Then an under reamer would further open the bore to increase the epoxy's thickness. A retrievable packer is then placed and set right under the corroded section then epoxy is placed above the packer to fill the place of the milled casing and any thief zones in the formation. The patent suggests that epoxy is either placed using a dump bailer or using coiled tubing. Both these placing methods are of course not suitable for the intended application of this thesis. The patent also suggested some epoxy based materials namely Shell's EPON-828 and Shell's EPON DPL-862 as the resin, a Sherling Berlin's diluent 7 as a reactive diluent, fine powder calcium carbonate or silica flour as a filler and lastly Sherling Berlin's Euredur[200] 3123 as a curing agent. The diluent's function is to increase pot life and gel time of the resin and decrease the epoxy's viscosity. The filler's function is to increase the specific gravity of the resin so the resin does not float and stay lying on the packer. The curing agent obviously causes the resin to cross-link and therefore harden. F**ig1** from the patent describes the process where epoxy is placed instead of the corroded casing and thief zones and then drilled off.
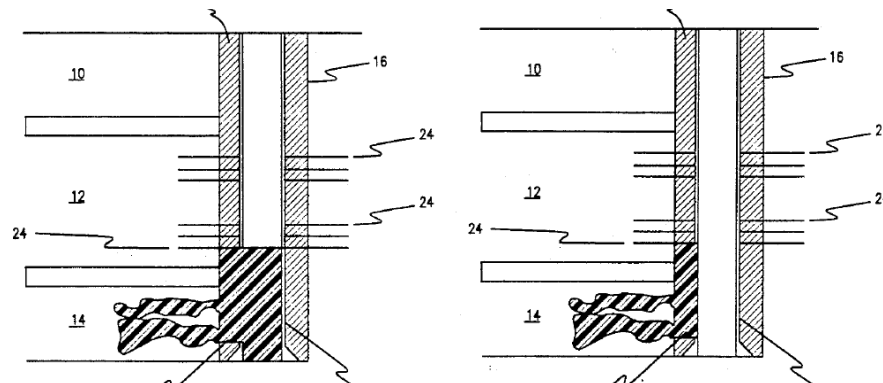
Fig1. Epoxy used for remedial casing procedure

An example of an epoxy used for formation plugging is discussed in SPE paper number 7083 by Knapp and Welbourn. It discusses the use of a resin in an emulsion where droplets are less than 1 micron in diameter to be able to seep through the pore spaces of the formation. The method they suggested is first pumping the resin in the formation and then pump the curing agent after it. This causes regions of high permeability in the formation to be preferentially sealed. The application of this process is for water or gas shut off. It is also used for controlling water in injection wells so it is not lost in useless parts of the formation. The resin would plug areas of high permeability and direct water injected to flow in the desired lower permeability zones of the reservoir.

The only resin product that has been applied for an application similar to the one we are focusing on is a product called Ultra-Seal from a company called Professional Fluid Systems. The company has applied this resin on a few similar applications. For example, High Island Block A330 platform was plugged and abandoned. Several years later gas seepage from the pressure cap of the well was detected by coincidence when a recreational driver was swimming by. The pressure cap was removed by a diamond saw. The gas seepage was found to be coming from micro-annuli between the cement and the casing/conductor walls. The tubing was then sealed with a CIBP and the pressure cap was reinstalled. Then the Liquid Bridge Plug (another name for the Ultra Seal resin) was pumped inside the micro-annuli and was waited on for 20 hours. The plug was successful and the gas seepage was stopped. Another application for the Ultra-seal was on Chevron's Vermillion 31 platform. The platform had a leaking packer and wanted a way to seal the packer without using rig equipment. The annular fluid was seawater and was 8.6 lb. /gal. The Ultra-Seal resin was weighted up with a filler material to increase its terminal velocity during its fall and therefore reducing the time of its travel. 168 gallons of the resin was loaded into the annulus and was allowed to fall for 14 hours and then set on the packer for an additional 24 hours. The plug then was pressure tested at 1000 psi and no pressure loss was detected indicating the success of the seal. The Ultra-

Seal resin was also applied in another five different wells for different plugging purposes especially hurricane damaged wells. (Ref 7)

CSI technologies did some fall tests on the Ultra-Seal but on a very small scale. A 2 inch diameter 5 feet in length clear glass pipe was used. A copper pipe was inserted in the first two feet of the pipe to act as a stringer. The pipe was filled with brine weighted with calcium bromide and had a density of 10.4 lb. /gal. Epoxy is then loaded into the copper pipe and time is measured when the epoxy exits the copper pipe until it reaches the capped bottom of the pipe. **Fig2** shows an illustration of the experiment.
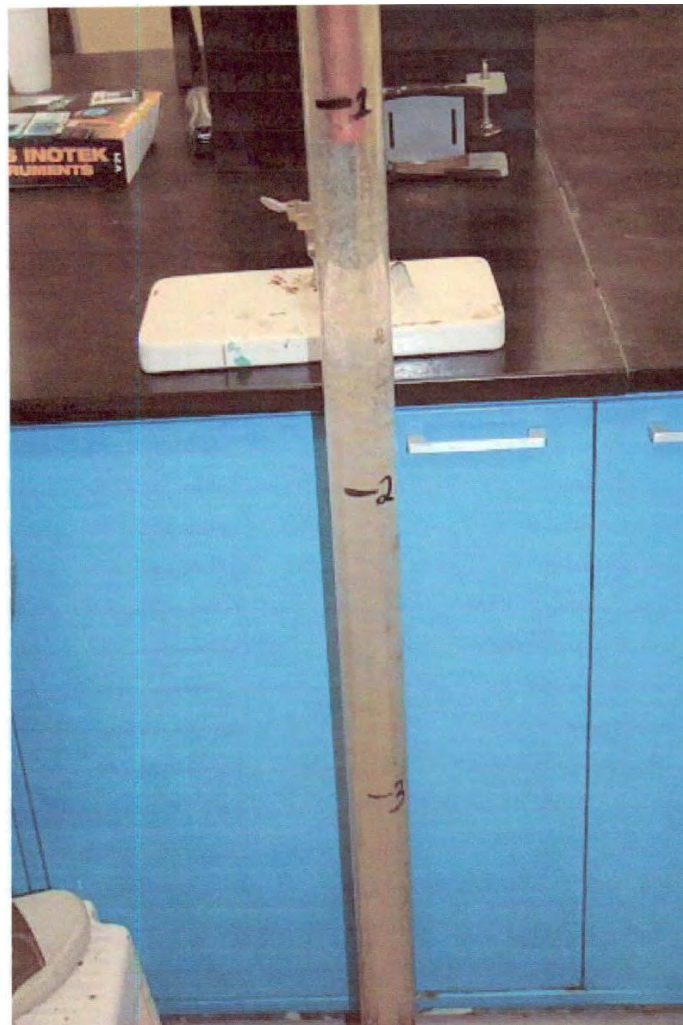
Fig2 (Ref 7). Test apparatus to measure epoxy's settling velocity.

Time is measured at every 1 foot interval over the 3 foot interval. The Ultra-seal was weighted with barite to a density of 16 lb. /gal. The time it took for the resin to fall over the 3 foot interval was 5 seconds, measured visually. The experiment was repeated 3 times yielding the same 5 seconds and therefore it was concluded that the fall rate of the resin would be 36 ft. /min. This experiment has many possible flaws. It did not study the effect of different parameters on the fall rate such as the pipe diameter, density and viscosity of resin and density and viscosity of annular fluid. Also the 3 foot interval is very short. Therefore, not only resin might not reach its terminal velocity during this interval, any small change in time would yield big changes in settling velocity. The 2" pipe diameter is also too small compared to real life application. (Ref 7)

3. THEORETICAL BACKGROUND

The concept of settling has been studied in many applications such as settling tank, catalytic converters, pneumatic conveying of solids, and gas migration in the oil field. There are a few fundamental concepts behind the theory of settling objects. The most known theory is Stokes' law. Stokes' law provides an equation to predict the settling of solids or liquid droplets in a fluid, either gas or liquid. It assumes that the settling object is a small sphere and that the difference in densities is not large. This is because Stokes' law takes into account only the viscous forces that cause drag and does not account for drag due to impact forces. Therefore, Stokes' law only applies where Reynolds number is very low. Stokes' law is given by the following equation (Batchelor 1967)

$$F_d = 6\,\pi\,\mu\,R\,V \ \ldots\ldots\ldots\ldots (1)$$

Where F_d is the drag force, μ is the fluid's viscosity, R is the sphere's radius and V is the particle's velocity. When the settling particle reaches terminal velocity then in that case the sum of forces must equal zero. Therefore the drag force must equal the difference between the force due to gravity and the buoyancy force. So F_d can be written as the following equation

$$F_d = \frac{4}{3}\,\pi\,R^3(\rho_{s-}\,\rho_f)g \ \ldots\ldots\ldots\ldots (2)$$

Where g is the acceleration due to gravity, ρ_s is the particle's density and ρ_f is the fluid's density. Now by equating equations (1) and (2) we can solve for the terminal velocity which will lead to the following equation

$$V = \frac{2R^2(\rho_{s-}\,\rho_f)g}{9\mu} \ \ldots\ldots\ldots\ldots (3)$$

Experimentally, it was found that at Reynolds number less than 0.1 the error is within 1%. From Reynolds number between 0.1 and 0.5 the error is within 3% and between 0.5 and 1 the error is within 9%. When Reynolds number is greater than 1, drag due to impact becomes significant and Stokes' law would lead to large errors. Reynolds number could be computed from the following equation. (Coulson 2002)

$$R_e = \frac{4R^3 g \rho_f (\rho_s - \rho_f)}{9\mu^2} \ldots\ldots\ldots (4)$$

When Reynolds number is large then impact forces become much more dominant and viscous forces can be ignored. In that case Newtonian drag applies. Newtonian drag identifies a parameter called the drag coefficient (C_D) that represents the ratio of the force exerted on the particle by the fluid divided by its impact pressure. The drag coefficient is given by. (Batchelor 1967)

$$C_D = \frac{2F_d}{\rho_f V^2 A} \ldots\ldots\ldots (5)$$

Where A is the projected area of the object that is perpendicular to the direction of flow. For example in case of a sphere the projected area in the direction of flow (or any other direction) is a circle and therefore $A = \pi\, r^2$. For a spherical particle settling in a fluid the terminal velocity using Newtonian drag could be obtained by equating equation (5) with equation (2) to obtain (Batchelor 1967)

$$V = \sqrt{\frac{4(\rho_s - \rho_f)gr}{3C_D \rho_f}} \ldots\ldots\ldots (6)$$

Table2 below gives rough estimates of drag coefficients for different applications. It must be noted that the drag coefficient varies with Reynolds number

C_D	Object
0.48	rough sphere (Re = 10e6)
0.005	turbulent flat plate parallel to the flow (Re = 10e6)
0.24	lowest of production cars (Mercedes-Benz E-Class Coupé)
0.295	bullet
1.0–1.3	man (upright position)
1.28	flat plate perpendicular to flow
1.0–1.1	skier
1.0–1.3	wires and cables
1.1-1.3	ski jumper
0.1	smooth sphere (Re = 10e6)
0.001	laminar flat plate parallel to the flow (Re = 10e6)
1.98–2.05	flat plate perpendicular to flow (2D)

Table2 (Ref 9). Drag coefficients of different objects.

Newtonian drag should be applied for Reynolds number above 1000. For intermediate values of Reynolds number where both viscous and impact forces are significant, a transitional drag regime occurs. An empirical equation was developed by Schiller and Naumann and is given by the following (Coulson 2002)

$$C_D = \frac{24}{R_e} \left(1 + 0.15\, R_e^{0.687}\right) \ldots\ldots\ldots (7)$$

By using equations (4), (6) and (7) we can solve for the terminal velocity.

The equations discussed all require that the particle has a known shape and they also are used for a particle that is in an infinite fluid. In our application however the shape may not be known and the epoxy is falling in an annulus so the pipe walls will definitely have an impact. This impact must be studied and its significance should be examined.

4. PROPOSED WORK

The experimental setup consists of a 25ft long pipe fixed on a pipe rack. The pipe rack is designed in such a way to be able to orient the pipe from horizontal to vertical or at any angle in between. The pipe can be full of any desired liquid that could be expected in the wellbore such as seawater, drilling fluid or oil. The setup should allow ease of adjustments, and services such as replacing pipe, replacing fluid in the pipe, installing pressure transducers on pipe, cleaning pipe, retrieving epoxy after it falls etc. Different pipe sizes and pipe materials could be used. Also two different pipe sizes can be inserted into one another to provide an annulus of desired size. The maximum size of pipe was chosen to be 7" diameter. Epoxy would then be dropped from the top of the pipe and the time taken for epoxy to reach different positions of the pipe will be measured. The epoxy is expected to be accelerating at first and then should reach a final terminal velocity. Since the distance between the injection point of the epoxy in the wellbore and the packer will be huge (around 7000ft), the time it takes to accelerate would be negligible compared to the rest of the journey. Therefore, the terminal velocity of the epoxy used is what will be sought. However, all data will be recorded in case it is needed at a later stage of the project. At start clear PVC pipe and fresh or synthetic sea water will be used to make measurements easier. During these starting experiments an ideal way of measuring the fall rate in an opaque pipe or opaque liquid will be investigated like for example a steel pipe or oil. For example, a pressure transducer could be installed to determine if the difference in hydrostatic pressure when epoxy passes the transducer is detectable or not. If pressure transducers fail other methods to predict fall rate in opaque steel pipe or opaque fluid will be sought.

To study whether weighting materials such barite will not separate from the epoxy, an epoxy that has a density less than water will be used .This epoxy will be weighted up with desired weighting material. This epoxy will then be dropped in the pipe until it either drops or fails to drop.

Lastly, it is important to determine how much epoxy would adhere to the walls of the pipe. This can be done by measuring the difference in volume between the epoxy injected and the epoxy collected at the bottom.

5. DESIGN AND IMPLEMENTATION

5.1 Preliminary Design

The pipe support was to be installed at the University Services Building. This building is the University's warehouse and each department has a plot about 75ft by 50ft. This building was chosen because its ceiling is 30ft high and therefore is the only building on campus that can hold the pipe support in vertical position. Before discussing the final design other alternative designs that were candidates will be introduced to show why the final design was thought to be the best and to give it more appreciation. It was decided that the maximum load that the pipe support would bear would be that of a 7 inch diameter steel pipe full of seawater since it is the most common packer fluid in the Gulf of Mexico. Taking the minimum casing weight which is a 6.54 inch ID the load would be.

7" diameter x 6.54" ID = 17.0 lb./ft

17.0lb/ft x 30ft length = 510 lb.

Seawater Volume $= \frac{\pi}{4} (\frac{6.54}{12})^2 \times 30 = 7ft^3$

Seawater Weight = 7ft^3 x 64.3 lb/ft^3 = 450 lb

Total Weight = (510 + 450) x 10% safety factor = 1056 lbs

The 10% safety factor is to account for any extra fittings and/or accessories. Now as explained in the previous section the pipe support has a few main functions. These functions are to bear the pipe's weight, keep it from moving during experiment and to orient the pipe at any desired angle. Cost was also an important issue to consider since the project has a fixed budget. The first conceptual design was as represented in **Fig3** below
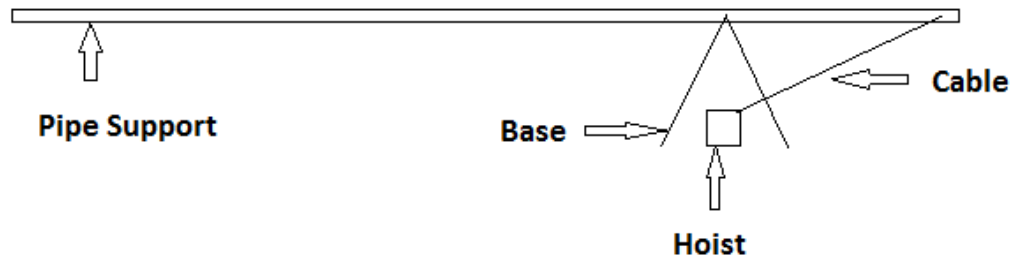
Fig3. First conceptual design.

As shown in the figure there would be a base that provides a pivot point for the pipe support the hoist would pull the pipe support from the right end as shown in the diagram to adjust the pipe support's position from horizontal to vertical or any angle in between. Now let us study the forces and moments on the pipe support. There are four forces acting on the pipe support.

1) Base
2) Hoist
3) Pipe
4) Pipe support's own weight

Now assuming a value of 350 lbs for the pipe support's weight, the load of the pipe and pipe support's weight can be represented as a distributed load of 46.87 lb/ft [(1056+350)/30] of the pipe support. **Fig4** shows a schematic of the force distribution on the pipe support.
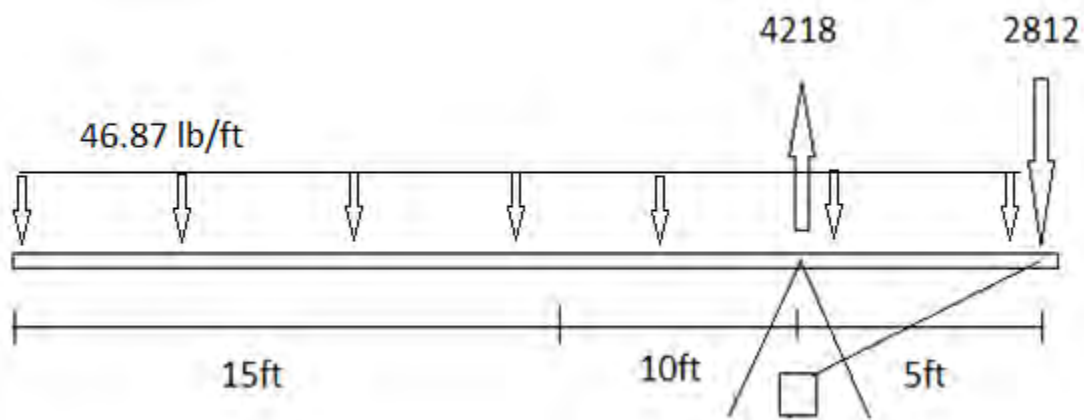
Fig4. Force distribution on first conceptual design.

The forces are represented in lbs. **Fig5** and **Fig6** below show the shear force and the moment distribution along the pipe support.
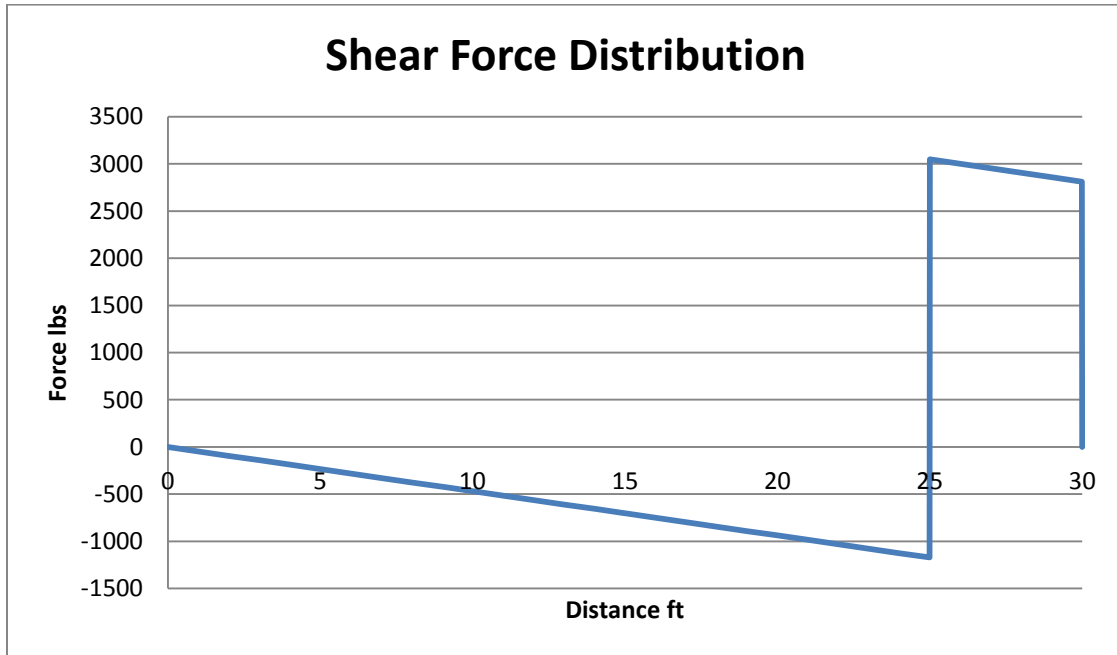
Fig5. Shear force distribution of first conceptual design.
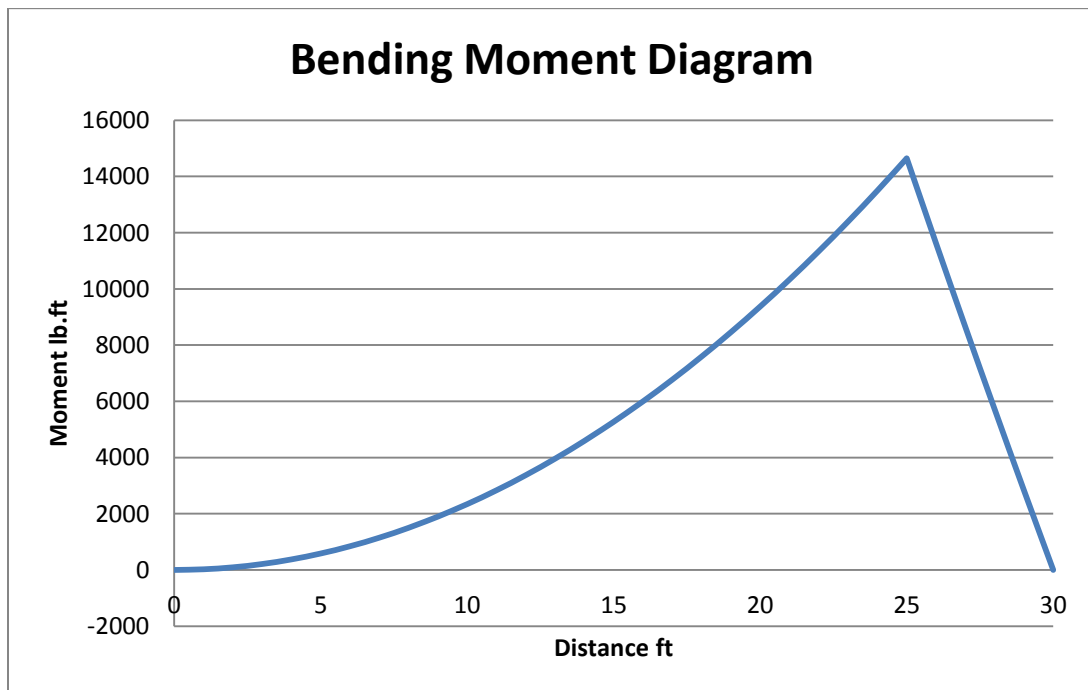
Fig6. Bending moment diagram of first conceptual design.

From the above charts it can be seen that the point of maximum stress is at distance 25ft. The shear force and the bending moment at this point are 4,218 lb. and 14,645 lb.ft respectively. The yield strength of steel is approximately 36,000 psi. Now we can calculate the moment of inertia (I) of the section.

$$I = M . y / Stress……….. (8)$$

Where M is the moment and y is the perpendicular distance between the force and the neutral axis. If we design at 75% of yield strength and assuming y =1 then I = 6.5 in^4. Assuming there would be 2 square steel tubes so each will carry half the stress then I = 3.25 in^4 per section. Therefore, the cheapest standard square steel tube that can carry the load is a 3.5x3.5x3/16" steel tube. The y assumed in equation was 1" while it is actually 1.75" for this specific steel tube so iteration is necessary to make sure it is safe. But let us assume that it is safe. The price of such a section is approximately 12$/ft. Since we will need a minimum of 60ft (30ft x 2) then the price is 720$ for just these two members. In addition to being expensive another major disadvantage is that the hoist will need to have a capacity of at least 4000lb assuming that the angle of the cable with the pipe support is 45 deg. What we currently have in the university is a 650lbs hoist this means we will have to buy a new hoist which will also cost a lot of money.

Another alternative that was considered is to have the base in the middle of the structure as shown in **Fig7** below
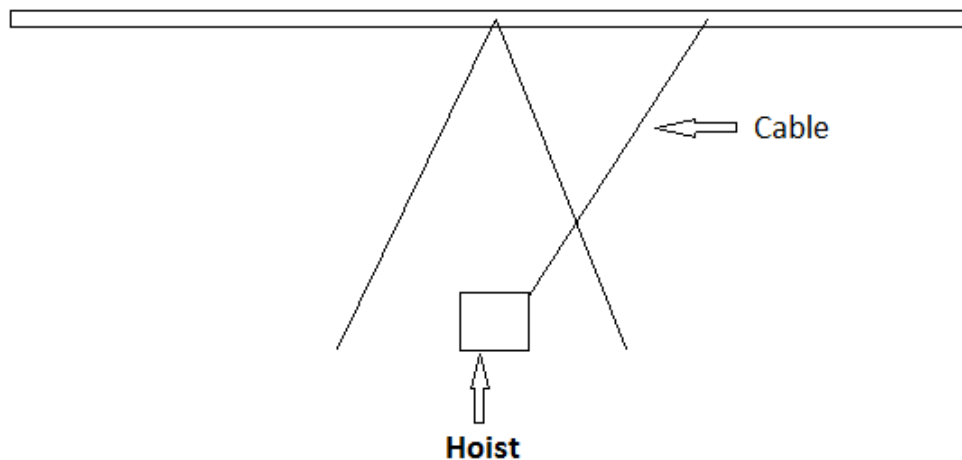
Fig7. Second conceptual design.

Assuming everything is the same, **Fig 8** shows the force distribution on the pipe support.
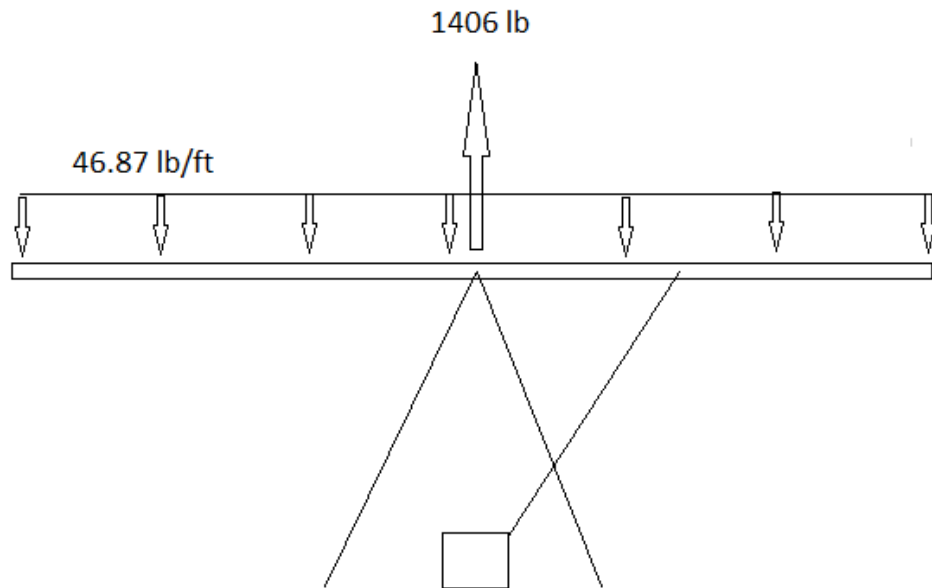
Fig8. Force distribution on second conceptual design.

The shear and moment diagram would be as shown in **Fig9** and **Fig10**.
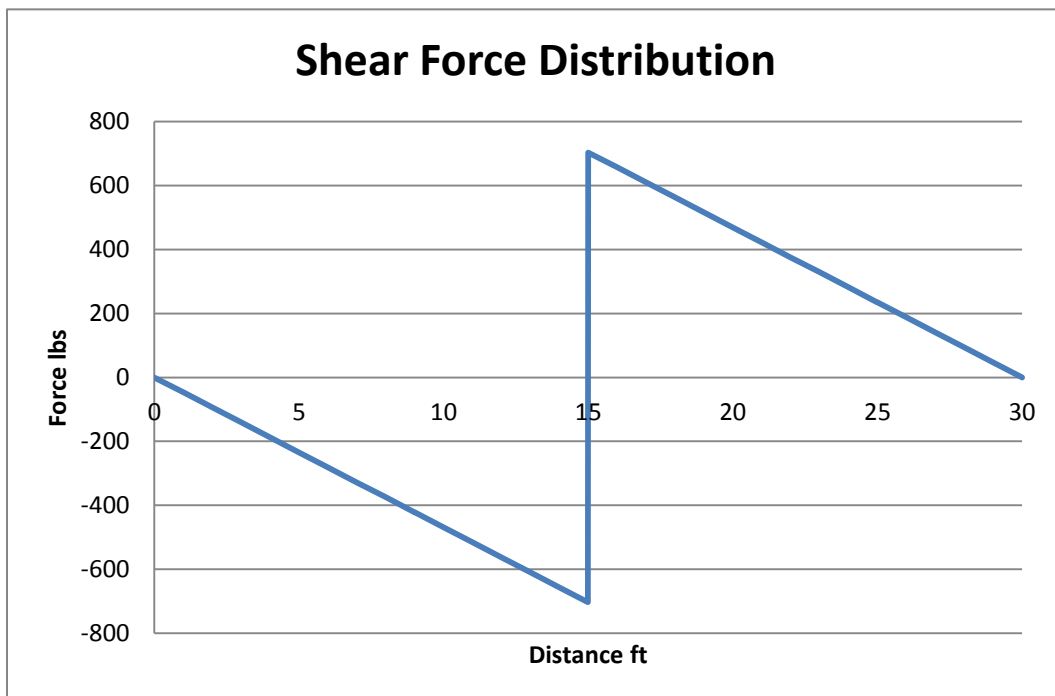
Fig9. Shear force distribution on second conceptual design.
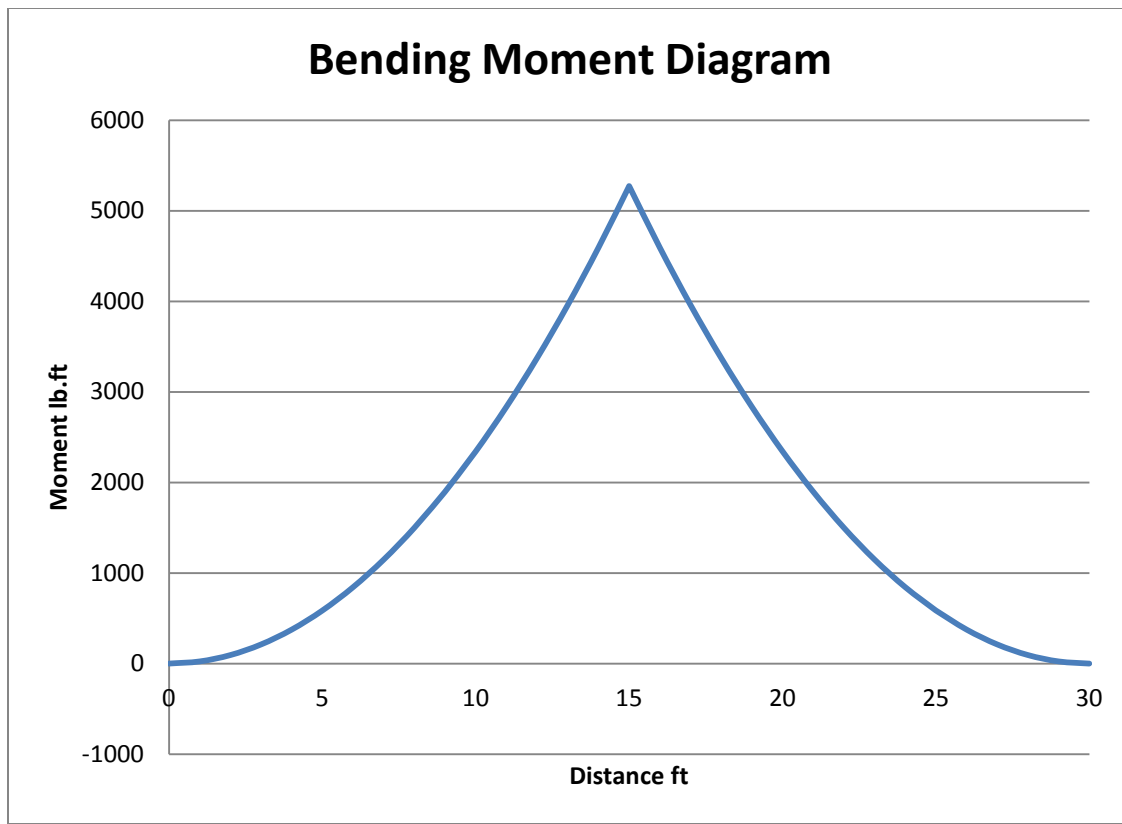
Fig10. Bending moment diagram of second conceptual design.

The maximum shear force and bending moment are 1406 lb. and 5272.5 lb.ft respectively. Using equation 8 and same criteria as before, we get $I = 2.343$ in^4. Assuming again we will have two square steel tubes carrying the load then $I = 1.2$ in^4 per steel tube. The cheapest square steel tube that can carry this load is a 2.5x2.5x3/16". The y assumed in equation was 1" while it is actually 1.25" for this specific steel tube so iteration is necessary to make sure it is safe. But let us assume that it is safe. This tube costs approximately 7.2$/ft giving a total cost for 60ft of 432$ which is significant savings compared to before. Another advantage is that the winch force is almost zero; it only needs to overcome the friction in the pivot and therefore, we could use the winch we already have. A disadvantage of this setup is that the base will be much bigger which might offset the savings but the main disadvantage of this setup is that the pipe will be at 15ft height when it is horizontal. This would make it very difficult to change the pipe,

add or remove fittings, add epoxy and so on. Also the installation of such setup would be very difficult.

This brings us to the design that has been chosen. The only way that we would have a lower stress than the one in the previous example is by having two supports instead of one. To achieve this then the hoist must act as a support along with the base. This is shown in the **Fig11** below
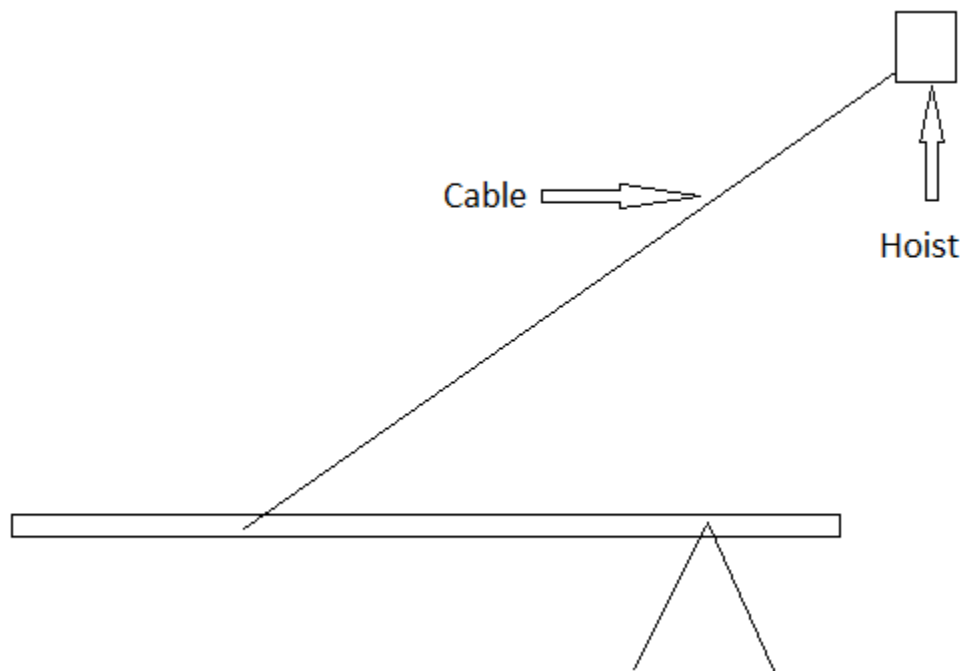
Fig11. Conceptual design of current setup.

The hoist would be attached at the ceiling of the building as shown in the picture. This would provide two support points instead of one. This should reduce the stress dramatically as compared to the first design. **Fig 12** shows the force distribution on the pipe support for this set up.
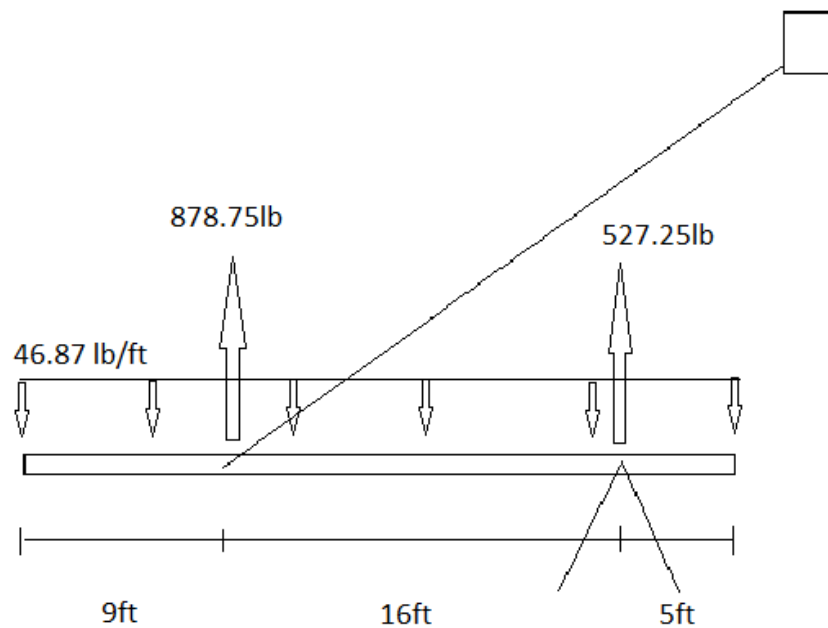
Fig12. Force distribution on current setup.

Now let us examine the shear force and bending moment diagrams as shown in **Fig13** and **Fig14**.
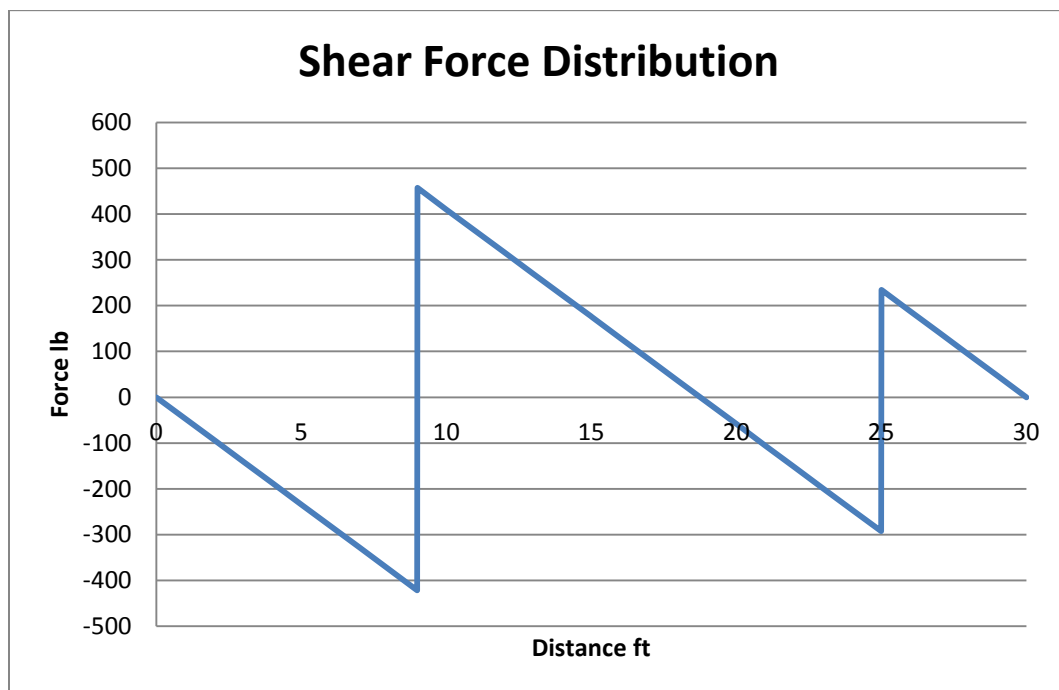
Fig13. Shear force distribution on current setup.

Bending Moment Diagram
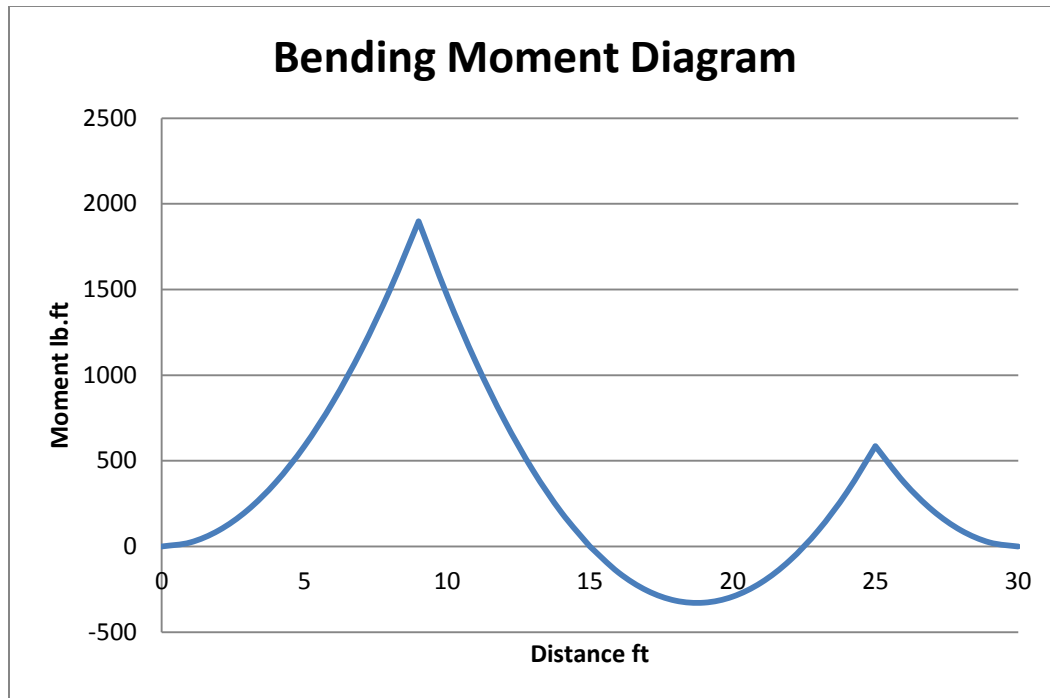
Fig14. Bending moment diagram of current setup.

From the diagrams we can see that the maximum shear force and bending moment are 878.75 lb. and 1898 lb.ft respectively. Using equation 8 and same criteria as before, except for using a stricter 50% of yield stress compared 75% from previous examples, we get $I = 1.265$ in^4. Assuming again we will have two square steel tubes carrying the load then $I = 0.633$ in^4 per steel tube. The cheapest square steel tube that can carry this load is a 2x2x3/16". In this case y is equal 1" as assumed and no more iteration is necessary. This tube costs approximately 5$/ft giving a total cost for 60ft of 300$ which is significant savings compared to any previous case. Another advantage of this setup is that the base is small. The capacity of the hoist in this setup is 1240 lbs assuming that the cable has a 45 degree angle with the pipe support. Though the hoist we had was only 650 lbs capacity we were still able to utilize it for this setup. This was done by using a double line setup which will be explained in or more detail later on in this report. The initial hand calculations concluded that using two 2x2x3/16" square steel tubes would be sufficient for our application. However, further analysis needs to be conducted to more accurately determine whether it is really sufficient or not. So the next step was

to create a three dimensional model of the proposed setup and then perform a finite element analysis to determine whether the pipe support would yield or not.

5.2 Detailed Design of the Pipe Support

The three dimensional model was implemented using the famous software Solidworks. The model consists of two main parts the pipe support and the base.

5.2.1   The Pipe Support

Fig 15 and Fig16 show the model for the pipe support.
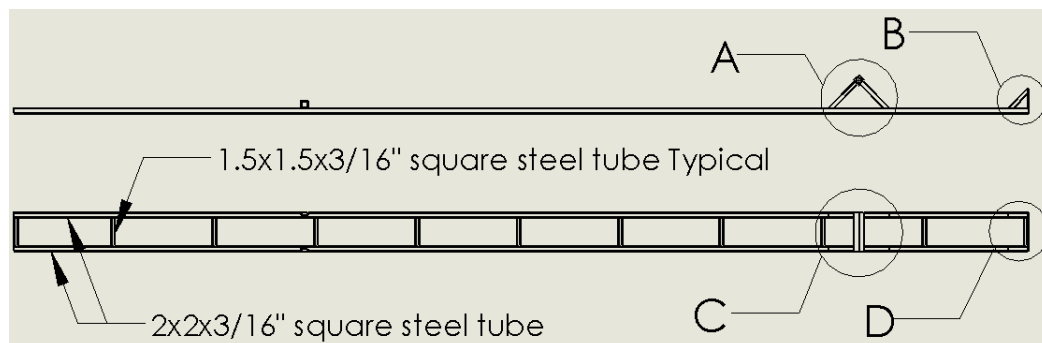
Fig15. 2-d representation of the 3-d model of the pipe support.
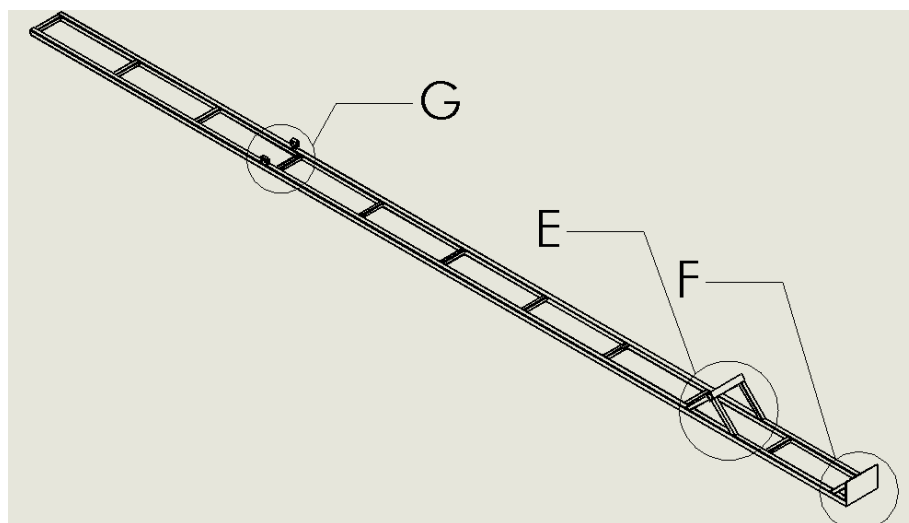
Fig16. Isometric view of the 3-d model of the pipe support.

The pipe support consists of two 30ft long square steel tubes with a 2x2x3/16" section. The two 30ft steel tubes are connected with 10" long square steel tubes that have a 1.5x1.5x3/16" section as shown in the figure above. Circles A, C and E show the pivot link where the pipe support connects to the base through a cylindrical pin. **Fig17**shows a blow out of these circles
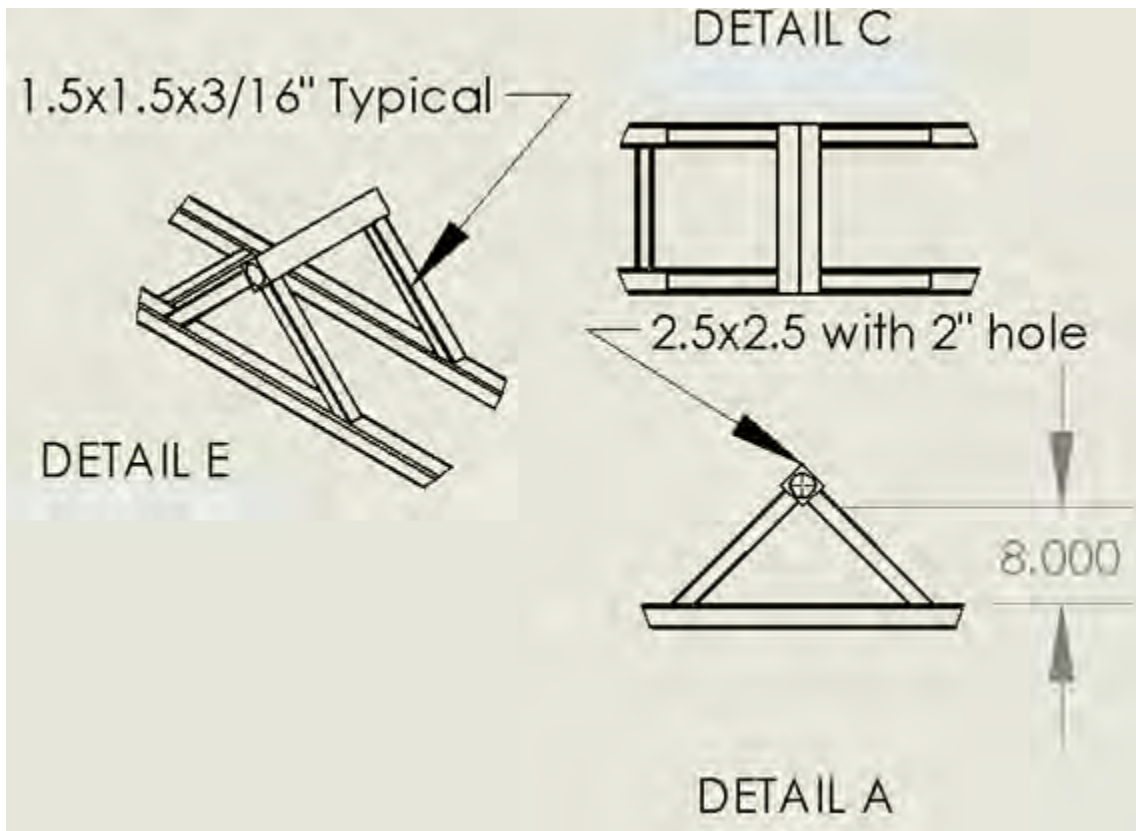
Fig17. Detail of the pivot on the pipe support.

The pivot consists of a 2.5x2.5 square steel tube with a 2" hole. It is positioned at 8 inches above the pipe support so the maximum pipe size of 7 inches can be inserted easily. This steel tube is connected to the pipe support through four 1.5x1.5x3/16" square steel tubes at an angle of 45 deg. A 2" cylindrical pin would be inserted into the 2" hole shown in the figure, to connect it to the base while allowing the pipe support to rotate around it. The 2" hole is above the pipe support to help prevent the pipe support from tumbling over. This will become clearer when we discuss the assembly. Circles B,

D and F highlight a steel plate at the end of the pipe support to prevent it from falling when it is in vertical position. The steel plate is 14x9x0.25". The steel plate is welded to the bottom of the two 2x2x3/16" square steel tubes. It is further supported by two 1.5x1.5x3/16" square steel tubes that connect the far end of the plate to the pipe support. **Fig18** shows a blow out of these circles.
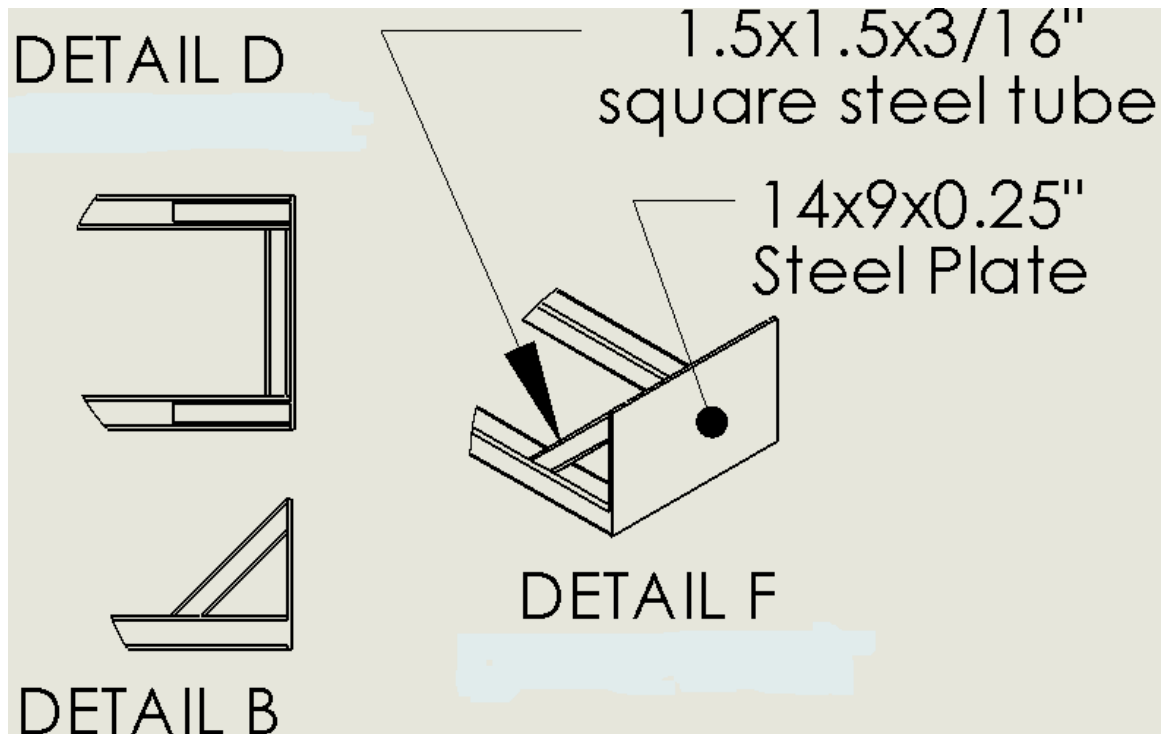
Fig18. Detail of the bottom steel plate.

The last detail in the pipe support is shown by circle G which is blown up by **Fig19**.
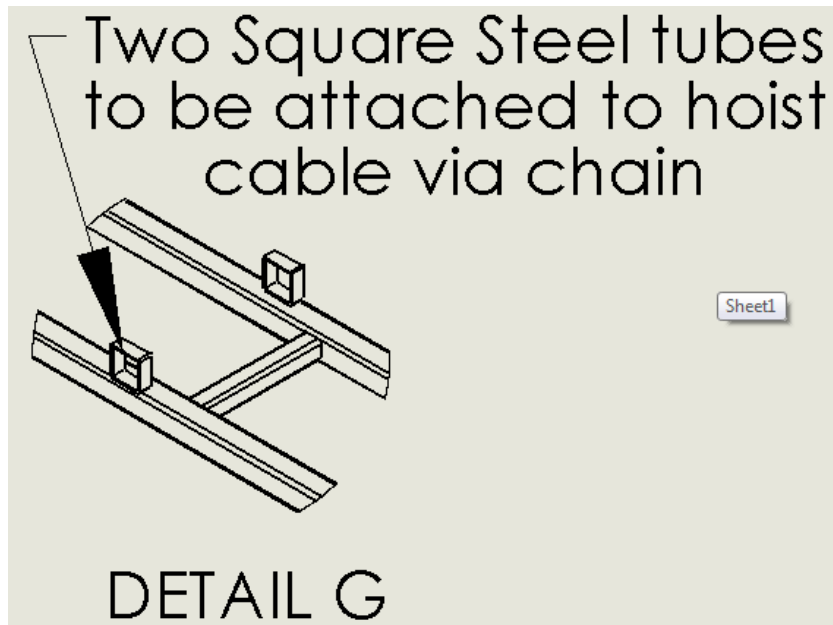
Fig19. Detail of the hoist cable attachment to the pipe support.

The two square steel tubes are to be attached to a chain that is attached in turn to the cable of the hoist to lift and lower the pipe support.

Total Volume of Pipe support = 1221 in^3 Total Weight = 353 lbs.

5.2.2   Base

The base's function is two provide support to the pipe support and provide a pivot point for the pipe support to be able to rotate about. **Fig20** shows the model for the base.

Fig20. 2-d representation of the 3-d model of the base.

The base consists of four legs anchored to the ground. Each leg consists of a 1.5x1.5x3/16" square steel tube. The legs diverge at an angle outward to increase the base area. This increases stability and helps prevent the structure from tumbling over. Each two legs connect to a 2.5x2.5" square steel tube with a 2" hole. The 2" hole holds the 2" cylindrical pin that connects it to the pipe support. The 2" hole goes all the way through to help assembly, so the cylindrical pin can be pushed from one end and pulled

from the other. To prevent the cylindrical pin from moving out during operation two small bolts fit into two holes at the end of the 2.5x2.5 square steel tube. This is shown in circle A in **Fig20** and blown up in **Fig21** below.
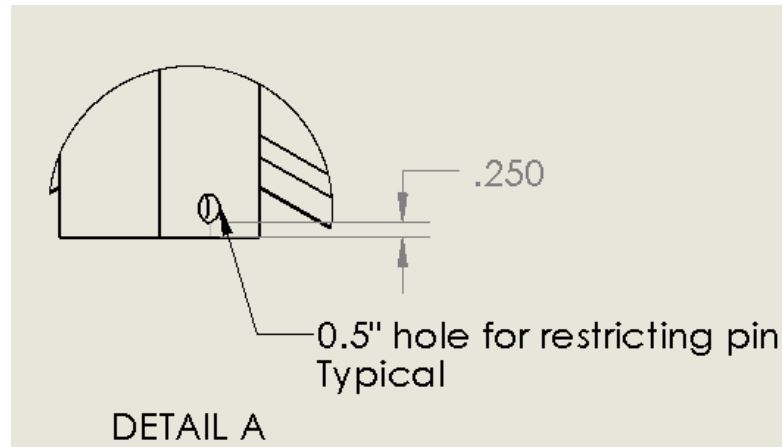
Fig21. Detail of the hole for the restricting pin.

The four legs are strengthened by three square steel tubes at the middle, two from the side with a section of 1x1x0.125" and one from the back with a section of 1.5x1.5x3/16". The one at the back has an additional function other than strengthening the base, which is to prevent the pipe support from tumbling after it reaches vertical position. It is equipped with two stops that bump into the 2 main 2x2x3/16" steel tubes of the pipe support, if it travels beyond the vertical position. The two stops are a 1x1x0.125" square steel tube. Each of the four legs of the base have a small steel plate with three holes as shown by circle C in **Fig20** and blown up in **Fig22**. This is to help anchor the base to the ground via steel bolts.
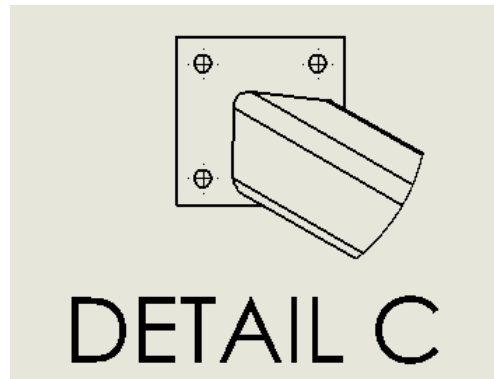
DETAIL C

Fig 22. Detail of how the base is anchored to the ground.

Total Volume of Base = 464 in^3 Total Weight = 132.5 lbs.

5.2.3   Assembly

Fig23 and **Fig24**below shows the pipe support and the base assembled together.
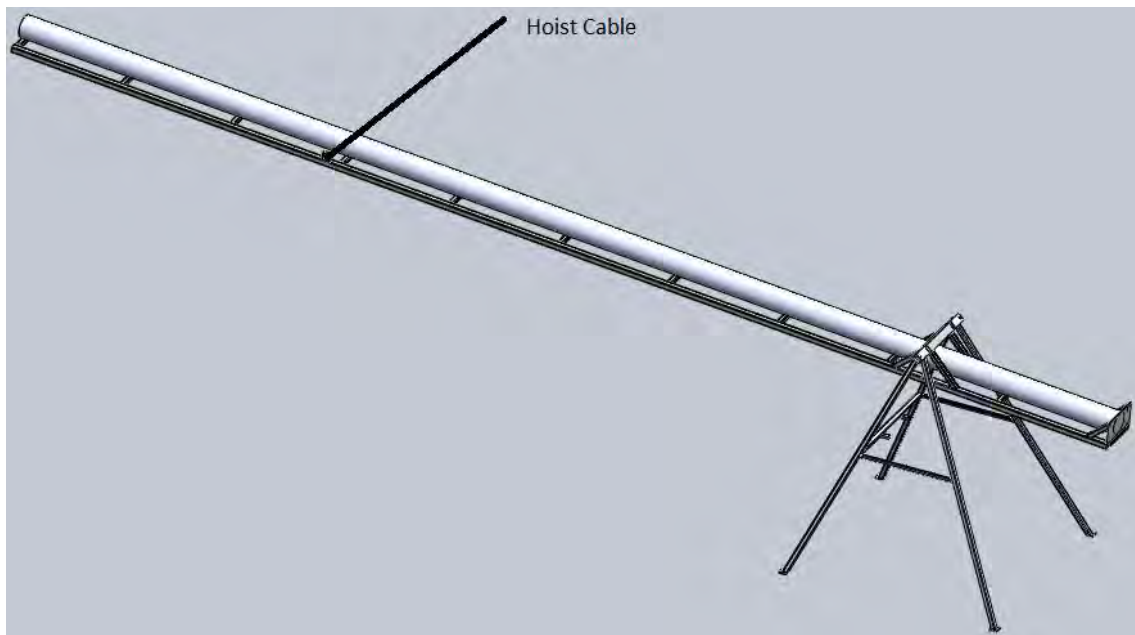
Fig23. 3-d model of the assembly
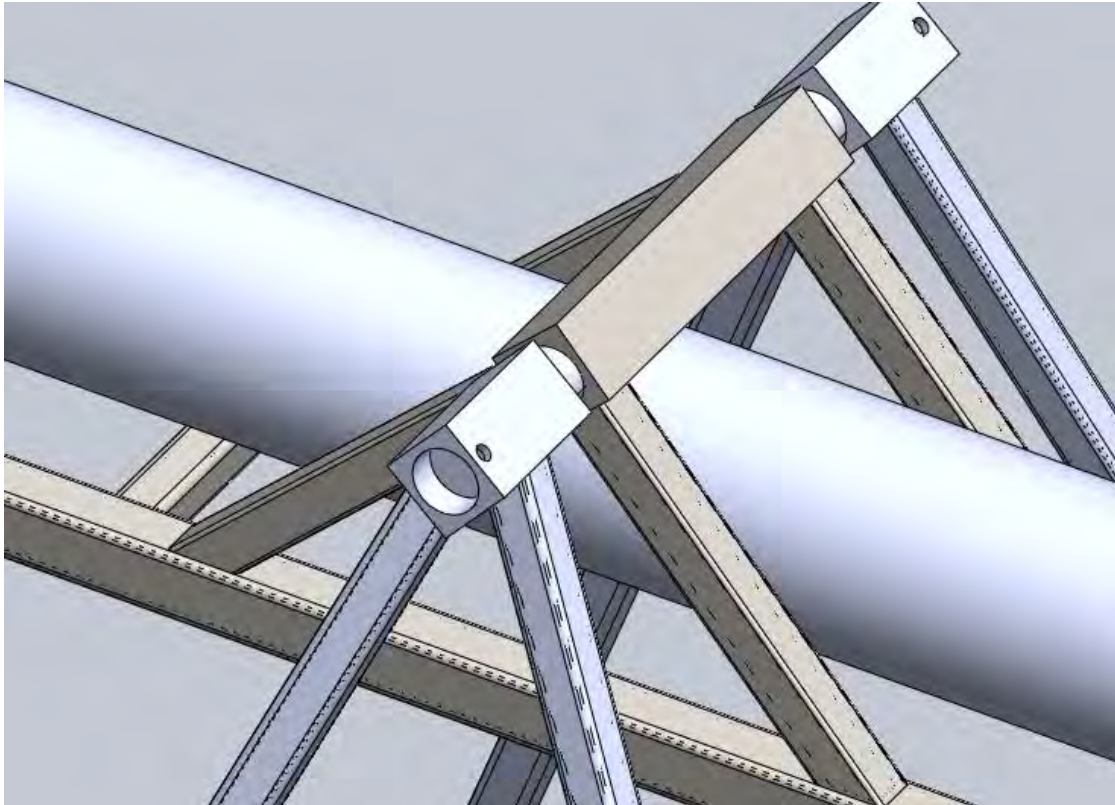
Fig24. The connection between the pipe support and the base.

The figure shows the base anchored to the ground, and a 2" pin connecting the pipe support to the base and a hoist cable pulling the pipe support and causing it to rotate around the pin connecting it to the base. **Fig24** shows a zoom in on the pin connecting the pipe support to the base.

Assembly is simply done by placing the pipe support's 2" hole concentrically with the base's 2" hole and pushing the pin inside. Then finally adding the two restricting bolts to restrict the pin from coming out. Disassembly is done by pushing the pin from one side and pulling it out from the other.

Since the hoist's cable can only pull the pipe support but cannot push it down, it must be made sure that the pipe support's weight always provides a torque in a direction opposite to that of the cable so it can lower itself in the right direction when the cable is slack. This is illustrated in **Fig25** below
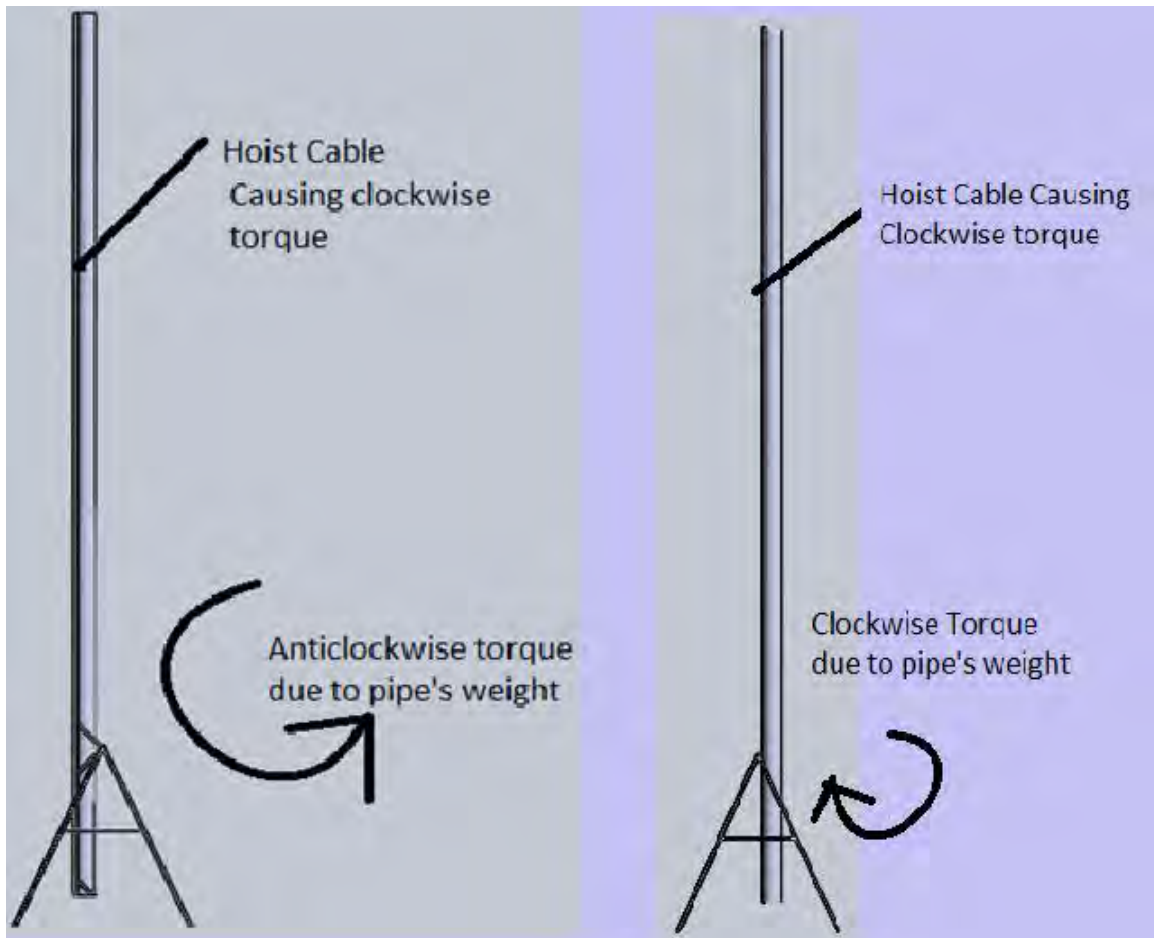
Fig25. Assembly is designed to prevent the pipe support from tumbling over.

The figure above shows two cases. The one on the left shows the pivot point above the pipe support similar to the actual design. The one on the right shows the pivot point below the pipe support. For the case on the left the weights of the pipe support and the pipe are causing a torque in an anticlockwise direction which prevents the pipe from tumbling over and also causes the pipe support to return to its original position when the cable is slacked. For the case on the right, the weight is causing a clockwise torque which will cause the pipe to tumble over. Even if there are stops to prevent this, the pipe support will not be lowered if the cable is slacked. The second feature that is clearer in assembly is the stops. The base has two stops to prevent the pipe from tumbling after reaching vertical position. **Fig26** shows the stops in action.
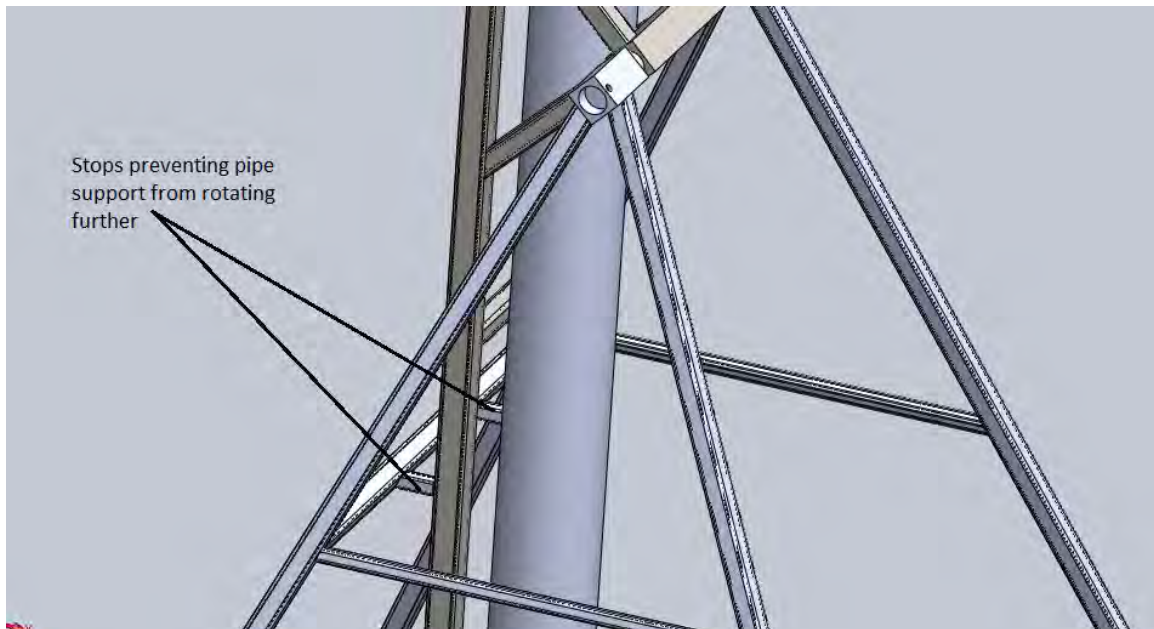
Fig26. The stops of the base in action.

In addition to the stops a limit switch should be added to stop the hoist from pulling further once vertical position has been reached. If hoist is still pulling while the pipe support is resting on the stop, the resulting bending moment will be too great for the pipe support members causing it to break. The limit switch should be designed in a way to prevent the hoist from pulling further at this position but still allow it to slack the cable and lower the pipe support.

5.2.4   Finite Element Analysis (FEA)

Although rough hand calculations were implemented a finite element analysis was necessary to make sure that the pipe support and the base are not over designed and more importantly not under designed. The finite element analysis was performed using Ansys. The three dimensional model was imported from Solidworks as an assembly into Ansys. The pipe support was tested in two different static positions, horizontal and vertical. These two positions represent two extremes. When in horizontal position the bending moment is maximized on the pipe support. When in vertical position the force is

maximized on the steel plate at the end of the pipe support. In vertical position the force is also maximum on the pin and on the base since at this position the hoist is almost carrying no load and all the weight is on the pin and the base. Any angle between these two extremes would have a stress either less on the pipe support members or less on the steel plate and pin.

The first step in the analysis is to import the geometry of the assembly from Solidworks either in horizontal position or in vertical position. Next, contact between parts of the assembly must be specified like for example between the pin and the base and the pin and the pipe support. Then the next step is to define the mesh which is the process of dividing the parts into small elements. Ansys has a very power meshing tool. A tetrahedral element is used to divide the parts into the elements for the analysis. Generally, the smaller the mesh size (element size) the more accurate the results are. The drawback to that is that it would require more computation time and more computer RAM. Time was not an issue so elements were made as small as the computer RAM could handle. For the computer used the smallest element size that could be handled was 0.5in. **Fig27** shows part of the pipe support with the meshed elements. **Fig28** shows a closer look on one of the members of the pipe support.
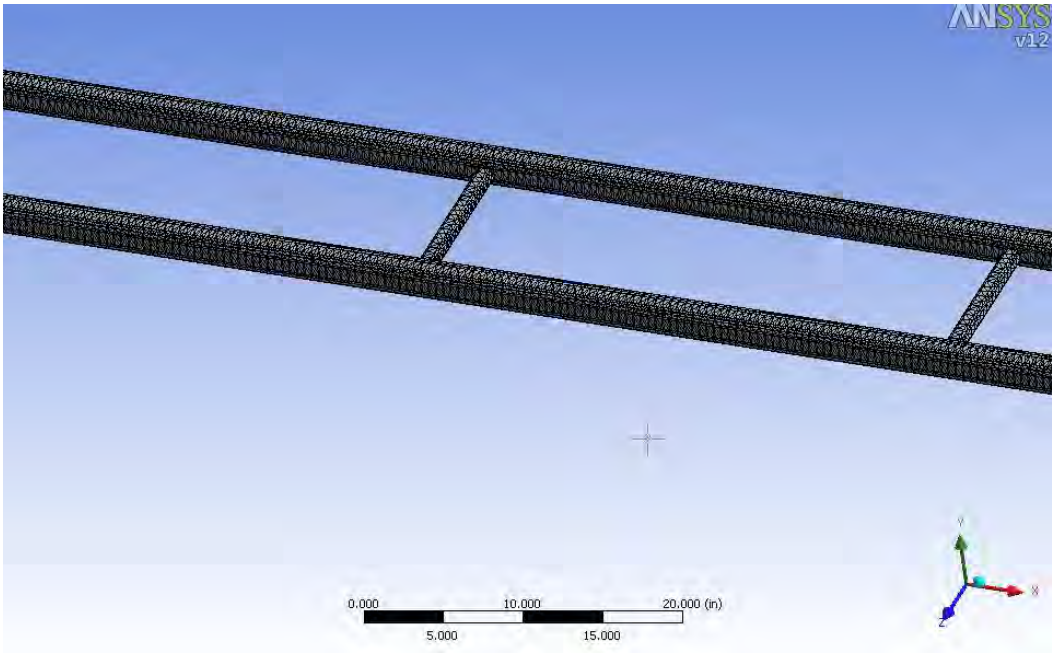
Fig27. The mesh for the FEA analysis.
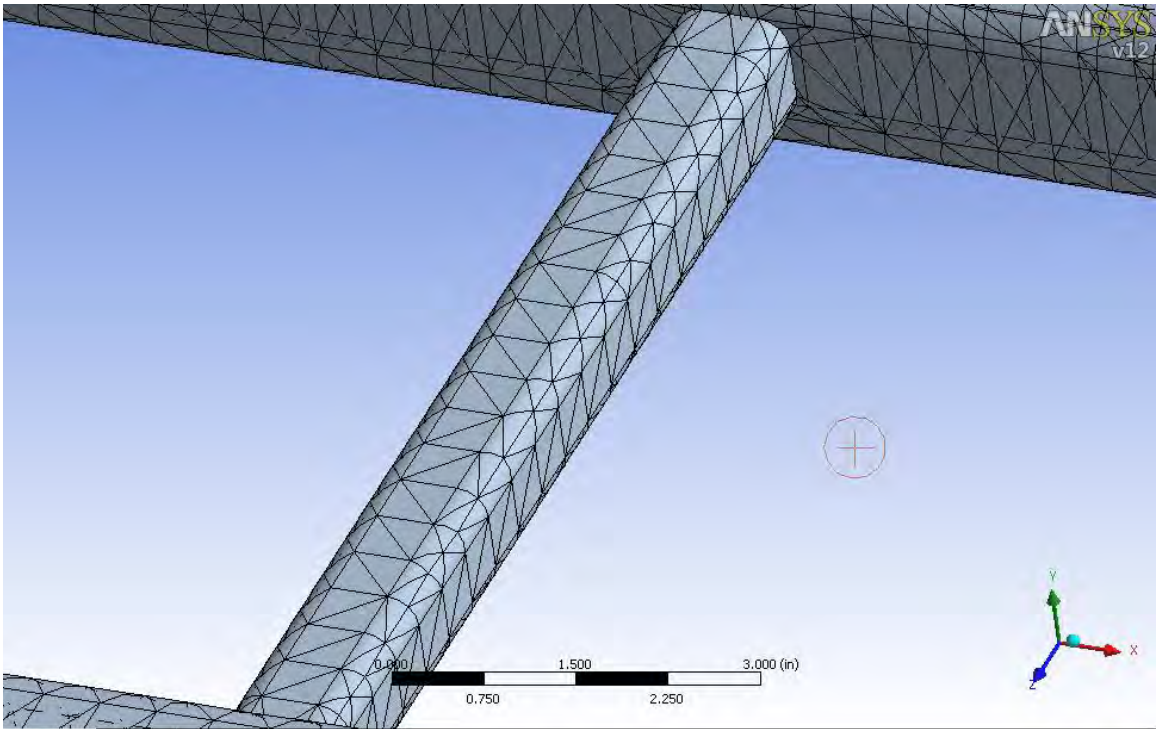
Fig28. Closer look on the mesh.

The element size was thought to be sufficient for this application. The next step was to define the forces and the boundary conditions. The forces that are exerted on the structure come from two sources. One is the weight of the pipe and the fluid inside of the pipe on the pipe support and the second source is the weight of the pipe support and the base on themselves. The latter is easily defined on Ansys by specifying a density for the pipe support, the base and the pin then specifying earth gravity in the desired direction. The weight of the pipe and the fluid were defined differently in the horizontal and vertical positions. For the horizontal position the pipe weight was distributed on a small area in the middle of 10" square steel tubes connecting the two 30ft square steel tubes of the pipe support. A small area was chosen rather than a point load because there will be small rubber pads between the pipe and the pipe support. These pads will distribute the force exerted on them over a small area on the pipe support rather than a point load or a line. The small area was chosen to be 0.5in^2 in the middle of each of the 10" square steel tubes. There are eleven 10" square steel tubes as shown in **Fig29** below.
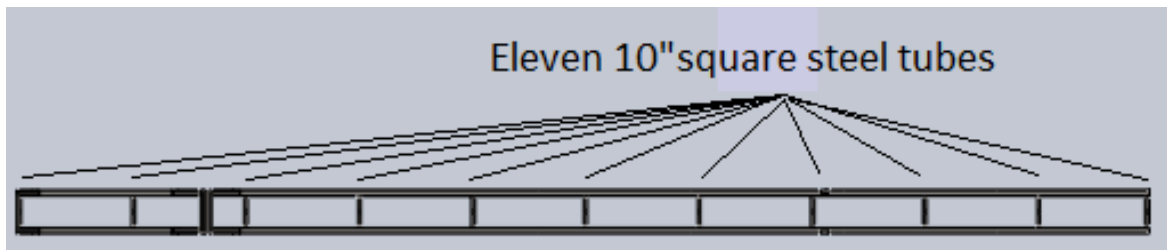
Fig29. Pipe support has 11, 10" long square tubes

Fig30 shows a close up to illustrate the small area on the 10" square steel tubes that the force was distributed on.
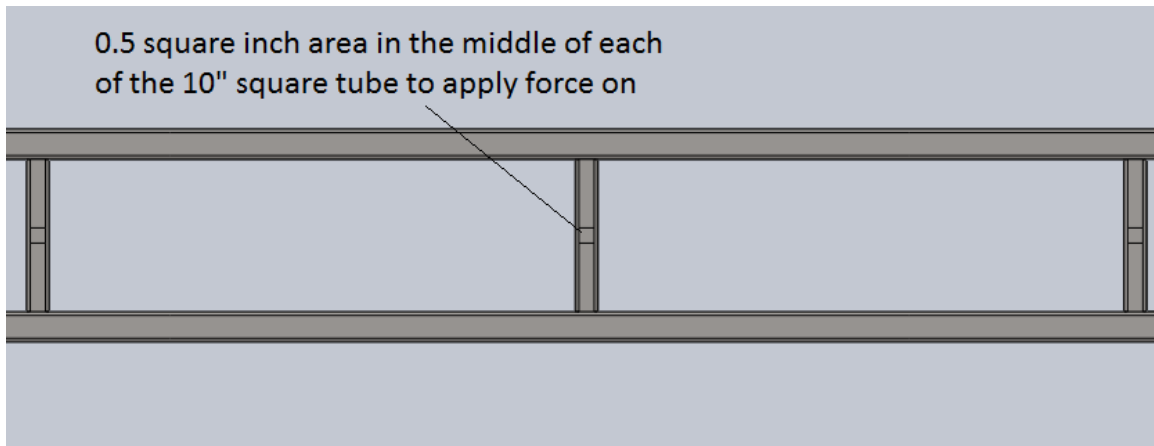
Fig30. The area where the pipe is resting on the pipe support.

The force of the pipe with the fluid in it was calculated in the detailed design section of this thesis and was concluded to be 1056lbs. Now the first and last 10" square steel tube will logically be carrying half the load of the remaining 10" square steel tubes. So then effectively each of the 10" square steel tubes will be carrying 10% of the total weight except the first and the last ones will be carrying 5% of the total load each. Since the force will be distributed on an area then it should be defined as a pressure where the pressure equals the force divided by the area. Since the area is 0.5in^2 then each 10" square steel tube will have a pressure of

Pressure = 1056 x 10% / 0.5 = 211.2 psi
For the first and the last square steel tubes pressure is = 105.6 psi

The force in the vertical position was applied on the bottom steel plate. An area on the plate that is equal to the pipe base area was defined and the total force of 1056lbs described earlier was distributed on that area. The pipe has a 7" diameter giving an area of 38.48in^2. Then the pressure that needs to be applied on that area would be the total force of 1056lbs divided by the area, giving a pressure of 27.44psi. This model is actually more extreme than the actual case since the pipe will be tied to the pipe support with tow straps at horizontal. When the pipe is raised into vertical position some of the vertical force will be carried by the tow straps through friction so not all of the vertical

force will be on the plate. However, modeling it that way would give us a safer estimate in case the straps were not tightened hard enough.

The next step after the forces are defined is to define restraints on the structure. In both the vertical and horizontal cases a full restraint was applied on the bottom of each leg of the base as they are anchored to the ground. The second restraint was added on the knob where the hoist cable would pull the pipe support.

After defining everything previously mentioned the model will be complete and ready to solve. **Fig31** shows the stress distribution on the structure when the pipe support is in the horizontal position. As per the analysis the maximum stress is 20,652 psi depicted by the red color. This occurs at the position where the hoist pulls the pipe support. This agrees with **Fig12** through **Fig14** where it was calculated that this point has the maximum shear force and the highest bending moment.
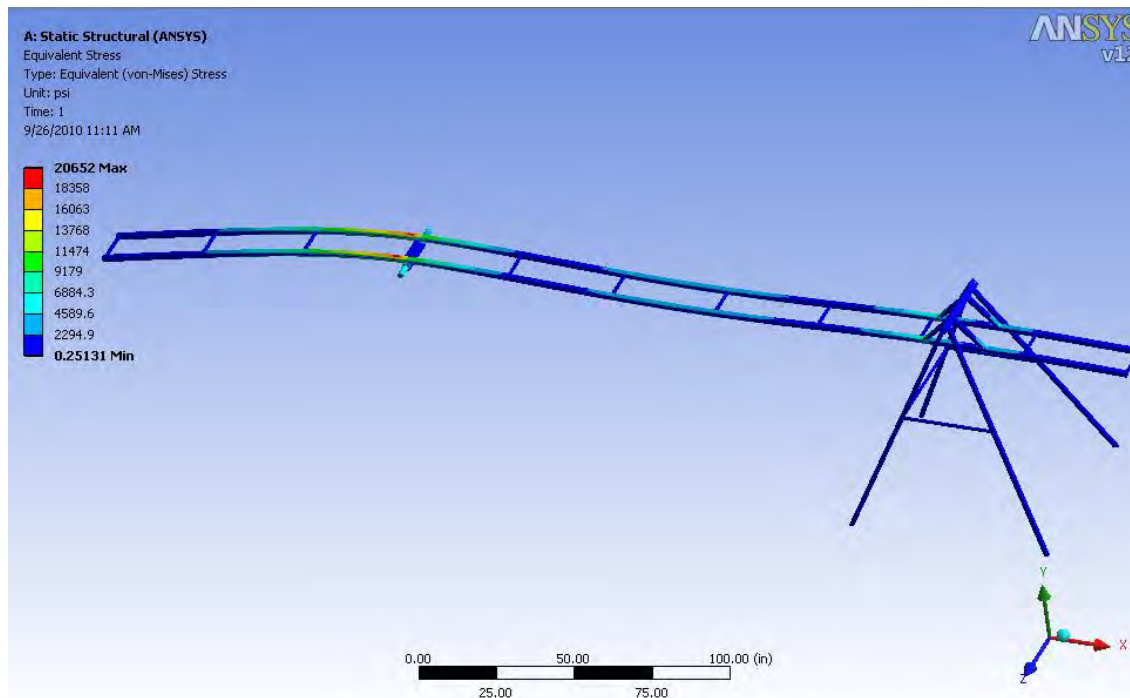
Fig31. Equivalent Von-Mises stress on the assembly in horizontal position.

Fig32 shows the safety factor distribution on the structure in the same position.
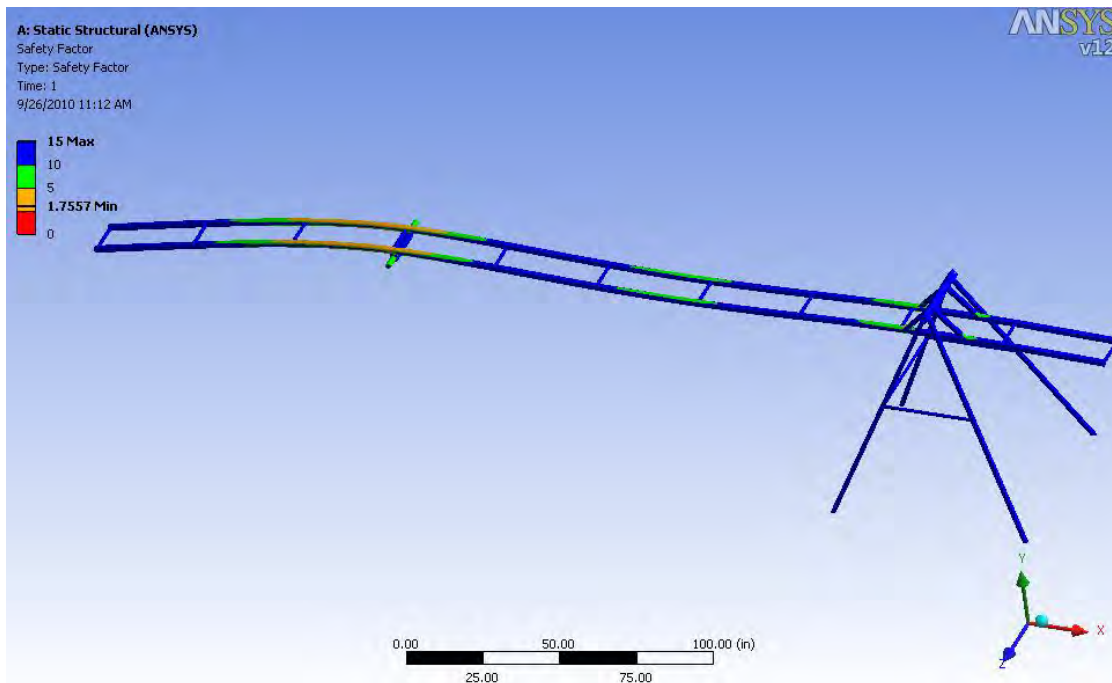
Fig32. Safety factor distribution on the assembly in horizontal position.

The minimum safety factor as per **Fig32** is 1.756 assuming that the steel's yield strength is 36,000 psi which is the strength of the weakest steel grade. This means that the maximum stress would be about 57% of the yield strength which gives evidence that the design is safe and sound in that position. **Fig33** shows the stress distribution in the vertical position.
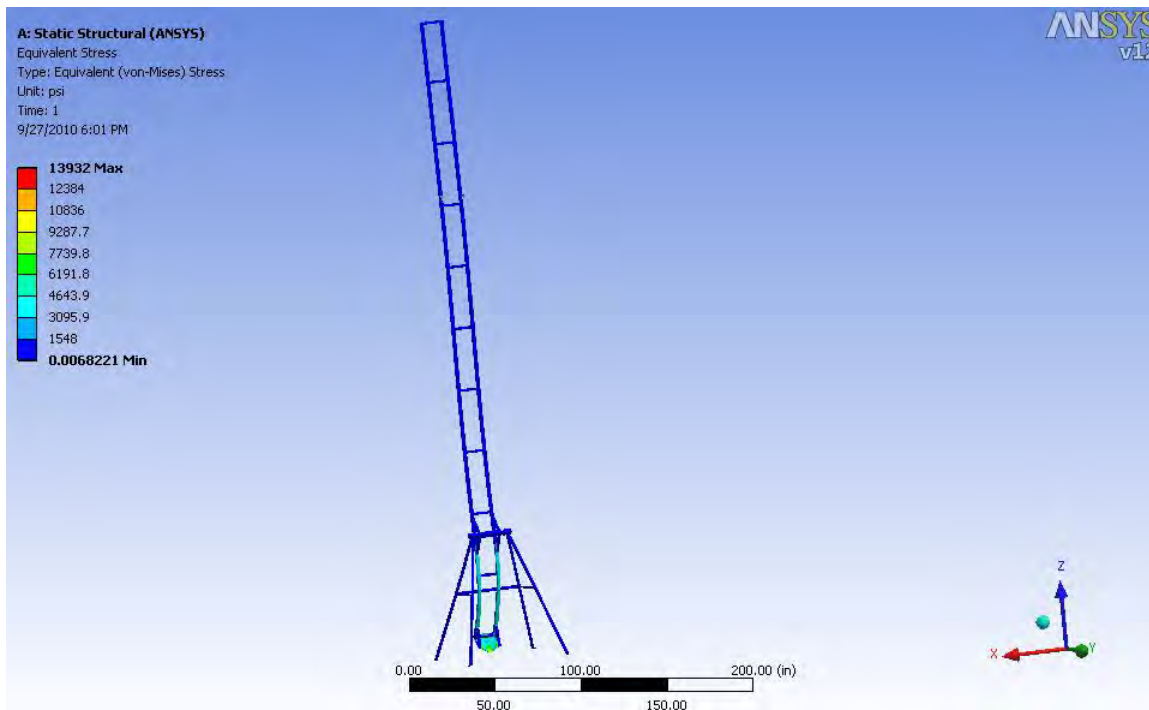
Fig33. Equivalent Von-Mises stress on the assembly in vertical position.

In the figure it can be seen that the maximum stress is 13,932 psi. It can also be seen from the figure that the most stressed area is the plate and the pipe support between the plate and the pivot. This is because this area sees a large bending moment. The area on top of the pivot only sees a small compressive stress due to the weight of the pipe support on itself. As expected the stress is much smaller than in horizontal position because the bending moment is smaller because the distance between the force and the support is much smaller. However, it was important to run the analysis at vertical position to correctly size the bottom steel plate and check if the 2" pin is strong enough. If the plate was of lesser thickness than 0.25in the plate would have yielded. **Fig34** shows a zoom in on the steel plate from the front and **Fig35** shows the steel plate from the back to show where the maximum stress occurs.
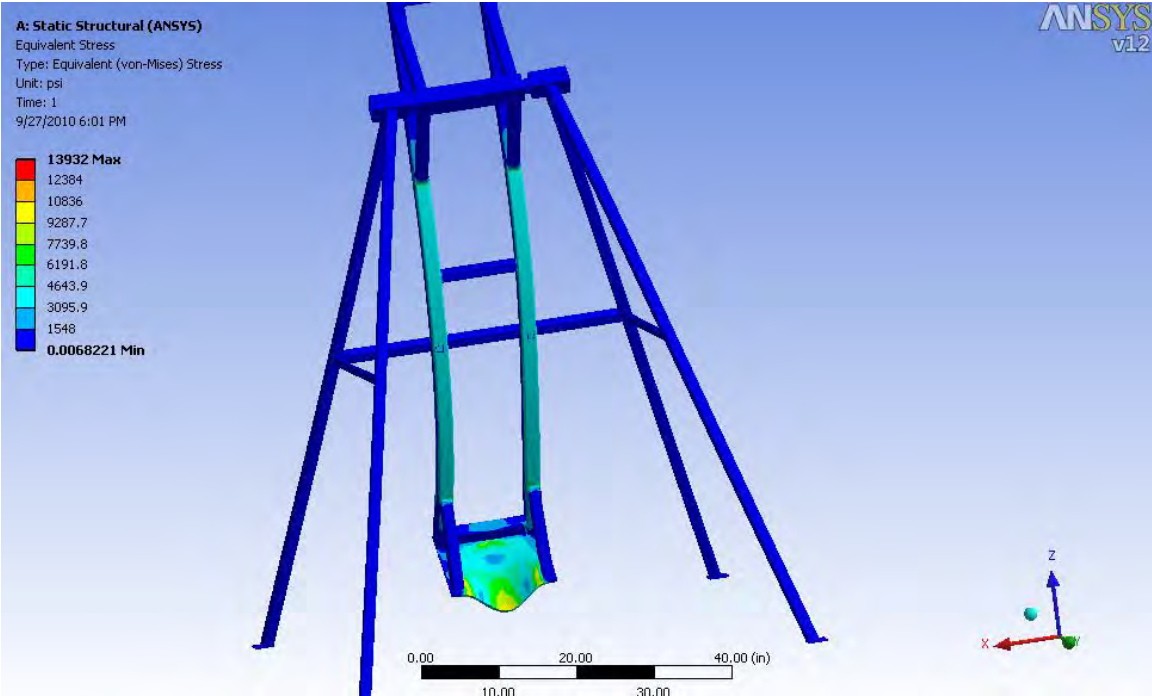
Fig34. Closer look on the equivalent Von-Mises stress on the assembly in vertical position.
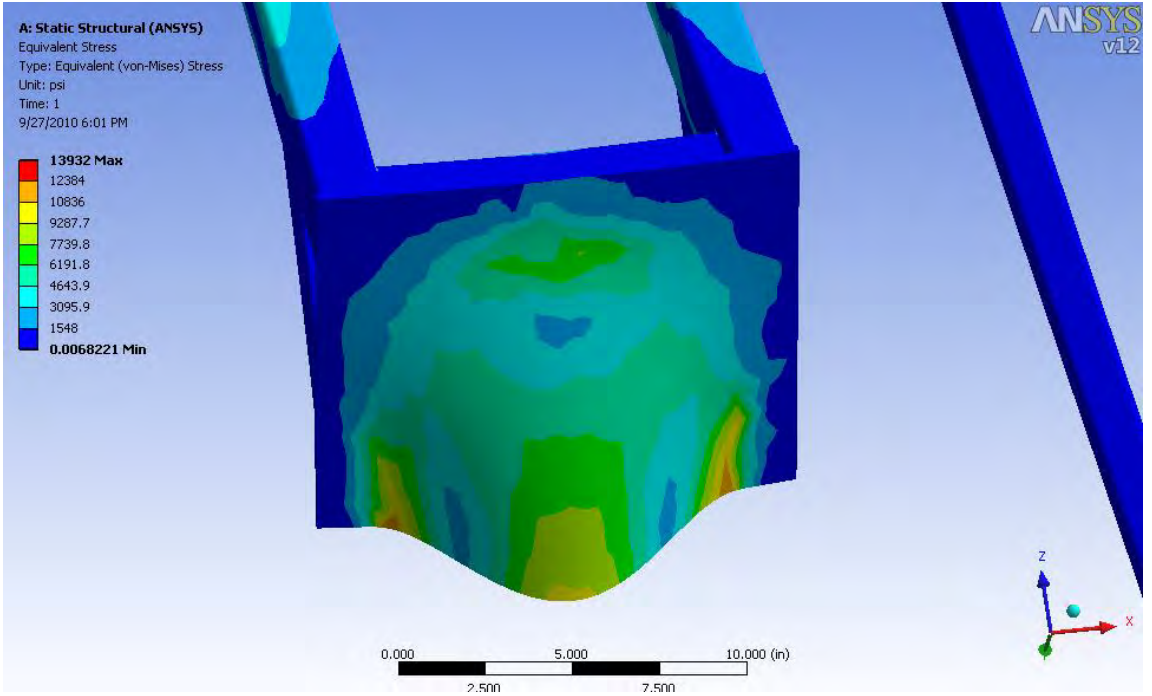
Fig35. Closer look on the equivalent Von-Mises stress on the back of the steel plate while pipe is in vertical position.

Fig36 through **Fig38** show the safety factor distribution for **Fig33** through **Fig35** respectively.
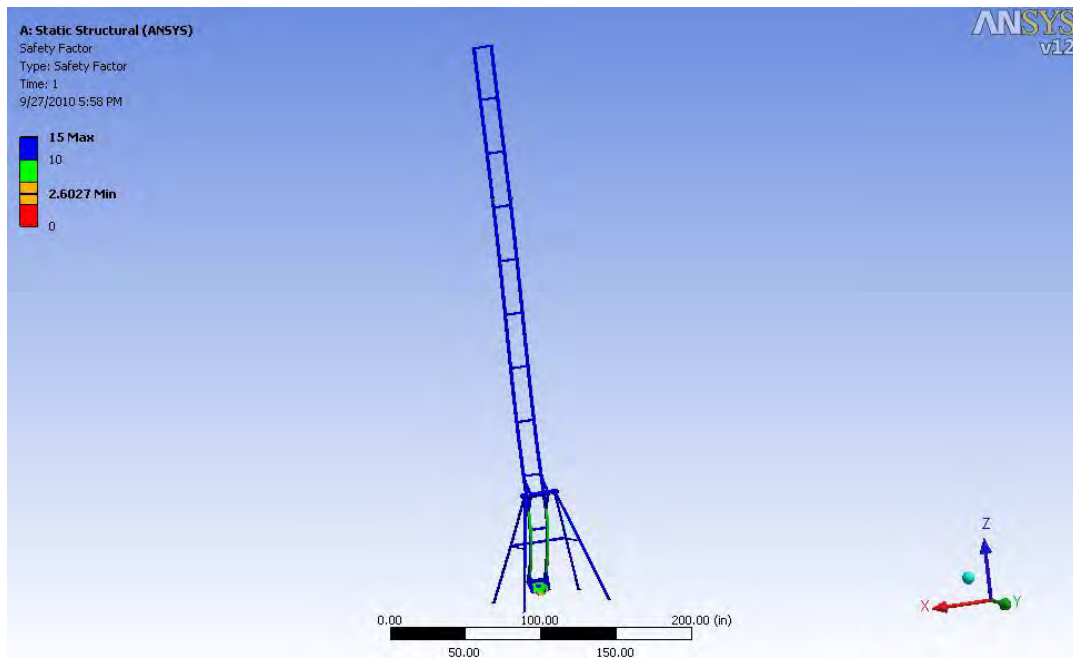
Fig36. Safety factor distribution on the assembly in vertical position.
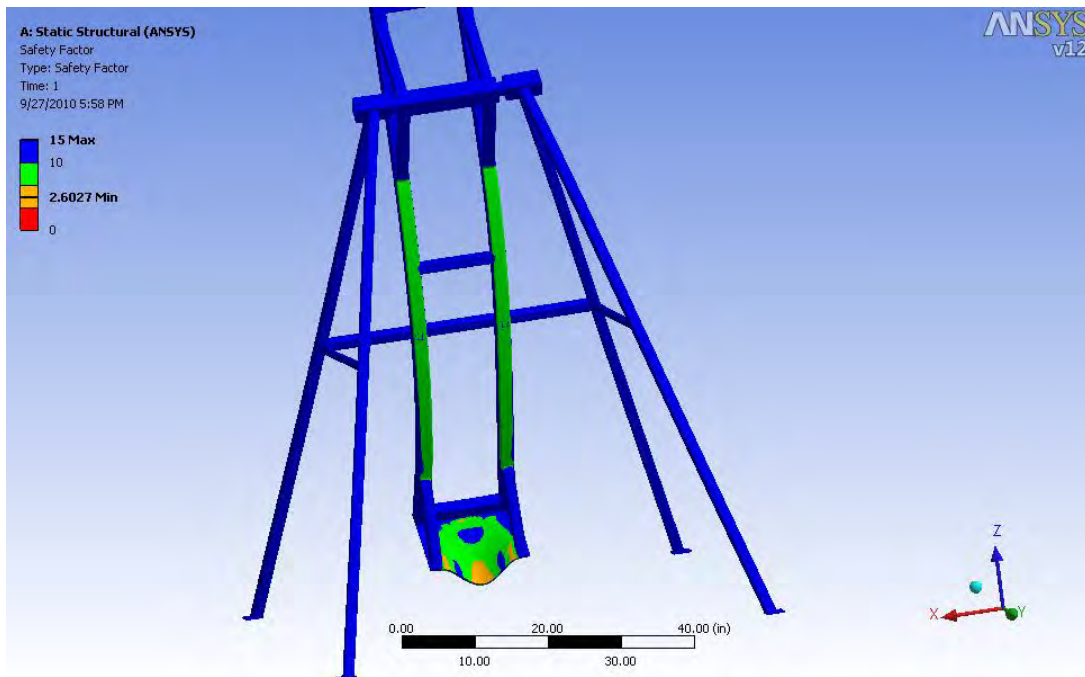
Fig37. Closer look on the safety factor distribution on the assembly in vertical position.
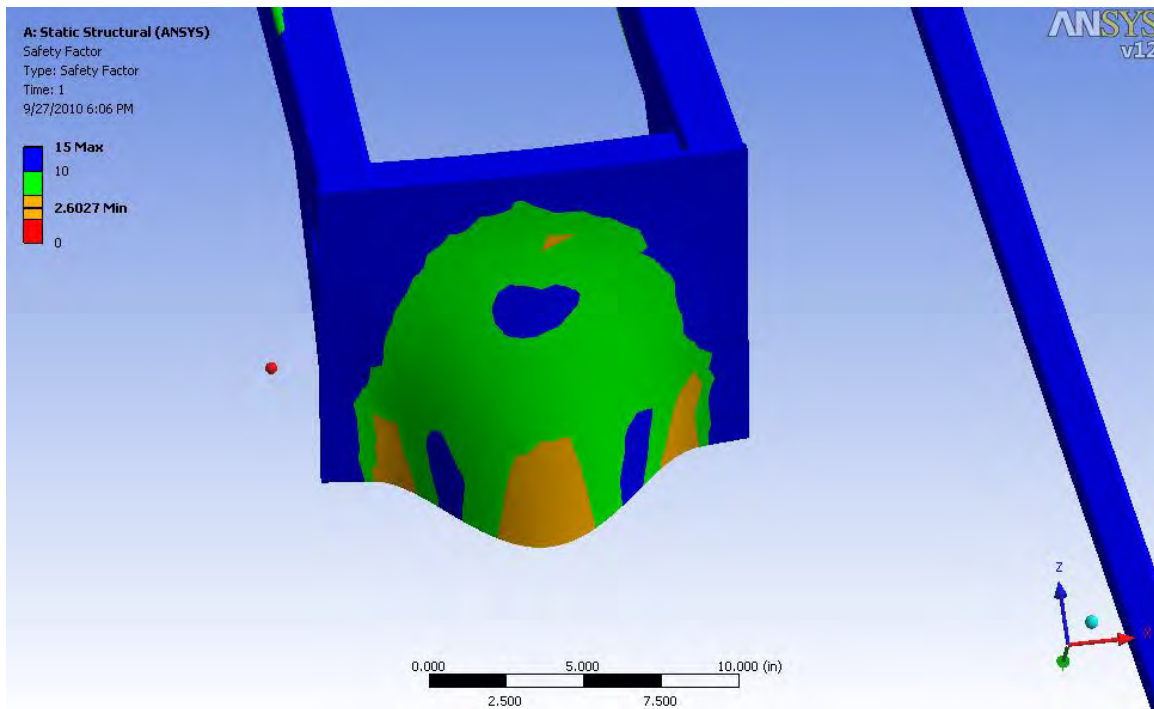
Fig38. Closer look on the safety factor distribution on the back of the steel plate while pipe is in vertical position.

As can be seen from all the previous figures the entire structure is safe and the minimum safety factor is 1.756. This occurs at the maximum design load when the pipe support is in the horizontal position. Static analysis was considered to be sufficient because the travel speed of the pipe support is very low and therefore excess stresses resulting from the movement of the pipe support could be ignored. At this step the design was deemed safe and implementation was carried out without need for further modifications.

5.3   Implementation

5.3.1   Pipe Support Assembly

As discussed before the experimental setup was to be installed in the University Services Building (aka TI Building). The building is a huge warehouse with each department owning a plot inside. The petroleum department owns a plot about 75ft x 50ft. This building was chosen because its ceiling just above 30ft high. The building also has an exposed steel structure that is ideal to mount our hoist and pulleys. The building has vertical I-beams 50ft apart in a square distribution. Resting on top of these I-beams are horizontal I-beams connecting the vertical I-beams in one direction. In the other direction the horizontal I-beams are connected to one another through small joists. As Shown in **Fig39**

Fig39. The steel structure of the University Services Building.

A certified structural engineer from the university's physical plant, conducted an analysis on the building's structure to make sure the building can withstand the load from the experimental setup. He was provided with the expected loads from the experimental setup. His conclusion and instruction was that the only safe place to mount the hoist and pulleys are very close to the vertical I-beam and that the small joists should not bear any load. This turned to be convenient because the hoist's remote controller is attached to the hoist through a cable that is only 5ft long and therefore the hoist needs to be at low level so that the remote controller can be reached. The final setup that was decided to be implemented is schematically shown in **Fig41**. As previously discussed the hoist that was available to us had a capacity of only 650lbs. and the maximum expected tension in the cable was approximately 1250lbs. So for the hoist to work we needed to have a double line setup. This is shown in **Fig41**. The cable goes from the hoist to a pulley (snatch block) attached to the horizontal beam at the ceiling then to another pulley attached to the pipe support then attached back to the horizontal beam. This means that even though the tension in the cable cannot exceed 650lbs. the setup can carry loads up to 1300lbs. There are two other advantages with this double line setup. The first is that the speed of the pipe support will be half of the speed of the cable. This is very important advantage because it reduces dynamic loading and enhances control of the positioning of the pipe support. The second advantage is that this setup will decrease the load on the building. **Fig40** illustrates this.
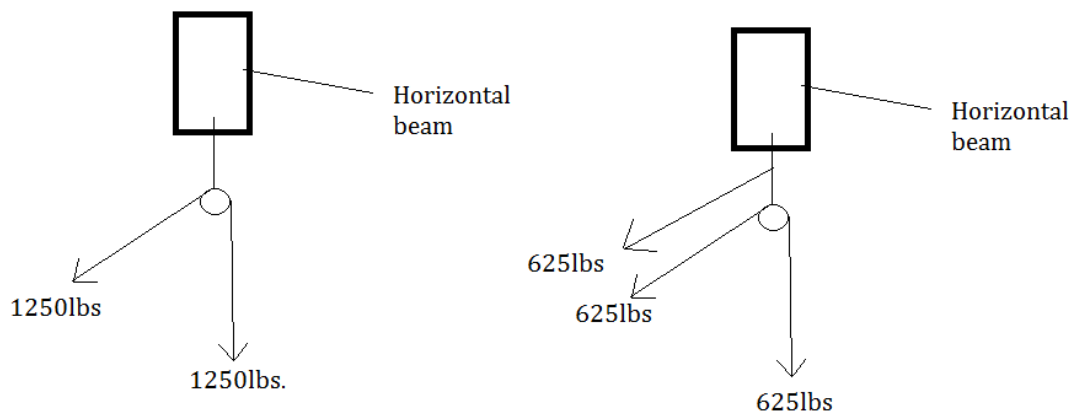
Fig40. Forces acting on the building's steel structure for single and double line setup.
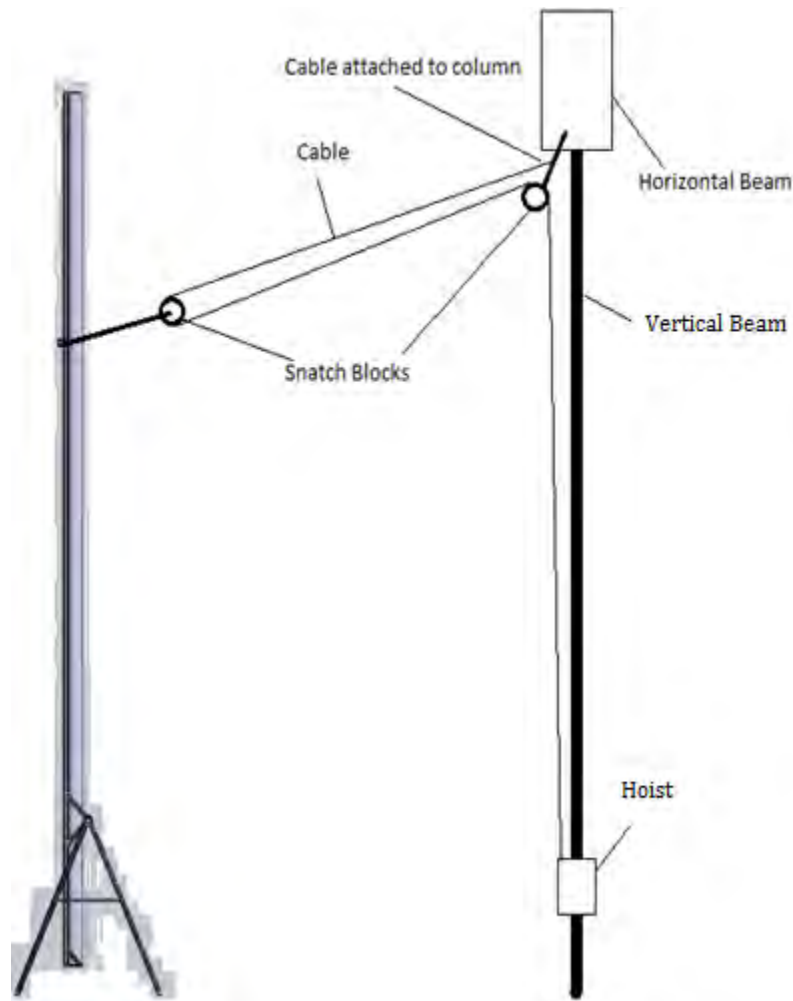
Fig41. Schematic of the double line setup.

After the analysis of the building was finished, 2d working drawings of the pipe support and the base were sent to a steel fabrication shop to begin the construction.

The hoist had a 50ft cable which was not long enough for the setup shown in the previous figure. In addition the cable had a kink in it and needed replacement anyway. A new 100ft cable was bought with the same dimensions as the original cable which is a 3/16" 7x19. (3/16" is the diameter of the cable and 7x19 means that there are 7 strands and each strand has 19 wires.) This cable had a strength of 840lbs which gives almost a 30% safety factor of the maximum expected load of 650lbs. A very important factor

affecting the cable strength is the pulley. If the pulley is too small the cable carrying capacity and life will decrease. **Table3** shows the effect of the pulley diameter on the cable strength.

Ratio "A" = Pulley DIA./Cable DIA.	Strength Efficiency Compared to Original Strength In %
40	95
30	93
20	91
15	89
10	86
8	83
6	79
4	75
2	65
1	50

Table3 (Ref 11). The effect of the pulley's diameter on the cable's strength.

The absolute minimum ratio of the pulley diameter over the cable diameter for a 7x19 cable is 18:1 which means the minimum pulley diameter is 3.4". (Ref 12) Therefore, the pulley selected was 4". To attach the pulley and the cable end to the top horizontal beam, a beam clamp has been used of suitable capacity. This is illustrated in **Fig42**.
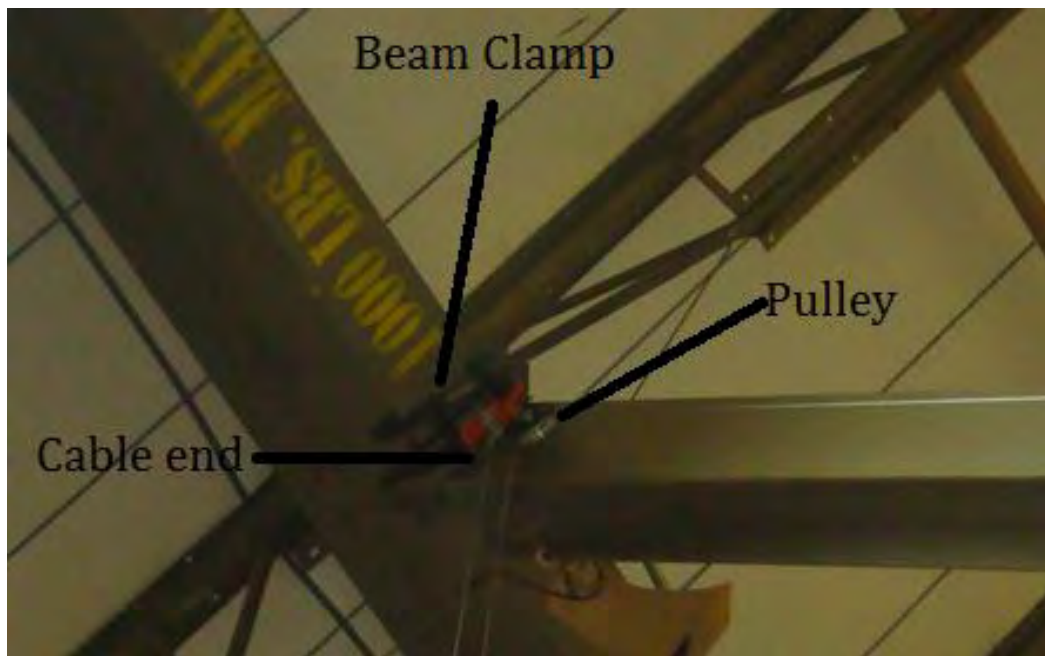
Fig42. The beam clamp and the first pulley.

To attach the hoist to the column a steel plate was welded to the column as per the instruction of the physical plant. They preferred to weld the plate rather than bolt it in the column. The plate has a seat for the hoist to be bolted on. **Fig43** illustrates this.

Fig43. The hoist.

Fig44 shows the pipe support with a pipe mounted on top. In the figure it can be seen that the design was closely implemented. The figure shows the base, pipe support, the bottom pulley attached to the pipe support via chain and at the far end there is another base. The second base is to carry the pipe support after the experiment is complete to relieve any load on the building. All steel parts were painted to minimize rusting. Tow straps were used to hold the pipe on the pipe support. Tow straps were compared with steel U-bolts to hold down the pipe but tow straps were preferred for several reasons. First they follow the shape of the pipe so the load would be distributed over an area for steel U bolts if the diameter of the pipe and the U bolt are not exactly equal the load will be applied on a single line rather than an area. Furthermore, the tow straps can accommodate any pipe size. Lastly, the straps will be softer on the plastic pipe where steel U bolts if they are tightened too much, might crack the plastic pipe. Tow straps have a 10,000lbs strength capacity which is much more than what is needed

Fig44. The pipe support assembly.

Rubber pads were placed between the pipe support and the pipe for the same reasons described, to distribute the force over an area rather than a line and to be softer on the pipe. An additional function of the rubber pads is to prevent sliding of the pipe due to its high friction coefficient.

Fig45 shows the pipe support in vertical position.

Fig45. The pipe support assembly in vertical position.

As described before precautions were taken to prevent the pipe support from tumbling over. **Fig46** shows the stops and part of the limit switch system.
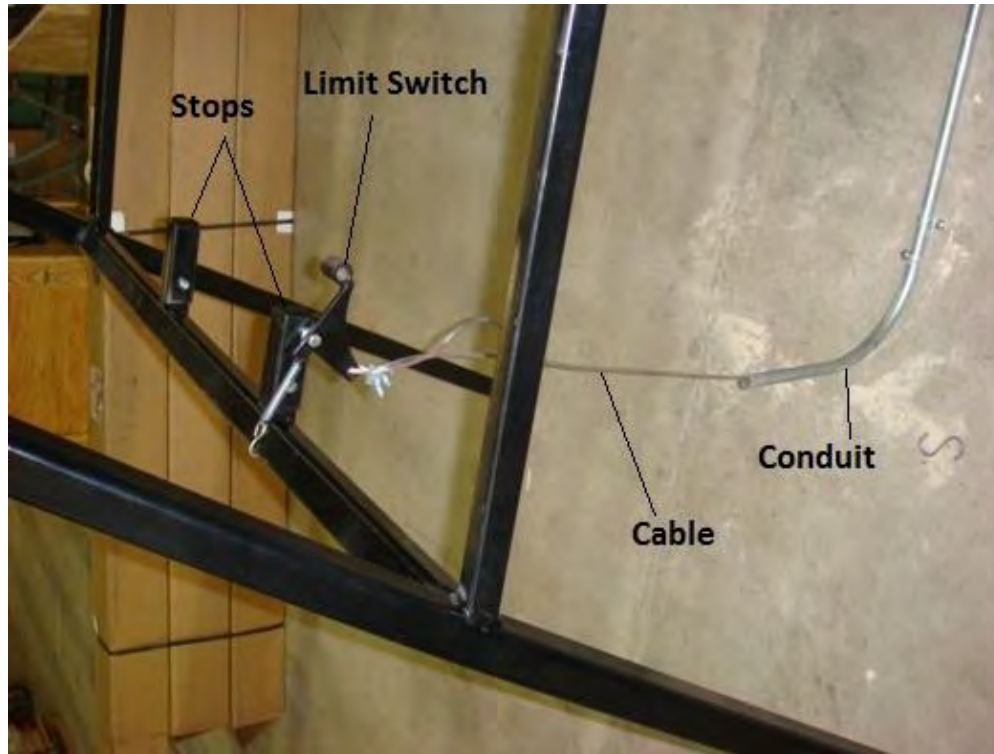
Fig46. The limit switch mechanism at base.

The stops prevent the pipe support from travelling too much and tumbling over. The limit switch, as seen in the figure, consists of a lever held forward with a spring and a cable attached to the lever at one end and the built-in limit switch in the hoist. **Fig47** and **Fig48** show the built-in limit switch of the hoist and the cable attached to it. The conduit shown in the figures is to provide a guide for the cable and to anchor it to the ground to minimize trip hazards.

Fig47. Limit switch handle on hoist.

Fig48. Limit switch mechanism at hoist.

Basically, when the pipe support reaches vertical position it bumps into the lever and pushes it back. The lever in turn pulls the cable up and the cable in turn pulls the built-in limit switch handle of the hoist down preventing further pulling of the pipe support. **Fig49** shows the pipe support pushing the limit switch lever back. **Fig50** shows the limit switch lever and the hoist relative positions to give an overview and a better understanding of the system.

Fig49. Limit switch mechanism in action.

Fig50. Overview of the limit switch mechanism.

The picture above also shows a boom that was laid on the ground to contain liquids in case of a spill and prevents it from reaching the neighboring plot as was required by the safety department.

.

5.3.2   Pipe

Starting at the bottom the pipe has a cap at the end that has a hole in its center which has a valve connected to it. A hole was drilled in the bottom steel plate so the valve could be connected to the bottom cap as seen in **Fig51**. The function of the valve 1 is to collect the epoxy that has settled at the bottom and then a hose can be connected (hose 1) as shown in the figure to guide the remaining water to the drain.

Fig51. Pipe fittings 1.

Next comes a 3.5ft long 6" in diameter clear PVC pipe which acts as a collection chamber for the epoxy. On top of that is a PVC tee (first tee) which 6x6x4" that connects the 6" pipe with a 4" tee (second tee) as seen in **Fig52**. One side of the 4in tee is connected to a 1" valve (valve 2) that closes and opens communication between the pipe and hose 2. The other side of the tee is connected to a 1" elbow that connects it to a third tee. The third tee connects to valve 3 on one side and a pressure transducer at the other as seen in **Fig53**. Valve three controls communication between the pipe and hose 3. Hose 3 is to fill the pipe with water. Hose 2 is connected to the drain and has two functions. One is to allow air to escape while hose 3 is filling the pipe with water. The second function is to drain the water above it when the pipe is vertical.
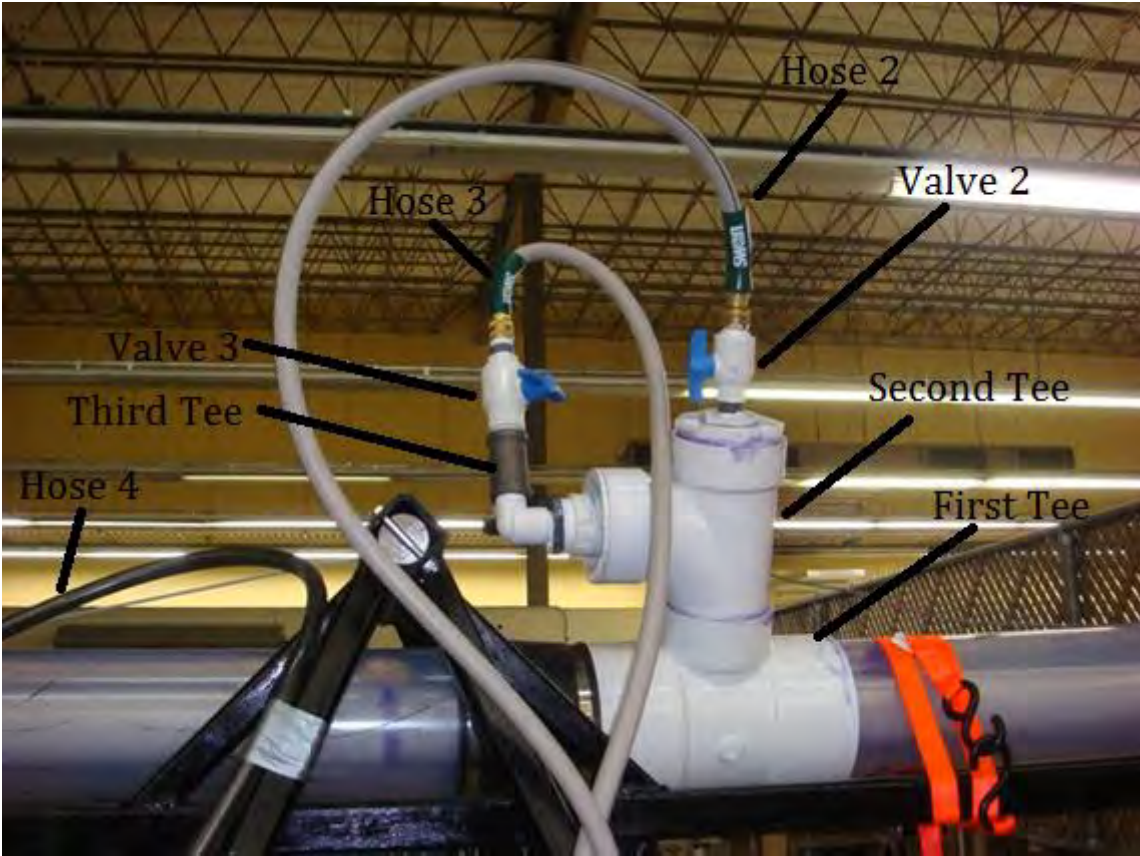
Fig52. Pipe fittings 2.
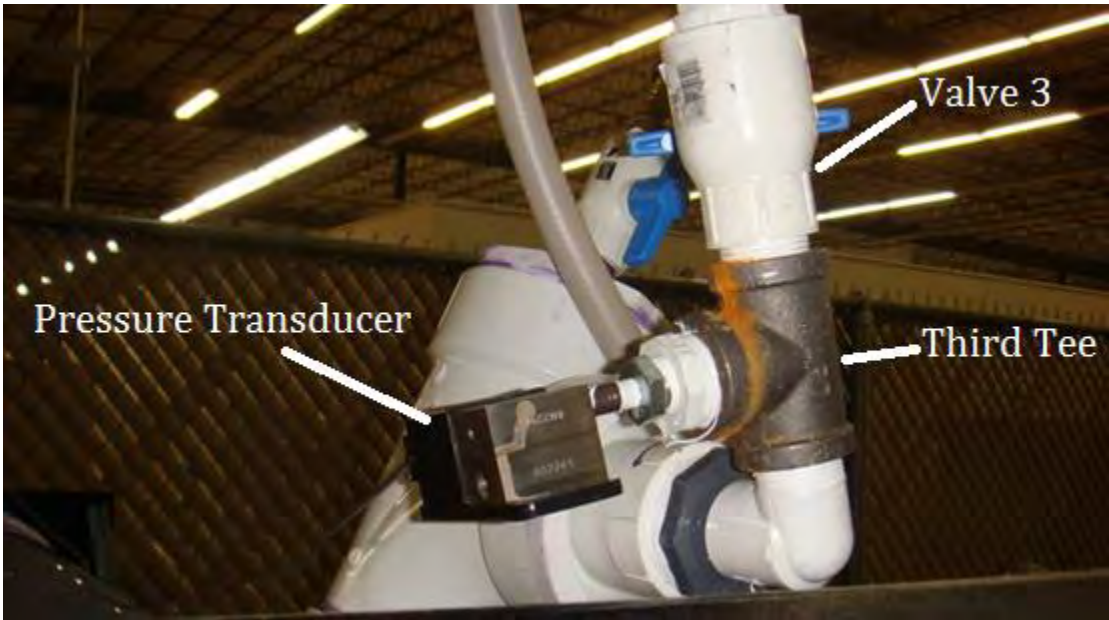
Fig53. Pipe fittings 3

Fig54. Pressure acquisition card and power supply of the transducer.

The pressure transducer connects to a data acquisition card to record the pressure to investigate whether this can be a useful way to measure the settling velocity in an opaque steel pipe. **Fig54** shows the data acquisition card and the power source to supply correct DC voltage to pressure transducer. DC voltage should be in the range of 10V to 50V. 25V was chosen to be in a safe range.

On top of the first tee is a 6" diameter rubber coupling as seen in **Fig52** and clearer in **Fig55**. The rubber coupling provides an easy way to access inside the pipe. This is needed either for cleaning purposes or to install and remove smaller pipes inside the 6" pipe to make epoxy flow in an annulus if desired.

Fig55. Pipe fittings 4.

Next comes 2 10ft long clear PVC pipes with a rigid coupling between them as can be seen in **Fig44** and **Fig45**. On top of those is a 6" PVC valve (valve 4). This valve is what separates the epoxy from the water before the experiment. Attached to the handle of the valve is a cable that allows opening the valve from the ground when the pipe is vertical. When the valve opens epoxy is released in the water and the settling begins. **Fig56** shows a picture of the valve with the cable attached to its handle.
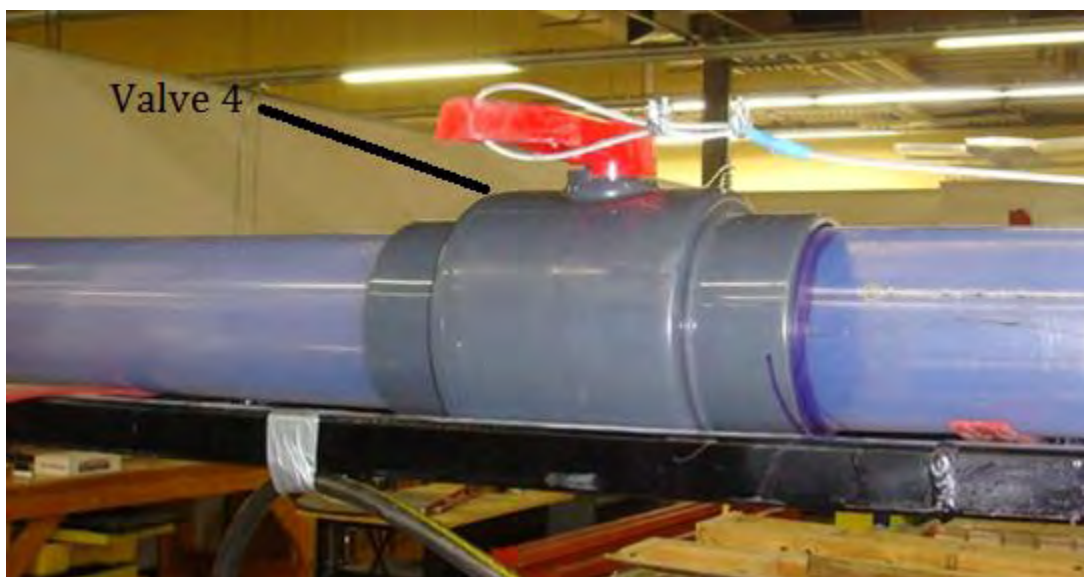
Fig56. Pipe fittings 5.

Next is a 3ft clear PVC pipe to hold the epoxy before it is released in the water at the end is a 90deg elbow to enter the epoxy in the pipe. **Fig57** shows this.

Fig57. Pipe fittings 6.

Hose 4 is used to clean the entire interior of the pipe by bringing the pipe to vertical and letting water flow through it. There is a nozzle at the end of the hose to distribute the water around the pipes circumference. During the experiment hose 4 is removed from the elbow.

It is desired to test the settling velocity of the epoxy in an open pipe and in an annulus. Two different pipe sizes have been used to create a small and large annulus. The diameters of those are 1.9" and 3.5". The smaller pipes are inserted by disassembling the rubber coupling then inserting the smaller pipe into the 6" pipe. The smaller pipes are capped at the top and bottom to prevent epoxy from entering them. Holes have been drilled through their walls on the side to allow the smaller pipes to fill with water while filling the 6" pipe otherwise the pipes would float when the pipe is brought to vertical and would exit from the top valve when opened. The holes are made at an angle that is in opposite direction of the falling epoxy to make sure epoxy would not enter inside the pipes. Centralizers specially designed and fabricated for our application has been used. Four of them are distributed throughout the pipe's length. The centralizers have three arms to ensure stabilization and are made to be easily assembled

and disassembled. They are made of steel and fitted with a piece of teflon board at their tips so when they are slid into the 6" pipe they do not scratch it and to minimize friction to ease the sliding. The centralizers were also painted to minimize rusting. **Fig58** and **Fig59** show a picture of the centralizer.

Fig58. Centralizer.
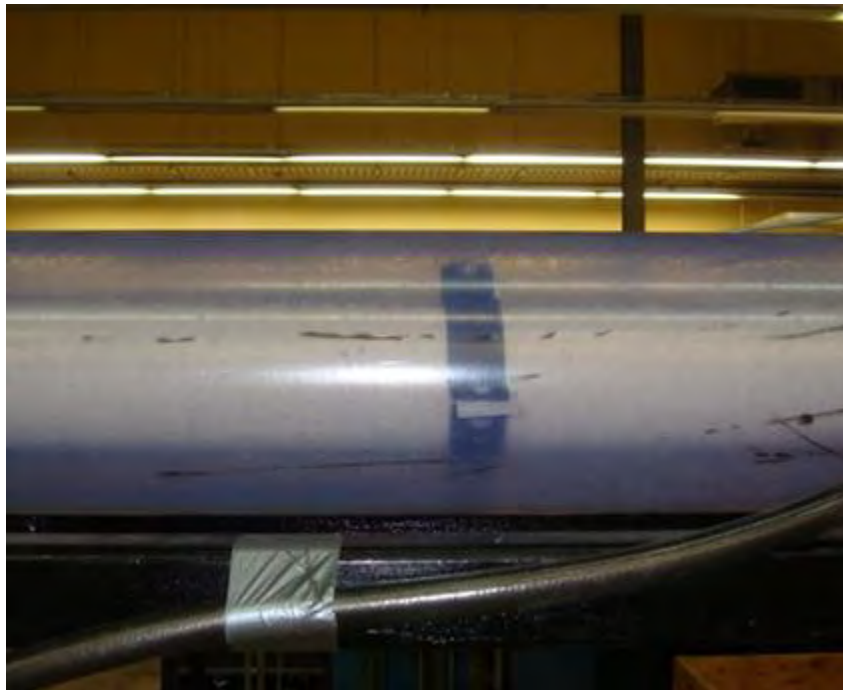
Fig59. Centralizer in pipe.

6. THE EXPERIMENT

6.1 The Epoxy

It was desired to test an epoxy that is representative to what would be used in real application. Professional Fluid Systems (PFS) is one of the well-known epoxy manufacturers in the industry. They have a product called Ultraseal that has been successfully used in similar applications to the one we are studying for, as discussed in the introduction. So Ultraseal was the main epoxy used. Ultraseal as with most other epoxies is a mixture of four main components, an epoxy (resin), a diluent, a hardener and a filler material. The epoxy or the resin consists of monomers or short chain polymers that have an epoxide group at their end. The epoxide group is a cyclic ether that consists of three atoms that form a shape that resembles an equilateral triangle. This shape makes the epoxide highly strained and therefore reactive. The hardener mainly consists of polyamine monomers such as triethylenetetraamine (TETA) that readily form stable covalent bonds with more than 1 epoxide (crosslinking) like for example TETA can form up to four bonds. The product therefore becomes heavily crosslinked and becomes hard and strong. The diluent is used to reduce viscosity of the epoxy to make it easier to pump. The diluent is also used to increase pot life and gel time. (Ng 1994) The filler is used to increase the density of the mixture. In the oil industry barite is the most common filler material even with epoxy.

To be able to try different densities and viscosities of epoxy mixtures each constituent was obtained separately from PFS. The constituents are then mixed at different ratios to obtain the different densities and viscosities desired. The hardener was not used because it was thought that it would damage the equipment by hardening on pipe walls and may cause the valves to get stuck etc. The hardener was not used also to be able to use the mixture more than once. So only the epoxy, the diluent and the filler were used in the mixtures.

6.2 Experiment Variables

1- Epoxy Formulations

Table4 shows the properties and constituents of the three main epoxy formulations that were used. They are classified as light, medium and heavy representing their relative densities.

Formulation	Density	Viscosity						Part A (epoxy)	Diluent	Barite
	ppg	R3	R6	R100	R200	R300	R600	g	g	g
light	11.5	4	7	96	192	272	>300	2819	904	1729
medium	13.2	5.5	11	148	294	>300	>300	2584	829	2950
Heavy	14.7	12	22	>300	>300	>300	>300	2352	755	4150

Table4. Epoxy formulations.

2- Annulus

Three different annuli were used to study the effect of annulus size. The outer pipe is a 6" ID for all three. The three inner pipes are 3.5" OD 1.9"OD and no inside pipe.

3- Angle

The angle is the angle of inclination of the pipe support measured from vertical.

6.3 Experimental Procedure

1) Get pipe support to horizontal position.
2) Make sure pipe is clean. If not see cleaning procedure.
3) Make sure all hoses are not kinked
4) Close Valve 1 (**see Fig51**) and make sure the 6" PVC valve (Valve 4, **Fig56**) is not stuck by opening and closing a couple of times then close it.
5) Open Valve 2 (**see Fig52**). (It is very important to open valve 2 before entering water into the pipe otherwise pressure will build up in the pipe and separate the pipe from the rubber coupling as it is not designed to hold against pressure)
6) Start filling pipe with water by opening Valve 3. (**see Fig52**).

7) Close Valve 3 when pipe is full. (Pipe will be full when Hose 2 (**see Fig52**) starts draining water). (If there is a smaller pipe to make an annulus, make sure it is full of water by inspecting if there are any air bubbles escaping the holes drilled at its side.

8) Close Valve 2.

9) Make sure epoxy is well mixed. Record its density, viscosity and weight. (this can be done before or during previous steps.

10) Remove hose 4 (**see Fig57**) from the elbow then pour the epoxy into the elbow.

11) Get the pipe to vertical or to desired angle.

12) Start recording data from the pressure transducer.

13) Two persons are needed starting from this step. One should be ready with a video camera to record the experiment and the other to pull the valve handle via the cable attached to it when the video camera starts recording.

14) Stop video recording and pressure data acquisition when all the epoxy falls to the bottom.

15) Start draining the water in the pipe by opening valve 2.

16) Remove hose 1 (See **Fig51**) and start collecting the epoxy at the bottom by opening valve 1.

17) Close valve 1 as soon as water starts to flow through the valve. (you will notice a great change in fluid velocity due to the two orders of magnitude difference in viscosity.)

18) Record the weight of the regained epoxy.

19) Connect hose 1 and start draining the remaining water by opening valve 1.

20) Clean (see cleaning procedure)

6.4 Cleaning Procedure

1) Get pipe support at a very small angle from horizontal where the elbow is the high point and reachable.

2) Make sure valve 4 and valve 1 are open.

3) Use hose 4 to flush the mud inside the elbow then insert hose 4 into the elbow.

4) Repeatedly close valve 4 for a while to build water behind it then open.

5) Close valve 4 and fill some water behind it with hose 4. Then close hose 4.

6) Get pipe support to vertical position.

7) Open valve 4.

8) Open hose 4 and allow enough time for water to flush entire pipe clean.

7. RESULTS AND DISCUSSION

Table5 and **Table6** summarize the results.

Experiment Number	Epoxy Formulation	Annulus	Angle
1 (13)	Light	6" - 0"	0
2 (3)	Medium	6" - 0"	0
2' (4)	Medium	6" - 0"	0
3 (14)	Heavy	6" - 0"	0
4 (12)	Light	6"-1.9"	0
5 (11)	Medium	6"-1.9"	0
6 (10)	Heavy	6"-1.9"	0
7 (8)	Light	6" - 3.5"	0
8 (6)	Medium	6" - 3.5"	0
9 (9)	Heavy	6" - 3.5"	0
10 (15)	Medium	6" - 0"	30
11 (16)	Medium	6" - 0"	45

Table5. Experiment variables.

Experiment Number	Time at Coupling (Visual) sec	Time at Pressure Transducer (Visual) sec	Time Lead (Visual) sec	Time Tail (Visual) sec	Time at Pressure Transducer from pressure readings sec	Time Tail at Pressure Transducer from pressure readings sec	dp after 100 secs psi
1 (13)	15	31	37	89	32	68	0.08
2 (3)	12	29	35	73	-	-	-
2' (4)	12	29	35	76	30	68	0.12
3 (14)	10	24	29	67	24	55	0.15
4 (12)	15	33	40	84	32.5	67	0.08
5 (11)	12	29	34	75	29	59	0.115
6 (10)	8	20	24	65	20.5	56	0.17
7 (8)	14	33	40	100	33.5	82	0.09
8 (6)	11	28	33	75	28	68	0.175
9 (9)	9	22	26	66	24	52	0.18
10 (15)	7	14	16	31	14	20	0.075
11 (16)	7	14	17	30	13.5	15.5	0.05

Table6. Epoxy settling times.

Table5 lists the experiment numbers and their corresponding variables that were controlled before the experiment. Experiment 2 was done before the pressure transducer was setup and therefore was repeated after it was setup. The number between brackets in the experiment numbers represents the original experiment numbers which were ordered by the date they were performed. They were re-numbered here by angle, annulus then epoxy formulation in order to make results more presentable. The angle represents the angle from vertical as previously discussed.

As can be seen in the experiment videos the epoxy does not fall as one part instead it spreads throughout the water column and then recollects at the bottom. This is shown in **Fig60**. **Fig60** also shows the lead of the epoxy column. Therefore, the "Time Lead" in **Table6** refers to the time in seconds from releasing the epoxy in the water by opening valve 4 (**Fig56**) to the time the lead reaches the bottom. "Time at Coupling" and "Time at Pressure Transducer" are the times from opening the valve till the lead reaches the coupling and the pressure transducer respectively. "Time Tail" is the time from opening the valve until almost all the epoxy recollects at the bottom. This latter entry is very difficult to measure and is somewhat subjective. This is because as the epoxy falls some of the adhered epoxy to the pipe begins to break out and fall. As a result, it will be seen that some epoxy continues to fall even several minutes after the start of the experiment. Moreover, as the epoxy falls in the water, the water becomes muddy from the barite and it is not clear enough to see when the epoxy fall rate actually stops or substantially decreases. The word "visual" in the table indicates that the time was measured visually from the experiment videos by actually seeing the epoxy through the clear pipe reaching its target.

Fig60. The epoxy spreads in the water column.

The times measured by the pressure transducer were obtained from plotting the pressure readings versus time. **Fig61** shows the plot for experiment 5 (11) as a typical representation of the other experiments. The remaining plots can be found in the appendix attached at the end of this report.
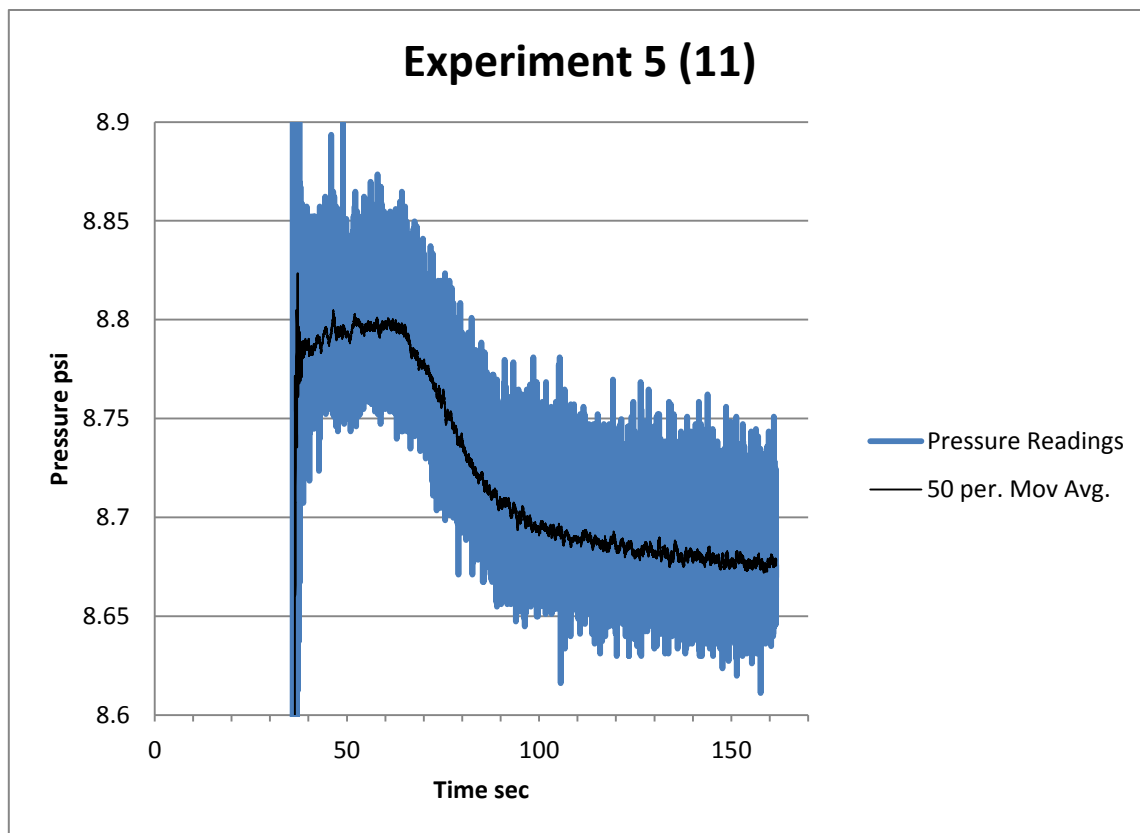
Fig61. Pressure readings taken by pressure transducer during experiment 5 (11).

The readings were fitted with a moving average trend line that averages the nearest 50 readings (±25) to smoothen the oscillatory readings and make them easier to interpret. The data acquisition card takes 100 readings per second therefore the trend line averages data over ±0.25 seconds. The sharp increase at 36 seconds marks the start of the experiment. "Time at Pressure Transducer from pressure readings" entry in **Table6** is the time from the experiment's start till the pressure starts declining which is approximately at 64 seconds in **Fig61**. This decline occurs when the epoxy passes the perpendicular opening of the "second tee" in **Fig52**. As can be seen from **Table6** the

visual values are very close to the time measured by the pressure transducer which indicates that the pressure transducer can be reliably used for this entry in case an opaque pipe is used. "Time Tail at Pressure Transducer from pressure readings" is the time from the experiment's start until the sharp decline of the pressure ends which occurs approximately at 95 seconds in the figure above. This latter entry of the table does not give an accurate reading of the tail and therefore was omitted from further consideration. However, the reason why it gives a false reading will be discussed later. Finally, "dp after 100 secs" is the difference in pressure before the pressure decline and the pressure after 100 seconds after the start of the experiment. In **Fig61** this would be the pressure at 64 seconds minus the pressure at 136 seconds which is 0.115psi. It can be seen from **Table6** that this value generally increases with density and decreases by increasing the angle.

There are several reasons for the sharp pressure increase at the experiment's start. First is that when the epoxy is released it increases the total hydrostatic pressure by about 0.1 to 0.3 psi. The second is that at the point when the pipe is being completely filled with water, the water flows in from hose 3 and out from hose 2. (see **Fig52**) As discussed before, valve 3 must be closed first then valve 2 to avoid pressure build up in the pipe that might separate the pipes at the rubber coupling. As soon as valve 3 is closed some water continues to exit through hose 2 due to a siphon effect which causes the pressure at the top side of the pipe to drop below atmospheric pressure. Since the pressure transducer reads differential pressure between the pipe and atmosphere the pressure transducer reads a negative pressure when the pipe is still horizontal. The longer the time lag between closing valve 3 and valve 2 the more the pressure would decrease below atmospheric pressure. When valve 4 is opened and epoxy is released atmospheric pressure is re-established at the top of the water column causing an increase in pressure. A third reason is when the pipe is filled and valves are closed and then brought from horizontal to vertical, the water column increases the pressure at the rubber coupling. This cause the rubber coupling to bulge outwards as seen in **Fig62** causing the very small volume of trapped air to expand causing a further decrease to the pressure.

This sharp increase in pressure is desirable because it shows the experiment's start clearly on the pressure plots.

Fig62. The rubber coupling bulges due to hydrostatic pressure of the water column.

It is important to discuss what the pressure transducer is actually sensing. A great misconception would be to think that the pressure transducer is able to sense the entire hydrostatic of the epoxy when it is inserted into the water. Consider **Fig63** below.
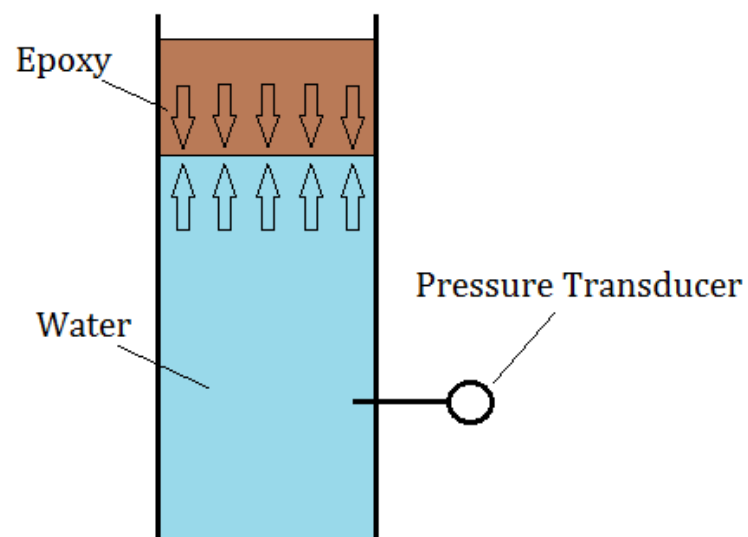
Fig63. Schematic of epoxy falling in a vertical pipe.

The only way that the pressure transducer would read the pressure of the water column above plus the pressure of the epoxy column is if the pressure at the water/epoxy interface equalizes. If the pressure at the interface equalizes then the epoxy will not settle because there would be no resultant force pushing it down so clearly this is not the case. Consider another example shown in **Fig64**.
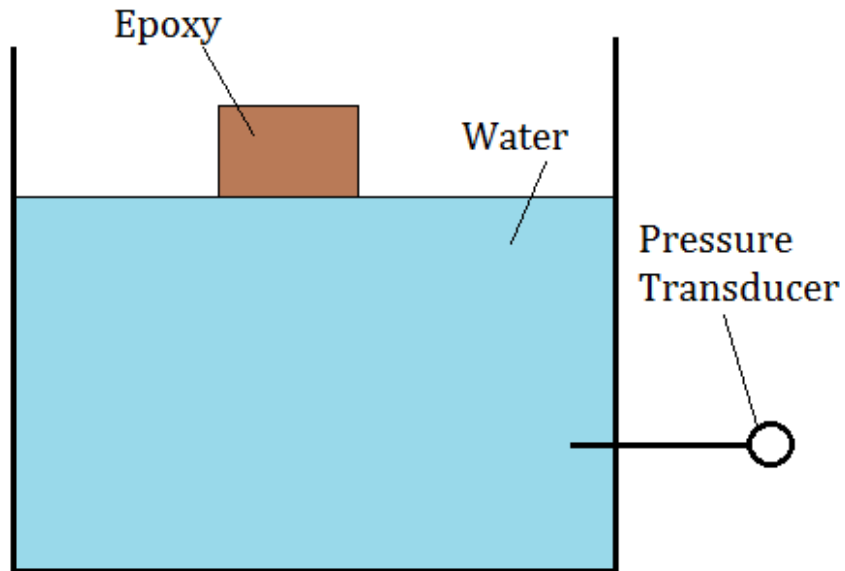
Fig64. Schematic of epoxy falling in a large tank.

In the case above the only change the pressure transducer will sense is the pressure change due to the increase of water height when the epoxy enters the water. If the same volume of epoxy was replaced with water the pressure transducer would not sense the difference. Going back to **Fig63** the situation is different. The difference is that in order for the epoxy to fall the water must be able to rise and therefore the pressure of the water will need to rise in order to be able to break through the epoxy. The difference between the two figures is that in **Fig63** the epoxy is much more concentrated. As the epoxy falls below the pressure transducer there is less epoxy above it and therefore less pressure is needed to force the water through the epoxy above. This concept is what causes the pressure to decline when the epoxy starts to fall below the pressure transducer. The pressure continues to decline until concentration of the epoxy above the pressure

transducer is not significant enough to inhibit the water from flowing upwards. Therefore, the reason why the "time tail from pressure readings" in **Table6** is not accurate is because some epoxy might still be above the pressure transducer but not causing significant pressure increase to be detected by the pressure transducer when they fall below it.

The proof that the pressure transducer does not sense the entire hydrostatic pressure of the epoxy comes by examining the difference in pressure when all the epoxy is above the transducer and when all of it is below it. For example, consider a heavy formulation falling in a 6"-3.5" annulus. The volume inserted is a little more than a gallon and therefore the height of epoxy is almost a foot in such an annulus. The hydrostatic pressure of a foot of 14.7ppg is approximately 0.764 psi. Subtracting the hydrostatic pressure of a foot of water that will replace it when the epoxy drops then the difference in pressure between the epoxy above and below the transducer is 0.33 psi. The maximum pressure drop observed with such a formulation was 0.18 psi.

Table7 below lists distances between different parts of the pipe that were used to calculate the epoxy's speed.

cap to bottom of valve 4	292	in
cap to top of coupling	178	in
cap to pressure transducer	54	In
cap to middle of first tee	46	In

Table7. Distances the epoxy travels during the experiment.

Based on the distances listed in **Table7** and the times listed in **Table6** average speed of the epoxy can be calculated. The speeds are listed in **Table8** in ft/min for visual readings and readings from the pressure transducer. "Time Tail from pressure readings" was neglected as discussed earlier.

Experiment Number	Speed from start to lead - ft/min	Speed from start to Tail - ft/min	Speed from coupling to lead ft/min	Speed from start to transducer ft/min	Speed from start to transducer by pressure readings ft/min
1 (13)	39.46	16.40	40.45	39.68	38.44
2 (3)	41.71	20.00	38.70	42.41	-
2' (4)	41.71	19.21	38.70	42.41	41.00
3 (14)	50.34	21.79	46.84	51.25	51.25
4 (12)	36.50	17.38	35.60	37.27	37.85
5 (11)	42.94	19.47	40.45	42.41	42.41
6 (10)	60.83	22.46	55.63	61.50	60.00
7 (8)	36.50	14.60	34.23	37.27	36.72
8 (6)	44.24	19.47	40.45	43.93	43.93
9 (9)	56.15	22.12	52.35	55.91	51.25
10 (15)	91.25	47.10	98.89	87.86	87.86
11 (16)	85.88	48.67	89.00	87.86	91.11

Table8. Epoxy's velocities.

A lot of information can be derived from **Table8**. First, it is clear that increasing the density of the epoxy increases its settling velocity which is expected. Although denser formulations are also more viscous, viscosity can only decrease settling by making it harder for the water to flow upwards. Therefore, the major contributor to the settling velocity is the density. The only way that the viscosity of the epoxy helps settling is by enhancing its ability to hold onto the barite and not allow it to separate. However, this was the case for the three formulations. Therefore this factor alone would not differentiate a formulation from another.

Another observation found in **Table8** is that experiments 10 and 11 which were done at an angle are much faster than experiments performed vertical with the same formulation namely experiments 2, 5 and 8. In fact their speeds are more than double of those performed vertical which shows that this observation is neither a coincidence nor an experimental error. At first this seems to be against logical reasoning because at an

angle the force pulling a settling particle in a vertical pipe is more than that in an inclined pipe as shown in **Fig65**.
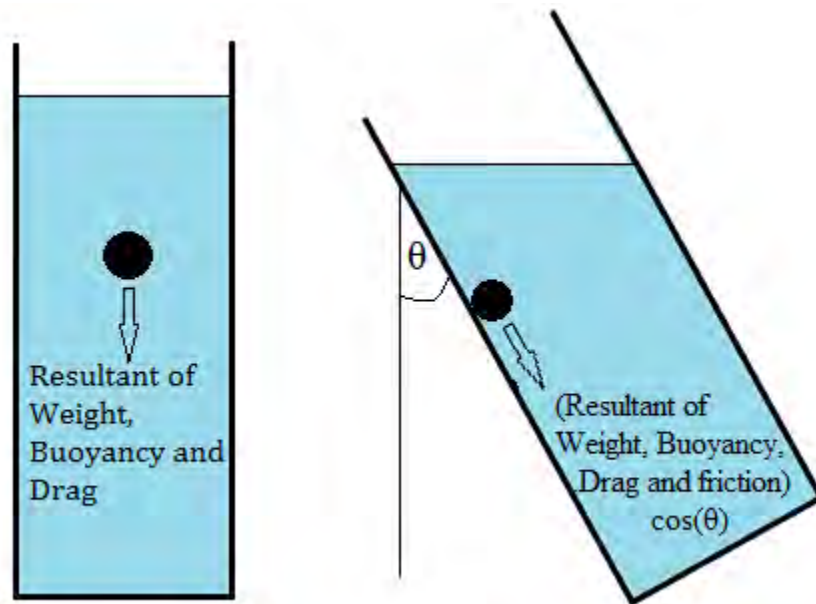
Fig65. Forces on a settling particle in vertical and slant pipe.

Fig65 clearly shows why at an angle the force is less. Not only there is friction from the pipe wall decreasing the resultant force but the resultant force is also multiplied by cosine the angle of inclination. However, there is another factor that comes into play causing this big difference in speed which is illustrated by **Fig66**.
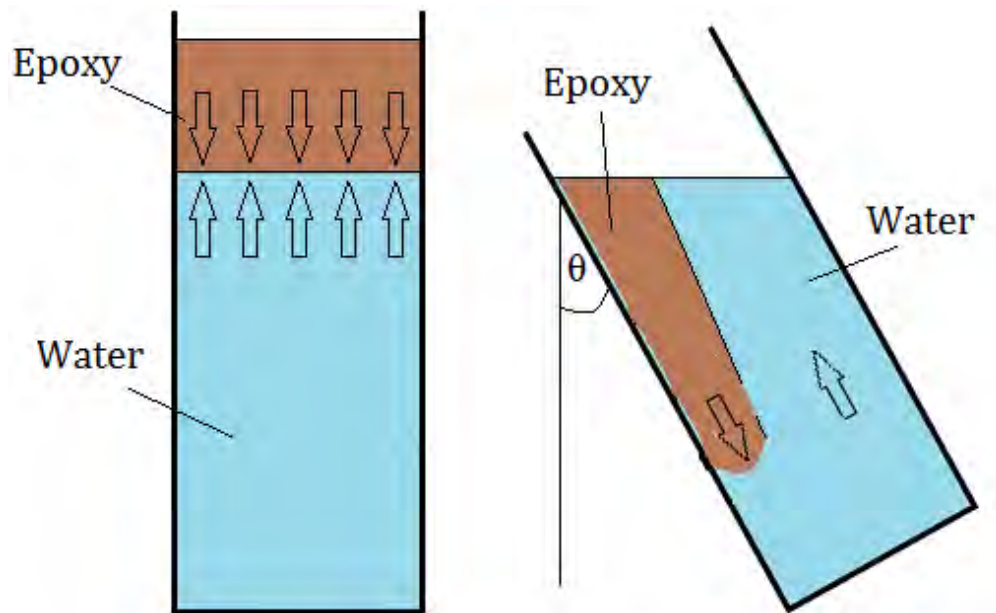
Fig66. Settling of epoxy in vertical and slant pipe.

For pipe on the left in **Fig66**, the water needs to rise and the epoxy needs to fall. The two motions oppose each other and therefore hinder the settling greatly. For the pipe on the right, the epoxy falls to the bottom side of the pipe first then starts to flow downwards. What makes the epoxy, for the pipe on the right, faster is that now the water has a big channel at the top side of the pipe to flow and therefore the epoxy can easily flow downwards at the bottom side and the water can easily flow upwards at the top side of the pipe. Another reason is as the epoxy starts to flow downwards its column gets longer and its hydrostatic pressure is increasing only on itself and not in the water which boosts the epoxy forward.

This latter phenomenon is caused by the placement method. Meaning, it is caused by dumping the entire volume of epoxy all at once in the water. This increases the concentration of epoxy in vertical pipes and inhibits the upward flow of water and the downward flow of epoxy. As a result, it is recommended to place the epoxy in small volume rates to prevent this phenomenon to occur in vertical pipes.

The annulus does not seem to cause any significant change in the settling velocity sometimes it makes the settling faster and sometimes slower and in both cases the change is not significant. It was expected that a smaller annulus would result in a

slower settling velocity since the cross sectional area is smaller and there would be more friction from the pipe walls which is proportional to the hydraulic perimeter of the annulus. A possible reason why the annulus did not affect the settling velocity could also be the placement method. Injecting epoxy in small volume rates might show otherwise.

Table8 also shows that the velocity of the epoxy is decreasing with depth for a vertical pipe. This is seen by comparing the "speed from start to lead" and "speed from coupling to lead". This is again the opposite of what is expected. It is expected that the epoxy would accelerate at first and then reach a terminal velocity and therefore the speed would increase and then stabilize. However, this expectation is opposite of what was observed for a vertical pipe. A possible reason might be that at first the epoxy is altogether and the layer of epoxy between the epoxy/water interface is seeing a big pressure difference between the epoxy above it and the water below it and therefore reaches a terminal velocity based on that pressure difference. As the epoxy spreads down the column of epoxy is not as significant on the lead as at the start of the experiment. Therefore there is a smaller pressure difference which causes the settling velocity to decrease. For experiments done at an angle the epoxy did accelerate as expected.

Experiment Number	Epoxy Formulation	Annulus	Angle	Epoxy Entered g	Epoxy Lost g	percentage
1 (13)	Light	6" - 0"	0	5350	1007	18.8
2 (3)	Medium	6" - 0"	0	6278	1211	19.3
2' (4)	Medium	6" - 0"	0	6284	1029	16.4
3 (14)	Heavy	6" - 0"	0	7170	2033	28.4
4 (12)	Light	6"-1.75"	0	5345	1332	24.9
5 (11)	Medium	6"-1.75"	0	6323	1634	25.8
6 (10)	Heavy	6"-1.75"	0	7137	2242	31.4
7 (8)	Light	6" - 3.5"	0	5359	1390	25.9
8 (6)	Medium	6" - 3.5"	0	6320	1665	26.3
9 (9)	Heavy	6" - 3.5"	0	6920	2237	32.3
10 (15)	Medium	6" - 0"	30	6323	1384	21.9
11 (16)	Medium	6" - 0"	45	6339	1753	27.7

Table9. Adhesion of epoxy on pipe walls.

The epoxy entered and the epoxy lost shows how much of the epoxy entered have adhered to the pipes while falling down. As can be seen that the amount of epoxy adhered is quite significant. This might give an indication that for 7000ft in real life application the entire volume of epoxy will adhere to the pipe before it reaches the bottom. However, there are very important factors that must be discussed before jumping to conclusions. It was noticed that most of the adhered epoxy was at the top and the adhesion decreases as the epoxy falls down. **Fig67** to **Fig69** show the pipe from top to bottom respectively after the experiment is complete and the water is drained out. These figures were taken after experiment 9 with the heavy epoxy formulation. The heavy epoxy formulation was the most adhesive to the pipes as shown in **Table9**. There are two possible explanations to why the adhesion decreases as the epoxy moves down. The first reason is that when the valve is open all the epoxy is released at once and therefore the concentration of epoxy at the top has more chance of bumping into the pipe walls and adhering to it. As the epoxy spreads down the concentration decreases and therefore has a less chance of bumping into the pipe walls. The second explanation is that at the top the epoxy is still slow and building up speed and therefore if it bumps into the pipe walls with no or small downward momentum it can easily stick to it. However, as the epoxy moves downward it builds up momentum and therefore becomes more difficult for it to adhere to the pipe walls.

From **Table9** it can be seen that adhesion is increases from the light formulation to the heavy formulation. The reason for this is not that the density has increased but is because that the viscosity increases significantly from one formulation to the next. This makes the epoxy has a stronger adhesion with the pipe walls and cohesion and therefore more epoxy is lost.

Also **Table9** shows that adhesion increases with increasing the inner pipe diameter. This is perfectly logical because a smaller annulus means a smaller flow area which means that there is more chance for the epoxy to bump into the pipe walls. In addition, the smaller the annulus, the larger the surface area of the pipe walls which means more area for the epoxy to adhere to.

Lastly, **Table9** also shows that increasing the angle of inclination increases adhesion. The reason for this is that the at an angle there is a smaller force pushing adhered epoxy down as explained in **Fig65**.

A recommendation to minimize adhesion of epoxy is to inject it at low volume rates so the concentration of epoxy relative to seawater in the pipe would be small. In addition, if the epoxy could be injected into the pipe while having an initial downward velocity that would also minimize adhesion.

Fig67. Adhesion of epoxy for a vertical pipe at top section.

Fig68. Adhesion of epoxy for a vertical pipe at middle section.

Fig69. Adhesion of epoxy for a vertical pipe at bottom section.

Experiments done at an angle showed the same concept of adherence as in vertical pipe but the difference is that almost all of the adherence took place at the bottom of the pipe. **Fig70** to **Fig72** illustrates the adherence from top to bottom respectively after experiment 11 (16).

Fig70. Adhesion of epoxy for a slant pipe at top section.

Fig71. Adhesion of epoxy for a slant pipe at middle section.

Fig72. Adhesion of epoxy for a slant pipe at bottom section.

Taking a look back at **Table6** it can be seen that there were 4 experiments that were not reported by looking at the original experiment numbering. One of them was the first experiment which was omitted because it was done without video recording and therefore the timing was not recorded. It was the first experiment that led us to decide to video record the rest of the experiments. The remaining three omitted experiments were

done using recycled epoxy which was recovered from an experiment that was already performed. They were omitted because their behavior was much different from the freshly made epoxy as can be seen in the experiments videos and the pressure recordings. There are two possible reasons for this. One when the epoxy is retrieved after an experiment some water must come along with it. Although the contaminant water volume is very small compared to the volume of recovered epoxy it can have significant effect on the formulation during the mixing stage affecting its viscosity. Another reason might be that the experiments were not performed on the same day. As a result, the barite in the epoxy settles to the bottom and clumps together. The mixer used might not have been strong enough to break the clumps of barite. **Table10** to **Table12** summarize the results for the recycled epoxies.

Experiment 12 (2)		
density	10	ppg
Viscosity	R3	2
	R6	4
	R100	56
	R200	111
	R300	165
	R600	above maximum (300)
Epoxy used =	Recycled epoxy	
Epoxy entered =	4466 g	
Epoxy recovered =	3077 g	
Epoxy Lost=	1389 g	
Time lead =	59 secs	

Table10. Recycled epoxy experiment 12 (2).

Experiment 13 (5)		
density	13.2	ppg
Viscosity	R3	3
	R6	5
	R100	70
	R200	140
	R300	205
	R600	above maximum (300)
Epoxy used =	Recycled epoxy	
Epoxy entered =	4500 g	
Epoxy recovered =	2390 g	
Epoxy Lost=	2110 g	
Time lead =	24 secs	

Table11. Recycled epoxy experiment 13 (5).

Experiment 14 (7)		
density	13.2	ppg
Viscosity	R3	5
	R6	9
	R100	140
	R200	235
	R300	above maximum (300)
	R600	above maximum (300)
Epoxy used =	Recycled epoxy	
Epoxy entered =	4515 g	
Epoxy recovered =	2300 g	
Epoxy Lost=	2215 g	
Time lead =	was not recoreded correctly	

Table12 Recycled epoxy experiment 14 (7).

Fig73 shows the pressure recording for experiment 7. Clearly the pressure behavior is different from that of a fresh epoxy.
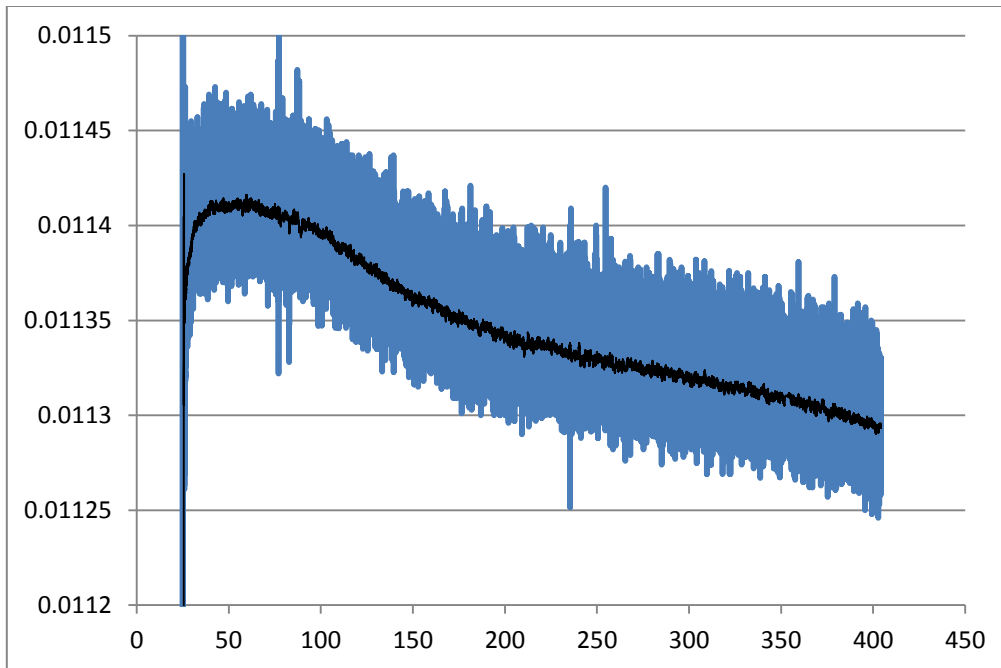
Fig73. Pressure readings for experiment 14 (7) which used recycled epoxy.

The pure epoxy that was used has a density that is less than water. Therefore, it was important to see if the epoxy could separate from the barite and float after it settles to the bottom. To test that, the medium formulation was kept in water after settling for a couple of hours. No significant floating of the barite was witnessed. For the heavy formulation it was noticed that most of the barite sags to the bottom of the epoxy column but there is still enough barite at the top keep it from floating. This is attributed to the strong adhesion properties of the pure epoxy.

8. CONCLUSION

1. Denser formulations have a faster terminal velocity.
2. Experiments at an angle are much faster than experiments done at vertical position, almost double the terminal velocity.
3. The annulus has no significant effect on terminal velocity for vertical pipes.
4. The pressure transducer is a good way to measure the time from the experiment's start till the lead of the epoxy passes it.
5. The more the viscosity of the epoxy formulation the more the adhesion to the pipe walls.
6. The larger the angle of inclination the more the adhesion to the pipe walls.
7. The smaller the annulus size the more the adhesion to the pipe walls.
8. Adhesion decreases with depth.
9. Recycled epoxy is not suitable to represent freshly mixed epoxy.
10. Although pure epoxy is less dense than water, it does not separate from the barite it is mixed with and therefore maintains a higher density and stays at the bottom.

REFERENCES

1) "Assessment of Fixed Offshore Platform Performance in Hurricanes Andrew, Lili and Ivan" MMS project number 549 final report. Jan 2006. http://www.boemre.gov/tarprojects/549/E05114MMSProject549FinalReport.pdf

2) "Assessment of Fixed Offshore Platform Performance in Hurricanes Katrina and Rita" MMS project number 578 final report. May 2007. http://www.boemre.gov/tarprojects/578/MMSProject578-Final%20Report.pdf

3) "MMS Completes Assessment Of Destroyed And Damaged Facilities From Hurricanes Gustav And Ike". MMS news release. 26 Nov 2008. http://www.mrm.boemre.gov/PDFDocs/20081121a.pdf

4) "MMS Updates Hurricanes Katrina and Rita Damage". MMS news release #3486. 1 May 2006. http://www.boemre.gov/ooc/press/2006/press0501.htm

5) Ng, R. C. (1994). Casing repair using a plastic resin.(5295541) Retrieved from http://www.freepatentsonline.com/5295541.html

6) H, K., R., & E, W., M. (1978). AN ACRYLIC/EPOXY EMULSION GEL SYSTEM FOR FORMATION PLUGGING: LABORATORY DEVELOPMENT AND FIELD TESTING FOR STEAM THIEF ZONE PLUGGING. Paper presented at the *SPE Symposium on Improved Methods of Oil Recovery,* Retrieved from OnePetro database.

7) "Liquid Bridge Plug" company brochures of professional fluid systems (PFS). www.professionalfluid.com

8) G.K. Batchelor, F. R. S. (1967). *An introduction to fluid dynamics*. Great Britain: Cambridge University.

9) John Metcalfe Coulson, John Francis Richardson, J. H. Harker, J. R. Backhurst. (2002). *Coulson and Richardson's chemical engineering: Particle technology and separation processes volume 2 of Coulson & Richardson's chemical engineering* (5th ed.) Butterworth-Heinemann, 2002.

10) http://www.engineeringtoolbox.com/drag-coefficient-d_627.html

11) http://www.savacable.com/pages/applic_10.html

12) http://www.tiedown.com/pdf/f236.pdf

APPENDIX
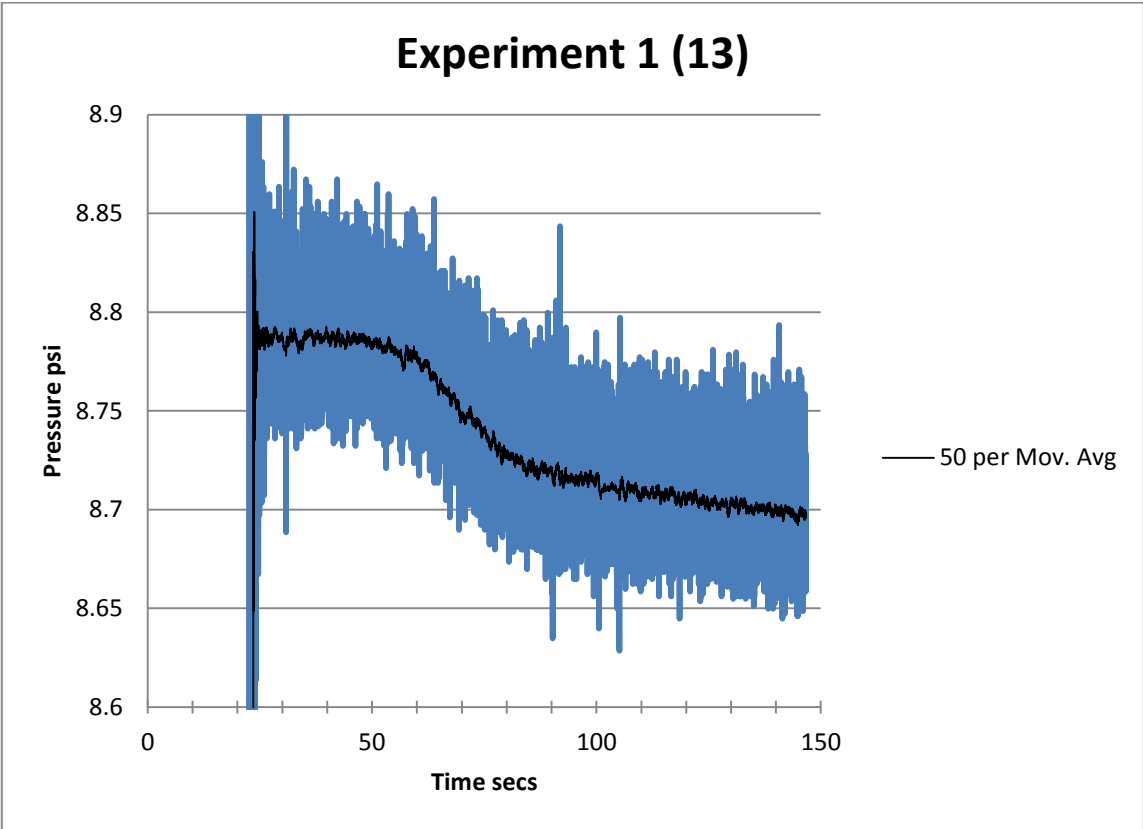
FigA1. Pressure Readings for Experiment 1 (13).
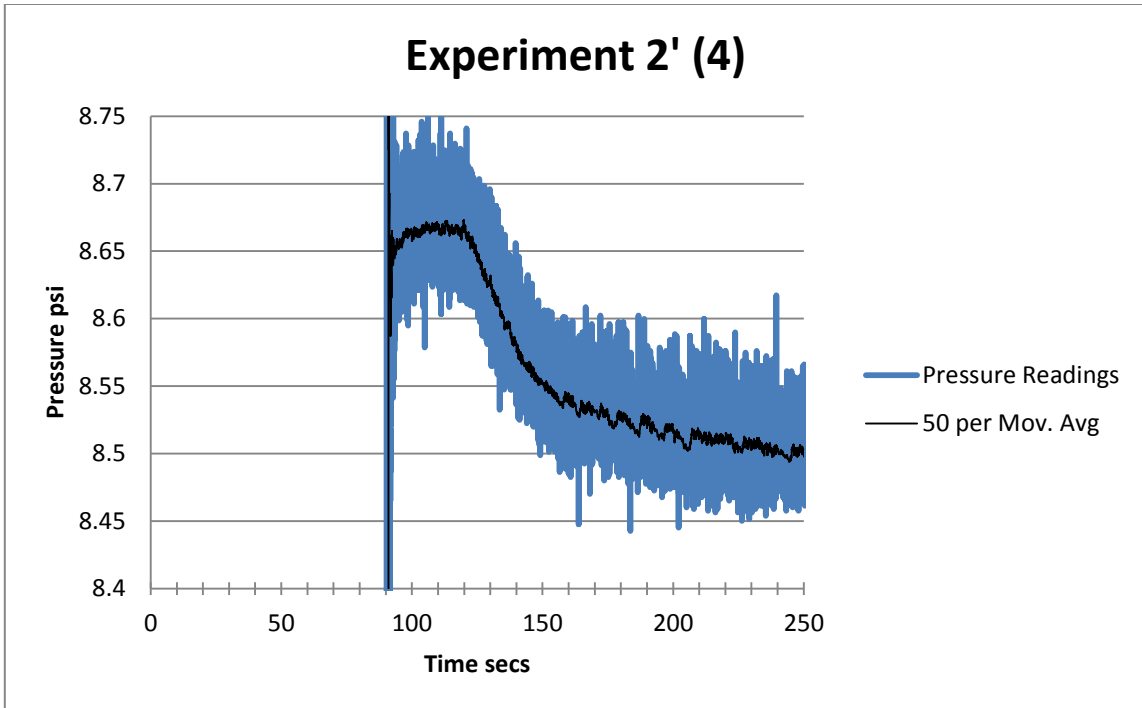
FigA2. Pressure Readings for Experiment 2' (4).
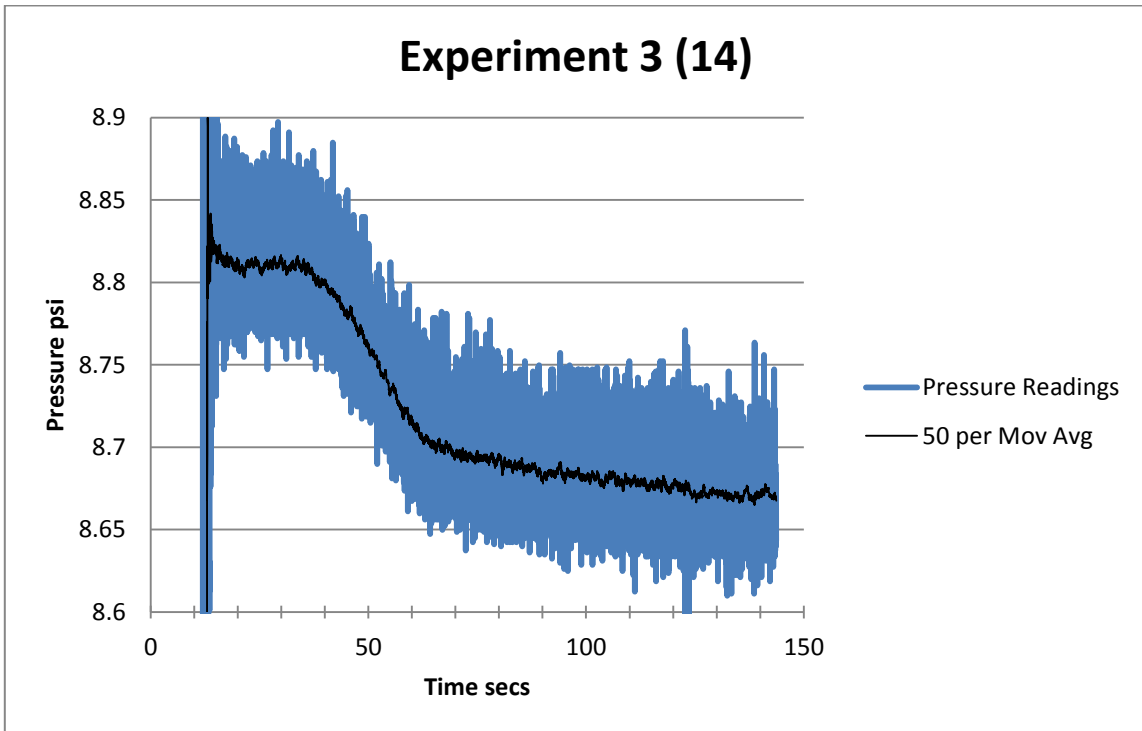
FigA3. Pressure Readings for Experiment 3 (14).
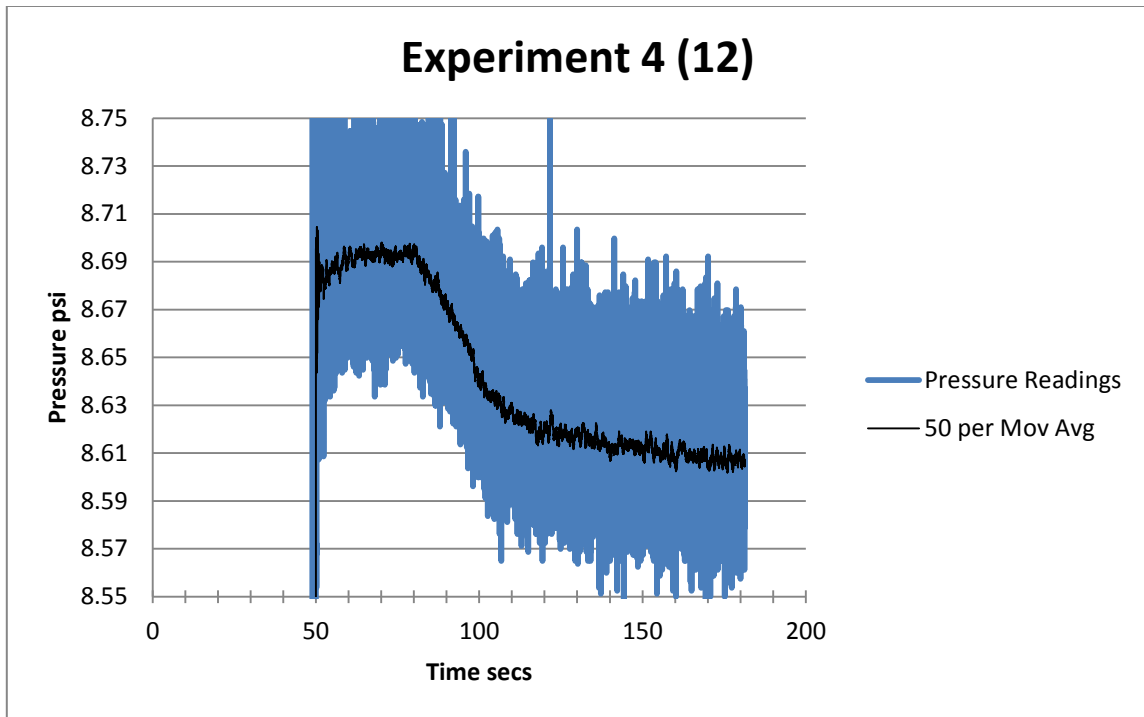
FigA4. Pressure Readings for Experiment 4 (12).
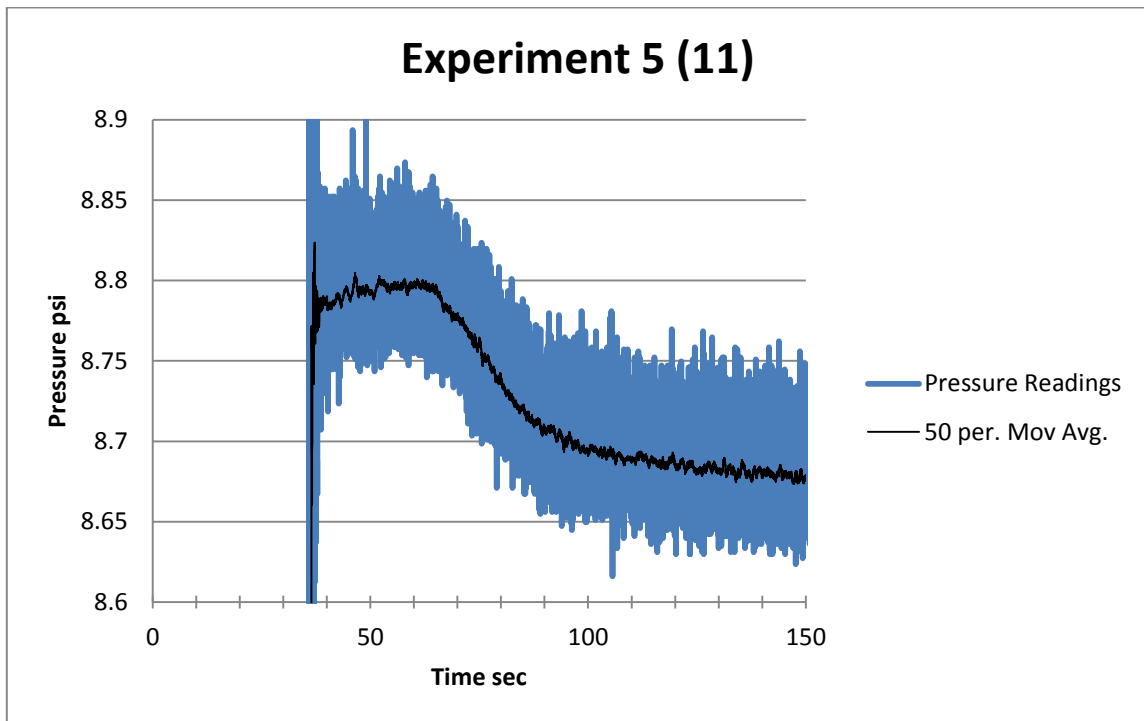
FigA5. Pressure Readings for Experiment 5 (11)
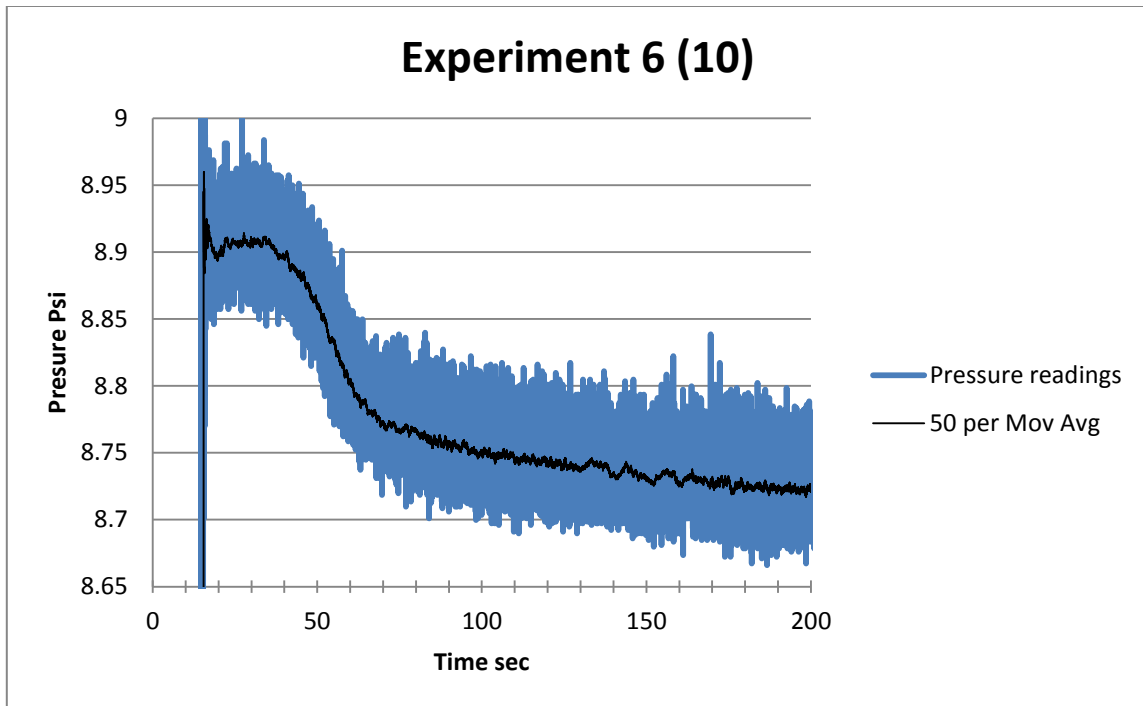
FigA6. Pressure Readings for Experiment 6 (10).
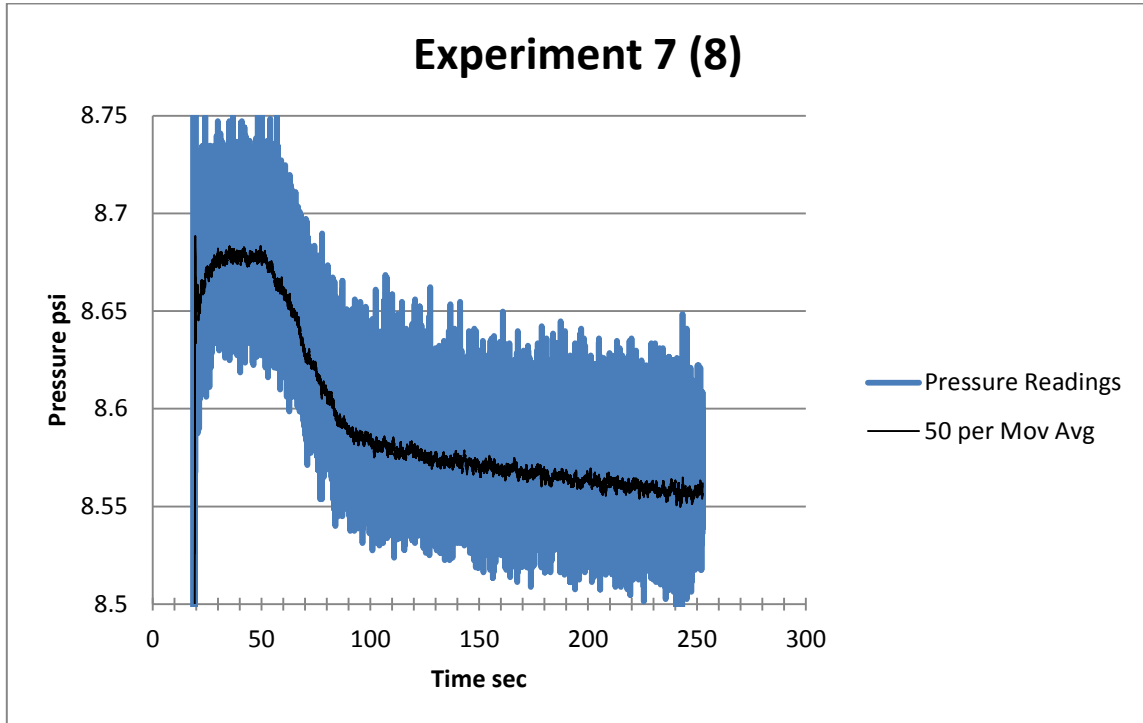
FigA7. Pressure Readings for Experiment 7 (8).
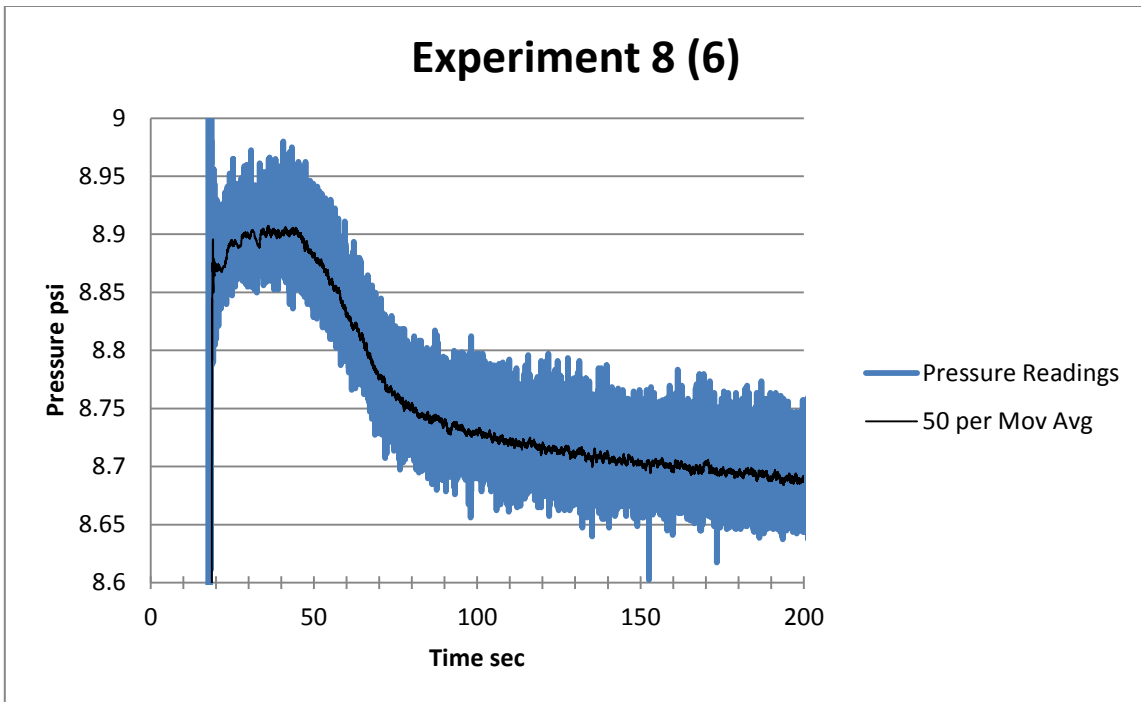
FigA8. Pressure Readings for Experiment 8 (6)
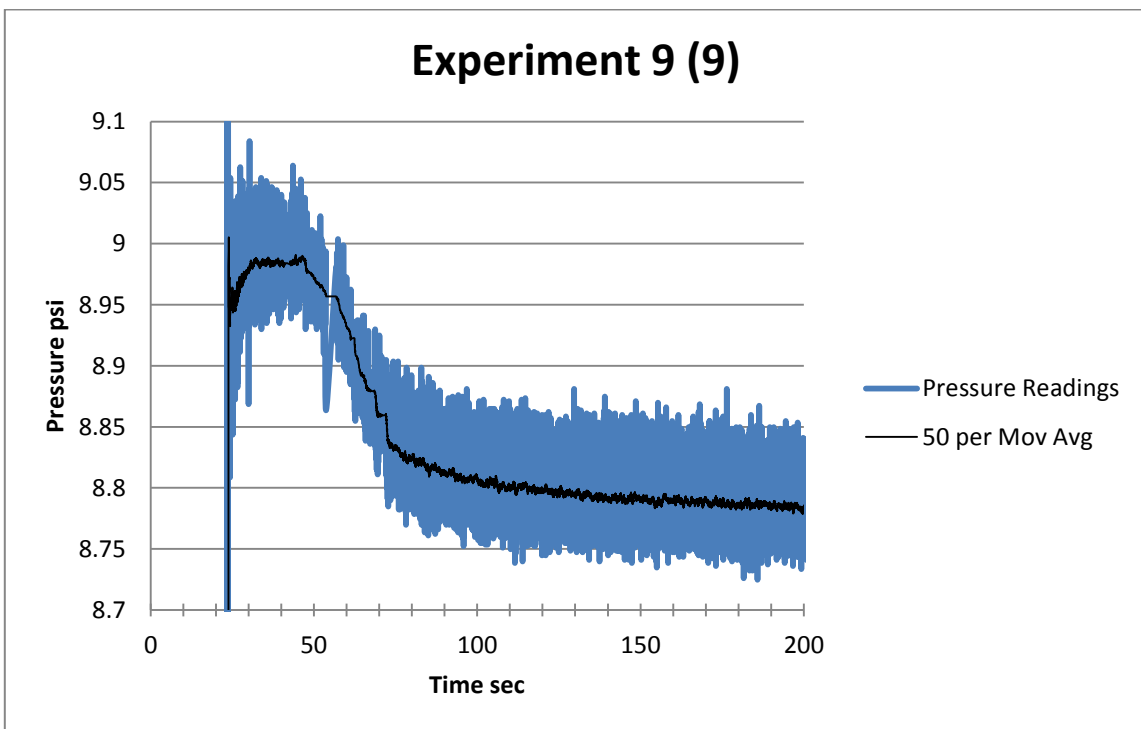
FigA9. Pressure Readings for Experiment 9 (9).
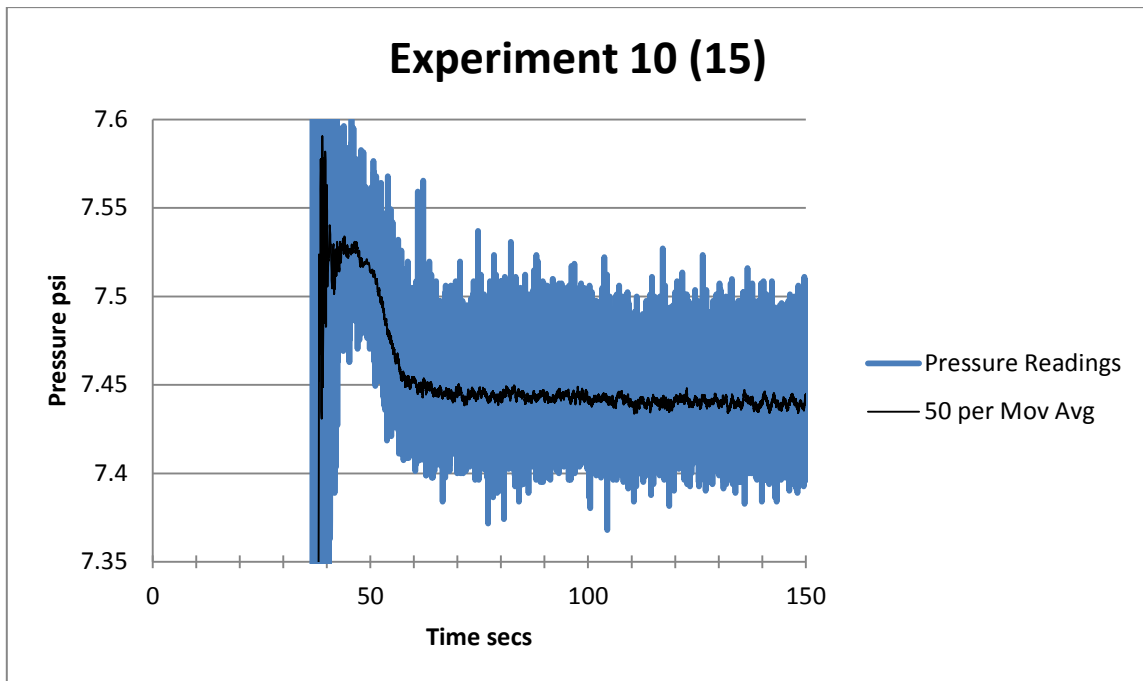
FigA10. Pressure Readings for Experiment 10 (15)
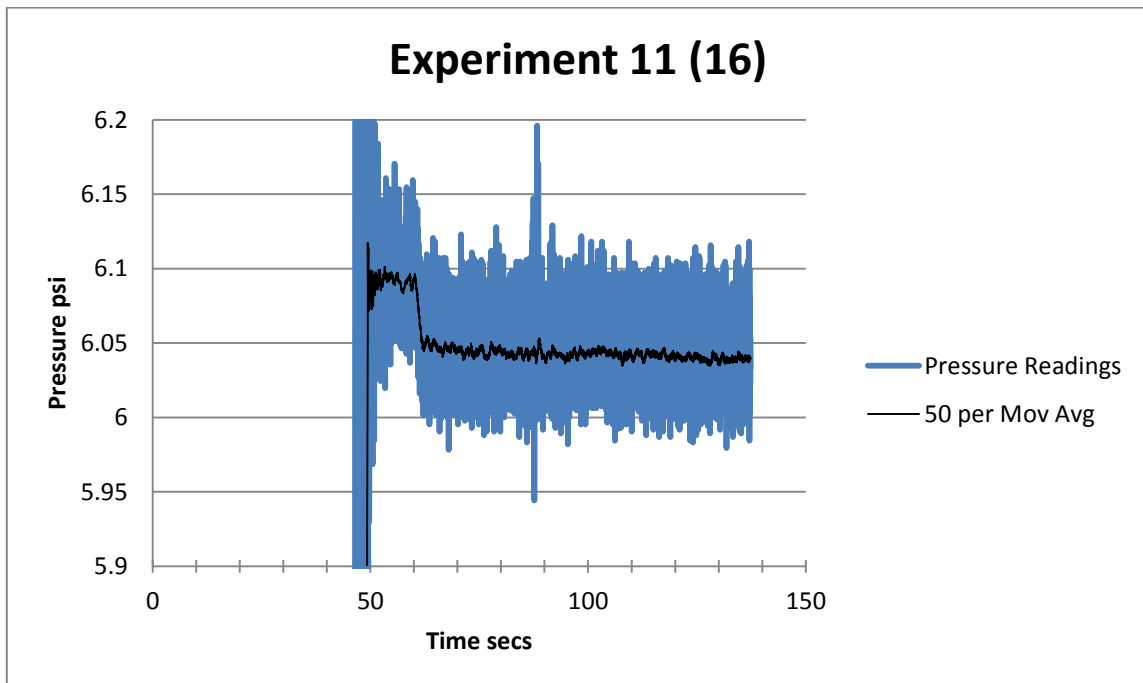
FigA11. Pressure Readings for Experiment 11 (16).

VITA

Name: Ibrahim Ismail El-Mallawany

Address: 4 Rashdan St. Dokki.
       Giza, Egypt

Email Address: mallo81@hotmail.com

Education: B.S., Mechanical Engineering, American University in Cairo. 2005

      M.S., Petroleum Engineering, Texas A&M University, 2010

DETERMINING THE TERMINAL VELOCITY AND THE PARTICLE SIZE OF

EPOXY BASED FLUIDS IN THE WELLBORE

A Thesis

by

HASAN TURKMENOGLU

Submitted to the Office of Graduate Studies of
Texas A&M University
in partial fulfillment of the requirements for the degree of

MASTER OF SCIENCE

August 2012

Major Subject: Petroleum Engineering

Determining the Terminal Velocity and the Particle Size of Epoxy Based Fluids in the

Wellbore

DETERMINING THE TERMINAL VELOCITY AND THE PARTICLE SIZE OF

EPOXY BASED FLUIDS IN THE WELLBORE

A Thesis

by

HASAN TURKMENOGLU

Submitted to the Office of Graduate Studies of
Texas A&M University
in partial fulfillment of the requirements for the degree of

MASTER OF SCIENCE

Approved by:

Chair of Committee,   Jerome J. Schubert
Committee Members,   Frederick Gene Beck
                     Yuefeng Sun
Head of Department,   A. Daniel Hill

August 2012

Major Subject: Petroleum Engineering

ABSTRACT

Determining the Terminal Velocity and the Particle Size of Epoxy Based Fluids in the

Wellbore. (August 2012)

Hasan Turkmenoglu, B.S., Middle East Technical University

Chair of Advisory Committee: Dr. Jerome J. Schubert

This thesis was inspired by the project funded by Bureau of Safety and Environment Enforcement (BSEE) to study the use of epoxy (or any cement alternative) to plug offshore wells damaged by hurricanes. The project focuses on non-cement materials to plug wells that are either destroyed or damaged to an extent where vertical intervention from the original wellhead is no longer possible. The proposed solution to this problem was to drill an offset well and intersect the original borehole at the very top and spot epoxy (or any suitable non-cement plugging material) in the original well. The spotted epoxy then would fall by gravitational force all the way down to the packer and then settle on top of the packer to plug the annulus of the damaged well permanently.

This thesis mainly concentrates on the factors affecting the fall rates and how to correlate them in order to derive an applicable test that can be conducted on the field or lab to calculate the terminal velocity of the known epoxy composition. Determining the settling velocity of the epoxy is crucial due to the fact that epoxy should not set prematurely for a better seal and isolation. The terminal velocity and the recovery for epoxy based plugging fluids were tested by using an experimental setup that was

developed for this purpose. The results were also validated by using an alternative experiment setup designed for this purpose. Factors affecting the terminal velocity and recovery of epoxy were studied in this research since the settling velocity of the epoxy is crucial because epoxy should not set prematurely for a better seal and isolation. The study was conducted by using an experiment setup that was specially developed for terminal velocity and recovery calculations for plugging fluids. Results obtained from the experiment setup were successfully correlated to epoxy's composition for estimating the terminal velocity of the mixture.

DEDICATION

Dedicated to…

Mom and Dad

&

Duygum

ACKNOWLEDGEMENTS

NOMENCLATURE

BSEE	Bureau of Safety and Environment Enforcement
TPAO	Turkish Petroleum Corporation
AIME	American Institute of Mining Engineers (former SPE)
SPE	Society of Petroleum Engineers
TETA	Triethylenetetraamine
PFS	Professional Fluid Systems
CIBP	Cast iron bridge plug
F_d	Drag force
μ	Fluid viscosity
R	Radius
V	Particle velocity
g	Acceleration due to gravity
$\boldsymbol{\rho_s}$	Particle density
$\boldsymbol{\rho_f}$	Fluid density
R_e	Reynolds Number
C_D	Drag coefficient
A_p	Projected area of an object
A	Area
Π	Number Pi
R	Radius of a circle

R1	Radius of an inner circle
R2	Radius of an outer circle
ID	Inner diameter
OD	Outer diameter
C_d	Weight percentage of diluent
C_b	Weight percentage of barite

TABLE OF CONTENTS

LIST OF FIGURES

Page

Page

LIST OF TABLES

1. INTRODUCTION

Epoxy polymer based plugging fluids are among the solutions considered for plugging the damaged offshore wells which are not possible to plug by conventional means using cement. These wells are destroyed to a point where re-entering the well is impossible due to casing related (buckled casing) or seafloor related (wellhead buried under seafloor mud) problems. This will prevent reaching a packer to set a cement plug. Since cement is a water based fluid, it is miscible with seawater or brine which is a common packer fluid for offshore wells. Long interaction time with these fluids can cause contamination or dilution of the cement mix which eventually will cause the cement to fail to thicken or fail to reach the required compressive strength. Therefore, wells destroyed or damaged enough to prevent conventional plugging are not suitable for plugging with cement slurry because the cement needs to be delivered to the point of interest with minimum or no interaction with the sea-water or brine. The only way to achieve this by conventional methods is to drill an intersection well which intersects the damaged borehole near the packer, meaning a drilling operation close to the full depth. This is most likely to be a very costly and time consuming operation which will probably offset the competitive price advantage of cement on the alternative plugging materials.

An alternative way to plug these wells is to drill an intersection well that intersects the original wellbore at the very top through perforations between the wells.

_____

This thesis follows the style of *SPE Drilling & Completion.*

Then the epoxy would be injected (spotted) inside the original wellbore. From this point to the packer, epoxy is expected to settle by gravity all the way down to the packer assuming the well is not flowing at the time of settling. Since the epoxy in general does not mix with water or brines, it is the best plugging fluid candidate for the proposed operation.

In the past years many oil platforms have been either completely destroyed or extremely damaged by hurricanes. **Table 1** shows the number of destroyed or extremely damaged platforms according to the BSEE released documents.

Table 1.1 Number of wells damaged or destroyed by hurricanes. (as of 2010)

Hurricane	No. Destroyed	No. Extremely Damaged
Rita & Katrina	113	144
Ike & Gustav	60	31
Ivan, Andrew & Lily	18	

Table 1.1 shows that the total number of destroyed or damaged platforms exceeds 350. All these wells need to be plugged prior to abandoning.

This thesis is part of a project funded by BSEE which investigates the applicability of epoxy based or other non-cement plugging fluid to plug hurricane damaged wells. The applicability of epoxy based plugging materials for abandonment

and plugging operations has not been adequately studied in the industry and this research aims to fill this gap.

The work conducted in this thesis is expected to help 2 points,

1) Determining whether epoxy material can effectively drop 7000 feet through a casing annuli and accumulate on top of the packer

2) Determining how long it takes the material to travel to the bottom of a casing annuli and cure.

The experiment setup designed and constructed by El-Mallawany (2010) was used to collect data for the fall rates and the collected data was analyzed to propose an applicable test method and correlation on estimating the fall rates for various epoxy compositions. I also tried estimate and report the amount of epoxy that would adhere to the walls of the pipe.

2. LITERATURE REVIEW

There are many examples of epoxy polymer used in the industry. Stabilizing emulsions (oil based), formation plugging applications, sand consolidation, resin coated proppants, remedial casing applications, plastic plugback applications, substituting emulsifiers, strengthening fractured formations for wellbore stability and many other applications.

In order to confront the more complex offshore drilling challenges, adaptation of the drilling mud composition and properties for the advanced well conditions (high temperature and low pressure) Audibert et al. (2004) suggested using epoxy polymers. They named it EMUL in their work, and compared the results they obtained from the lab work to the other commercially available systems. It is stated that the mud stability can be achieved and formation of hydrates can be prevented by using this new system.

Bosma et al. (1998) studied the possibility of abandoning wells by a cost effective through tubing well abandonment method. The idea was to reduce the cost by proposing an alternative to the traditional abandonment method where the operator needs to remove the tubing and set a mechanical barrier before the plug. The authors argued that significant saving could be made if wells could be abandoned by a coiled tubing operation, during which the production tubing could be left in the well. Epoxy polymer was one of the alternatives to the regular cement along with the silicone rubber and silicone gel. Experiment setup used in their work is show on **Figure 2.1**.
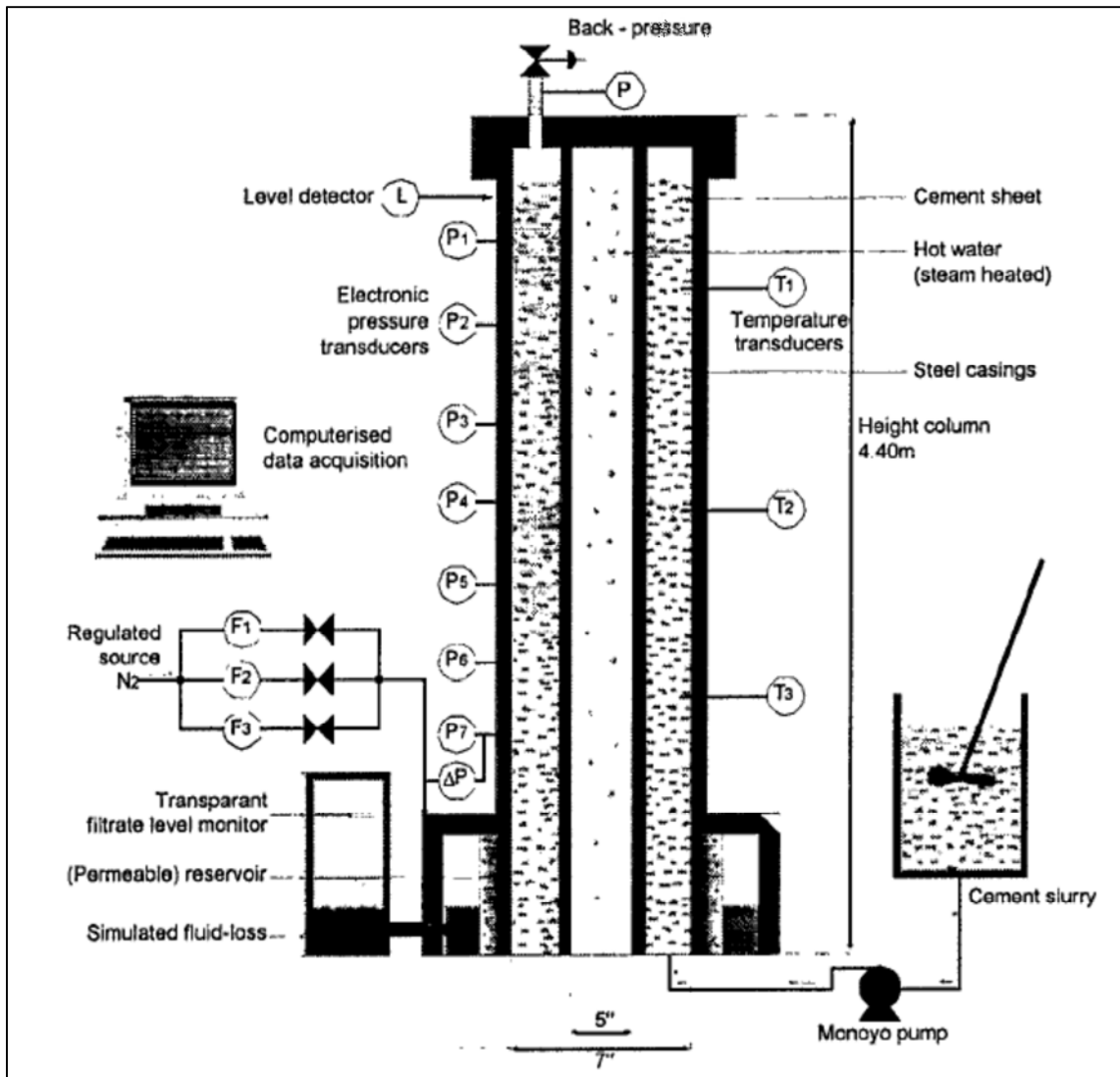
**Figure 2.1 Schematic of the experiment setup used in Bosma et al.'s work
(Bosma et al. 1998)**

Nguyen et al. (2004) studied the possibility of stabilizing wellbores in unconsolidated, clay-laden formations by using epoxy polymers while Knapp et al. (1978) suggested that and acrylic/epoxy emulsion gel system could be used for formation plugging in their laboratory work. **Figure 2.2** shows the images obtained

before and after flooding the clay formation in Nguyen et al.'s work. A Case Study of Plastic Plugbacks on Gravel Packed Wells in the Gulf of Mexico was presented at the SPE Production Operations Symposium in Oklahoma City, Oklahoma by Rice (1991). Rice argued that a special chemical mixture can be used instead of cement for wells with a conventional screen such as gravel packs to isolate the water producing zones. He suggested that the cement does not adequately fill the desired section thus a new chemical mixture (containing epoxy polymer) would be more appropriate for plastic plugback technique that was first introduced in 1988 by Carrol and Bullen. The success rate reported in his paper was a high as 67% in isolating the water producing zones in 21 field applications conducted by Chevron USA Inc.
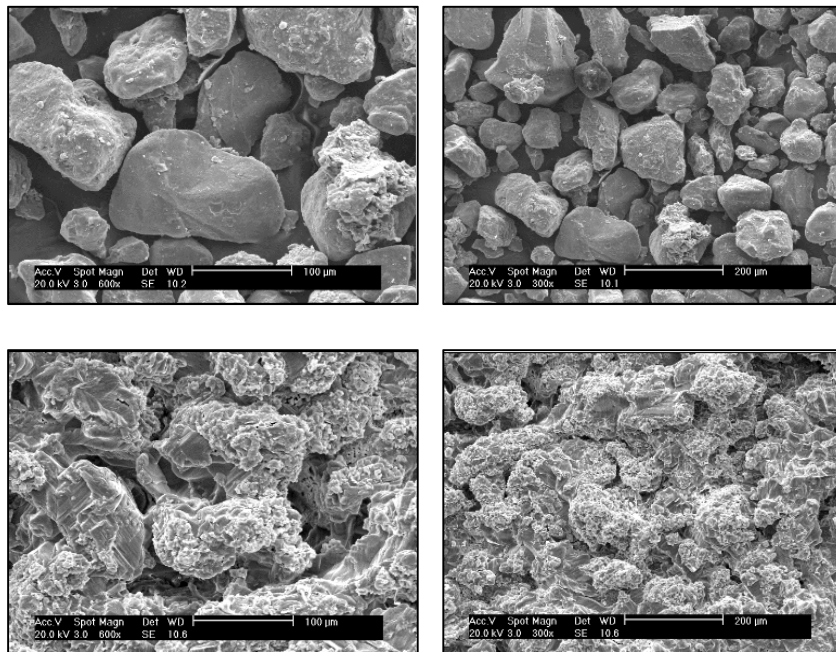
Figure 2.2 Epoxy flooded formations under microscope (Nguyen et al. 2004)

In one of the studies conducted by Soroush et al. (2006) epoxy polymer was suggested as a formation consolidation chemical especially for fractured formations to provide wellbore stability by increasing the formation strength. The term "chemical casing" was used to identify the interval saturated thus strengthened by epoxy polymers. Many advantages and disadvantages of using various chemicals were discussed in their paper Investigation into Strengthening Methods for Stabilizing Wellbores in Fractured Formations.

There is also a US patent Ng et al. (1992) that discusses using epoxy polymers to repair corroded casing in a wellbore. It is suggested in the patent that the corroded casing section is milled out and a retrievable packer is placed under the milled section. The epoxy is placed above the packer to fill the milled section and any thief formation section. The patent suggests that the epoxy is either placed using a dump bailer or using coiled tubing.

Both of these placement methods mentioned in the patent are of course not suitable for the intended application of this thesis. The patents also suggests some epoxy based materials namely Shell's EPON-828 and Shell's EPON DPL-862 as the resin and a Sherling Berlin's diluent 7 as a reactive diluent and fine powdered calcium carbonate or silica flour as a filler and lastly Serling Berlin's Euredur200 3123 as a curing agent. The diluent's function is to increase the pot life and gel time of the resin and decrease the epoxy's viscosity. The filler's function is to increase the specific gravity of the resin so the resin does not float and start settling on the packer. The curing agent's job is to make the resin crosslink and therefore harden.

Figure 2.3 from the patent describes the process where epoxy is placed to repair the corroded casing and thief zones and then drilled off.
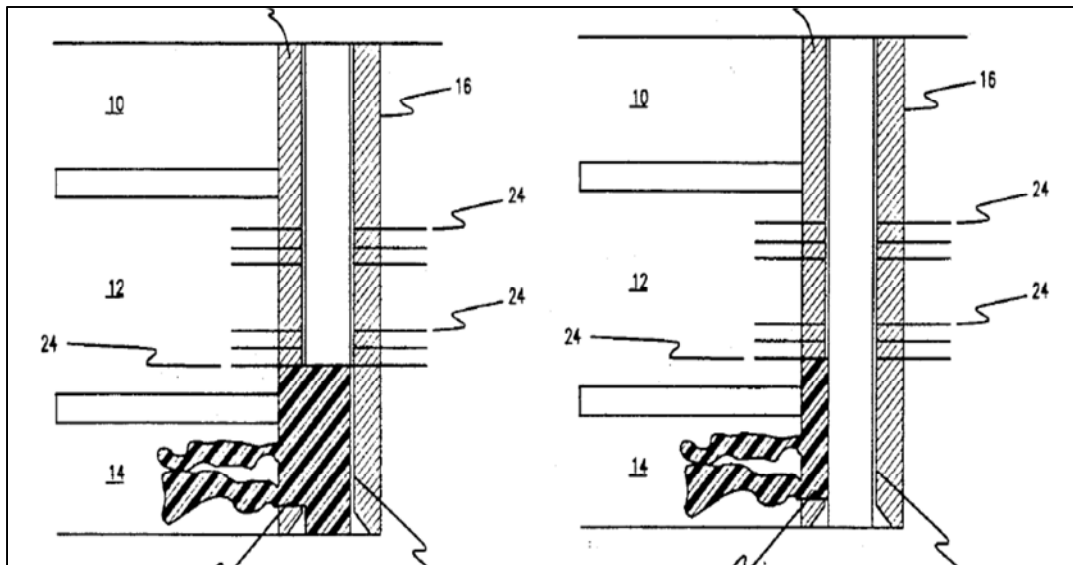
Figure 2.3 Epoxy used for remedial casing procedure (Ng 1994)

Knapp and Welbourn (1978) discussed the possible use of epoxy for formation plugging in their research which was also mentioned in their paper that was presented at the fifth Symposium on Improved Method for Oil Recovery of the Society of Petroleum Engineers of AIME held in Tulsa. It suggests the use of a resin in an emulsion where droplets are less than 1 micron in diameter which are able to seep through the pore spaces of the formation. They suggest pumping the resin in the formation first then pump the curing agent after it. This causes regions of high permeability in the formation to be preferentially sealed. The reason for this application is the cut the water or gas production from a formation. It is also used to control water injection wells to make sure

the water is not lost in unwanted zones. The resin's use here is to plug the areas of high permeability and direct the injected water to flow in the desired sections of the reservoir.

The only resin product that has been applied for a similar application to the one we are focusing on is a product called Ultra-Seal from a company named Professional Fluid Systems. The company has applied this resin on similar applications that are limited in number. High Island Block A330 platform that plugged and abandoned, and is an example of these applications. Several years after abandoning, gas seepage from the pressure cap of the well was detected by coincidence when a recreational diver was swimming by. When the company removed the pressure cap by using a diamond saw, they observed that the seepage was coming from the micro-annuli between the cement and the casing walls. The tubing was then sealed with a CIBP and the pressure cap was reinstalled. Liquid Bridge Plug (Ultra-Seal) was pumped inside the micro-annuli and was waited on for 20 hours. The plug was tested to be successful in sealing and the gas seepage was stopped. Another example of the application of Ultra-seal is Chevron's Vermillion 31 platform. When the platform had a leaking packer and the company wanted a way to seal the packer without using the rig equipment, Ultra-seal was used. Annular fluid in this case was 8.6 lb/gal seawater and ultra-seal was weighted up with a filler material to increase its terminal velocity (or settling velocity) during its fall through the seawater thus reducing the total time required to reach the packer. A total of 168 gallons of the resin was loaded into the annulus and was allowed to fall for 14 hours and then set on the packer for an additional 24 hours. After curing, the plug was pressure tested at 1,000 psi and no pressure loss was detected.

CSI technologies has some laboratory work on the Ultra-Seal fall rates but these are very small scale compared to the experiment setup that was used in this work. A 2 inch diameter 5 feet in length clear glass pipe was used. A copper pipe was inserted in the first two feet of the pipe to act as a stringer.
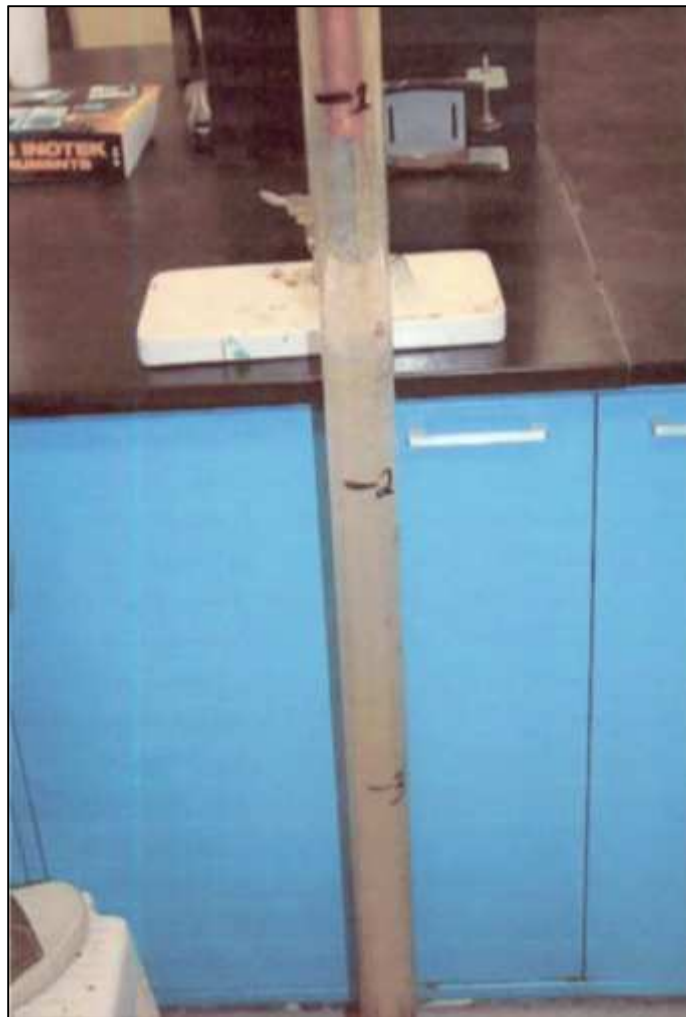
Figure 2.4 Experiment setup that was built by CSI Technologies

The whole system was filled with brine weighted with calcium bromide and had a density of 10.4 lb./gal. Epoxy was then loaded into the copper pipe and time was measured to calculate the speed of epoxy from the copper pipe to the bottom of the clear pipe. **Figure 2.4** shows the experimental setup that was used in this study.

The clear tubing shown on the Figure 2.4 was divided into 3 equal sections (1 foot each) and time was measured at every 1 foot interval as the particle fell. Barite was used as a filler to weight the epoxy to a density of 16 lb./gal. The time it took for the resin to reach the bottom of the cleat tube was measured as 5 seconds. The measurement was made visually. The experiment was repeated 3 times giving the same result of 5 second for 3 feet section. The fall rate was accepted to be 36 ft./min. Although this is a simple and logical way to obtain the fall rate data for epoxy, this experiment has many possible flaws. The first and most important deficiency of this experiment was that the effects of different parameters such as pipe diameter, epoxy density and viscosity, annular fluid density and viscosity were not taken into consideration. 3 foot interval for terminal velocity observation is probably not long enough to claim that the fluid reached its terminal velocity before the pipe ends. Having a small length of tube for the observation will also yield large errors in the velocity calculation.

3. THEORETICAL BACKGROUND ON TERMINAL VELOCITY

Determining the terminal velocity of a particle in a liquid medium has been an issue for petroleum engineers for quite a long time. Slip velocity of particles in a drilling mud, migration velocity of gas bubbles in a kick during well control operations, settling particles in a tank and many other examples in the petroleum industry have the same concept behind the working mechanism.

There are a few fundamental concepts behind the theory of settling objects. The most famous and known theory is the Stokes' law. Stokes' law provides an equation to predict the settling of solids or liquid droplets in a fluid, either gas or liquid. The law assumes that the settling object is a small sphere and that the difference in densities is not large. This is because Stokes' law takes into account only the viscous forces that cause drag and does not account for drag due to impact forces. Therefore, Stokes' law only applies where Reynolds number is very low. Stokes' law is given by the following equation (Batchelor 1967).

$$F_d = 6\,\pi\,\mu\,R\,V \tag{1}$$

where F_d is the drag force, μ is the fluid's viscosity, R is the sphere's radius and V is the particle's velocity.

When a settling particle reaches the terminal velocity, we can say that the net forces acting on the particle are equal to zero since the particle is not accelerating anymore. This implies that the drag force should be equal to the difference between the

gravitational forces and buoyancy forces. Having said that, we can rearrange the formula

for drag forces as the following

$$F_d = \frac{4}{3} \pi R^3 (\rho_{s-} \rho_f) g \tag{2}$$

where g is the acceleration due to gravity, ρ_s is the particle's density and ρ_f is the fluid's

density.

Now by equating equations (1) and (2) we can solve for the terminal velocity

which leads to the following equation

$$V = \frac{2R^2 (\rho_{s-} \rho_f) g}{9\mu} \tag{3}$$

It was found that (experimentally) the error margin is within 1% when the

Reynolds number is less than 0.1 for this equation. When the Reynolds numbers varies

between 0.1 and 0.5 then the error increases to 3% and between 0.5 and 1.0 the error

reaches to 9% margin. When the Reynolds number is greater than 1, drag due to the

impact becomes so significant that the Stoke's law yields larges errors due to the nature

of the estimation (it neglects the drag due to impact). Reynolds number can be calculated

by using the following equation (Coulson et al. 2002).

$$R_e = \frac{4R^3 g \rho_f (\rho_s - \rho_f)}{9\mu^2} \tag{4}$$

When the Reynolds number is greater than 1, then the impact forces become

much more significant and dominant where viscous forces can be ignored. In this case,

Newtonian drag is the determining factor for the terminal velocity. Newtonian drag

introduces a new parameter called the drag coefficient (C_D) that represents the ratio of

the force exerted on the particle by the fluid divided by its impact pressure. The coefficient can be calculated by (Batchelor 1967),

$$C_D = \frac{2F_d}{\rho_f V^2 A_p} \tag{5}$$

where A_p is the projected area of the object that is perpendicular to the direction of flow. For a sphere, the projected area of its shape is a circle and can be calculated by $A_p = \pi r^2$.

For a spherical particle settling in a fluid at a terminal velocity, Newtonian drag could be obtained by integrating equation (5) into (2) to obtain the following (Batchelor 1967),

$$V = \sqrt{\frac{4(\rho_s - \rho_f)gr}{3C_D \rho_f}} \tag{6}$$

Table 2.1 has some examples of drag coefficients for different shapes and materials. It should be noted that the drag coefficient also depends on the Reynolds number.

Table 2.1 Drag coefficients of different objects (Coulson et al. 2002)

C_D	Object
0.48	rough sphere (Re = 10e6)
0.005	turbulent flat plate parallel to the flow (Re = 10e6)
0.24	lowest of production cars (Mercedes-Benz E-Class Coupé)
0.295	bullet
1.0–1.3	man (upright position)
1.28	flat plate perpendicular to flow
1.0–1.1	skier
1.0–1.3	wires and cables
1.1-1.3	ski jumper
0.1	smooth sphere (Re = 10e6)
0.001	laminar flat plate parallel to the flow (Re = 10e6)
1.98–2.05	flat plate perpendicular to flow (2D)

Newtonian drag should be applied to particles with Reynolds number above 1000. For the cases which fall in between 1 and 1000 (intermediate values) for Reynolds number where both viscous and impact forces have significant effects on the terminal velocity, a transitional drag regime can be observed. An empirical equation for such cases was developed by Schiller and Naumann and is given by the following equation (Coulson et al. 2002),

$$C_D = \frac{24}{R_e} \left(1 + 0.15\, R_e^{0.687}\right) \tag{7}$$

By using equations (4), (6) and (7), terminal velocity of a particle can be calculated. The only problem in applying these equations to epoxy fall tests is that they

all require the particle size and shape (sphere). In my research however, shape is unknown and the velocity is measured with the help of the experiment setup. My main objective in this research is to correlate the velocity of the epoxy with at least one of its properties and substitute this property of the epoxy with the unknown size and shape of the particle so that estimating the terminal velocity of epoxy would be possible.

4. CONDUCTED WORK

After gathering enough data from the experimental setup that was developed by Ibrahim El-Mallawany, these results were tabulated and the relationship between the terminal velocity and the rheological properties of the epoxy were discussed. As an alternative to the already constructed experimental setup, a smaller scale experimental setup was built for further investigation and data validation.

The experimental setup at hand (static) consists of a 25 ft long pipe fixed on a pipe rack. The pipe is mounted on the rack which is able to be oriented the pipe from horizontal to vertical or any angle in between. The pipe acts as the wellbore in this experiment setup. The pipe is filled with the completion fluid which is sea water or simply fresh water. The setup allows the user to retrieve epoxy after it falls and clean the pipe after each run. There are pressure transducers for observing the pressure change along the pipe. For simplicity, the experimental setup is used with only one fixed pipe dimension. Different combinations were used when necessary. Terminal velocity obtained from the experiments was used as a constant velocity for the real-life scenario. In reality, the epoxy will accelerate first before reaching the terminal velocity but the distance covered with terminal velocity will be large compared to the acceleration zone in a 7000 ft. well. Thus the acceleration section was ignored and the velocity of the epoxy derived from the experimental setup was considered as constant terminal velocity.

The new experimental setup consists of a closed pipe system where the water is circulated at a constant rate and the annular velocity is kept close to the results obtained

in the previous experiment to validate the results obtained from the previous setup. After reaching a stabilized flow in the closed system, small amounts of epoxy were injected into the pipe with a help of syringe or similar device. The expectation was that the epoxy droplet would be suspended in the upward flowing water thus validate the results obtained from the first experimental setup. Specifications of the new experimental setup will be discussed in the next sections of this thesis.

5. EXPERIMENTAL SETUP

There is two experimental setups studied in this research. The first one is the setup that was constructed by Ibrahim El-Mallawany for the epoxy fall tests in 2010. The second experimental setup was constructed to validate the results obtained from the previous setup. The first setup has a static water column in the 7" clear pipe, thus it will be called the "static setup" for convenience while the second experiment will be called the "dynamic setup" due to the fact that it has flowing water system in the 3" clear pipe. Details for the both setups will be discussed under this topic and experimental data will be discussed in the next section of this thesis.

5.1 The Static Experiment Setup Design

There are two main components to the static experiment setup: the pipe support and the base for the pipe support.

5.1.1 Static Design Assembly

The 3D representation for the completed system is shown in F**igure 5.1** and **Figure 5.2.** The pipe support along with the 7" pipe attached to it is mounted on the base and the hoist cable is attached to the pipe support for moving the system to different angles. The base of the experiment setup is anchored to the ground in order to prevent the setup from being tumbled over.
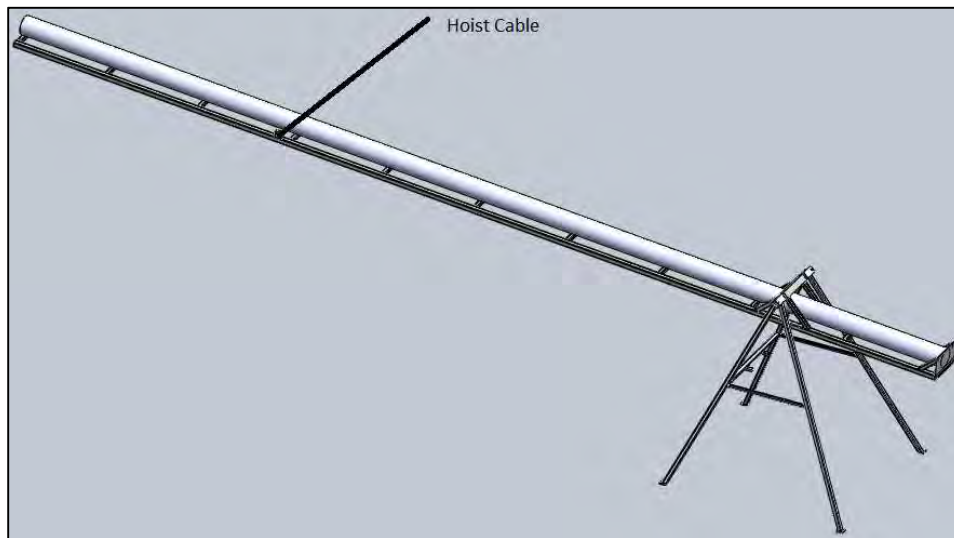
Figure 5.1 3-D model of the assembly (El-Mallawany 2010)
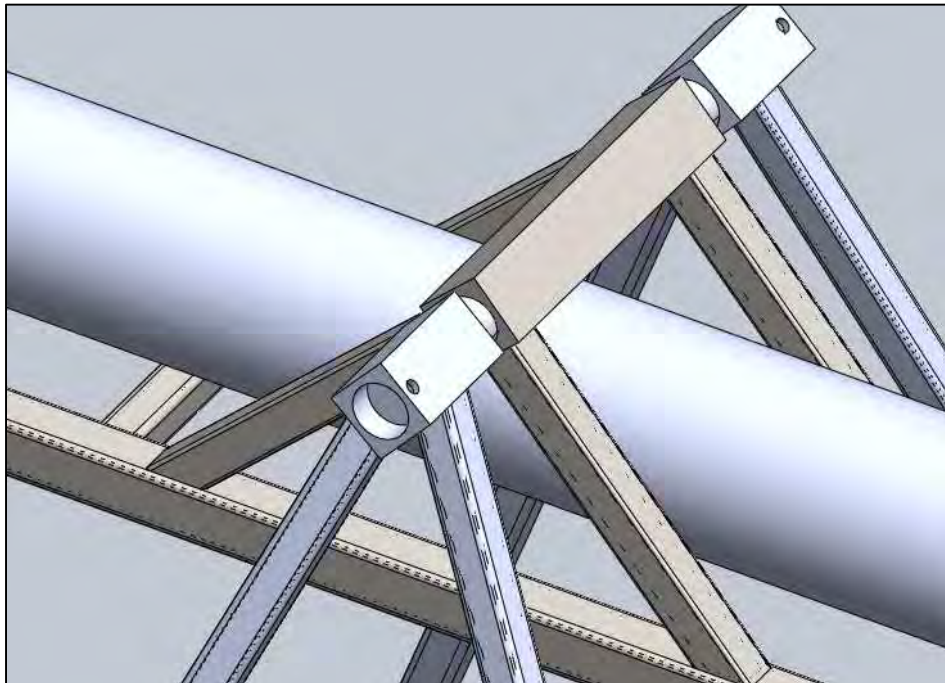
Figure 5.2 Zoomed 3-D view of the connection between the pipe support and the base (El-Mallawany 2010)

Assembly is simply put together by placing the pipe support's 2" hole concentrically with the base's 2" hole and pushing the pin inside. Then finally adding the two restricting bolts to restrict the pin from coming out.

Since the hoist's cable can only pull the pipe support but cannot push it down, it was made sure that the pipe support's weight always provided a torque in a direction opposite to that of the cable so it can lower itself in the right direction when the cable is slack.

The base has two stops to prevent the pipe from tumbling after reaching vertical position. **Figure 5.3** shows the stops in action.
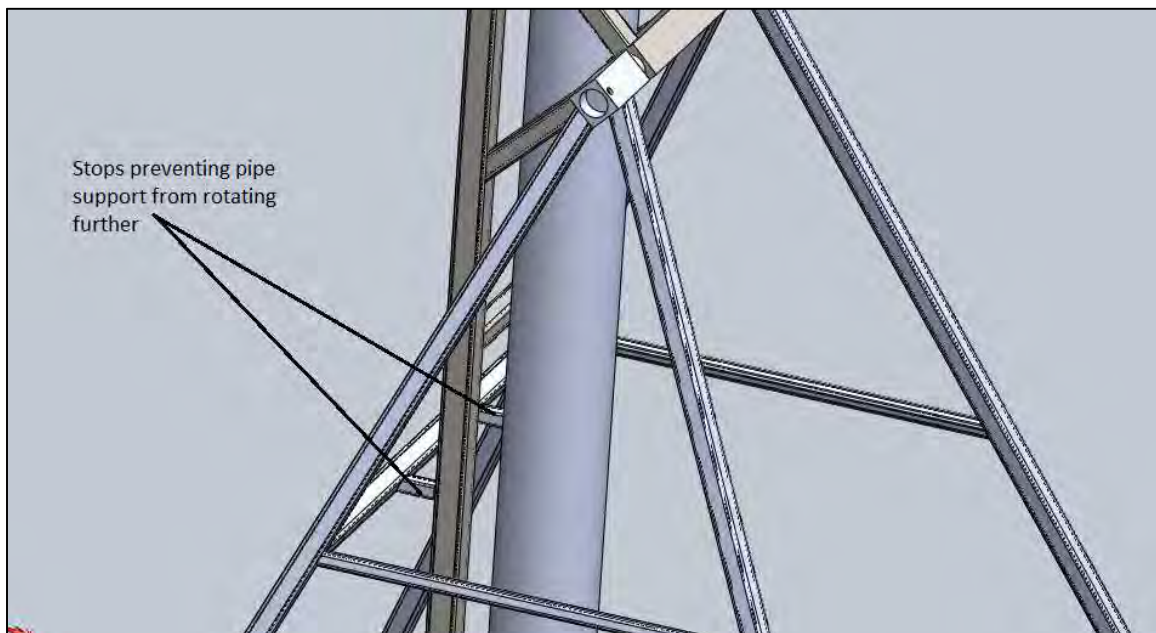
Figure 5.3 The stops of the base in action (El-Mallawany 2010)

5.2 The Dynamic Experimental Setup Design

The purpose for building the dynamic experimental setup was to validate the results obtained from the static setup. If the turbulence in the pipe allows the epoxy particle to be observed in the clear pipe, then the results obtained from the static setup can be put to test in this dynamic setup. The dynamic setup simply consists of a closed system with a 3-inch clear tubing in vertical position. The orientation of the clear tubing can be adjusted if required. The power required for the circulation is derived from a ¾" pump which is capable of pumping 24 gal/min water (@1 ft. head). Specifications for the pump will be discussed in the next sections of this thesis.

5.2.1 The Pump

The pump used in the assembly was a ¾" inlet and ¾" outlet pump with a pressure rating up to 150 psi. It can be found in most home-care stores under the name "hot water circulator pump". This specific pump was manufactured by Bell & Gossett Company. The technical specifications for the pump are shown on **Table 5.1**.

Table 5.1 Technical specifications for the pump used for the research.

Item	Circulator Pump
Type	Closed Loop
Series	NRF
Style	Wet Rotor
Speed	3
HP	1/15
Voltage	115
Phase	1
Amps	1.1
Inlet/Outlet	Flanged
Housing Material	Cast Iron
Face to Face Dimension (In.)	6-3/8

Table 5.1 Continued.

Max. Working Pressure (PSI)	150
Flange/Union Included	No
Shut-Off (Ft.)	18.5
RPM	2950
Impeller Material	Noryl
Shaft Material	Ceramic
Thermal Protection	Auto
GPM of Water @ 1 Ft. of Head	24
GPM of Water @ 5 Ft. of Head	19
GPM of Water @ 6 Ft. of Head	18
GPM of Water @ 7 Ft. of Head	16
GPM of Water @ 8 Ft. of Head	15
GPM of Water @ 9 Ft. of Head	14
GPM of Water @ 10 Ft. of Head	13
GPM of Water @ 11 Ft. of Head	12
GPM of Water @ 12 Ft. of Head	10.5
GPM of Water @ 13 Ft. of Head	10
GPM of Water @ 15 Ft. of Head	6.5
Best Efficiency GPM @ Head (Ft.)	15 @ 8
Min. GPM @ Head (Ft.)	1 @ 18
Drive Type	Direct
Bearing Type	Sleeve
Watts	125
Feet of Head @ 20 GPM	4

Figure 5.4 ¾" Pump specifications mentioned on the label of the pump

Figure 5.5 ¾" Pump (The pump has 3 different speeds that can be adjusted by the switch)

Figure 5.6 ¾" Pump inlet view
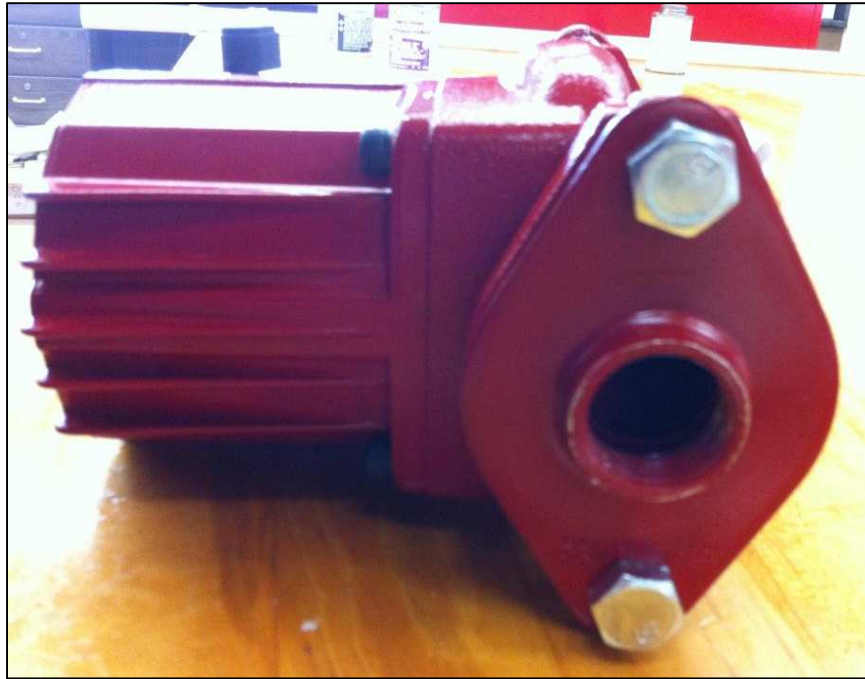
Figure 5.7 ¾" Pump outlet view

5.2.2 The Valves

There are two valves in the assembly. The first valve is placed right after the pump to regulate the flow if necessary. The second valve is simply the drainage valve for draining the 3" tubing when necessary. This valve is placed right before the 3" tubing with a "T" connection. Both of the valves a socket ball type with 1" ID. The valves are connected with hard pipes of 1" in ID.

Figure 5.8 1" PVC valve used in the assembly

Figure 5.9 1" PVC valve with threaded connection used in the assembly

Figure 5.10 1" Hard pipes with threaded connections

5.2.3 The Flow-meter

Flow meter's function in this assembly is to make sure that the system has a stable and constant water flow before each trial. The display unit for the screen is in gallons. The flow meter has screw type connections which are 1" in diameter. Technical specifications are shown on **Table 5.2.**

5.2.4 The 3-inch Vertical Tubing

3" clear tubing is the main component of the whole assembly. The reason for having clear tubing for this assembly was to be able to observe the water flow in the tubing while injecting the epoxy. The behavior of the epoxy was observed both in static

Table 5.2 Technical specifications for the flow meter

Item	Flowmeter
Type	Turbine, For Water
Housing Material	Nylon
Fitting Size (In.)	1
Flow Material	Water
Fitting Type	FNPT
Accuracy (%)	+/-5
Wetted Materials	304 SS, Nylon, Tungsten Carbide, Ceramic
Pressure Rating (PSI)	150
Fluid Temp. Range (Deg. F)	14 to 130
Max. Viscosity	5cP
Sensor Type	Magnetic
Rotor Type	Nylon
Display Units	Gallon
Display Type	Standard LC Display
Flow Range	3 to 30 gpm
Repeatability	0.50%
Fluid Temp. Range (Deg. C)	0 to 60
Strainer	55 Mesh
Agency Compliance	CE

Figure 5.11 1" Flow meter

water and flowing water conditions. Length of the tubing was initially set to 6 ft. and observed that it was a sufficient length for the purpose of this work. The 3" clear tubing is connected to the 1" pipe system with an adapter. Switching from a narrow clearance to larger tubing would cause instability in the water flow but this was not an issue since the epoxy was injected from the top of the clear tubing.

Figure 5.12 3" OD tubing with 6' length

5.2.5 The Reservoir

Since it is a closed water circulation system, there is no need for a constant water supply or such kind. Having a closed system also enables us to use a relatively small reservoir to act as an intermediate medium for the pump and the circulated water. In this research, a plastic cylindrical 4 gallon tank was used.

Figure 5.13 Reservoir for the pump's water supply. Once the system is filled with water, the only function of this reservoir was to act as an intermediate medium for the circulated water.

The tank is connected to the pump via ¾" clear hose with ¾" fittings. **Figure 5.13** shows the tank's shape and the connection method to the pump.

5.2.6 The Supporting Infrastructure

In order to keep the 3" tubing in a vertical position and support it during the experimental runs, a supporting structure was built. The supporting structure was built by joining uni-struts together by simply using bolts on the joints.

Figure 5.14 The support structure

The structure was built on four wheels in order to move the assembly when needed (for water refill or drainage purposes). Height of the assembly is 105 inches, width is 33 inches and the length of the platform is 49 inches.
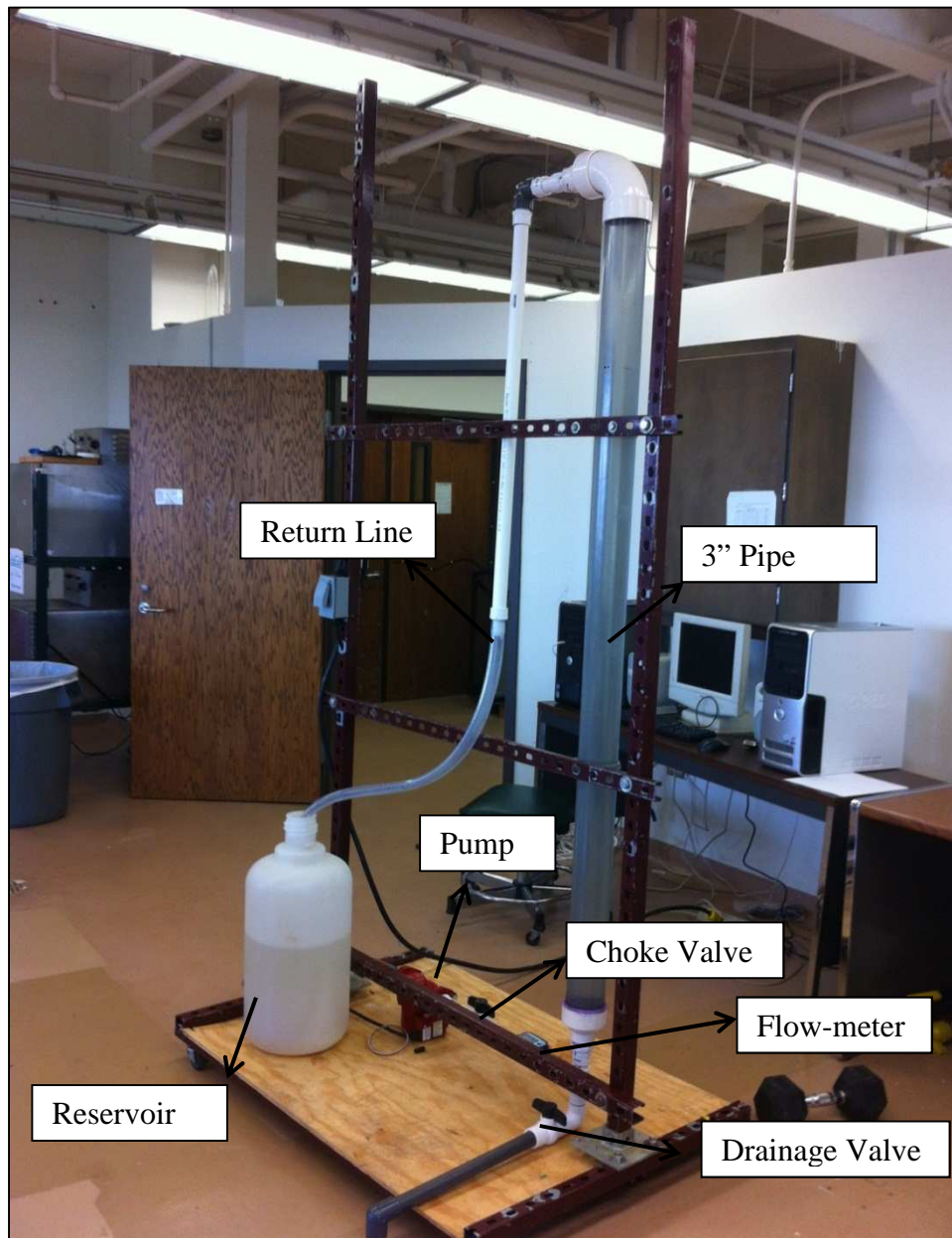
Figure 5.15 The completed experimental setup

6. THE EXPERIMENTS

The objective of this thesis was to test an epoxy sample that is representative to what would be used in a real application. Ultra-Seal, which is produced by one of the well-known manufacturers in the industry Professional Fluid Systems (PFS) was used in the tests. Ultra-Seal has been successfully used in similar applications to the one that we are studying (see the introduction for more information). It's prior use in the industry was the main reason for using Ultra-Seal in this research.

Ultra-Seal as with most other epoxies is a mixture of four main components, an epoxy (resin), a diluent, a hardener and a filler material. *The epoxy or the resin* consists of monomers or short chain polymers that have an epoxide group at their end. The epoxide group is cyclic ether that consists of three atoms that form a shape that resembles an equilateral triangle. This shape makes the epoxide highly strained and therefore reactive. *The hardener* mainly consists of polyamine monomers such as triethylenetetraamine (TETA) that readily form stable covalent bonds with more than 1 epoxide (crosslinking) like for example TETA can form up to four bonds. The product therefore becomes heavily cross-linked and becomes hard and strong. *The diluent* is used to reduce viscosity of the epoxy to make it easier to pump. The diluent is also used to increase pot life and gel time. (Ng 1994) *The filler* is used to increase the density of the mixture. In the oil industry *barite* is the most common filler material even with epoxy.

To be able to try different densities and viscosities of epoxy mixtures each constituent was obtained separately from PFS. The constituents are then mixed at different ratios to obtain the different densities and viscosities desired. The hardener was not used because it was thought that it would damage the equipment by hardening on pipe walls and may cause the valves to get stuck etc. The hardener was not used also to be able to use the mixture more than once. So only the epoxy, the diluent and the filler were used in the mixtures.

Since two different experimental setups were used in this experiment, there will be one section for each experimental setup and the data obtained from them. Each setup and procedure will be discussed in details. In the first section, the static experiment setup will be discussed. This experimental setup has a static fluid column in the plastic tubing and that is why it is called the static experiment setup. The second setup is the dynamic experiment setup and as it can be referred from the name, this experiment setup has a dynamic water column in the tubing that flows from bottom to top.

6.1 Static Experiment

6.1.1 Experiment Variables

Table 6.1 shows the properties and constituents of the epoxy formulations that were used. As it can be seen on the table, most of the readings for the majority of the samples were out of range (300).

Table 6.1 Epoxy formulations

Sample#	Density, ppg	Viscosty						Part A (epoxy), g	Diluent, g	Barite, g
		R3	R6	R100	R200	R300	R600			
1	9.00	3	12	200	>300	>300	>300	1000	178	0
2	9.60	9	16	236	>300	>300	>300	1000	182	100
3	9.15	9	17	255	>300	>300	>300	1002	181	51
4	9.60	8	14	205	>300	>300	>300	1000	250	53
5	9.60	6	11	153	>300	>300	>300	1001	310	25.1
6	9.65	9	16	226	>300	>300	>300	1000	210	52
7	9.90	6.5	12	183	>300	>300	>300	1017	250	53
11	9.40	9	17	235	>300	>300	>300	1002	154	50
12	9.60	4	7	97	195	300	>300	1002	400	50
13	9.80	4	6	91	183	274	>300	1006	402	100
14	10.50	4	6	85	169	251	>300	1003	422	204
16	13.50	16	30	>300	>300	>300	>300	1011	182	1000
17	15.20	26	48	>300	>300	>300	>300	1005	180	1527
18	14.00	22	40	>300	>300	>300	>300	1000	180	1250
20	12.20	17	34	>300	>300	>300	>300	1000	179	730
21	11.30	12	22	>300	>300	>300	>300	1030	179	500
22	17.20	43	80	>300	>300	>300	>300	1050	179	2094
23	8.90	3	10	186	>300	>300	>300	1000	230	0
24	10.60	12	22	>300	>300	>300	>300	1000	184	403
25	11.80	16	30	>300	>300	>300	>300	1004	183	650

A constant annular size was used in this study since the effect of the annular size was already studied by El-Mallawany. His observations for the annular size and epoxy were used as a reference for the interpretations about the annular size. The outer pipe has 6" ID and the inner pipe has 1.9"OD.

The angle is the angle of inclination of the pipe support measured from vertical. All the tests were done in vertical for simplicity. Inclined tests were discussed in the thesis.

6.1.2 Experimental Procedure

1) Get pipe support to horizontal position.

2) Make sure pipe is clean. If not see cleaning procedure.

3) Make sure all hoses are not kinked

4) Close Valve 1 (**Figure 6.1**) and make sure the 6" PVC valve (Valve 4, Figure 6.2) is not stuck by opening and closing a couple of times then close it.

5) Open Valve 2 (**Figure 6.2**). (It is very important to open valve 2 before entering water into the pipe otherwise pressure will build up in the pipe and separate the pipe from the rubber coupling as it is not designed to hold against pressure)

6) Start filling pipe with water by opening Valve 3 (**Figure 6.3**).

7) Close Valve 3 when pipe is full. (Pipe will be full when Hose 2 (Figure 6.2) starts draining water). (If there is a smaller pipe to make an annulus, make sure it is full of water by inspecting if there are any air bubbles escaping the holes drilled at its side.

8) Close Valve 2.

9) Make sure epoxy is well mixed. Record its density, viscosity and weight. (this can be done before or during previous steps.

10) Remove hose 4 (**Figure 6.4**) from the elbow then pour the epoxy into the elbow.

11) Get the pipe to vertical or to desired angle.

12) Start recording data from the pressure transducer.

13) Two persons are needed starting from this step. One should be ready with a video camera to record the experiment and the other to pull the valve handle via the cable attached to it when the video camera starts recording.

14) Stop video recording and pressure data acquisition when all the epoxy falls to the bottom.

15) Start draining the water in the pipe by opening valve 2.

16) Remove hose 1 (Figure 6.1) and start collecting the epoxy at the bottom by opening valve 1.

17) Close valve 1 as soon as water starts to flow through the valve. (you will notice a great change in fluid velocity due to the two orders of magnitude difference in viscosity.)

18) Record the weight of the regained epoxy.

19) Connect hose 1 and start draining the remaining water by opening valve 1.

20) Clean (see cleaning procedure)

Figure 6.1 Pipe fittings 1.
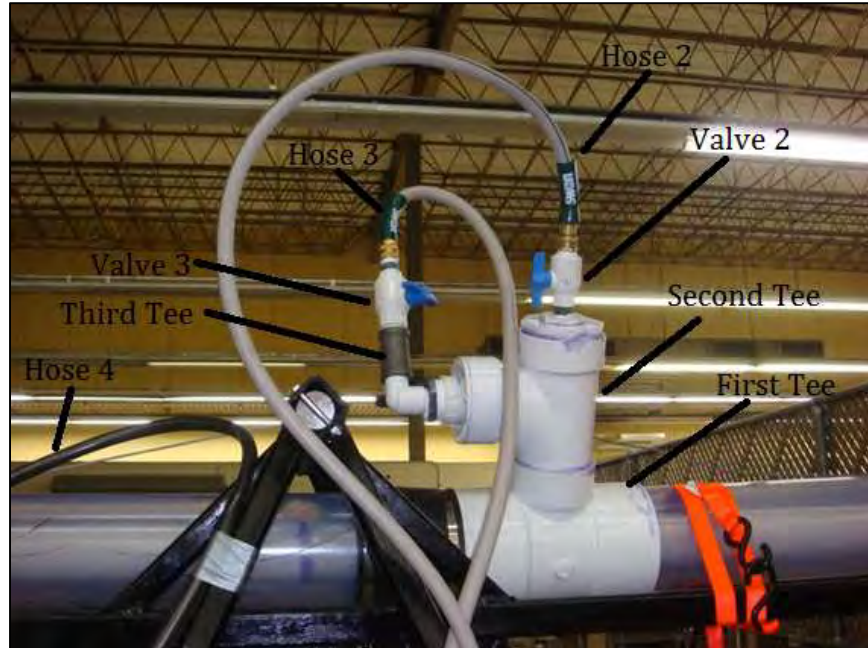
Figure 6.2 Pipe fittings 2.
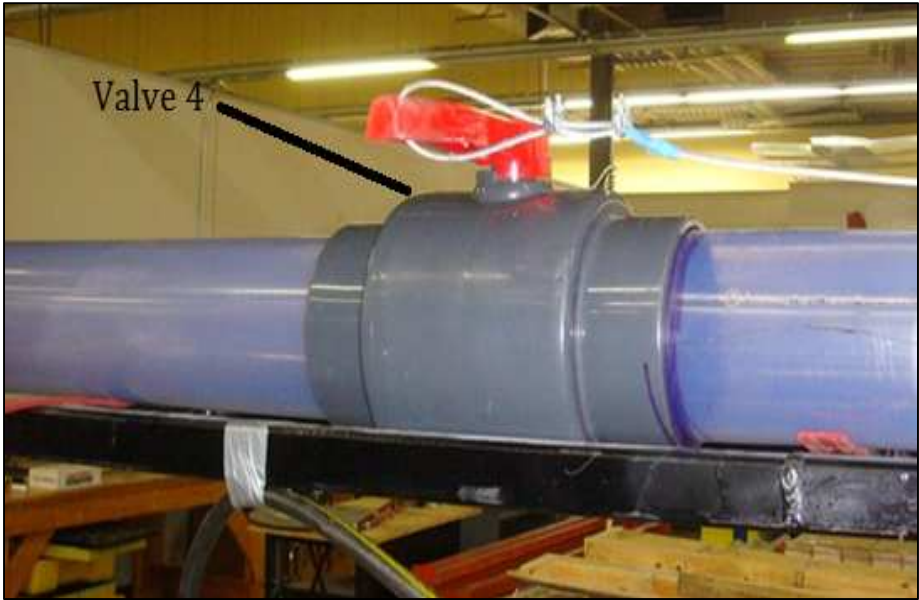
Figure 6.3 Pipe fittings 3.

Figure 6.4 Pipe fittings 4

6.1.3 Cleaning Procedure

1) Get pipe support at a very small angle from horizontal where the elbow is the high point and reachable.

2) Make sure valve 4 and valve 1 are open.

3) Use hose 4 to flush the mud inside the elbow then insert hose 4 into the elbow.

4) Repeatedly close valve 4 for a while to build water behind it then open.

5) Close valve 4 and fill some water behind it with hose 4. Then close hose 4.

6) Get pipe support to vertical position.

7) Open valve 4.

8) Open hose 4 and allow enough time for water to flush entire pipe clean.

6.2 Dynamic Experiment

6.2.1 Experiment Variables

There were two variables in this experiment. The first variable was the flow rate and the second variable was the epoxy composition. Pipe diameter was kept constant at 3" and the flow rates were kept close to the values obtained from the static experiment to see the effects on the epoxy particle. The same epoxy formulations as the static experiment were used to verify the results and validate the data. Since the epoxy specimens from the static experiment were contaminated with water, new samples were prepared by using the same mass ratio from the static experiment.

6.2.2 Experimental Procedure

1) Fill the reservoir with water (keep the valve 1 open during the fill)

2) Start the pump at slow rate (1st speed on the switch)

3) By using the flow-meter, make sure to have the desired flow rate, choke the flow in order to reach the desired rate or increase the pump speed by using the switch on the panel.

4) Make sure the system has a stable flow-rate and there are no leaks.

5) Mix the epoxy to the desired ratio and make sure the final product is homogenous.

6) Record the density, viscosity and weight of the epoxy.

7) By using the provided syringe, inject the epoxy in the 3" tubing slowly until the epoxy breaks free from the needle. Record the amount of epoxy injected.

8) Observe the epoxy and record the time if the particle starts falling down the tubing.

9) Decrease the pump rate if the epoxy starts to move up after breaking free from the needle.

7. RESULTS AND DISCUSSION

7.1 Static Experiment Results

7.1.1 Fall Rates for Vertical and Inclined Pipe

Since most of the epoxy samples had higher readings than 300 for R200, R300 and R600 readings, viscosity of these samples were not considered as a determining factor for the terminal velocity, thus not reported in the results section.

Table 7.1 Terminal velocities for each epoxy

Experiment / Sample Number	Epoxy Formulation				Time, sec	Terminal Velocity, ft/sec
	Epoxy, g	Diluent, g	Barite, g	Density, ppg		
23	1000	230	0	8.9	57	0.427
12	1002	400	50	9.6	55	0.442
13	1006	402	100	9.8	52	0.468
5	1001	310	25.1	9.6	51	0.477
1	1000	178	0	9	48	0.507
11	1002	154	50	9.4	45	0.540
3	1002	181	51	9.15	45	0.541
14	1003	422	204	10.5	45	0.541
6	1000	210	52	9.65	44	0.553
4	1000	250	53	9.6	43	0.566
7	1017	250	53	9.9	43	0.566
2	1000	182	100	9.6	40	0.608
24	1000	184	403	10.6	40	0.608
21	1030	179	500	11.3	38	0.640
25	1004	183	650	11.8	35	0.695
20	1000	179	730	12.2	34	0.715
16	1011	182	1000	13.5	31	0.785
18	1000	180	1250	14	28	0.869
17	1005	180	1527	15.2	27	0.901
22	1050	179	2094	17.2	27	0.901

Weight was one of the properties that was successfully measured and recorded for each epoxy sample that was used in the experiment. **Table 7.1** summarizes the results from the tests.

Table 7.1 has the results obtained from the static experiment setup for different compositions of epoxy mixtures. As it can be observed from the table above, terminal velocity and density tend to have the same trend with some exceptions. It is most likely that this behavior is caused by the diluent amount in the epoxy which is directly proportional with the overall viscosity of epoxy. Viscosity of epoxy is thought to be the main factor behind how much barite can be held within the mixture. Since the viscometer readings are of the maximum scale, an alternative way to relate the viscosity with the terminal velocity will be suggested in the next sections of this research. This alternative method will not require an experiment setup, thus it is hoped that it can be used in the field without the need for an expensive device.

The epoxy does not fall as one part, instead it spreads throughout the water column and then recollects at the bottom. This is shown in **Figure 7.1**. **Figure 7.1** also shows the lead of the epoxy column. The "Time" in **Table 7.1** refers to the time in seconds from releasing the epoxy in the water by opening valve 4 (**Figure 6.3**) to the time the lead reaches the bottom. There are two parts to the falling epoxy; the lead and the tail. What was recorded in the "time" section is the time observed for the lead to reach to the bottom. The time for the tail however, is very difficult to measure and is

Figure 7.1 The epoxy spreads in the water column.

somewhat subjective. This is due to the fact that as the epoxy falls, some of the adhered

epoxy on the pipe begins to break out and fall. As a result, it was seen that some epoxy

continues to fall even several minutes after the start of the experiment. Moreover, as the

epoxy falls in the water, the water becomes blurry from the barite and it is not clear

enough to see when the epoxy fall process actually stops or substantially decreases. The pressure transducers were able to pick up the time where the epoxy was first released in the tube but could not detect the pressure change while the epoxy passed the transducer. As it can be seen from the **Figure 7.2** the spike in the pressure is the indication of the epoxy falling in the tube but after that, the expected pressure drop is not observed. This is most likely that the sensitivity of the pressure transducers were not high enough to pick up the pressure drop caused by the epoxy falling down the tube. Thus, the recordings obtained from the pressure transducers were neglected. Visual observation was the only source for the data collection. The word "visual" indicates that the time was measured visually from the experimental videos by actually seeing the epoxy through the clear pipe reaching its target.
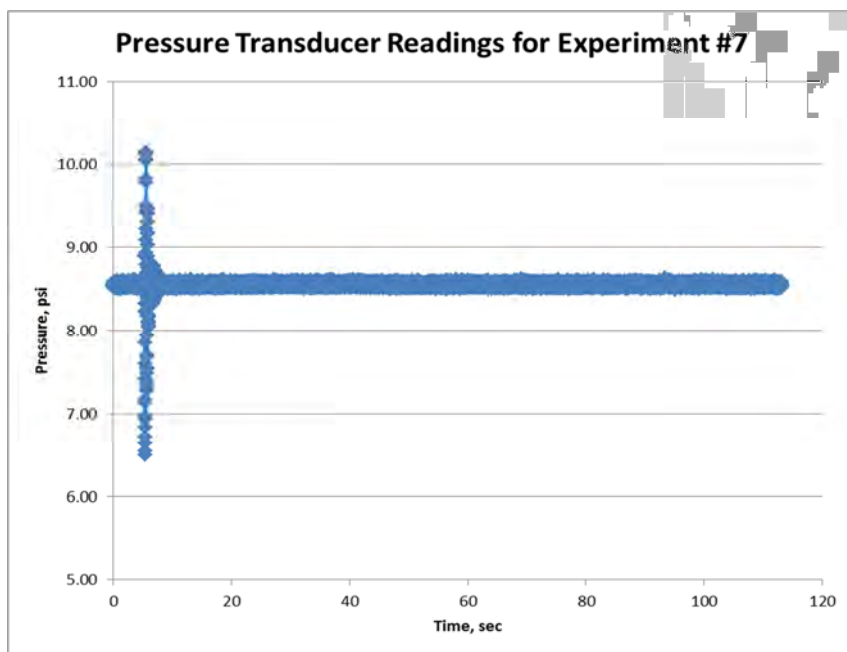
Figure 7.2 Pressure transducer readings

The information that can be derived from **Table 7.1** is as follows. First, it is clear that increasing the density of the epoxy (adding more filler to the mixture) increases its settling or terminal velocity which is expected. Although the denser epoxy compositions have higher viscosities, which decrease the terminal velocity by resisting the water to flow through the epoxy section in the initial stage of the flow/fall, it is safe to say that the main contributor to the terminal velocity is the density of the epoxy. It should also be noted that viscosity of the mixture increases the ability to hold the barite within the mixture and increase the terminal velocity. If we compare the sample#11 which has 154g diluent and 50g barite with a density of 9.4 ppg is actually faster than the sample#13 which has 100g the barite in the mixture but 248g more diluent than the sample#11. Although the sample#13 has higher density than sample#11 in normal conditions, sample#11 can hold on to barite better than sample#13, which gives the advantage of having higher density during the fall in the water column. Before jumping to any conclusions, the relation between the viscosity and density of the epoxy should be studied further in details. Since measuring the viscosity of the epoxy compositions were not possible with conventional fann viscometer, a simpler but effective way of relating the viscosity to the weight of the mixture needed to be derived.

After investigating the terminal velocities in vertical orientation, the effect of the deviation from the vertical was studied by using 30, 45 and 60 degrees deviation from the vertical. The same experiment setup and procedure was used only changing the deviation to desired angle. **Table 7.2** shows the data collected from the tests.

Table 7.2 Formulation and terminal velocities of epoxy mixtures in inclined tubing

Experiment / Sample Number	Epoxy Formulation				Time, sec	Terminal Velocity, ft./sec	Angle
	Epoxy, g	Diluent, g	Barite, g	Density, ppg			
10	1000	243	51	9.6	29.0	0.839	30
34	1500	270	1000	12.4	20.0	1.217	30
36	1500	270	800	12.2	20.0	1.217	30
35	1500	270	1200	12.8	18.5	1.315	30
37	1570	270	2003	13.8	17.0	1.431	30
38	1500	270	2500	15.9	16.0	1.521	30
39	1500	270	3000	17.3	14.0	1.738	30
27	888	157	187	10.5	26.0	0.936	45
8	1000	260	50	9.5	25.0	0.973	45
28	1500	270	320	10.5	23.0	1.058	45
30	1500	270	800	11.4	21.7	1.121	45
29	1500	265	660	11.5	18.8	1.294	45
19	1006	183.8	519	11.3	18.0	1.352	45
31	1530	270	1000	12.4	17.8	1.367	45
32	1500	270	1200	12.8	17.0	1.431	45
33	1500	270	1400	13.4	15.0	1.622	45
9	1000	254	51	9.6	30.0	0.811	60
40	1500	270	700	11	16.0	1.521	60

An important observation that can be inferred from **Table 7.1** and **Table 7.2** is that even though the epoxy has similar properties, it flows faster in an inclined section that it does in vertical. Deviating 30 degrees from the vertical increases the fall rate roughly by 100% - 110%, deviating 45 degree from the vertical increases the fall rate roughly by 110% - 130% and increasing the deviation further usually causes the epoxy to flow very slow or even make it stop before reaching the target. Two of the tests

however, yielded similar results to 45 degrees inclination results. 60 degrees inclination however, should be treated with care and the viscosity of the epoxy should be kept at minimum to make sure that the epoxy does not stop before reaching the target.

The most important conclusion that can be derived from these results is although the epoxy is expected to fall faster in a vertical it is possible for epoxy to flow faster in a deviated well. This can be explained by the epoxy's rheological properties and the physics behind the flowing mechanism of epoxy in inclined section. The reason for not flowing in 60 degrees inclination in these tests it that thought to be the thixotropic like behavior of epoxy which makes it harder for the mixture to flow once it becomes slow enough or even come to a full stop. The phenomenon of having a greater velocity in the inclined section compared to vertical is also explained by I. El-Mallawany in his research. He simply compares the behavior of a particle and a fluid body in the wellbore to explain the logic behind this phenomenon.
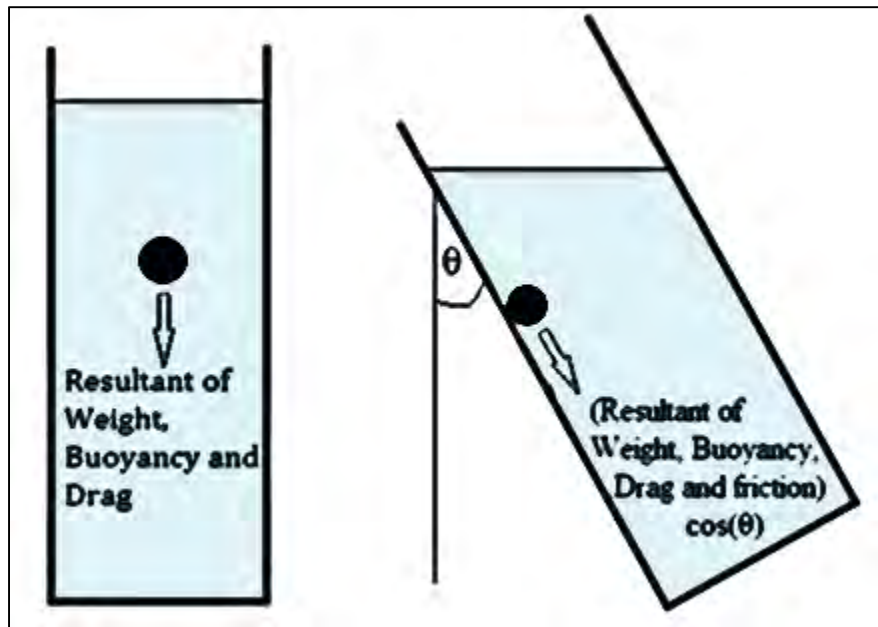
Figure 7.3 Forces on a settling particle in vertical and slant pipe
(El-Mallawany 2010)

The main reason for expecting a lower fall rate in the inclined pipe compared to the vertical is that the gravitational force on the particle is less than the vertical. There is also more frictional force acting on the particle in the inclined pipe compared to the vertical where the only friction force is the resistance to particle flow by water. **Figure 7.3** clearly shows why at an angle the downward force is less. Not only is there friction from the pipe wall decreasing the resultant force but the resultant force is also multiplied by cosine the angle of inclination. However, there is another factor that comes into play causing this big difference in speed which is illustrated by **Figure 7.4**.
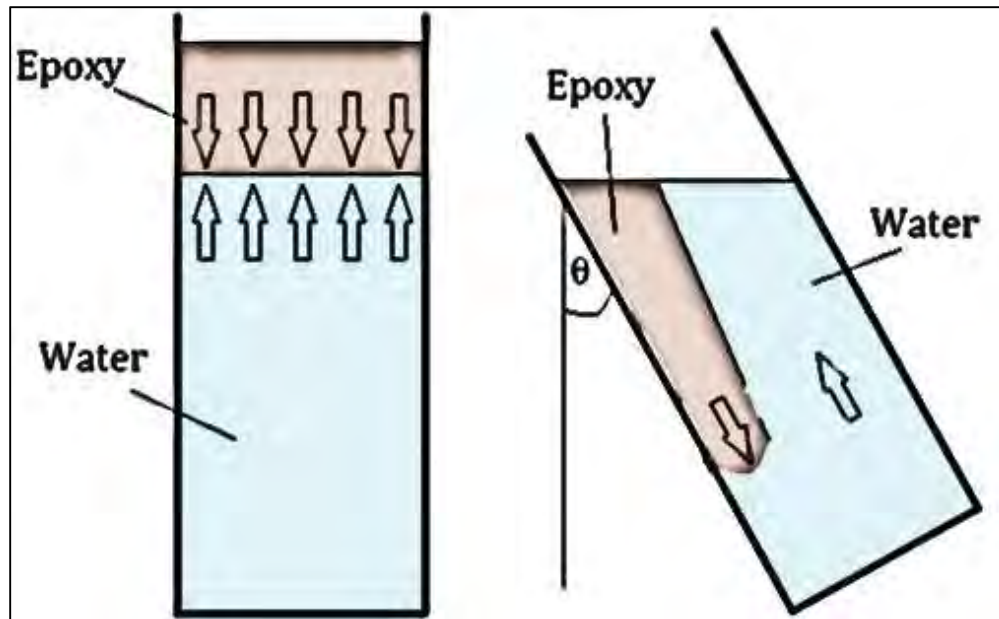
Figure 7.4 Settling of epoxy in vertical and slant pipe. (El-Mallawany 2010)

For pipe on the left in **Figure 7.4**, the water needs to rise and the epoxy needs to fall at the initial stage of the flow. The two motions oppose each other and therefore resist the settling greatly. For the pipe on the right, the epoxy falls to the bottom side of the pipe first then starts to flow downwards. What makes the epoxy, for the pipe on the right, faster is that now the water has a channel to flow above the epoxy layer and therefore the epoxy can easily flow downwards at the bottom side and the water can easily flow above the epoxy layer. "*Another reason is as the epoxy starts to flow downwards its column gets longer and its hydrostatic pressure is increasing only on itself and not in the water which boosts the epoxy forward*" (El-Mallawany 2010).

The next reason is the placement method for the vertical pipe. What is meant here is that this is caused by dumping the entire volume of epoxy all at once in the water.

This increases the concentration of epoxy in vertical pipes and inhibits the upward flow of water and the downward flow of epoxy. As a result, the initial stage of the epoxy fall is slowed down by this phenomenon. It is recommended to inject the epoxy in small volume rates to prevent this phenomenon to occur in vertical pipes.

"*The annulus does not seem to cause any significant change in the settling velocity sometimes it makes the settling faster and sometimes slower and in both cases the change is not significant. A possible reason why the annulus did not affect the settling velocity could also be the placement method. Injecting epoxy in small volume rates might show otherwise*" (El-Mallawany 2010).

7.1.2 Adhesion on the Pipe

The adhesion of the epoxy on the pipe is also an important factor to take into consideration when designing a remedial job offshore. If the amount of epoxy is not calculated correctly then the chances of failure are high. Overestimating the epoxy amount is probably the best option to make sure of the success of the job but this will increase the cost. For the fall rate tests conducted in the static experimental setup, the amount of epoxy mixture placed in the pipe and the amount of epoxy taken out were recorded and tabulated in order to figure out how much epoxy was lost due to adhesion. Since the pipe is 24.33 ft. long, epoxy adhered to the walls of the pipe per foot can also be calculated. This number however, will also depend on the surface area inside the pipe (annular size). Thus, the annular size also plays a great role in calculating the exact (or

estimate) amount of epoxy adhered to the walls of the well. **Table 7.3** shows the data obtained from the tests conducted in the static experiment setup.

<p align="center">Table 7.3 Epoxy recovery percentages</p>

Experiment Number	Epoxy Formulation				Time, sec	Recovery, %	Angle, degrees
	Epoxy, g	Diluent, g	Barite, g	Density, ppg			
22	1050	179	2094	17.2	27	17.76	0
3	1002	181	51	9.15	45	54.38	0
11	1002	154	50	9.4	45	59.29	0
5	1001	310	25.1	9.6	51	59.88	0
4	1000	250	53	9.6	43	60.78	0
7	1017	250	53	9.9	43	61.45	0
23	1000	230	0	8.9	57	63.41	0
2	1000	182	100	9.6	40	63.81	0
17	1005	180	1527	15.2	27	64.01	0
20	1000	179	730	12.2	34	67.37	0
14	1003	422	204	10.5	45	67.96	0
1	1000	178	0	9	48	69.78	0
6	1000	210	52	9.65	44	70.92	0
12	1002	400	50	9.6	55	71.76	0
13	1006	402	100	9.8	52	72.94	0
24	1000	184	403	10.6	40	75.61	0
21	1030	179	500	"11.3	38	77.24	0
16	1011	182	1000	13.5	31	82.95	0
18	1000	180	1250	14	28	83.13	0
25	1004	183	650	11.8	35	91.34	0
39	1500	270	3000	17.3	14.0	48.05	30
10	1000	243	51	9.6	29.0	48.69	30
38	1500	270	2500	15.9	16.0	63.07	30
37	1570	270	2003	13.8	17.0	75.05	30
34	1500	270	1000	12.4	20.0	80.18	30

Table 7.3 Continued

Experiment Number	Epoxy Formulation				Time, sec	Recovery, %	Angle, degrees
	Epoxy, g	Diluent, g	Barite, g	Density, ppg			
36	1500	270	800	12.2	20.0	86.77	30
35	1500	270	1200	12.8	18.5	88.48	30
19	1006	183.8	519	11.3	18.0	0.00	45
26	988	206	1012	13.5	90.0	0.00	45
27	888	157	187	10.5	26.0	46.43	45
8	1000	260	50	9.5	25.0	55.88	45
28	1500	270	320	10.5	23.0	58.37	45
33	1500	270	1400	13.4	15.0	72.43	45
29	1500	265	660	11.5	18.8	78.35	45
30	1500	270	800	11.4	21.7	78.60	45
32	1500	270	1200	12.8	17.0	83.33	45
31	1530	270	1000	12.4	17.8	83.57	45
9	1000	254	51	9.6	30.0	0.00	60
40	1500	270	700	11	16.0	48.05	60

While epoxy recovery by percentage is a useful data to have a rough estimation about how much epoxy to lose during the fall, it does not necessarily give us an accurate result. This is because the recovery percentage heavily depends on the length of the pipe, the inner surface area of the pipe (diameter) and the amount of epoxy used in the test. On a drilling rig, the crew would be more interested on how much epoxy would be lost due to adhesion during the remedial work. Thus, data obtained from each test was re-tabulated into a new table (**Table 7.4**). The amount of epoxy lost in each test was reported in terms of epoxy lost per foot to show how much epoxy would be lost for a field trial. It should be kept in mind that this is for a 6" ID tubing with 1.9" OD pipe

inside. The data on Table 333 can further be tabulated and reported as epoxy loss per ft^2 of inner surface area.

Table 7.4 Epoxy adhesion concentration on the tubing (g/ft)

Experiment Number	Epoxy Formulation				Time ,sec	Adhesion per ft., g/ft.	Angle, degrees
	Epoxy, g	Diluent, g	Barite, g	Density, ppg			
25	1004	183	650	11.8	35	6.54	0
1	1000	178	0	9	48	14.63	0
6	1000	210	52	9.65	44	15.08	0
16	1011	182	1000	13.5	31	15.37	0
24	1000	184	403	10.6	40	15.91	0
21	1030	179	500	"11.3	38	15.99	0
13	1006	402	100	9.8	52	16.77	0
18	1000	180	1250	14	28	16.85	0
12	1002	400	50	9.6	55	16.85	0
23	1000	230	0	8.9	57	18.50	0
2	1000	182	100	9.6	40	19.07	0
11	1002	154	50	9.4	45	20.18	0
7	1017	250	53	9.9	43	20.91	0
4	1000	250	53	9.6	43	21.00	0
14	1003	422	204	10.5	45	21.45	0
5	1001	310	25.1	9.6	51	22.03	0
3	1002	181	51	9.15	45	23.14	0
20	1000	179	730	12.2	34	25.60	0
17	1005	180	1527	15.2	27	40.12	0
22	1050	179	2094	17.2	27	112.32	0
36	1500	270	800	12.2	20.0	13.97	30
35	1500	270	1200	12.8	18.5	14.06	30
34	1500	270	1000	12.4	20.0	22.57	30
10	1000	243	51	9.6	29.0	27.29	30
37	1570	270	2003	13.8	17.0	39.41	30

Table 7.4 Continued

Experiment Number	Epoxy Formulation				Time ,sec	Adhesion per ft., g/ft.	Angle, degrees
	Epoxy, g	Diluent, g	Barite, g	Density, ppg			
38	1500	270	2500	15.9	16.0	64.81	30
39	1500	270	3000	17.3	14.0	101.85	30
31	1530	270	1000	12.4	17.8	18.91	45
32	1500	270	1200	12.8	17.0	20.35	45
29	1500	265	660	11.5	18.8	21.58	45
30	1500	270	800	11.4	21.7	22.61	45
8	1000	260	50	9.5	25.0	23.76	45
27	888	157	187	10.5	26.0	27.13	45
28	1500	270	320	10.5	23.0	35.76	45
33	1500	270	1400	13.4	15.0	35.92	45
19	1006	183.8	519	11.3	18.0	70.23	45
26	988	206	1012	13.5	90.0	90.67	45
40	1500	270	700	11	16.0	52.74	60
9	1000	254	51	9.6	30.0	53.64	60

Data obtained from **Table 7.4** would be useful for studies which have the same dimension as the static experiment setup. There is however, a better way to report the amount of epoxy adhered to the walls of the tubing, so that it can be correlated to any experiment or well for volume calculations and similar operations. Instead of quantifying the amount of epoxy lost per foot for this setup, it is wiser to report the concentration of epoxy adhered to the walls of the experimental setup by simply converting the previous data (g/ft.) to a universal and easy to correlate data (g/ft^2). Since the total amount of the epoxy adhered to the walls of the pipe is a function of the inner surface area of the annulus and rheological properties of the epoxy, surface area of the

equation can be taken out of the equation by reporting the epoxy concentration by unit area. This is possible by calculating the inner surface area which is simply done by using modified version of the equation below.

$$A = 2\pi R * 1ft \tag{8}$$

where A is the inner surface area and R is the radius of the pipe.
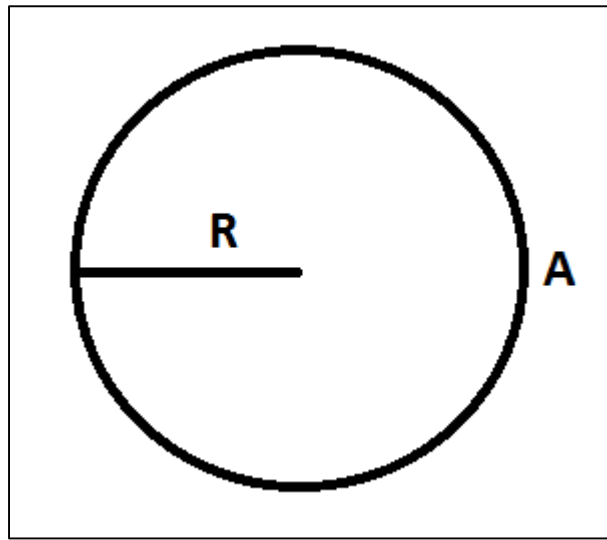
Figure 7.5 Area of a circle

The first section of the equation is simply the circumference of a circle and the second section converts it to area of a cylinder. Since there were two pipes inside each other for the dynamic setup, we will modify the equation to the below.

$$A = 2\pi (R_1 + R_2) * 1ft \tag{9}$$

where R_1 is the inner radius of the outer pipe and the R_2 is the outer radius of the inner pipe.
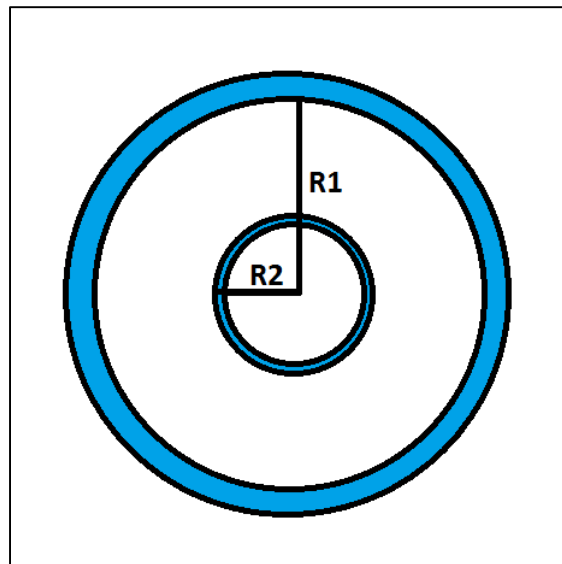
Figure 7.6 Total inner surface area of the dynamic experiment setup

This gives us the total inner surface area that the epoxy will be interacting during the fall. Multiplying the result with 1 ft assures the unit area that will be used for correlations.

Table 7.5 Adhesion concentration of epoxy (g/ft^2)

Experiment Number	Epoxy Formulation				Time, sec	Adhesion per ft^2, g/ft^2	Angle, degrees
	Epoxy, g	Diluent, g	Barite, g	Density, ppg			
25	1004	183	650	11.8	35	3.161	0
1	1000	178	0	9	48	7.075	0
6	1000	210	52	9.65	44	7.293	0
16	1011	182	1000	13.5	31	7.431	0
24	1000	184	403	10.6	40	7.692	0
21	1030	179	500	"11.3	38	7.730	0

Table 7.5 Continued

Experiment Number	Epoxy Formulation				Time, sec	Adhesion per ft^2, g/ft^2	Angle, degrees
	Epoxy, g	Diluent, g	Barite, g	Density, ppg			
13	1006	402	100	9.8	52	8.109	0
18	1000	180	1250	14	28	8.147	0
12	1002	400	50	9.6	55	8.149	0
23	1000	230	0	8.9	57	8.944	0
2	1000	182	100	9.6	40	9.220	0
11	1002	154	50	9.4	45	9.757	0
7	1017	250	53	9.9	43	10.113	0
4	1000	250	53	9.6	43	10.156	0
14	1003	422	204	10.5	45	10.372	0
5	1001	310	25.1	9.6	51	10.653	0
3	1002	181	51	9.15	45	11.187	0
20	1000	179	730	12.2	34	12.379	0
17	1005	180	1527	15.2	27	19.397	0
22	1050	179	2094	17.2	27	54.309	0
36	1500	270	800	12.2	20.0	6.757	30
35	1500	270	1200	12.8	18.5	6.799	30
34	1500	270	1000	12.4	20.0	10.911	30
10	1000	243	51	9.6	29.0	13.195	30
37	1570	270	2003	13.8	17.0	19.055	30
38	1500	270	2500	15.9	16.0	31.338	30
39	1500	270	3000	17.3	14.0	49.245	30
31	1530	270	1000	12.4	17.8	9.142	45
32	1500	270	1200	12.8	17.0	9.839	45
29	1500	265	660	11.5	18.8	10.434	45
30	1500	270	800	11.4	21.7	10.930	45
8	1000	260	50	9.5	25.0	11.486	45
27	888	157	187	10.5	26.0	13.116	45
28	1500	270	320	10.5	23.0	17.291	45
33	1500	270	1400	13.4	15.0	17.368	45
19	1006	183.8	519	11.3	18.0	33.959	45
26	988	206	1012	13.5	90.0	43.840	45
40	1500	270	700	11	16.0	25.500	60
9	1000	254	51	9.6	30.0	25.934	60

As it can be seen from **Table 7.5**, the general trend for the amount of epoxy adhered to the walls of the tubing is expected to be directly proportional to the amount of barite used and inversely proportional with the diluent used in the experiment. Since there are more than one parameters affecting the amount of epoxy adhered and the flow of epoxy in the system is more chaotic than expected, the amount of epoxy adhered to the walls of the tube cannot be related to any of the variables directly. However, it is safe to give an interval for the expected amount of epoxy that will adhere to the walls of the well by using the **Table 7.5**. The maximum amount of epoxy loss for a vertical well will be between 3.161 g/ft^2 and 12.379 g/ft^2. For an inclined well which has a 30 degree inclination is expected to have 6.757 g/ft^2 to 19.055 g/ft^2 epoxy loss. For 45 degree inclination this number varies between 9.142 g/ft^2 and 17.368 g/ft^2. For a 60 degree inclination however, most of the tests failed to give any recovery thus it is not recommended to use high viscosity epoxy mixtures in order to increase the success rate of the remedial job. Another important conclusion that can be inferred from **Table 7.5** is that the amount of barite that can successfully be used in the epoxy mixture should be considered carefully. As far as the tests conducted in the static experiment setup suggest, the density of the mixture should be kept around 14 ppg or less to increase the recovery of the epoxy. This means more epoxy can be delivered to the target if the density of the epoxy is 14 ppg or less and less mixture will be required to accomplish the same operation. A clear example of this case is the Experiment #22 from the vertical case. As it can be observed, the recovery of the expoy is 17%. This is mainly due to the amount of barite that was added to the mixture. Since the amount of barite that the mixture can

hold during the fall is limited, excess barite particles break free from the mixture, adhering to the walls and losing barite on the way causes a much lower recovery of the epoxy at the end of the test. The barite particles that cannot be recovered after the test are simply flushed away with the water. The highest recovery rates are observed for epoxy mixtures with 11.8 ppg to 14 ppg. One should also take into consideration that the viscosity of the epoxy is an important factor affecting the maximum amount of barite it can hold. Thus, the diluent ratio should also be kept at minimum in order to prevent barite from breaking free from the mixture.

As it can be observed from the **Figure 7.7,** the adhesion of epoxy is not a thin layered film or similar but has more like a spotted pattern. This makes the estimation of "epoxy volume lost due to adhesion" harder by using small scale experiment setup. Although the pattern in a well would most likely look similar to the pattern on **Figure 7.7,** the size of the well size and the tubing inside the well (annular space) would affect the final outcome. This phenomenon should further be investigated by a larger scale experimental setup or even by a field experiment. The data at hand suggests that the adhesion pattern will look like the **Figure 7.7** and the concentration of the epoxy lost will be within the intervals mentioned in the previous paragraph.

The effect of inclination on the adhesion of epoxy is already discussed in the previous paragraphs but it is worth stating once more that the inclination tends to increase the amount epoxy adhered to the walls of the tube in the static experiment setup.

Figure 7.7 Adhesion of epoxy for a vertical pipe at middle section
(El-Mallawany 2010)

Figure 7.8 shows an example of adhered epoxy on the experimental setup. As it can be observed, the epoxy tends to move towards the lower wall of the inclined pipe and accumulate there. On the upper wall however, there are less spots due to the fact that the interaction with the epoxy is less compared to the vertical tests. It is most likely that the increase in the interaction on the lower walls of the tubing makes it possible for epoxy to adhere more than the vertical case.

Figure 7.8 Adhesion of epoxy for a slant pipe at middle section

Also, the flow of epoxy for the inclined pipe is very different from the vertical case. Instead of spreading and flowing in a chaotic manner, the epoxy slides on the lower wall of the tubing. This naturally increases the interaction (more contact with the tubing) and the amount of epoxy lost due to adhesion.

7.1.3 Summary of Results for Static Experiment Setup and Conclusions

1) Denser formulations tend to have faster terminal velocity with some exceptions. The exceptions are thought to have a connection with the amount of diluent used. Further study needs to be done to increase the accuracy of terminal velocity estimations.

2) Tests conducted on the inclined tubing yielded higher terminal velocities compared to the vertical tests.

3) Viscosity of the epoxy is directly proportional to the amount of epoxy that will adhere to the walls of the system but the recovery of epoxy is a function of both viscosity and density. Increasing the density of epoxy above 14 ppg causes the barite to break free during the fall and decrease the recovery.

4) Higher inclinations will cause higher adhesion thus decrease the amount of epoxy delivered to the target.

5) Smaller annular size will usually lead to less epoxy loss due to smaller inner surface area.

6) As the epoxy flow stabilizes towards the bottom of the well, interaction with the walls will decrease and the adhesion concentration will also decrease.

7) Barite is a good candidate for epoxy weighting for up to 14 ppg mixture density.

7.2 Dynamic Experiment Results

After analyzing the results from the static experiment setup, terminal velocity values were used to estimate the required flow-rate values for the dynamic experiment setup. The objective was to validate the results obtained from the static experiment setup by using the dynamic setup developed as a part of this study. The same epoxy compositions as the previous tests were prepared by using the same ratio for each sample. Since the required amount of mixture for this part is a fraction of the amount used in the static setup, values were simplified by a factor of 5 to reduce the cost and labor. **Table 7.6** shows the simplified compositions and the required flow rate for each sample that is used in the dynamic experiment setup. Note that only vertical tests were used to validate the results since the inclined tests indicate a different flow behavior that is difficult to observe in the dynamic setup.

Terminal velocity calculation for the dynamic experiment setup results required a step by step procedure. Since the particles in the water were stabilized and not suspended in the flowing water, it was assumed that the velocity of water around the particle was equal to the terminal velocity of the particle in static water column. The flow rate for the water was recorded by the flow meter. Calculations for the water velocity required the inner diameter of the clear tubing which is 3 inches. Flow rates required for each sample to suspend in water are given on **Table 7.7.**

Table 7.6 Comparison of the dynamic and the static experiment results

Experiment / Sample Number	Epoxy Formulation				Velocity from Static Experiment, ft/min	Velocity from Dynamic Experiment, ft/min
	Epoxy, g	Diluent, g	Barite, g	Density, ppg		
23	200	46	0	8.9	25.6	17.7
12	200	80	10	9.6	26.5	19.3
13	202	80	20	9.8	28.1	20.1
5	200	62	5	9.6	28.6	19.3
1	200	36	0	9.0	30.4	19.6
11	200	30	10	9.4	32.4	20.7
3	200	36	10	9.15	32.4	20.4
14	200	84	21	10.5	32.4	20.9
6	200	42	10	9.7	33.2	20.4
4	200	50	11	9.6	33.9	20.4
7	202	50	11	9.9	33.9	21.2
2	200	36	20	9.6	36.5	20.7
24	200	36	81	10.6	36.5	27.0
21	206	36	100	11.3	38.4	27.0
25	200	36	130	11.8	41.7	27.5
20	200	36	146	12.2	42.9	27.5
16	202	36	200	13.5	47.1	29.7
18	200	36	250	14.0	52.1	31.8
17	202	36	305	15.2	54.1	32.3
22	210	36	419	17.2	54.1	34.4

After recording the flow rate values for each sample, these results were converted to velocity values in order to make it suitable for comparison. Since the water in the tubing is flowing in a laminar regime, it should be noted that the velocity distribution for the flowing water is much like a streamline flow where the fluid is faster at the center and relatively slower close to the pipe. If the epoxy sample followed a certain flow-path, this phenomenon would affect the results but since the particles moved around the pipe

in a random manner during the flow, so this effect was neglected. It was assumed that the calculated velocity is the average velocity for each epoxy sample.

Table 7.7 Required flow rates for each epoxy samples to suspend in water

Experiment / Sample Number	Epoxy Formulation				Required Flow Rate, gal/min
	Epoxy, g	Diluent, g	Barite, g	Density, ppg	
23	200	46	0	8.9	6.7
12	200	80	10	9.6	7.3
13	202	80	20	9.8	7.6
5	200	62	5	9.6	7.3
1	200	36	0	9.0	7.4
11	200	30	10	9.4	7.8
3	200	36	10	9.15	7.7
14	200	84	21	10.5	7.9
6	200	42	10	9.7	7.7
4	200	50	11	9.6	7.7
7	202	50	11	9.9	8.0
2	200	36	20	9.6	7.8
24	200	36	81	10.6	10.2
21	206	36	100	11.3	10.2
25	200	36	130	11.8	10.4
20	200	36	146	12.2	10.4
16	202	36	200	13.5	11.2
18	200	36	250	14.0	12
17	202	36	305	15.2	12.2
22	210	36	419	17.2	13

The equation that was used to convert the flow-rate values to the velocity is given below.

$$Velocity = \frac{FlowRate/7.4805}{ID^2 * \frac{\pi}{4}/144} \tag{10}$$

where *Velocity* is in feet per minute, *Flow Rate* is in gallons per minute and the *ID* (inner diameter of clear tubing) is in inches.

As it can be observed from Table 7.6, the results from the dynamic experiment setup and the static experiment setup support each other from slowest to fastest epoxy mixtures. The numeric results however, are not in complete agreement. This is due to the nature of these two experiments which are a lot different from each other. As it was mentioned earlier in the thesis, barite that is in suspension in epoxy settles down in a static epoxy mixture. Since the epoxy specimen in the static experiment setup rests in the top chamber before the experiment can be conducted, this allows the barite to settle down in the epoxy mixture. Since the settled part is the first to flow in the pipe, the velocity obtained for the lead is actually greater than the average velocity of the epoxy mixture. Notice that the difference between the two experiment setup results increase as the concentration of barite increases in the mixture. This is due to the fact that the amount of barite settled in epoxy increases as the barite concentration increases.

7.2.2 Predicting the Terminal Velocity

As it was mentioned in the theory section of the thesis, there are several approaches to estimate the terminal velocity for settling substances in liquids. Stokes approach is the most commonly used and accepted approach for spherical solids falling in liquids. In this research, the objective was to correlate the particle size with two variables which are density and the viscosity to use in Stokes correlation. Since the viscosity is not possible to measure with conventional equipment, the diluent mass percentage was used as variable. Since one variable was used as a percentage, density was also correlated to the weighting material namely barite percentage in the mixture. Compositions for each sample and the corresponding weight percentage are given on **Table 7.8.**

The visual representation of the **Table 7.8** is given on **Figure 7.9.** As it can be seen from this chart, it is difficult to determine which parameter is dominant on the particle size. There is however, a cross over between the barite and diluent concentrations around 12.5% barite concentrations. In order to observe the effect, the data were split from 12.5% barite concentration. **Figure 7.10** and **Figure 7.11** show the same set of data as the **Figure 7.9** where **Figure 7.10** is up to 12.5% barite concentration and **Figure 7.10** is the visual representation for the 12.5% barite concentration and higher.

Table 7.8 Weight percentage and particle size for epoxy mixtures

Sample #	Particle Volume, ml	Flow Rate, gal/min	Speed, ft/min	Barite, %	Diluent, %
23	0.2500	6.7	17.7	0.0%	18.7%
12	0.1563	7.3	19.3	3.4%	27.5%
13	0.1667	7.6	20.1	6.6%	26.7%
5	0.1786	7.3	19.3	1.9%	23.2%
1	0.2778	7.4	19.6	0.0%	15.1%
11	0.2941	7.8	20.7	4.1%	12.8%
3	0.2778	7.7	20.4	4.1%	14.7%
14	0.1351	7.9	20.9	12.5%	25.9%
6	0.2439	7.7	20.4	4.1%	16.6%
4	0.2174	7.7	20.4	4.1%	19.2%
7	0.2273	8.0	21.2	4.0%	18.9%
2	0.1852	7.8	20.7	7.8%	14.2%
24	0.1351	10.2	27.0	25.4%	11.6%
21	0.1163	10.2	27.0	29.3%	10.5%
25	0.1111	10.4	27.5	35.4%	10.0%
20	0.1163	10.4	27.5	38.2%	9.4%
16	0.0877	11.2	29.7	45.6%	8.3%
18	0.0641	12.0	31.8	51.4%	7.4%
17	0.0375	12.2	32.3	56.3%	6.6%
22	0.0353	13.0	34.4	63.0%	5.4%
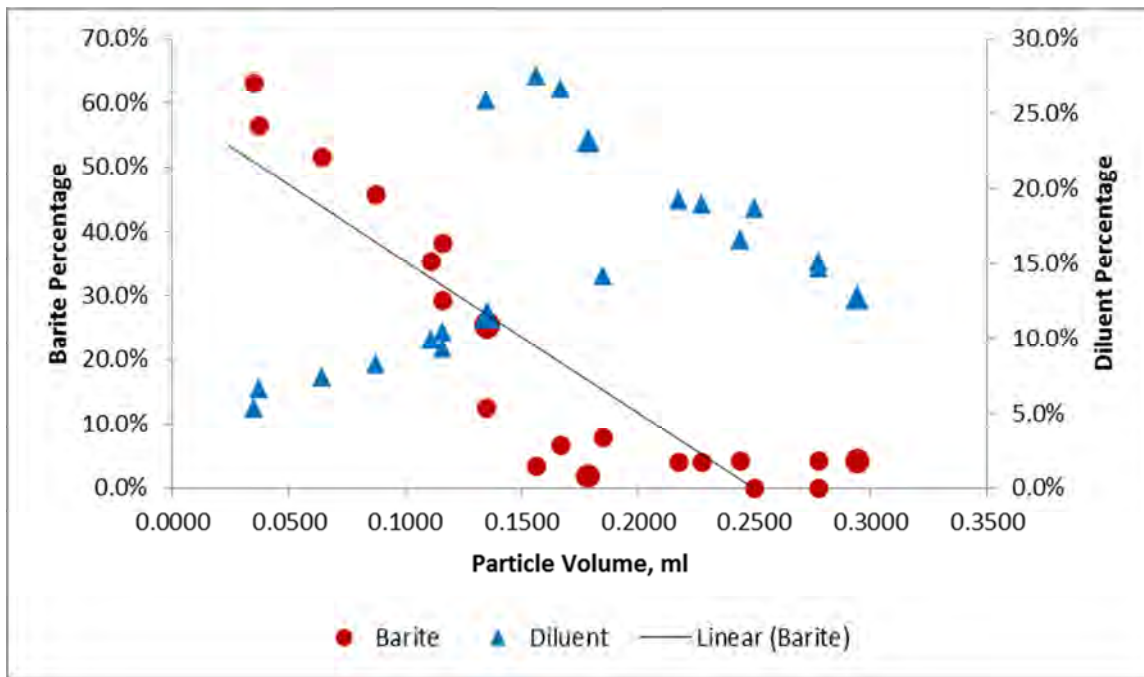
Figure 7.9 Total data from dynamic dxperiment
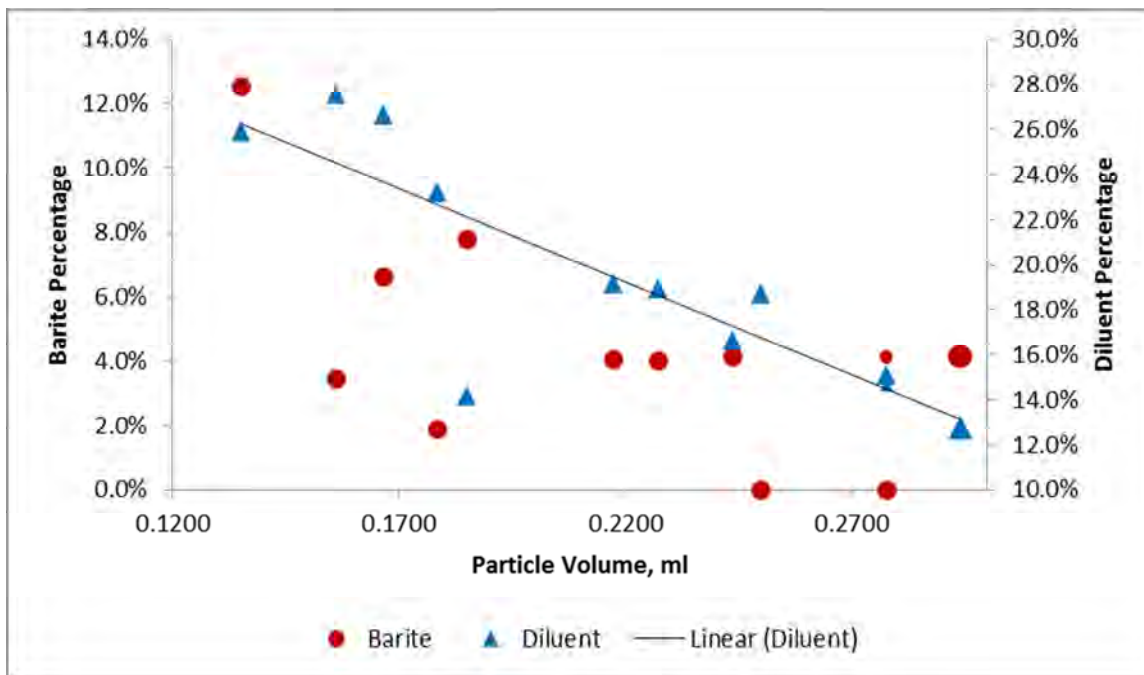
Figure 7.10 Results up to 12.5% barite from dynamic experiment

Figure 7.10 shows that the particle size depends heavily on the diluent percentage used in the mixture. This is valid up to 12.5% barite concentrations. After 12.5%, barite concentration seems to be the dominant factor on the particle size. This is also shown on **Figure 7.10**.

As you can see from the chart, the diluent percentage and the particle size are inversely proportional, which is not the general trend for the rest of the tests. This can be explained by the high concentrations of barite in the mixture. Barite increases the weight, thus the particle size decreases due to higher velocity in the water column.
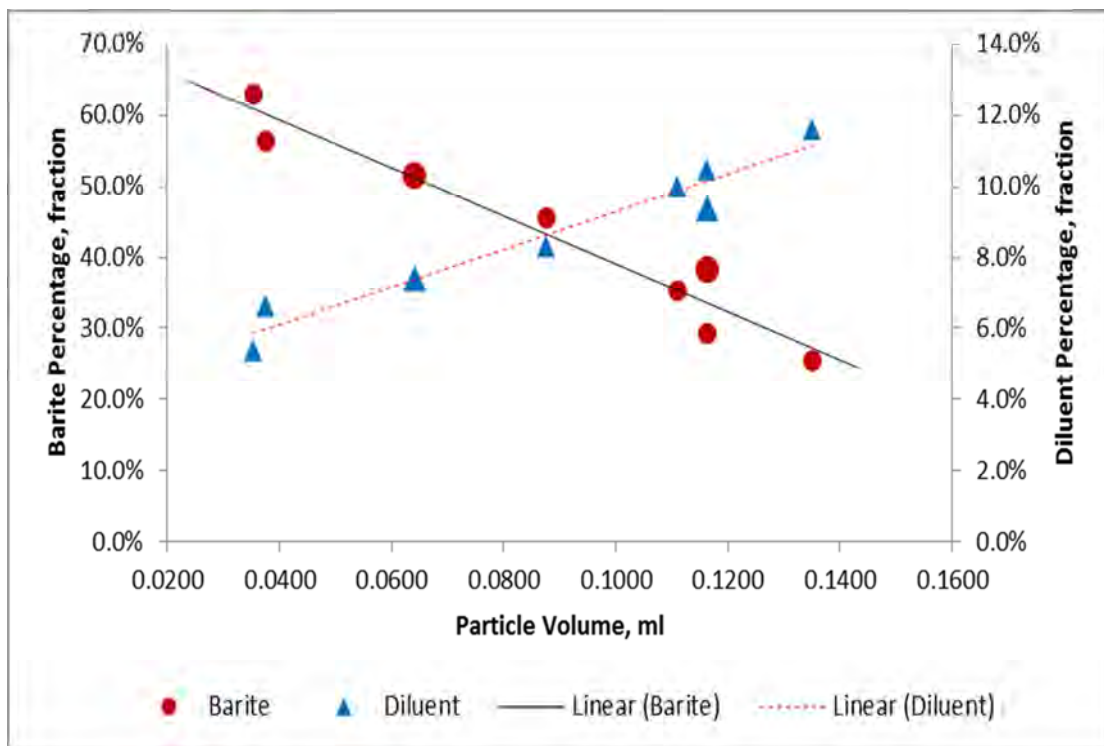
Figure 7.11 Results for 12.5% barite and higher concentration

It is possible to correlate the particle size with two variables such as diluent and barite percentage in the mixture. The results obtained from the correlation however, will yield a certain amount of error. Since the epoxy particles are not perfect spheres but rather look like hamburger buns, the Stokes correlation will also yield further error in the results. To overcome this problem, the percentages for barite and diluent were correlated with the terminal velocity values obtained from the dynamic experiment setup. The procedure is explained below.

It is easy to predict the result for a given data set if there are only one variable effecing the results. In this case, there were two variables affecting the outcome of the experiment; barite and diluent concentration. In order to correlate these two variables, a program called GRACE was used. The GRACE program generates an optimal correlation between a dependent variable (say, y) and multiple independent variables (say, x1, x2, x3 .....up to x30). This is accomplished through non-parametric transformations of the dependent and independent variables. Non-parametric implies that no functional form is assumed between the dependent and independent variables and the transformations are derived solely based on the data set.

The final correlation is given by plotting the transformed dependent variable against the sum of the transformed independent variables. The correlation thus obtained can be shown to be optimal (Breiman and Friedman, 1985; Xue et al, 1996).

Before coming up with the optimum correlation, the program transforms the independent variables (curve fitting). The alternating conditional expectation (ACE) algorithm of Breiman and Friedman (1985) is used by the GRACE program. **Figure 7.12** and **Figure 7.13** shows the optimal transform results for barite and diluent respectively. After obtaining the optimal transform equation, the program then calculates the optimum regression for velocity, the dependent variable. Using the transformed velocity values from **Figure 7.14** and velocity values from the test results optimal inverse transform relation is obtained. Finally, by using the transformed independent variables and dependent variable (velocity), the effect of barite and diluent concentration on the velocity is shown on **Figure 7.15.** The program evaluated both optimal transform and optimal inverse transform and chooses the most accurate correlation. The calculations for terminal velocity values are done according to the chosen transformation.
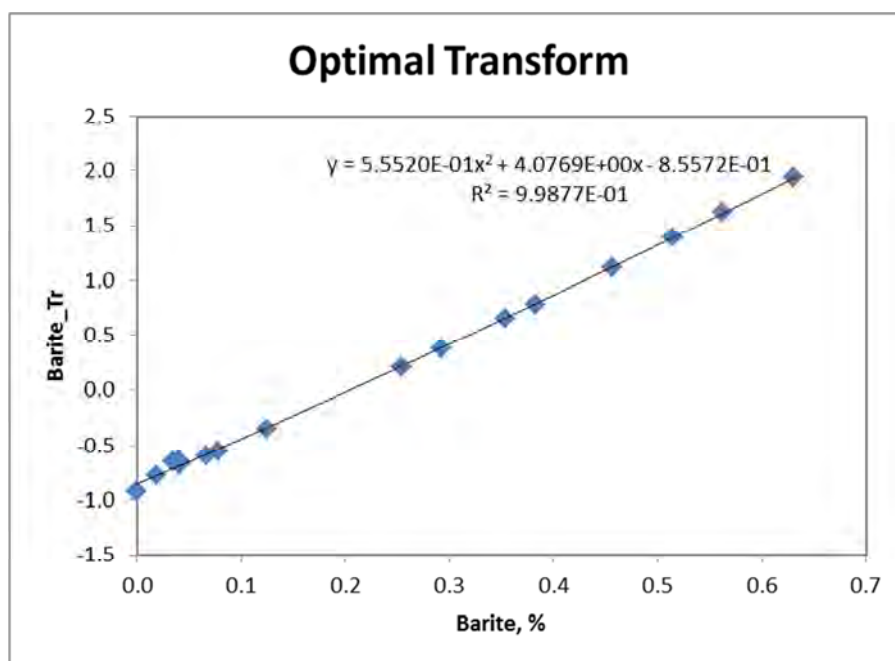
Figure 7.12 Optimal transform for barite
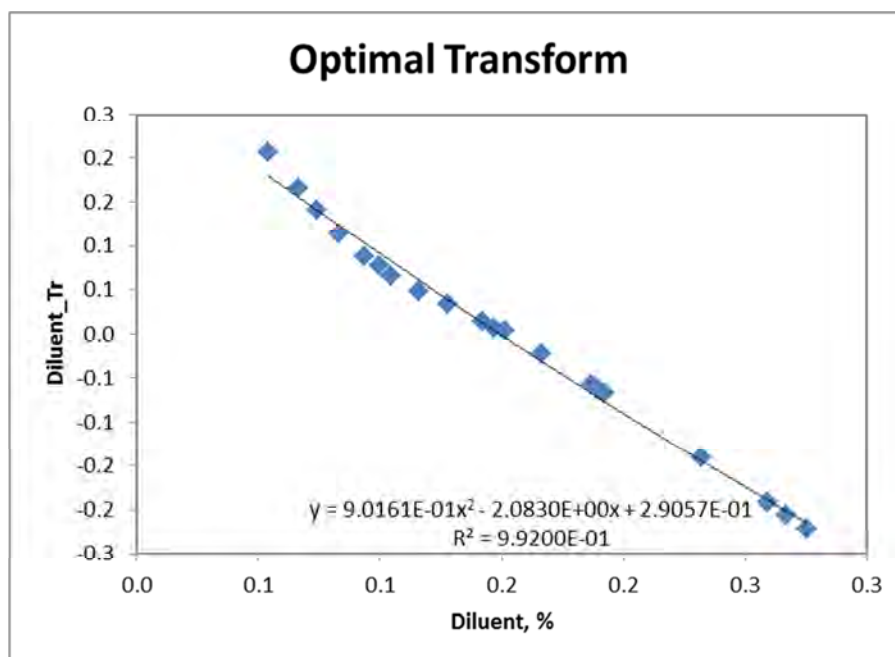
Figure 7.13 Optimal transform for diluent
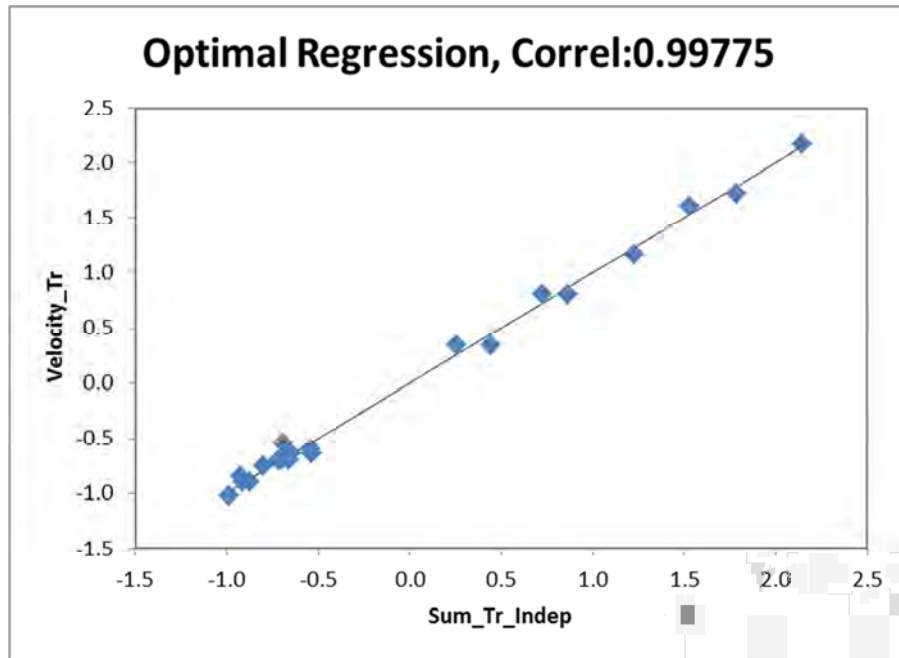
Figure 7.14 Optimal regression for velocity
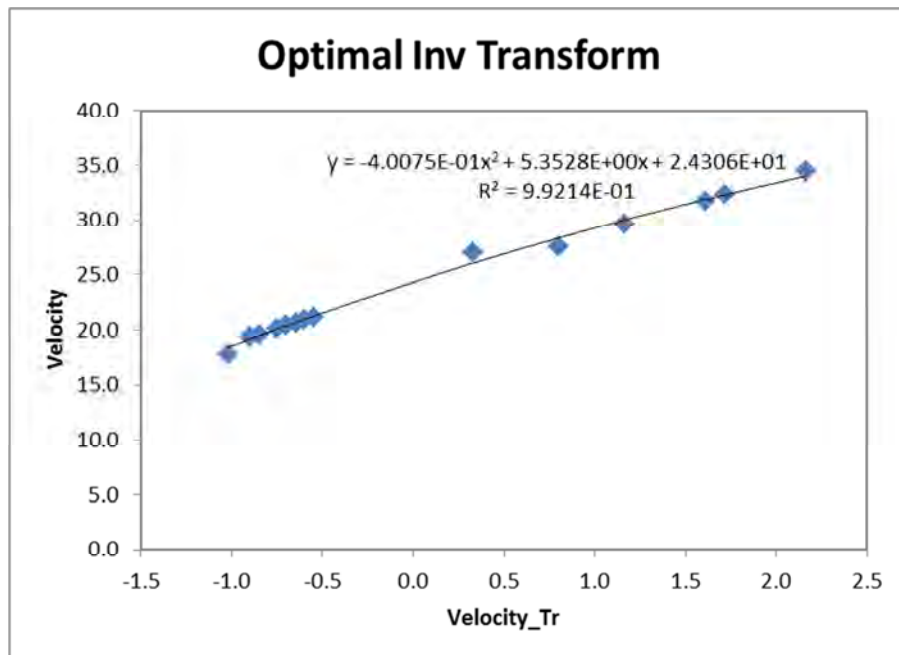
Figure 7.15 Optimal inverse transform for velocity
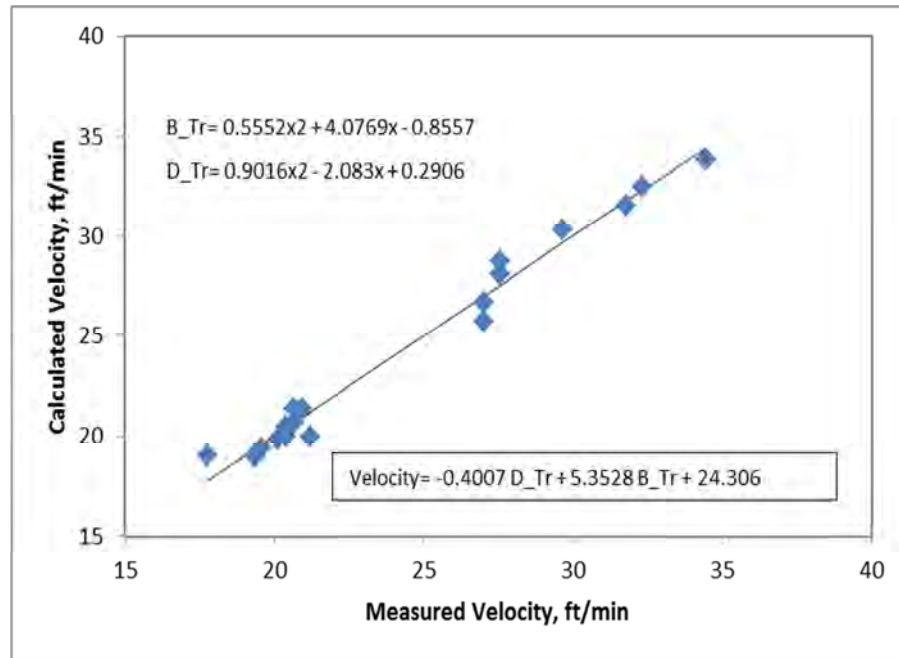
Figure 7.16 Comparison of the measured and calculated results for vertical

Figure 7.16 compares the test results to the results obtained from the correlation. As it can be seen on the chart, the correlation can predict the results quite accurately. The equation given on the chart can predict the test results within %3 error range. This is an acceptable error margin for field use. Results obtained from the static setup were used to plot the charts on **Figure 7.17** and **Figure 7.18.** Corresponding equations are also given in the following figures.
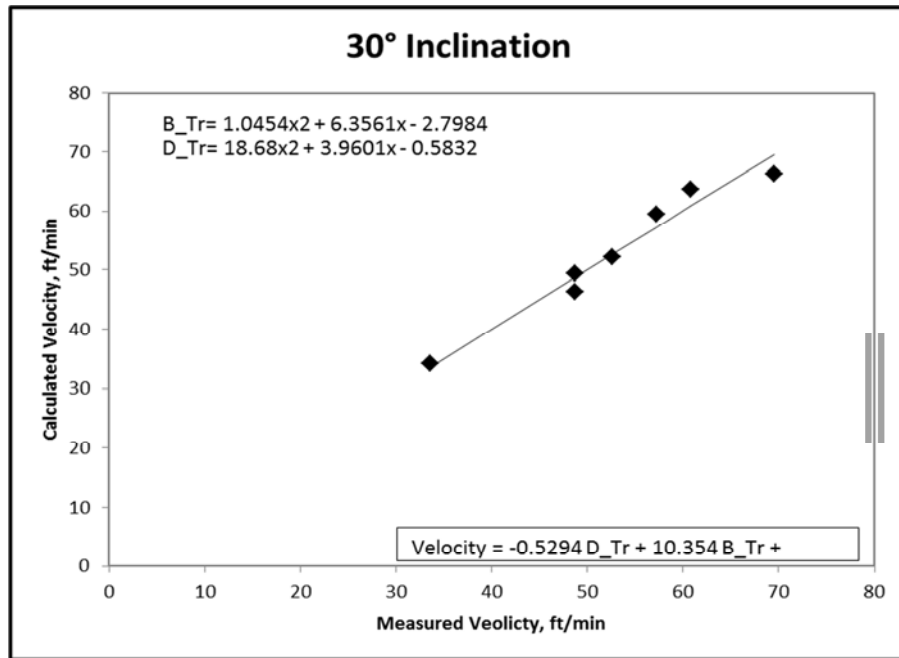
Figure 7.17 Comparison of the measured and calculated results for 30°
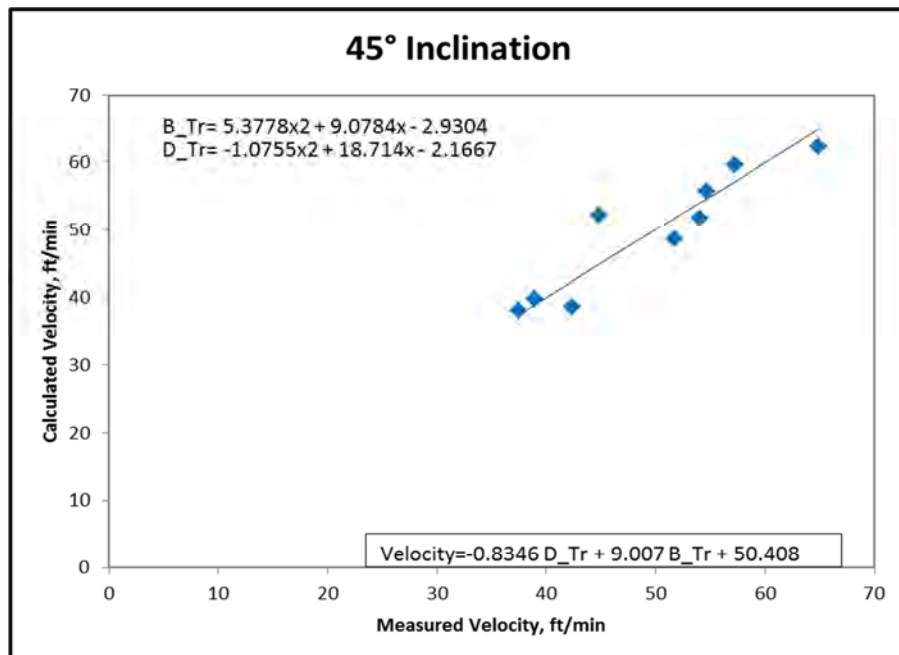
Figure 7.18 Comparison of the measured and calculated results for 45°

7.2.3 Summary of Results for Dynamic Experiment Setup and Conclusions

The dynamic experiment setup results were consistent with the static experiment setup results in terms of the velocity trend for each epoxy formulation. The numeric results however, were always lower for the terminal velocity values. This can be explained by the settling behavior of the barite in the epoxy mixture. Since the samples in the static experiments were put in the top compartment of the setup and had time for barite to settle on the bottom, the lead of the epoxy was always denser than the whole mixture. Heavier lead had higher terminal velocity and thus the results were always higher than the dynamic experiment results. It is safer to conclude that the results obtained from the dynamic experiment setup are more reliable than the static experiment due to the fact that sample has more barite in suspension (more homogenous). It is also better to use the slower terminal velocity values for settling calculations to be on the safe side.

The two variables, –barite concentration and the diluent concentration– were successfully (%3 error) correlated to the terminal velocity of the epoxy mixture. The terminal velocity for any epoxy formulation can be calculated by using the equation provided.

$$TerminalVelocity$$
$$= -0.4007\left(0.9016 * C_d{}^2 - 2.083 * C_d + 0.2906\right)$$
$$+ 5.3528\left(0.5552 * C_b{}^2 + 4.0769 * C_b - 0.8557\right) + 24.306 \qquad (11)$$

where *TerminalVelocity* is in ft/min, C_d is weight percentage of diluent, C_b is weight percentage of barite.

For the inclined section, there should be enough accumulation at the kick-off point of the well for the epoxy to flow like it was shown on **Figure 7.4** and since the flow is proved to be faster on the inclined section, it is recommended to use the velocity on the vertical as the average velocity of the epoxy.

Under the guidance of the results obtained from the tests, for a well that is 7,000-ft deep, and average epoxy (let's say 12 lbm/gal density) would need;

$$\frac{7000ft}{32ft/min} = \mathbf{218\ minutes}$$

This is around **3 hours and 38 minutes**, which is fast enough to keep the epoxy from curing before reaching the bottom.

For the same well (vertical), with 7 inch production casing and 1.9 inch tubing it would be required to have additional epoxy mixture between:

$$7000ft * \left(\frac{7}{12} + \frac{1.9}{12}\right) * \pi * \frac{3.161g}{ft^2} * 453.59\frac{lb}{g} * \frac{1gal}{12lbm} = \mathbf{9.47 gallons}$$

to

$$7000ft * \left(\frac{7}{12} + \frac{1.9}{12}\right) * \pi * \frac{12.379g}{ft^2} * 453.59\frac{lb}{g} * \frac{1gal}{12lbm} = \mathbf{37.09 gallons}$$

in order to compensate the epoxy loss in the wellbore.

8. CONCLUSIONS

1) Denser epoxy formulations tend to have higher terminal velocity with some exceptions. The exceptions are thought to have a connection with the amount of diluent used. Further study needed to be done to increase the accuracy of terminal velocity estimations and "The Static Experiment Setup" was developed for this purpose.

2) The terminal velocity for any epoxy formulation can be calculated by using the equation provided.

$$TerminalVelocity$$
$$= -0.4007\left(0.9016 * C_d{}^2 - 2.083 * C_d + 0.2906\right)$$
$$+ 5.3528\left(0.5552 * C_b{}^2 + 4.0769 * C_b - 0.8557\right)$$
$$+ 24.306 \tag{11}$$

3) For well inclinations from 30 degrees to 45 degrees, the fall rate of epoxy will increase by 100% to 130% compared to the vertical cases. It is recommended that the velocity calculated from the equation should be used as the average velocity to be on the safe side.

4) Maximum amount of epoxy loss for a vertical well is estimated to be between 3.161 g/ft^2 and 12.379 g/ft^2.

5) For an inclined well which has a 30 degree inclination is expected to have 6.757 g/ft^2 to 17.368 g/ft^2 epoxy loss.

6) For 45 degree inclination this number varies between 9.142 g/ft^2 and 19.055 g/ft^2.

7) For a 60 degree inclination however, most of the tests failed to give any recovery thus it is not recommended to use high viscosity epoxy mixtures in order to increase the success rate of the remedial job.

8) As far as the tests conducted in the static experiment setup suggest, the density of the mixture should be kept around 14 ppg or less to increase the recovery of the epoxy. After 14 ppg, barite tends to break free from the mixture as it falls through water.

9) Higher inclinations will cause higher adhesion thus decrease the amount of epoxy delivered to the target. The volume of epoxy prepared for the inclined sections should always be kept more than the vertical case in order to assure the success of the work.

10) Smaller annular size will usually lead to less epoxy loss due to smaller inner surface area.

11) As the epoxy flow stabilizes towards the bottom of the well, interaction with the walls will decrease and the adhesion concentration will also decrease.

12) Barite is a good candidate for weighting epoxy mixtures up to 14 ppg density. It will however, break free from the mixture significantly if the density exceeds this number.

REFERENCES

Assessment of Fixed Offshore Platform Performance in Hurricanes Andrew, Lili and
Ivan. MMS project number 549 final report. Jan 2006.
http://www.boemre.gov/tarprojects/549/E05114MMSProject549FinalReport.pdf.
Downloaded 15 January 2012

Assessment of Fixed Offshore Platform Performance in Hurricanes Katrina and Rita
MMS project number 578 final report. May 2007.
http://www.boemre.gov/tarprojects/578/MMSProject578-Final%20Report.pdf.
Downloaded 15 January 2012

Audibert, A., Dalmazzone, C., Dalmazzone, D., and Dewattines, C., 2004. Special Non
Polluting Emulsifier for Non Aqueous Drilling Fluids in Deep Offshore Drilling.
Paper presented at the SPE Annual Technical Conference and Exhibition,
Houston, Texas. SPE 89989. DOI: 10.2118/89989-ms.

Batchelor, G.K. 1967. *An Introduction to Fluid Dynamics*. Cambridge Mathematical
Library Series. United Kingdom: Cambridge University Press. Original edition.
ISBN 0521663962.

Bosma, M.G.R., Cornelissen, E.K., Reijrink, P.M.T., Mulder, G.S., and de Wit, A. 1998.
Development of a Novel Silicone Rubber/Cement Plugging Agent for Cost
Effective through-Tubing Well Abandonment. Paper presented at the IADC/SPE
Drilling Conference, Dallas, Texas. IADC/SPE 39346. DOI: 10.2118/39346-ms.

Coulson, J. M., Richardson, J.F., Harker, J.H., and Backhurst, J.R. 2002. *Particle Technology and Separation Processes*. Coulson and Richardson's Chemical Engineering. Woburn, Massachusetts: Elsevier Science. Original edition. ISBN 0750644451.

El-Mallawany, I. 2010. An Experimental Setup to Study the Fall Rate of Epoxy Based Fluids. Master of Science, Texas A&M University.

Knapp, R.H. and Welbourn, M.E. 1978. An Acrylic/Epoxy Emulsion Gel System for Formation Plugging: Laboratory Development and Field Testing for Steam Thief Zone Plugging. Paper presented at the SPE Symposium on Improved Methods of Oil Recovery, Tulsa, Oklahoma. 1978 Copyright 1978, American Institute of Mining, Metallurgical, and Petroleum Engineers, Inc. 7083. DOI: 10.2118/7083-ms.

Liquid Bridge Plug. Professional Fluid Systems. www.professionalfluid.com. Downloaded 15 January 2012.

MMS Completes Assessment Of Destroyed And Damaged Facilities From Hurricanes Gustav And Ike. MMS news release. 26 Nov 2008. http://www.mrm.boemre.gov/PDFDocs/20081121a.pdf. Downloaded 15 January 2012

MMS Updates Hurricanes Katrina and Rita Damage. MMS news release #3486. 1 May 2006. http://www.boemre.gov/ooc/press/2006/press0501.htm. Downloaded 15 January 2012

Nguyen, P.D., Dusterhoft, R.G., Ali, S.A., and Lockman, R.R. 2004. Stabilizing Wellbores in Unconsolidated, Clay-Laden Formations. Paper presented at the SPE International Symposium and Exhibition on Formation Damage Control, Lafayette, Louisiana. SPE 86559. DOI: 10.2118/86559-ms.

Ng, R.C., Mcpherson II, T.W., and Hwang, M.K. 1994. *Casing Repair Using a Plastic Resin*, 12/22/1992 Cong. Doc. 5295541, pt. United States: Mobil Oil Corporation (Fairfax, VA).

Rice, R.T. 1991. A Case Study of Plastic Plugbacks on Gravel Packed Wells in the Gulf of Mexico. Paper presented at the SPE Production Operations Symposium, Oklahoma City, Oklahoma. SPE 21671. DOI: 10.2118/21671-ms.

Soroush, H., Sampaio, J.H.B., and Nakagawa, E.Y. 2006. Investigation into Strengthening Methods for Stabilizing Wellbores in Fractured Formations. Paper presented at the SPE Annual Technical Conference and Exhibition, San Antonio, Texas, USA. SPE 101802. DOI: 10.2118/101802-ms.

Xue, G., Datta-Gupta, A., Valko, P., and Blasingame, T. 1997. Optimal Transformations for Multiple Regression: Application to Permeability Estimation from Well Logs. *SPE Formation Evaluation* (2): 85-94. DOI: 10.2118/35412-pa

VITA

Name: Hasan Turkmenoglu

Address: Turkish Petroleum Corporation, Söğütözü Mahallesi, 2180. Cadde
                 No: 86, 06100 Çankaya – Ankara / TURKEY

Email Address: hasanturkmenoglu@gmail.com

Education: B.S., Petroleum Engineering, Middle East Technical University at
                 Ankara, 2009
                 M.S., Petroleum Engineering, Texas A&M University, 2012